Publications of the Astronomy
Department of the Eötvös University
No. 10.

STAR CLUSTERS AND ASSOCIATIONS

(BUDAPEST 1989)

Budapest 1990

Publications of the Astronomy
Department of the Eötvös University
No. 10.

STAR CLUSTERS AND ASSOCIATIONS

EDITED BY
B. A. BALÁZS and
G. SZÉCSÉNYI – NAGY

Published by the Roland Eötvös University and the
Konkoly Observatory of the Hungarian Academy of Sciences
Budapest 1990

HU ISSN 0238–2423

Készült az ELTE Sokszorosítóüzemében
300 példányban
Felelős kiadó: Dr. Klinghammer István
Felelős vezető: Arató Tamás
ELTE 90124

C O N T E N T S

PREFACE 5
LIST OF PARTICIPANTS AND CONTRIBUTORS 7
1. ENERGY OUTPUT OF ASSOCIATIONS AND STAR COMPLEXES by V.S. Avedisova 9
2. THE MASS SPECTRUM OF UNRESOLVED DOUBLE STARS by B. Stecklum 17
3. THE ESTIMATES OF TIDAL SIZES OF OPEN STAR CLUSTERS IN THE GALAXY by V.M. Danilov & G.V. Beshenov . . . 23
4. A COMPUTER PROGRAMME FOR ESTIMATION OF OPEN CLUSTER CHARACTERISTICS by A.V. Loktin & N.V. Matkin . . . 29
5. METALLICITY OF OPEN STAR CLUSTERS by W. Götz . . . 39
6. ELECTROPHOTOMETRIC OBSERVATIONS OF TRAPEZIUM TYPE MULTIPLE STARS IN uvbyβ SYSTEM by G.N. Salukvadze & G.Sh. Dzhavakhishvili 45
7. ON THE ORIGIN OF THE UV CETI TYPE STARS by L.V. Mirzoyan 51
8. THE USE OF CCD DETECTORS IN H-ALPHA EMISSION STUDIES OF FLARE STARS by G. Szécsényi-Nagy 55
9. AGE CALIBRATION FOR OPEN STAR CLUSTERS ON THE BASIS OF INTEGRATED COLOURS AND MAGNITUDES by B.A. Balázs 77
10. KINEMATICS OF STAR FORMING REGIONS IN OUR GALAXY by J. Palouš 85
11. AN IRAS BASED STUDY OF YOUNG OBJECTS IN A CEPHEUS REGION by L. Pásztor & L.V. Tóth 91
12. SOME CONSIDERATIONS ON DATA BASES AND CATALOGS by C. Jaschek 99
13. INVESTIGATIONS BASED ON "CATALOGUE OF STAR CLUSTERS AND ASSOCIATIONS" DATA by O.P. Pyl'skaya 103
14. SOME INFORMATION ON THE BIBLIOGRAPHIC CATALOGUE OF VARIABLE STARS by S. Rössiger 111
15. LARGE VOIDS OF RICH CLUSTERS OF GALAXIES by K.Y. Stavrev 115

16. A CATALOGUE OF BLUE STARS IN M33 by G.R. Ivanov . . 125
17. ASSOCIATIONS IN M31 AND M33 by N.S. Nikolov 135
18. BRIGHT ASSOCIATIONS IN M33 by G.R. Ivanov 147
19. THE STRUCTURE OF STELLAR ASSOCIATION N 104 (LUCKE AND HODGE) IN THE LARGE MAGELLANIC CLOUD by P.E. Zakharova 163
20. FUORLIKE VARIABLES IN THE ORION ASSOCIATION by K.G. Gasparian, A.S. Melkonyan, G.B. Oganian & E.S. Parsamyan . . 167
21. AP AND AM STARS IN YOUNG STELLAR GROUPS by Ts. Radoslavova 175
22. INTERSTELLAR EXTINCTION OBSERVED IN SPECTRA OF Be STARS by W. Wegner, J. Papaj & J. Krełowski 181
23. MULTIDIMENSIONAL STATISTICAL ANALYSIS OF STAR CLUSTERS AND COMPLEXES by A.M. Ejgenson & O.S. Yatsyk . 189
24. DYNAMICAL MASSES OF GALACTIC GLOBULAR CLUSTERS by N. Spassova, G. Mandushev & A. Staneva 191
25. THE "COCl A", A CATALOGUE OF OPEN CLUSTER AGES by M. L. Roth-Höppner 201
26. DISTANCE CORRECTIONS FOR 203 OPEN STAR CLUSTERS AND 8 ASSOCIATIONS (supplement) by B.A. Balázs I

PREFACE

The 6th symposium of the Subcommission No. 6 -- Star Clusters and Associations -- of the multilateral cooperation "Physics and Evolution of Stars" held in Visegrád (near Budapest, Hungary) during June 5-9, 1989, was simultaneously the 8th conference of the subcommission. It was organised by the Konkoly Observatory of the Hungarian Academy of Sciences and the Astronomy Department of the Roland Eötvös University. The Local Organising Committee was headed by B. A. Balázs.

36 astronomers of 8 countries participated in the symposium and contributed to the discussions on "The Role of Star Clusters and Associations in Cosmogony and in the Study of Galactic Structure". The field "Computer-based Compilation and Evaluation of Astronomical Catalogues and Archives" (project No. 3 of the cooperation) was also included in the scope of the meeting. Thus the following fields were dealt with in the scientific programme:

-- star forming regions, young stellar groups;
-- cluster morphology, age, kinematics, metallicity;
-- variable and peculiar objects in clusters;
-- photometry of clusters;
-- clusters of galaxies;
-- cluster catalogues, data banks.

The general purpose of the meeting was the quick dissemination of results of the multilateral cooperation and the deepening of contacts with astronomers of neighbouring countries.

In the volume we present the papers read at the meeting. It is the honour of the editors to express their appreciation to all those who contributed to the success of the symposium.

The Editors

Budapest, December 30, 1989

LIST OF PARTICIPANTS AND CONTRIBUTORS

Bulgaria

Bonev, T.
Ivanov, G.
Mandushev, G.
Nikolov, N.
Radoslavova, Ts.
Spassova, N.
Staneva, A.
Stavrev, K.

Czechoslovakia

Palouš, J.

France

Jaschek, C.

GDR

Götz, W.
Rössiger, S.
Stecklum, B.

GFR

Roth-Höppner, M. L.

Hungary

Balázs, B.
Barlai, K.
Kun, M.
Pásztor, L.
Szécsényi-Nagy, G.
Tóth, L. V.
Vincze, I.

Libya

Abuzeid, Kalifa B.

Poland

Krełowski, J.
Papaj, J.
Wegner, W.

USSR

Avedisova, V. S.
Beshenov, G. V.
Dzhavakhishvili, G. Sh.
Danilov, V. M.
Dlushnevskaya, O. B.
Efremov, Yu. N.
Ejgenson, A. M.
Gasparian, A. S.
Geraschenko, A. N.
Loktin, A. V.
Matkin, N. V.
Melkonian, A. S.
Mirzoyan, L. V.
Oganian, G. B.
Parsamyan, E. S.
Pyl'skaya, O. P.
Rastorguev, A. S.
Salukvadze, G. N.
Sat, L. A.
Surdin, V. G.
Zakharova, P. E.
Yatsyk, O. S.

ENERGY OUTPUT OF ASSOCIATIONS AND STAR COMPLEXES

Veta S. Avedisova
Astronomical Council of the USSR Acad. Sci.
Pjatnitskaya, 48
109017, Moscow
USSR

ABSTRACT. Average values of O stars and supernova progenitors per an association (N_{OA}=25 and N_{SNA}=130) and per a star complex (N_{OC}=150 and N_{SNC}=800) are estimated on the basis of the Catalogue of Supergiants and O Type Stars in Associations and Clusters and the Catalogue of Star Formation Regions in the Galaxy. Average energy outputs produced by sequential supernova explosions in an association and in a star complex are estimated as about $2*10^{53}$ erg and $(6-8)*10^{53}$erg, correspondingly. These amounts of energy are sufficient to form superclouds and numerous observing large-scale structures in the ISM, calculated with more real value of efficiency of transformation the initial energy deposition into the ISM kinetic energy, than one suggested earlier.

1. INTRODUCTION.

Looking closely at the hierarchical structure of spiral galaxies one can distinguish subsequent levels in their structure. The first level is a division of a galaxy into disk and halo components. The second level is spiral arms. These two levels are well known and prominent. Recently we have came to the third one. It is a star complex level. The star complexes were discovered by Efremov (1978, 1979) in our Galaxy and by Elmegreen (1983) in external galaxies.

Star complexes are the main structure of spiral arms. They are formed from superclouds with masses of $10^7 M_\odot$. In its turn such superclouds are resulted of the gravitional instability in differentially rotating gas disk, by Elmegreen's (1987) assumption. However, in the real conditions of extremely inhomogeneous distribution of the interstellar matter (ISM) in the disk the action of the mechanism is hardly possible. Recently Tenorio-Tagle and Palous (1987)

"Star Clusters and Associations"
Publ. Astron. Dep. Eötvös Univ.
No.10, Budapest (1990)

suggested an alternative model of supercloud formation, needed an anormous energy deposition of 10^{53}erg in a limited volume during limited time interval with an efficiency of transformation the released energy into a kinetic one of 30%.

The local significant energy output is also required by numerous observational objects, such as Heiles's structures: HI shells, supershells, shell-like objects, "worms" et cetera. On the other hand, the existance of OB associations and their groups in the form of star complexes is accomponied by a prominent energy output during enough short interval of time. This energy must affect very much not only a thermal state, but also dynamics of a surrounding ISM.

In an extendent survey Tenorio-Tagle and Bodenheimer (1989) considering various sources of energy for construction the large-scale structures in the galaxies went to conclusion that the main energy input into the ISM is given by the sequentual supernova events in the OB associations and clusters. Survey of various works where the estimations of the number of massive stars in the associations were made led the authors to the conclusion that the average number of stars with masses of $M>8M_{\odot}$(progenitors of Type II supernovae) is 40 and the maximum value of stars can reach of 120 - 330 stars in the exceptionally rich associations.

This article concentrates on the estimations of the number of O stars (N_O)and the number of supernova progenitors (N_{SN})in the typical stellar association and in their groups - star complexes. It allows finally to estimate more realistic values of typical and maximum energy depositions in the ISM and a value of efficiency of transformation the released energy into kinetic energy of the ISM.

2. DESCRIPTION OF DATA

For the estimation of an amount of massive stars in the galactic associations the Catalogue of Supergiants and O Type Stars in Associations and Clusters by Humphreys and McElroy (1984) (futher HM) was used. It contains all known O and early B stars and supergiants being members of the galactic associations. For each star of the catalogue associations a spectral type, UBV photometry and also values of absolute visual and bolometric magnitudes calculated in the assumption that all association stars are located at the same distance from the Sun are given. In present study several association distances were changed in comparison with the catalogue values on the basis of nowadays investigations.

Besides the visible in optics associations the star

complexes contain some HII regions with invisible young associations or star clusters. For the estimation of amount of invisible massive stars immersing into gas and dust shells the Catalogue of Star Formation Regions in the Galaxy by Avedisova (1988) was used. The radio observational data taken from it allow to determine the ionizing photon fluxes from HII regions and to calculate the number of hidden stars.

3. THE NUMBER OF O STARS IN THE GALAXY ASSOCIATIONS

The counts of O stars in OB associations must take into account the selection effects of HM Catalogue. According to the analysis of the sample of the OB stars and supergiants of the Catalogue made by the authors (1984) the completeness of the data is provided for the objects with the distances within 3 kpc from the Sun and for stars with bolometric magnitudes, $M_B<-8.0$ mag. However, our analysis showed that it is necessary to limit the counts by the distances of 2.5 kpc from the Sun. According to the evolutionary tracks by Maeder (1981, 1983) and the spectral and luminocity calibration by de Jager and Nienwenhuijzen (1987) the limit of $M_B=-8.0$ mag corresponds to the stars with an initial mass of 30 $M_\odot$ and spectral type of O8. The counts of all stars with $M_B<-8.0$ were made for all associations within 2.5 kpc from the Sun. Then the expected numbers of all O stars (including $M = 18.5\ M_\odot$ which corresponds to the spectral type of O9.7) were calculated for the chosen associations by extrapolating the initial mass function (IMF) with the slope of -1.6.

In Fig.1 the number distribution of the amount of O stars in each association of Humphreys' list is shown. On can see in the figure two maxima, one is at about 8 O stars per association and another one at 25 O stars per association. The filled squares show associations located along the prominent spiral arms and into star complexes. Among them there is only one maximum at 25 O stars.

A conception of "an association" is quite unclear. Probably they are born as clusters and then after sweeping up the significant part of the initial cloud mass by O star wind they disperse into association, expending and mixing with the neighbouring associations. That is why the evolved association whithin star complex becomes more and more rich and extendent. It explains the right tail in the distribution.

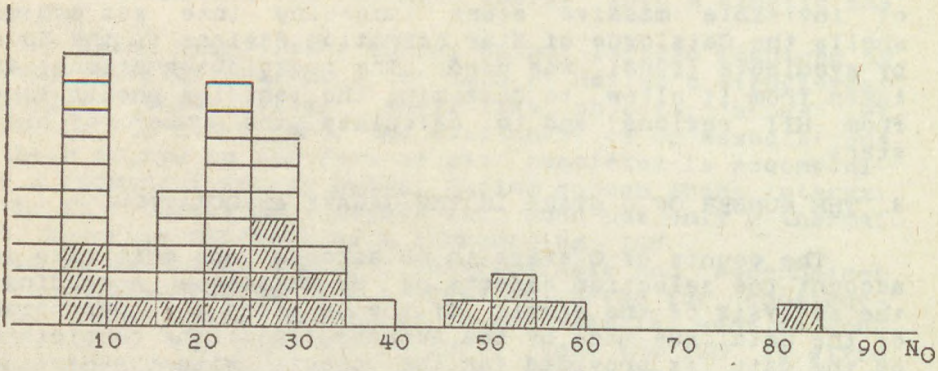

Fig. 1. The distribution of the number of O stars in the associations. Filled squares - associations whithin the star complexes.

The first maximum can be explained on the one hand by the small and poor associations situated between the spiral arms and outside the star complexes. On the other hand it is due to the very young associations whithin the star complexes, like the clusters Tr 14, Tr 15, Tr 16 and Cr 228, which are the future association, like Car OB1.

Therefore the normal association has about 25-30 O stars. More rich associations such as Cyg OB1, Cen OB1, Car OB1 and Sco OB1, have about 50 O stars, and the most rich, like Per OB1, about 80 O stars.

Among the most young associations there are HII regions where a visual absorption is very high (some tens magnitudes) and which are uncovered by their radio fluxes. In this case the amount of massive stars can be estimated on the basis of the value of radio flux density, due to O stars in general. From the Catalogue of Star Formation Regions the powerful HII regions situated in the star comlexes of the table were chosen. Assuming that the optical depth at 5GHz is small the total quantities of Lyman photons can be estimated from the values of radio flux densities. The number estimations of N_{O+BO} stars, radiating the Lyman photon flux, N_L, were made using the calculations of Lyman photon quantities, radiating by O star atmospheres (Avedisova, 1979):

$$N_{O+BO} = [(N_L / 2*10^{47})]^{1/2}$$

Using this relation the expected values of O stars were found for the chosen HII regions.

4. AMOUNT OF SUPERNOVA PROGENITORS IN THE ASSOCIATIONS

At first the typical OB association inputs in the ISM the stellar wind energy. But in spite of that a whole amount of energy per one star from the wind and a supernova explosion is the same (about 10^{51}erg), the numbers of stars taking part in both processes are differs by a decade. The thing is, that only very massive ($M > 30\ M_\odot$) stars have enough strong stellar wind, but supernova progenitors have much lower masses $M > 8\ M_\odot$. The expected number of supernova progenitors in our associations was also estimated by extrapolation of the IMF down to $8M_\odot$ (Sp.T. ~B2). It is found that N_{SN} is about from 4.5 to 6 times exceeded the number of O stars, N_O, depending on the spectral type of the earliest star. If N_O is 25, then N_{SN} is about 130, and for the very rich associations can be 250-400 stars. It means that during the evolution of a typical association the released energy may be about $(2-3)10^{53}$ erg, and in the rich association the energy deposition can reach $4*10^{53}$ erg.

5. ENERGY OUTPUTS IN STAR COMPLEXES

In the lagre-scale structures of spiral galaxies, extending along a kiloparsec, the main energy sources can be also concentrated into a part of this area. Distribution of associations in complexes often is enough compact. There is a reason to estimate the total energy released in a star complex as a possible energy source for formation of superclouds.

The most prominent star complexes are located along the main spiral arms in the Galaxy. The table describes the most well-known star complexes, located within 2.8 kpc from the Sun. It gives the associations and the powerful HII regions containing in each complex. One can see that the energy deposition in star complexes can reach $(7 - 8)10^{53}$erg during about $3*10^7$ years. Such high enegry input in the ISM allows to lower the efficiency value of transformation of released energy into the kinetic energy of the ISM. That is very important for the action of processes of superstructure formation. In this case the efficiency may be as low as several (2-4%) procents, that is real enough for the ISM.

Table. DISTRIBUTION of N_O and N_{SN} STARS among ASSOCIATIONS and HII REGIONS of the STAR COMPLEXES (SC)

SC	ASSOCIATIONS					HII REGIONS			ΣN_{SN}	E_{SN} (10^{53} erg)
	Name	D kpc	N_O	N_{SN}	N_O	N_{SN}	Name	N_O	N_{SN}		
SGR	Sgr OB1	1.60	24	110	112	520	S 45 G15.09-0.74	30	150	670	6.7
	Sgr OB7	1.74	7	36							
	Sgr OB4	2.00	10	48							
	Ser OB1	1.90	34	155							
	Sct OB3	1.66	9	46							
	Ser OB2	2.00	28	125							
CYG	Cyg OB3	2.20	27	124	159	761	G78.8 +3.60 G78.88+1.39 G82.28+2.42 G82.60+0.40 G84.84+3.91 G85.49-0.99	13	65	826	8.3
	Cyg OB1	1.80	59	286							
	Cyg OB8	2.30	22	104							
	Cyg OB9	1.20	23	122							
	Cyg OB2	1.80	28	125							
PER	Cas OB8	2.50	9	57	123	604	G133.7+1.2	15	75	680	6.8
	Per OB1	2.30	82	402							
	Cas OB6	2.20	32	145							
CAR	Car OB1	2.50	53	260	138	658				658	6.6
	Car OB2	2.20	30	147							
	Tr 14	2.90	9	39							
	Tr 15	2.60	6	34							
	Tr 16	2.60	24	106							
	Cr 228	2.50	16	72							

REFERENCES

Avedisova V.S., 1988, A Catalogue of Star Formation Regions in the Galaxy.
Avedisova V.S., 1979, Astron.Zh., 56, 965.
de Jager C., Nienwenhuijzen H., 1987, Astron.Astrophys., 177, 217
Efremov Yu.N., 1978, Pis'ma Astron.Zh., 4, 125.
Efremov Yu.N., 1979, Pis'ma Astron.Zh., 5, 21.
Elmegreen B.G., Elmegreen .M., 1983, MNRAS, 203, 31.
Humphreys R.M., McElroy D.B., 1984, A Catalogue of Supergiants and O Type Stars in Associations and Clusters.
Humphreys R.M., McElroy D.B., 1984, Astrophys.J., 284, 565.
Maeder A., 1981, Astron.Astrophys., 102, 401.
Maeder A., 1983, Astron.Astrophys., 120, 113.
Tenorio-Tagle G., Palous J., 1987, Astron.Astrophys., 186, 287.
Tenorio-Tagle G., Bodenheimer P., 1989, Ann.Rev., 26, 145.

THE MASS SPECTRUM OF UNRESOLVED DOUBLE STARS

B. Stecklum
Karl-Schwarzschild Observatory, Tautenburg, 6901,
and
University-Observatory, Jena, 6900
GDR

ABSTRACT. The derivation of the stellar mass spectrum (MS) by converting an observed stellar luminosity distribution using a mass-luminosity relation (MLR) assumes implicitely that all stars are single. However, due to the limits of angular resolution a fraction of double stars remains unresolved. The derived MS is a superposition of the MS of both single stars and unresolved double stars (UDS) for which a mass is estimated according to the total luminosity. The paper presents mass spectra of UDS for different distributions of stellar masses and mass ratios, respectively. The influence of the MLR on the resulting MS is illustrated.

The presence of UDS changes the low-mass end of the MS, whereas the MS slope at the high-mass end remains. If the mass ratio q is distributed in an uniform manner a relatively broad cut-off at the low-mass end appears. The cut-off becomes steeper for mass-ratio distributions peaked at q=1. If low values of q are more likely the MS resembles that of the primaries.

For a fixed number of stars, and a given stellar density distribution the fraction of UDS depends strongly on the angular resolution.

1. INTRODUCTION

In the derivation of the MS by transforming a stellar luminosity distribution it is often neglected that due to the limits of angular resolution a fraction of double or multiple stars remains unresolved. In the context of the following it does not matter if these stars are really bound or close together by projection. In the case of an UDS (or an unresolved multiple star - UMS) a mass is estimated according to the total luminosity. Therefore, the derived MS of a stellar system is a superposition of the MS of single stars and the MS of UDS (and UMS, respectively).

With the development of high-angular resultion techniques (speckle interferometry, lunar occultation) a number of former believed single stars turned out to be double or even multiple (McAlister, 1989). The same effect has the improvement of image quality by active optics (Wilson, 1989). The question is not only how do UDS influence the shape of

"Star Clusters and Associations"
Publ. Astron. Dep. Eötvös Univ.
No. 10, Budapest (1990)

the MS, but to which masses extends the MS at all?
The first chapter of the paper contains the derivation of the MS of UDS for two specific MS of single stars, and two different MLR. These results will be compared with Monte-Carlo simulations. In the next chapter a method will be presented to estimate the probable number of UDS for a given limit of angular resolution in the case of a polytropic stellar density distribution. At the end of the paper the results will be summarized.

2. THE MASS SPECTRUM OF UNRESOLVED DOUBLE STARS

For the derivation of the MS of UDS $n_2(m)$ two initial MS $n(m)$ of single stars will be used, the classical Salpeter-MS (Salpeter, 1955), and the Miller-Scalo-MS (Miller and Scalo, 1979). The MS were cut-off at $0.1M_\odot$, and $50M_\odot$.

$$\begin{aligned} &\text{Salpeter} && n(m) = C_S\, m^{-2.35}, \\ &\text{Miller/Scalo} && n(m) = C_{MS}\exp(-(\ln m+2.3025)^2/4.605)/m. \end{aligned} \qquad (1)$$

Both distributions were normalized

$$\int_{0.1}^{50} n(m)dm=1 \ . \qquad (2)$$

It will be assumed that the distances of the stars are equal and known, e.g. for members of a star cluster, so that the luminosities are available. To illustrate the influence of the MLR $l(m)$ two different MLR were adopted, a simple power law, and the MLR according to Heintze (1973)

$$\begin{aligned} &\text{"simple"} && l(m) = m^4, \\ &\text{Heintze} && l(m) = \begin{cases} m^{4.85(1-0.07774\ln m)} & m>0.7M_\odot \\ 0.4093\ m^{2.48} & m\leq 0.7M_\odot \end{cases} . \end{aligned} \qquad (3)$$

The basic equation for the present purpose is given by

$$n(l)\ dl = n(m)\ dm, \qquad (4)$$

from which the MS can be derived if the luminosity distribution is known or vice versa. In the case of an UDS a resulting mass m_2 is obtained by inverting the MLR

$$m_2 = m(l_P+l_S) \ , \qquad (5)$$

where l_P, l_S are the luminosities of the primary (brighter) and secondary (fainter) components, respectively. The resulting MS $n_R(m)$ in the presence of UDS can be written as

$$n_R(m) = (1-f)\ n(m) + f\ n_2(m) \ , \qquad (6)$$

where f is the fraction of UDS (see next chapter). For the derivation of the MS of the UDS $n_2(m)$ it will be assumed that the luminosities (or masses, respectively) of primaries and secondaries are not correlated. The total luminosity of an UDS is $l_2=l_P+l_S$. Using the assumption it follows that the luminosity distribution of UDS $n_2(l)$ is the convolution of the luminosity distribution of single stars

$$n_2(l) = \int_{l_P(0.1)}^{l_P(50)} n(l_P)n(l-l_P)dl_P \quad . \tag{7}$$

Using Eq.(4) the MS of UDS is obtained

$$n_2(m) = n_2(l)\,|dl/dm| \quad . \tag{8}$$

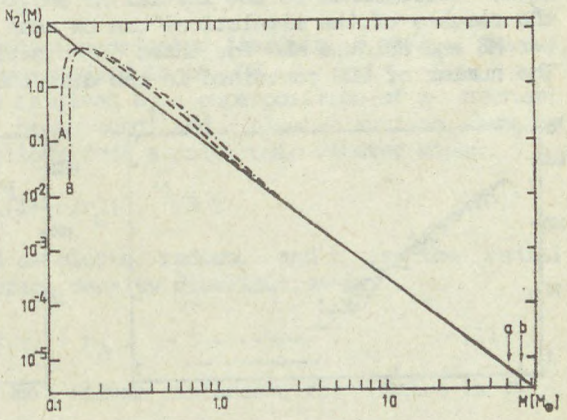

Fig.1a: MS of UDS for the initial Salpeter-MS and two different MLR (A -"simple", B -Heintze)

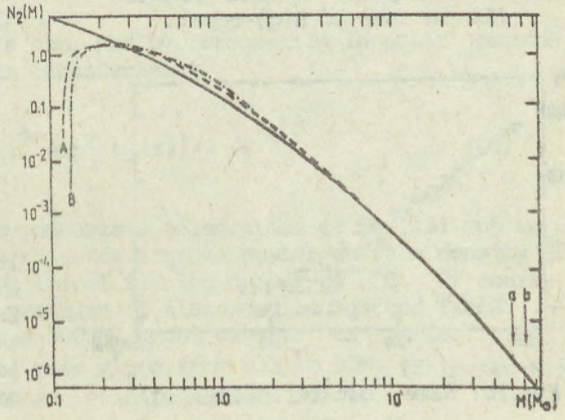

Fig.1b: Same for initial Miller-Scalo-MS;a,b - high-mass cut-off of initial and resulting MS (simple MLR), respectively;

Fig.1 shows the MS of UDS for the initial Salpeter- and Miller-Scalo-MS, respectively. For both cases the low-mass cut-off is shifted to somewhat higher masses. At the low-mass end a turn-over appears, which is broader in the case of the Miller-Scalo-MS. In the mass region below $1M_\odot$ the resulting MS differs signifcantly from the initial MS, whereas in the high-mass range the shape of the MS of UDS is essentially the same as that of the initial MS. However, the MS of UDS extends to higher masses (high-mass cut-off at $50M_\odot$ for the initial MS - a, at $69M_\odot$ for the simple MLR - b, at $74M_\odot$ for the Heintze-MLR). The appearance at the low-mass end depends on the actual location of the cut-off which was chosen arbitrarily.

For comparison several Monte-Carlo simulations have been performed using different distributions n(q) of the mass ratio $q=m_S/m_P$, $q\in[0,1]$. The above result corresponds to a uniform distribution $n(q)=\text{const}$. Two other cases are trivial. If $n(q)=\delta(q)$, i.e. no secondaries present, the MS of UDS is identical with the initial MS. In the case $n(q)=\delta(1-q)$ primaries and secondaries are of equal mass and luminosity, therefore, $n_2(m)$ corresponds to the initial MS shifted to higher masses. In Fig.2 the results of the simulations can be seen for the combination of Salpeter-MS and Heintze-MLR for three distributions n(q) (const, q^2, $(1-q)^2$). The number of UDS contained in the distribution is 10^4.

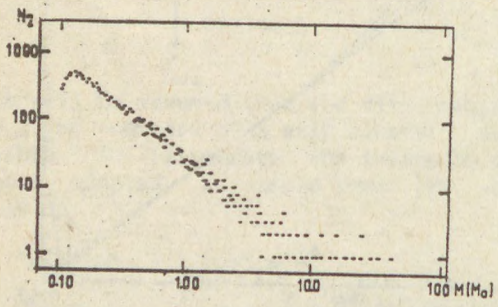

Fig.2a:Monte-Carlo-Results for initial Salpeter-MS and Heintze-MLR in case of n(q)=const.

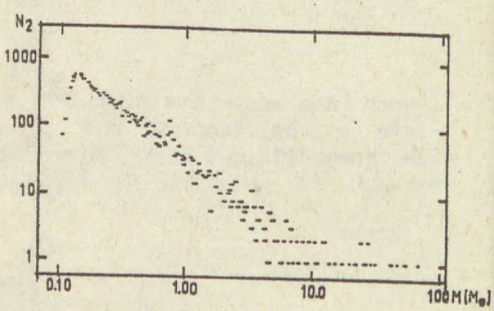

Fig.2.b: Same, but for $n(q)\sim q^2$.

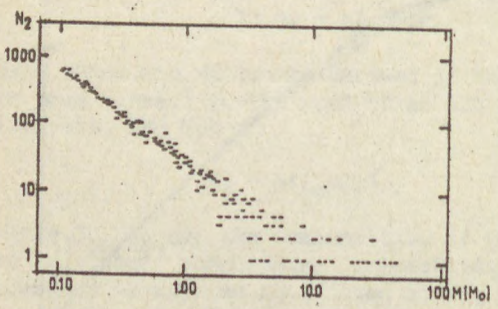

Fig.2c: Same, but for $n(q)\sim(1-q)^2$.

It is straightforward to extend the rigerous method to estimate the MS of UMS. However, due to the multiple convolution the computational effort increases considerably.

2. THE FRACTION OF UNRESOLVED DOUBLE STARS

Besides the form of the MS of UDS it is of interest how many UDS contribute to the resulting MS (see Eq.(6)). In the following an evaluation of the fraction f is given which assumes that the number of stars n in an area element dA of the sky is governed by Poisson's distribution.

$$p(n) = n_*(x,y)^n \exp(-n_*(x,y))/n! \quad . \tag{9}$$

The case of a uniform surface density distribution corresponds to n_*=const (e.g. number of stars per square degree). The mean number N of stars within an area A of the sky is then $N=n_*A$.

Now consider the area A_S of a disk having a radius that corresponds to the observational angular resolution of the telescope, which will be called the effective seeing disk (ESD). The mean number of stars per ESD is $n_S=n_*A_S$. The probability of the occurence of two stars in one ESD is according to Eq.(9)

$$p(2) = n_S^2 \exp(-n_S)/2 \quad .$$

The total number of ESDs in the investigated field is $N_S=A/A_S$. So, a number $N_2= p(2)N_S$ of stars are expected to be UDS.

A more realistic description is given by a superposition of a constant surface density n_B (stellar background) and a cluster surface density distribution $n_C(x,y)$ which follows from a polytropic cluster model.

$$n_C(r) = 4n_o r_C(1+(r/r_C)^2)^{-2}/3 \quad , \tag{10}$$

where r_C may be considered as cluster radius, and r is the radial distance. So, the overall surface density distribution is

$$n(x,y) = n_C(x,y) + n_B \quad . \tag{11}$$

The mean number of stars within a ESD at distance r from centre is

$$n_s(r) = \iint_{A_S(r)} n(u,v)\, du\, dv \quad . \tag{12}$$

The expected number of UDS is obtained by integration in polar coordinates over the area taken into consideration

$$N_2 = 2\pi \int_0^\infty n_s(r)^2 \exp[-n_s(r)]/2\, dr/A_S \tag{13}$$

Values for N_2 were obtained by numerical integration of Eq.(13) out to 5 cluster radii. It turned out that for a given number surface density of stars the size of the ESD is critical for the number of UDS. Of course, this number is higher in the presence of a crowded background field.

Table I gives results for a $3000M_\odot$ model cluster of radius r_C=15' having N_C=8772 members in the mass range from 0.1 to $50M_\odot$ (Salpeter-MS) for two ESD diameters without, and with background stars.

Table I.
Number of UDS for a model cluster of radius 15' containing 8772 members

ESD diameter	0".3		3".0	
n_B */□°	N_2	%	N_2	%
0	0.356	0.004	35.11	0.420
44640	29.08	0.012	2836	1.260

In the presence of background stars the corresponding surface density is equal to the maximum surface density of the cluster $n_C(0)$. The percentage of UDS is defined as N_2 divided by the number of observed stars $N_C+n_B\pi(5r_C)^2-N_2$. It is obvious that a tenfold increase in angular resolution reduces the fraction of UDS by about two orders. From the results the conclusion may be drawn that the fraction of UDS is too small to influence the estimation of the MS. However, one must be cautious because the lower limit of the MS may be smaller than $0.1M_\odot$ which results in a much larger number of cluster stars, and, in addition, the cluster may be more concentrated than in this model. Therefore, in some cases a fraction of UDS of about 5 per cent seems not unrealistic. The application to photographic images of star fields should include the effects of light scattering in the photoemulsion enlarging the stellar image in dependence on both stellar brightness and focal length, and as a consequence, the number of UDS.

4. SUMMARY

The question of the influence of UDS on the estimation of the MS has been investigated. The shape of the MS of UDS shows significant differences at the low-mass end (presence of a turn-over) compared with the initial MS, whereas at the high-mass end the slope of the initial MS is conserved. This conclusion agrees with the results of Malkov and Piskunov (1989) for the stellar luminosity function.

On the base of a polytropic density distribution for the star cluster the expected fraction of UDS has been computed for two cases of the effective angular resolution in the presence, and absence of a stellar background. The results indicate that improving the angular resolution is a severe way to avoid the influence of UDS. Images of a concentrated star cluster in a crowded field obtained under bad seeing conditions may contain a significant fraction of UDS, especially if taken by photography.

References:

Heintze, J.R.W.(1973). in B.Hauk and B.E. Westerlund (eds.), Problems of Calibration of Absolute Magnitudes and Temperatures of Stars, D. Reidel Publ. Co., Dordrecht, Holland, p.265.
Malkov, O.Ju, and Piskunov, A.E.(1989). Nauchn. Inform. 65, 155.
McAlister, H.; Hartkopf, W.I.; Sowell, J.R.; Dombrowski, E.G., and Franz, O.G.(1989). Astron.J. 97, 510.
Miller, G., and Scalo, J.M.(1979). Astrophys.J.Suppl. 41, 513.
Salpeter, E.E.(1955). Astrophys.J. 121, 161.
Wilson, R.(1989).ESO Messenger 56, 1.

THE ESTIMATES OF TIDAL SIZES OF OPEN STAR CLUSTERS IN THE GALAXY

V.M.Danilov, G.V.Beshenov
Astronomical Observatory of the Urals State University,
620083 Sverdlovsk
USSR

ABSTRACT. The stability of open star clusters (OCl) embedded in the joint gravitational field of the Galaxy and a gas-star complex with mass $\sim 10^7 M_\odot$ and size $\lesssim 1$ kpc has been investigated. The influence of this field reduces the OCl tidal radius r_t by factor 1.5 - 2.5 as compared with r_t in the case of the Galaxy field only.
Three different estimates of the tidal radius r_t of OCl having noncircular orbits in the Galaxy field have been performed. The value of tidal radius of OCl with noncircular orbits coincide with r_t of OCl moving in Galaxy at corresponding central circular orbit.

Study of the structure of open star clusters in solar neighbourhood shows, that old OCl-s have larger average values of relative radii (in units of tidal radius r_t) than young OCl-s (see fig. 3, in paper Danilov, Seleznev, 1988). Stars in young OCl-s are on the average situated deeper under the tidal surface defined by gravitational field of the Galaxy, than in old clusters, that points on a large stability of young OCl-s in tidal field of the Galaxy. However, the mean life-time of young OCl-s is less that of old clusters (Wielen,1971). It may be coursed by the disruption of young OCl-s by collisions with giant molecular clouds (GMC) in galactic disc (Wielen, 1985). Recently published data of GMC catalogues (Dame et al., 1987; Solomon et al.,1987) lead to notably less values of concentrations of GMC and their mean masses in solar neighbourhood, than it was assumed earlier by (Wielen, 1985; Danilov, 1987a; Danilov, Beshenov, 1987), that makes disruption times of OCl-s approximately three times larger (Danilov, Seleznev, 1988b). Thus the mechanism, which was not taken into account in this estimates of OCl-s disruption times that notably decreases the stability of OCl-s in outer force fields has to work in solar neighbourhood. Effect of such mechanism on young OCl-s dynamics may be caused by gravitational fields of gas-star complexes (GSC), which contain this OCl-s. The examples of such

"Star Clusters and Associations"
Publ. Astron. Dep. Eötvös Univ.
No.10, Budapest (1990)

systems, arguments for GSC to be gravitationally bounded and for stability of comoving neutral hydrogen superclouds are presented in papers of Efremov, 1986; Elmegreens, 1987. According to this papers HI superclouds (and probably GSC-s) have masses of 10^7 $M_\odot$ and sizes up to 1 kpc.

The purpose of present paper is to analyse OCl stability in Galaxy field with (and without) of the GSC effect on stability of OCl comoving with GSC in Galaxy.

As an approximation to solution of one of these problemsthe stabiliti of OCl, which moves in orbit of radius r_o with constant angular velocity around the center of massive GSC (in coordinate system centered and fixed with GSC) was considered. The following assumptions are used in present paper. The mass center of GSC moves along cirsular orbit with constant angular velocity ω_c about Galaxy center. OCl's and GSC's orbits are situated in Galaxy plane. The cluster is simulated by homogeneous gravitating sphere. There are considered two models of GSC: homogeneous and unhomogeneous spheroids, which are oblate along Z axis. The density of unhomogeneous spheroid is assumed as decreasing from its mass center by the low: $\rho \sim (1 - f)^2$, $f = (r/a)^2 + (Z/c)^2$; a and c are spheroid semiaxes, Z axis is perpendicular to Galaxy plane, r - distance from Z-axis of GSC.

Linearized equations of star motion in OCl orbit plane are written in coordinate system, which is motionless relative to cluster, with respect to force fields of OCl, GSC and of Galaxy ($r/R \ll 1$, $R/r \ll 1$; R is the radius of the orbit of SC, R is the radius of OCl):

$$\frac{d\vec{\xi}}{dt} = Y(t)\vec{\xi} + \vec{b}, \quad \vec{b} = \text{const}, \tag{1}$$

where t is time, ξ_i is components of radius-vector and of velocity vector of star in assumed reference frame. Matrix Y(t) is periodic with period $T = 2\pi/\omega_\varphi$. The solutions of stability problem for the system of equations (1) may be reduced to analysis of solutions stability of corresponding systems of linear homoeneous equations (Demidovich, 1967; Jackubovitch, Stardzinsky, 1972)

$$\frac{dX}{dt} = Y(t)X, \quad X(0) = E, \tag{2}$$

where X is the matrix of the fundamental solutions of system (1) with $\vec{b} = \emptyset$ and E is unit matrix.

There is considered the particular case of $\omega_\varphi = \omega_c$, $\vec{\omega}_\varphi \parallel \vec{\omega}_c$ in present paper. Such conditions may exist in outer regions of the most extended gravitationally bounded GSCs or in certain parts of OCl's orbit in unbounded complexes. In this case matrix Y not depends on the time t and in this paper the formula for cluster's tidal radius r_t has been obtained. The value r_t depends on angle φ between directions from mass center of GSC towards mass center of OCl and towards galactic anti-center:

$$r_t(\varphi = \pm\pi/2) > r_t(\varphi = \pi) > r_t(\varphi = 0).$$

In more general case, when $\omega_\varphi > \omega_c$, integration of equations (2) for t from $\emptyset$ to T allows to derive monodromy matrix X(T) (see Demidowich, 1967; Jackubovitch, Stardzinsky, 1972). The analysis of the stability of

OCl in plane of its orbit for the unhomogeneous Gsc with the help of multipliers of matrix X(t) shows, that on "direct" orbits ($\omega_\varphi > 0$) OCl has smaller values of tidal radius r_t, than on "retrograde" orbits ($\omega_\varphi < 0$). It is well known that the greater stability of "retrograde" orbits of individual stars in cluster, which moves along circular orbit in the Galaxy (Keenan, 1981). The cluster stars with "retrograde" motions in GSC in our case form the bunch of the orbits within gas-star complex, which are more steady than that in the case of "direct" orbits. This leads to greater stability of OCl on "retrograde" orbits.

In the case of "direct" orbits of clusters in GSC the value r_t for OCl is in a good agreement with

$$r_t = \left[\frac{GM_c}{2(A-B)(A+\omega_\varphi) - \gamma/2 + |\gamma/2+s|}\right]^{1/3}, \quad \gamma = \left(\frac{1}{r}\frac{\partial\Phi}{\partial r} - \frac{\partial^2\Phi}{\partial r^2}\right)_{r=r_o}, \quad (3)$$

$$s = gr_o^2/4R_o^2, \quad g = -(\alpha_1 + R_o(\partial^3\Psi/\partial R^3)_{R=R_o}), \quad \alpha_1 = 4A(B-A),$$

where M_c is the cluster's mass, A and B are the Oort's constants, Φ and Ψ -gravitational potentials of GSC and Galaxy. Value r_t in (3) is derived by the averaging of matrix Y(t) over period T. In the case of $\omega_\varphi < 0$ for inhomogeneous GSC formula (3) corresponds to boundary of OCl stability region in outer parts of gas-star complex.

There were executed numerical experiments for study of dynamical evolution of OCl by the numerical integration of motion equations for N=500 stars of equal masses in models of OCl, which is virialized at t=0 and which moves near the circular orbits around the center of GSC in the joint gravitational field of the Galaxy and GSC. It is assumed that mass center of GSC moves along the circular orbit in galactic plane. The methods of integration, of setting of initial conditions and the forms of galactic and GSC potentials are described in (Danilov, 1985; Kutuzov,Ossipkov, 1980; Chandrasechar, 1973). The position of minimum of star tangential velocities distribution over star distances from mass center of cluster is used for estimation of OCl tidal radius, as well as in (Allen,Richstone, 1988). The results of determination of r_t in numerical experiments are in close agreement with the theoretical results, obtained in linear approximation. That allows to use formula (3) for OCl tidal radius estimation in the joint gravitational field of GSC and Galaxy.

If GSC mass is (1 - 2) $10^7 M_\odot$ and its semiaxes are a = 300 - 400 pc, c = 35 - 100 pc, then the tidal radius of OCl averaged over the region of GSC becomes 1.5 times smaller for the "direct" orbits of OCl for homogeneous GSC and 2 - 2.5 times smaller for inhomogeneous GSC than the values r_t, which caused by the effect of Galaxy field only. This can lead to increase of instability degree estimations of OCl in the solar neighbourhood (Danilov, 1987b) and permit to coordinate OCl disruption times with observation data on age and lifetimes of such clusters (Danilov, Seleznev, 1988b) with new data on GMCs (Dame et al., 1987; Solomon et al., 1987) that actively affects the disruption of OCl.

There were used three different approaches for investigation of tidal sizes of OCl with noncircular orbits (disregarding of GSC field) in this paper.

1. The equations of motion of star of cluster with epicyclic galactical orbit in cylindrical galactocentric coordinates (R, Θ, Z) where written down. As before it is assumed the rotational symmetry of Galaxy potential. For the case, when sizes of clusters and semiaxes of OCl motion in R and Z coordinates in the Galaxy are small in comparison with the distance of OCl from Galaxy center (Condition 1), the analysis of cluster stability in linear approximation was carried out. It is shown that cluster tidal radius on such orbits is equal to tidal radius of OCl, which moves along the central galactic circular orbit (King, 1965), which correspond to the given epicycle. The use of Condition 1 by the linearization of equations of star motion in OCl makes possible to suppose the constancy of the matrix Y for our case. The elements of matrix Y in this case are equal to values of matrix Y elements, when cluster moves along the central circular orbit.

2. If the matrix Y depends on position of OCl on epicycle of its orbit, the stability of cluster in plane of OCl orbit may be investigated by means of euations (1), in which the terms corresponding to GSC are excepted. As a simplification let us consider circular epicycle of cluster orbit, which placed in Galaxy plane. In this case the matrix Y is periodical on time with period $T_1 = 2\pi/\omega_1$, where ω_1 is epicyclical frequency of motion in Galaxy field, and the OCl motion is "retrograde".

The analysis of OCl stability with the aid of multipliers of the corresponding matrix $X(T_1)$ (see (2)) shows that the tidal radius of OCl with a high precision is equal to constant value $0.97r_t$ over the considered range of epicycle radius r_o = 50 - 800 pc, where r_t is calculated according to (King, 1965) for central circular orbit of OCl. The difference of multiplier at r_t from 1 is caused by assumption about circular shape of epicycle.

The method of estimation of the value of tidal radius for the cluster, which is similar to that considered here, was used in (Angeletti et al., 1983, 1984; Angeletti, Giannone, 1983), where the analysis of stability of star clusters in linear approximation for the orbits with large eccentricities are carried out. However, the shape of the boundary of "dominating" stability region of cluster, introduced in these papers, $\nu = \nu(e)$ (see fig. 4 in (Angeletti et al., 1983) or fig. 1 in (Angeletti, Giannone, 1984)) is too rough at $e \sim 0 - 0.1$ and therefore it is not applicable for the stability analysis of the most OCls in the solar neighbourhood. It is necessary to assume the limiting value of $\nu(e)$ to be constant in the range of values $e = 0 \div 0.1$.

3. The numerical experiments by the integration of equations of motion for N = 500 stars with equal masses are carried out in this paper. These stars form the cluster, which moves along the plane noncircular orbits and along corresponding central circular orbit with a radius of 8200 pc. Let us the half width of noncircular orbit "box" ΔR measuring along axis "center-anticenter" in the Galaxy is equal to 356 pc. Accordingly to (Barkhatova et al., 1981), the orbits with ΔR = 356 pc are characteristic for OCls with ages $t \lesssim 2\ 10^8$ years. The estimations of tidal radii of OCls by N-body simulation of clusters moving on the noncircular and on corresponding central circular orbits are well accord with each other. These estimations are near to that of r_t, obtained by (King, 1965) for the central circular orbits.

The use of Galaxy potential in the form (Kutuzov,Ossipkov, 1980) with allowance for results of this part of paper permits to estimate the maximal error $\delta r_t/r_t$. This error is entering to the estimates of tidal radius due to assumption that cluster orbits are circular. Let us $e=(R_a-R_n)/(R_a+R_n)$, where R_a and R_n are the apocentric and the pericentric distances of OCl from the center of Galaxy. If e=0.05 or e=0.1 for OCl from solar neighbourhood then we have $\delta r_t/r_t=\pm 0.036$ or $\delta r_t/r_t=\pm 0.075$ correspondingly. These are smaller than mean error in determination of limit sizes of such OCl (~10%) in the framework of method of star counting (Danilov et al.,1985).

REFERENCES.

Allen A.J.,Richstone D.O. Astrophys. Journ.,1988,v.325,p.583.
Angeletti L. et al. Astron. Astrophys.,1983,v.121,p.183.
Angeletti L. et al. Astron. Astrophys.,1984,v.138,p.404.
Angeletti L.,Giannone P. Astron. Astrophys.,1984,v.138,p.396.
Barkhatova et al. In "Dvizhenie iskusstv. i estestv. nebesnykh tel.Ural. Univ.Press.Sverdlovsk,1981,p.8.
Chandrasekhar S. Ellipsoidal figures of equillibrium,M.,Mir,1973.
Dame T.M. et al. Astrophys. Journ.,1987,v.322,p.706.
Danilov V.M. Astron. Zh.,1985,v.62,p.704.
Danilov V.M. Astron. Tsirk.,1987a,N 1492,p.1.
Danilov V.M. Astron. Tsirc.,1987b,N 1522,p.2.
Danilov V.M.,Beshenov G.V. Astron. Tsirk.,1987,N 1520,p.5.
Danilov V.M. et al. Astron. Zh.,1985,v.62,p.1065.
Danilov V.M.,Seleznev A.F. Kinematika i phys. neb. tel,1988a,v.4,p.51.
Danilov V.M.,Seleznev A.F. Astron. Tsirk.,1988b,N 1534,p.9.
Demidovitch B.P. Lectures on mathemat. theory of stability,M.,Nauka, 1967.
Efremov Ju.N. Astron. Tsirc.,1986,N 1447,p.1.
Elmegreen B.G.,Elmegreen D.M. Astrophys. Journ.,1987,v.320,p.182.
Jackubovitch V.A.,Stardzinsky V.M. Linear diff. equations and their applications,M.,Nauka,1972.
Keenan D.W. Astron. Astrophys.,1981,v.95,p.334.
King I.R. Astron. Journ.,1965,v.67,p.471.
Kutuzov S.A.,Ossipkov L.P. Astron. Zh.,1980,v.57,p.28.
Solomon P.M. et al. Astrophys. Journ.,1987,v.319,p.730.
Wielen R. Astrophys. Space Sci.,1971,v.13,p.300.
Wielen R. Dyn. star clusters,Proc.IAU Symp.,113,1985,p.44.

A COMPUTER PROGRAMME FOR ESTIMATION OF OPEN CLUSTER CHARACTERISTICS

A.V.Loktin, N.V.Matkin
Astronomical Observatory Urals State University,
620083 Sverdlovsk, USSR

ABSTRACT. An algorythm of computer determination of main charcteristics of the open clusters from UBV photometry is presented. The examples of deriving reddenings, distances, ages and in some cases metallicities are shown. There is briefly discussed the distribution of 76 open clusters in the galactic plane and found zero-point of the period-luminosity relation from Cepheids in galactic clusters as a preliminary results.

The main characteristics of open clusters such as reddening, distance from the Sun and age, are usually estimated from photometrical data. In order to get a large set of homogeneous characteristics of clusters we decide to develope the computer programme for estimation of such values, analogous to that discussed by Cameron (1985), but more suitable for determination of cluster ages and not so exacting to the quality of photometrical measurements and selection of cluster members. Such approach after the accumulation of photometrical data on magnetic carriers will provide the opportunity of fast reevaluation of characteristics of many clusters using any new sets of isochrones, reddening lines or distance scale.

By now there exists a large amount of photometrical investigations of open clusters, especially in UBV system, and it is obvious to start with the data of that photometrical system, though we have plans to use RGU and Stromgren systems later. In that short paper we consider the operation of our programme and some preliminary results concerning

"Star Clusters and Associations"
Publ. Astron. Dep. Eötvös Univ.
No.10, Budapest (1990)

young open clusters, most interesting in connection with the investigation of structure of the Galaxy.

For estimation of reddening we use common procedure of the best fit of observational data on two-colour diagram by shifting data along appropriate reddening lines. The best fit is fixed by minimisation of the sum of deviations of (U-B) color index, but using such fitting procedure we are faced on with problem of the influence of nonmembers, which make the distribution of points around unreddened color-color relation asymmetrical. We try to avoid that problem by using the minimization of less than 2 powers of deviations, which makes fitting procedure less sensitive to large deviations. The power by our experience is calculated as P=50/N, where N is number of stars used. Such method permit us to use in most cases the photometrical data contaminating by nonmembers and to imitate the by-eye fitting, because minimization of small powers of deviations gives estimates lying close to the mode of distribution.

For reddening lines we use the expression of the form

$$E(U-B)=(0.72+0.05*E(B-V))*E(B-V) \qquad (1)$$

where the values of coefficients are taken from Straizys (1977) for main-sequence stars.

After the evaluation of colour excess some stars with the largest deviations are rejected to prevent the disturbing effect of such stars (mainly nonmembers) on the determination of distance and age.

With the estimated value of colour excess the V-magnitudes of stars are dereddened with the ratio of total to selective absorption

$$R=Av/E(B-V)=3.34+0.18*(B-V)_o+0.027*E(B-V) \qquad (2)$$

This expression was evaluated with the data taken from Straizys (1977) for MS-stars.

For the estimation of distance modulus we decide not to use ZAMS fitting procedure because of evolutional deviations of stars, but to make the best fit of appropriate isochrone to get the simultaneous estimates of distance and age of cluster. This method allowes to use all the photometrical material for the determination of distance modulus, not only the unevolved MS-stars as in the case of ZAMS fitting procedure. In order to use the programme for clusters of various

ages we use 10 isochrones for ages from zero to $15 \cdot 10^9$ years, which we get which we get from Mermilliod and Maeder (1986), Heilesen (1980), VandenBergh (1985). The lower parts of the youngest isochrones are replaced by those calculated by Iben for contracting pre-MS stars.

We have slightly shifted the luminosity scale of isochrones to permit distance modulus to be equal to $3.^m42$ for Hyades cluster accoding our estimation (Loktin et al.,1987). In the case of isochrone fitting we use color index (U-V) instead of conventionally used (B-V) or (U-B) because of better sensitivity of (U-V) to differences in effective temperatures for young stars.

After the preliminary determination of distance modulus and age some stars with largest deviations from appropriate isochrone are rejected and the procedure of estimation of colour excess and modulus-age determination is repeated to get better quality of the estimates. We have to mention, that for clusters older than 10^8 years the programme calculates the metallicity by searching for the best fit between the colour-colour diagrams of unreddened stars of various metallicities taken from Cameron (1985).

Table 1. Parameters of some clusters provided by programme discussed

Object	Source of photometry	Initial number of stars	E(B-V)	[Fe/H]	(V_0-M_V)	lgt	Phot
IC1805	Hoag et al.(1961)	65	0.788	-	11.585	6.643	pe+pg
	Ishida (1969)	26	0.788	-	11.276	6.613	pe
	Joshi,Sagar(1983)	117	0.788	-	11.694	6.724	pe
h Per	Muminov (1982)	371	0.546	-	11.794	7.079	pg
	Wildey (1964)	192	0.554	-	11.651	7.497	pg
	Mermilliod (1976)	50	0.575	-	11.399	6.898	pe
M67	Murrey (1965)	285	0.11	-0.12	9.594	9.418	pg
	Racine (1971)	159	0.07	-0.03	9.594	9.608	pe
	Eggen (1964)	183	0.06	-0.07	9.555	9.652	pe

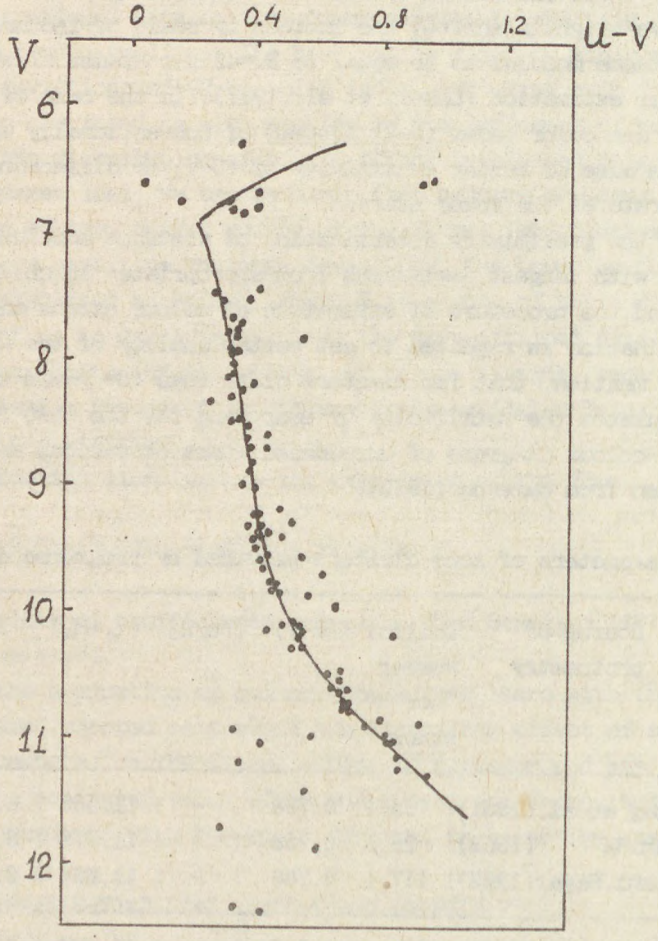

Fig.1. The example of isochrone fitting for Praesepe cluster.

The check of quality of our programme is performed by using of photometrical data for Hyades and Praesepe clusters (Loktin et al.(1987). For the Hyades members we get $E(B-V)=0.^m007$, $[Fe/H]=+0.15$, $(V_o-M_v)=3.^m42$ and age $t=6.27\cdot10^8$ years. For Praesepe cluster there are performed two solutions. First solution we make for all stars from catalogue of Mermilliod (1976) and derived $E(B-V)=0.^m010$, $[Fe/H]=+0.02$, $(V_o-M_v)=6.^m27$, $t=7.16\cdot10^8$ years. For second solution we use only doubtless members, whose membership are justified by proper motions and radial velocities. Here we have $E(B-V)=0.^m020$, $[Fe/H]=+0.01$, $(V_o-M_v)=6.^m260$ and $t=6.93\cdot10^8$ years. The comparison between two solutions shows, that the procedure of rejecting stars with large deviations works perfectly. The colour-magnitude diagram of Praesepe cluster and isochrone found by the programme is shown on fig.1.

In Table 1 we give another examples of the results of programme operation. In last column of the table we point out what kind of photometry, photoelectric (pe) or photographic (pg) is used.

The inspection of Tabl.1 shows, that for numerous photometric determinations the programme can give estimates of good quality in most cases, even if we use photographic photometry without selection of members.

Fig.2 shows the opportunity of the use of small powers minimization (SPM) for best fit procedures. Here on Fig.2 is drawn the color-magnitude diagram of very young open cluster NGC1893, the photometry is taken from Hoag et al.(1961). The isochrones found by SPM-method is shown by solid line, while dashed line represents the isochrone selected by least squares method. The difference between distance moduli of that two solution is equal to about 1^m.

On fig.3 we show the distribution of clusters in the projection on the galactic plane. Here considering clusters of equal ages one can see the location of spiral arms. We have to mention, that to drawn that figure we use incomplete data for 76 clusters, that is why this picture must be taken as preliminary. On fig.3 one can see some multiple clusters such as the group consisting of clusters IC4725, Cr394 and NGC6716. Some space characteristics of that group of clusters are collected in Table 2. The diameter of that group equals 67 pc. The little scatter of ages for clusters in groups shows good quality of our ages.

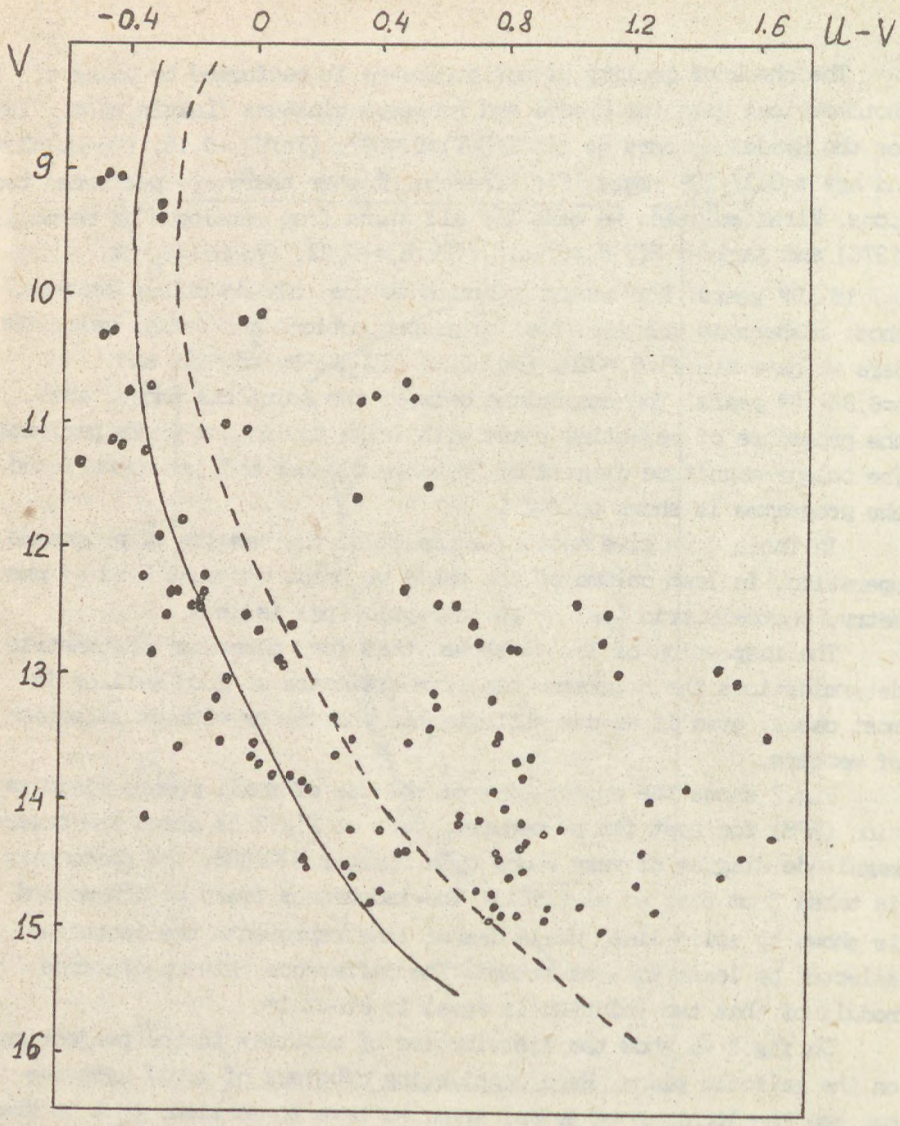

Fig.2. The isochrone fitting by small powers minimization (solid line) and least squares method (dashed line) for NGC1893.

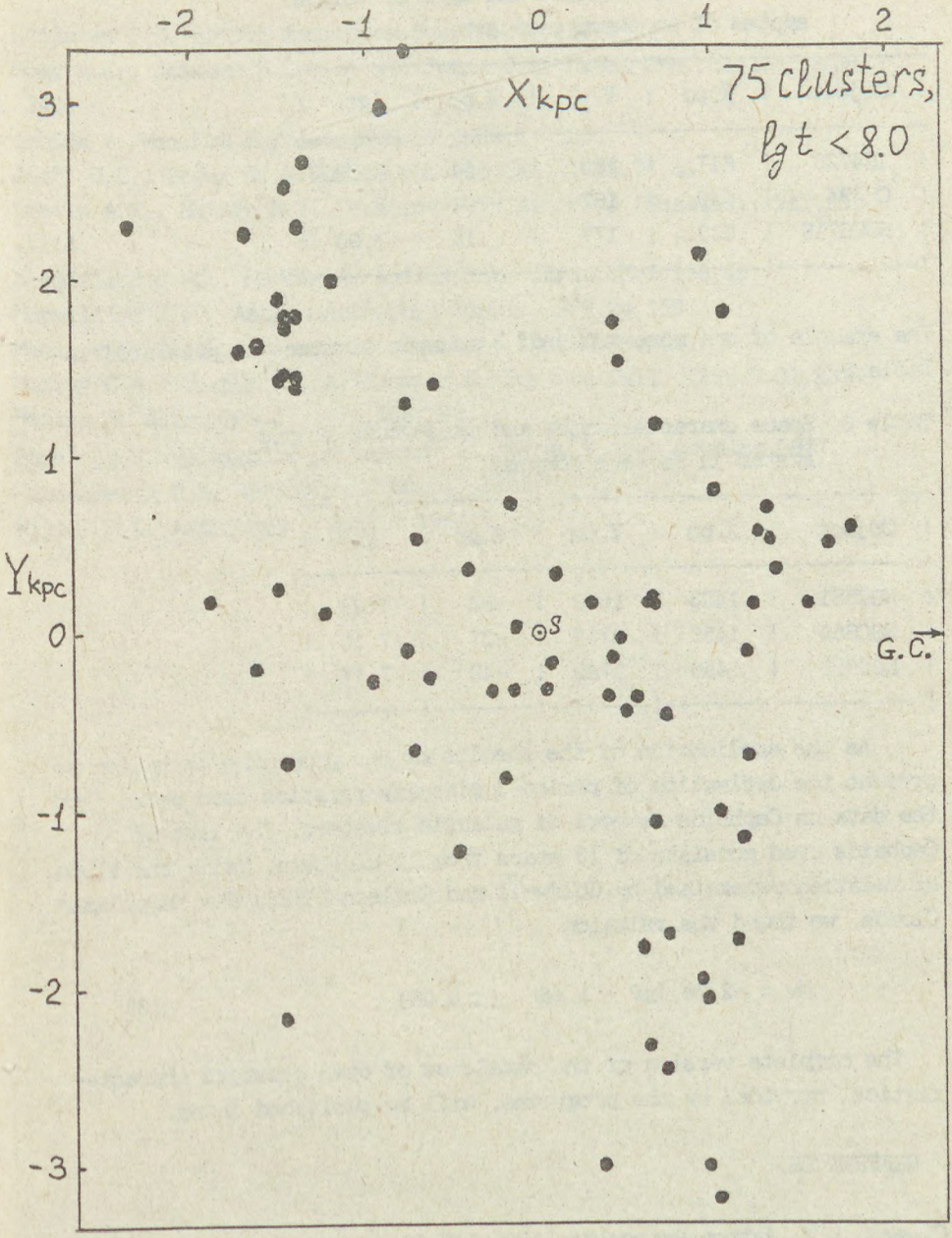

Fig.3. The distribution of young open clusters in the galactic plane. "S" denotes the position of Sun.

Table 2. Space characteristics and ages of triple system of southern clusters.

Object	X,pc	Y,pc	Z,pc	lgt
IC4725	617	153	-54	7.89
Cr394	620	167	-101	7.87
NGC6716	630	177	-115	7.90

The example of one more group of 3 younger clusters is presented in Table 3.

Table 3. Space characteristics and ages-young triple system in Perseus complex.

Object	X,pc	Y,pc	Z,pc	lgt
NGC581	1403	1803	-93	7.23
NGC654	1450	1783	-27	7.10
NGC663	1450	1740	-40	7.17

As the application of the results of our programme operation we present the derivation of period-luminosity relation zero point from the data on Cepheids-members of galactic clusters. The list of Cepheids used consists of 13 stars from 11 clusters. Using the slope of relation determined by Coldwell and Coulson (1986) for Magellanic Clouds, we found the relation

$$Mv = -2.78.\lg P - 1.46 \quad (\pm 0.06) \qquad (3)$$

The complete version of the cataloque of open clusters characteristics, provided by the programme, will be published later.

REFERENCES.

Cameron L.M. Astron.Astrophys.,1985,146,59.
Coldwell J.A.R., Coulson I.M. Mon.Not.Roy.Astron.Soc.,1986,218,223.
Eggen O.J., Sandage A.R. Astrophys.J.,1964,140,130.

Heilesen P.M. Astron.Astrophys.Suppl.,1980,39,347.
Hoag A.A., Johnson H.L., et al. Publs U.S. Naval Obs.,1961,17,part 7, 343.
Ishida K. Mon.Not.Roy.Astron.Soc.,1969,144,55.
Joshi U.C., Sagar R. J.Roy.Astron.Soc.Can.,1983,77,40
Loktin A.V., Matkin N.V., Fedorov V.V. Astron.J.(Russian),1987,64, 1114.
Mermilliod J.-C., Maeder A. Astron.Astrophys.,1986,158,45.
Mermilliod J.-C. Astron.Astrophys.Suppl.,1976,24,159.
Muminov M. Tsirk.Astron.Inst.,Tashkent,1982,N.98(445),3.
Murray C.A., Corben M., Allchorn M.R. Roy.Obs.Bull.,1965,N.91,E327.
Racine R. Astrophys.J.,1971,168,393.
Straizys V. Multicolor photometry of stars. Vilnus,Mokslas,1977.
VanderBergh D.A. Astrophys.J.Suppl.,1985,58,711.
Wildey R.L. Astrophys.J.Suppl.,1964,8,439.

METALLICITY OF OPEN STAR CLUSTERS

W. GÖTZ
Zentralinstitut für Astrophysik,
Sternwarte Sonneberg
Sonneberg, PF 55/27-28
DDR 6400

ABSTRACT. The noteworthy deviations and differences given in the individual values of the metal abundance of open clusters were studied. It could be shown that the metal abundance of open clusters, which are situated in or near the galactic plane ($|Z| \leq 0.3$ Kpc) are not only correlated with the galactocentric distance (R(GC)) but also with the galactic longitude l of the clusters. This correlation is not given in the open clusters of high $|Z|$-distances. There, the metal abundance is connected as well with the galactocentric radius (R(GC)) as with the distances of the objects from the galactic plane.

INTRODUCTION

This report will be about the metal abundance in open clusters and its correlations to the position of these objects in our Galaxy. First findings derived from data of 60 open clusters have been published in 1986.

Meanwhile values of metallicity are known of 87 clusters. Among them are those given by JANES (1979), which were obtained with different methods, and those given by CAMERON (1985), which were found by means of the ultraviolet excess of open clusters. Here, other than in my former paper, the new solar distance to the galactic centre, d = 8.5 Kpc, is taken into consideration.

MATERIAL AND METHODS

The metal abundance of an open cluster is generally given by the logarithmic ratio of Ferrum to Hydrogen relative to that of the sun,

$$(Fe/H) = \log(N_{Fe}/N_H)_{Cl} - \log (N_{Fe}/N_H)_{\odot} \qquad (1).$$

JANES, in 1979, was the first to show on the basis of 41 open clusters that there exists an abundance gradient with

"Star Clusters and Associations"
Publ. Astron. Dep. Eötvös Univ.
No.10, Budapest (1990)

the galactocentric radius, R(GC). The value of this gradient is given with

$$d(Fe/H)/d\,R(GC) = -0.05 \pm 0.01\ Kpc^{-1} \qquad (2),$$

and shows that the metal abundance in open clusters decresses with increasing distance from the galactic centre.

On the basis of 87 clusters the correlation between the metal abundance (Fe/H) and the galactocentric radii is shown in Figure 1, where clusters with distances $|Z| \geq 0.3$ Kpc from the galactic plane are marked with circles. The observations of CAMERON are marked with big dots, while the others represent metal abundances published by several other authors and are gathered in the catalogue of LYNGA. These observations are reduced to the system of CAMERON by the equation

$$(Fe/H)_{Cam} = 0.715\ (Fe/H) - 0.079 \qquad (3).$$

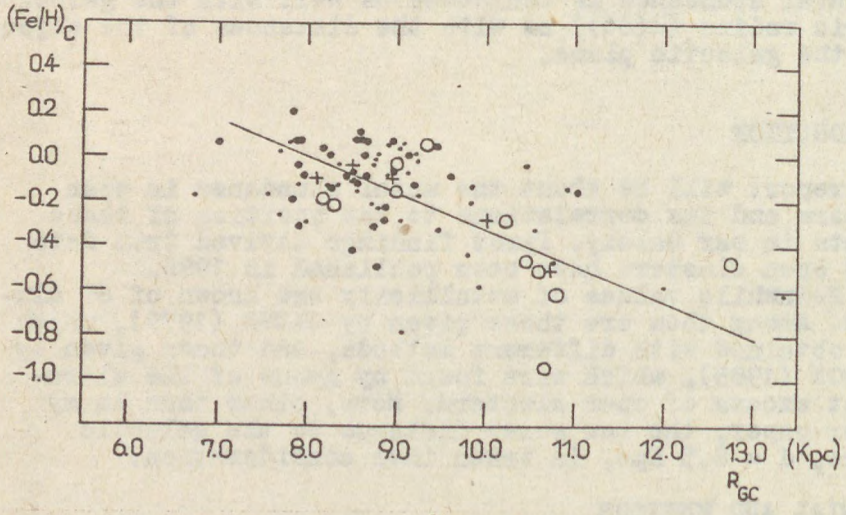

Fig. 1 The abundance gradient with the galactocentric radius

The crosses drawn in are mean values of all observations. At the solar distance the mean value of its vicinity, (Fe/H) = -0.04, is given. The straight line represents the mean correlation, which is given by

$$(Fe/H)_{R(GC)} = -0.163\ R(GC) + 1.316 \qquad (4).$$

It is worth mentioning, in this connection, that -0.163 is the mean value of the gradient d(Fe/H)/d R(GC) between R(GC) = 6.5 Kpc and R(GC) = 9.5 Kpc, which is smaller than

the mean taken over 9.5 Kpc < R(GC) < 13.5 Kpc. From equation 4 results a metal abundance of the solar vicinity of (Fe/H) = -0.07, which is a little smaller than the observed value of (Fe/H) = -0.04.

RESULTS AND DISCUSSION

From Figure 1 it can also be seen that the individual metal abundances show noteworthy deviations. This is true for the open clusters at large as well as small distances from the galactic plane.

The suspicion is obvious that there are still other parameters which influence the individual metal abundances.

In 1986 I could show that the galactocentric distance dependence of the metal abundance is still superimposed by two other correlations, which belong to the two different groups of open clusters, to those at small distances from the galactic plane ($|Z| \leq 0.3$ Kpc) and to those at larger distances ($|Z| > 0.3$ Kpc).

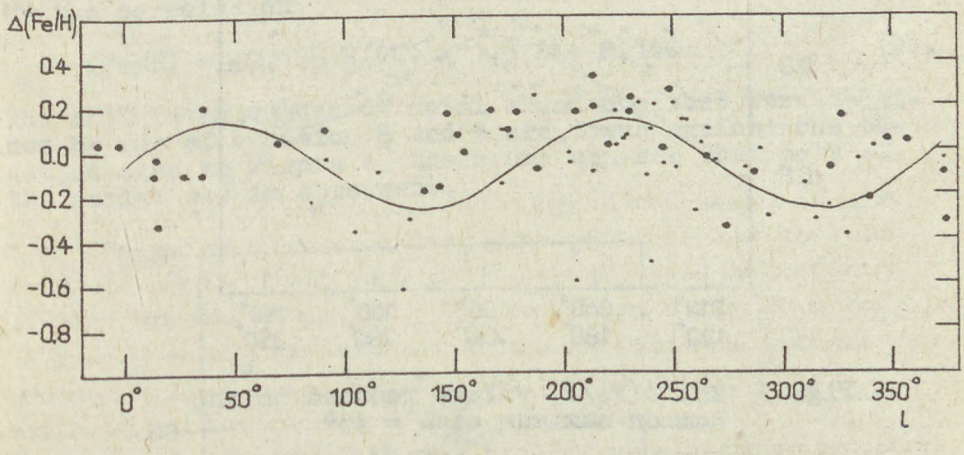

Fig. 2 Correlation between the differences Δ (Fe/H) and the galactic longitudes

From the group of lower plane distances a correlation between the metal abundance and the galactic longitude was found. In Figure 2 the differences

$$\Delta\,(Fe/H) = (Fe/H)_{obs} - (Fe/H)_{R(GC)}$$

between the observed metal abundance and those obtained by the galactocentric distance correlation corresponding to equation 4 are plotted against the galactic longitudes of the open clusters. From the diagram can be seen that the distribution of the Δ(Fe/H) - values is not homogenous,

but arranged in a double wave. Maxima of that distribution are situated at l = 45° and l = 235°, while the minima can be seen at l = 135° and l = 315°. The mean correlation drawn in Figure 2 is given by the equation

$$\Delta (Fe/H) = 0.20 \sin 2\,l - 0.07 \qquad (5).$$

The double wave distribution of the differences Δ(Fe/H) can also be seen in Figure 3, where all observations are reduced to a common maximum at l = 45°. In Figure 2 as well as in Figure 3 the differences Δ(Fe/H) derived from observations given by CAMERON are marked with big dots. Comparing this with the results obtained in 1986, we can state that the representation of the longitude correlation is better on the basis of 87 clusters.

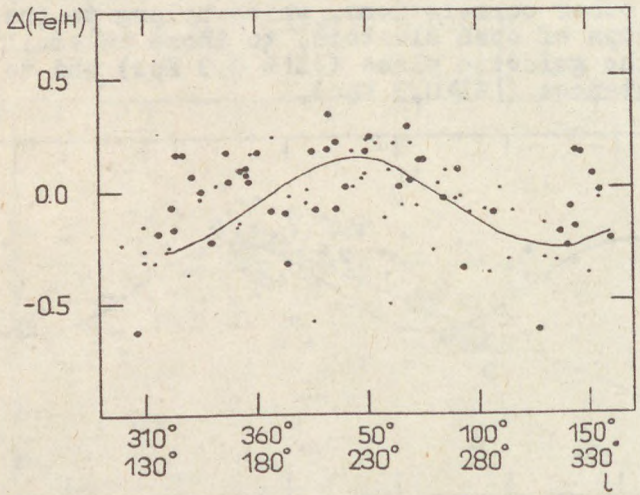

Fig. 3 The Δ(Fe/H)-values reduced to the common maximum at l = 45°

The longitude correlation of the metal abundance can be explained by the fact that the correlation with the galactocentric distances is an "orientated" parameter in the sense that it itself is a function of R(GC). The exact explanation of this statement I have given in my publication of 1986. Besides, we know similar relations from the radial velocities and the proper motions, which made it possible to explain the rotation of our Galaxy.

Another explanation of the metal abundance longitude correlation can be excluded because according to FERNIE (1968) the absorption coefficient of different regions in our Galaxy goes with a single sine function like

$$K_V = 0.90 + 0.28 \sin (l + 49°) \text{ mag Kpc}^{-1} \qquad (6).$$

As to the group of open clusters with high distances to the galactic plane, there is a correlation effective wich is different from the longitude dependence. In this group there is a correlation between the differences Δ (Fe/H) and the distances from the galactic plane, which can be characterized by

$$\Delta (Fe/H) = -1.5\ |Z| + 0.85 \qquad (7).$$

This correlation shows that the metal abundances become smaller with increasing distances from the galactic plane, thus indirectly confirming the results of STROBEL concerning the existence of two groups of open clusters.

Considering the given correlations, the metal abundance of clusters near or in the galactic plane ($|Z| \leq$ 0.3 Kpc) can be described by

$$(Fe/H) = -0.163\ R(GC) + 0.20 \sin 2\,l + 1.246 \qquad (8)$$

and that of the group with high distances ($|Z| = \geq 0.3$ Kpc) by the correlation

$$(Fe/H) = -0.163\ R(GC) - 1.5|Z| + 2.166 \qquad (9).$$

The calculated values of metal abundance that were obtained by use of equation 8 and 9 are drawn against the observed ones in Figure 4. There one can see that both of the series are in agreement.

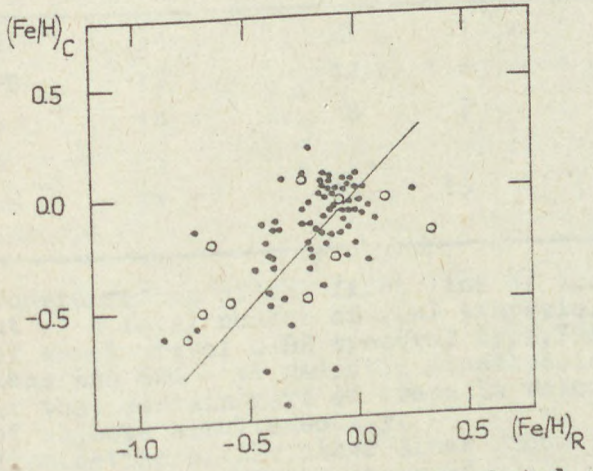

Fig. 4 Comparison of the calculated and observed metallicities

CONCLUSION

In conclusion we can stress that the remarkable deviations and differences in the individual values of metal abundance of open clusters are not only correlated with the galactocentric distance but also with the galactic longitude for the group of clusters situated near or in the galactic plane or with the distance from the galactic plane for clusters with high |Z|-distances.

REFERENCES:

CAMERON, L.M.: 1985, Astron. Astrophys. 147, 39-46,
CAMERON, L.M.: 1985, Astron. Astrophys. 147, 47-53,
FERNIE, J.D.: 1968, Astron. J. 73, 995-999,
GÖTZ, W.: 1986, Astron. Nachr. 307, 371-378,
JANES, K.A.: 1979, Astrophys. J. Suppl 39, 135-156,
LYNGA, G.: 1983, Catalogue of Open Cluster Data, Centre de Donnees Stellaires, Strasbourg,
STROBEL, A.: Metallicity of Open Star Clusters, lecture given Nov./Dec. 1987 at Babelsberg Observatory

ELECTROPHOTOMETRIC OBSERVATIONS OF TRAPEZIUM TYPE MULTIPLE STARS IN uvbyβ SYSTEM

G. N. Salukvadze, G. Sh. Dzhavakhishvili
Astrophysical Observatory,
383762 Abastumani, Georgia, USSR

Soon after the discovery of stellar association numbers of multiple stars were observed in them. Table I lists the results of a special investigation of the relation of Trapezium type multiple stars to associations and galactic clusters [1] .

TABLE I. Spectral Type Distribution of Trapezium Type Multiple Systems Entering Associations and Clusters

Spectr. class	Numb. of real trapezia	Numb. of trap. entering		Percent of trap. entering	
		assoc.	clus.	assoc.	clus.
O-B2	34	27	21	79	62
B3-B5+B	17	12	6	75	35
B8-B9	14	8	2	57	14
Unknown spectrum	99	32	10	32	10

Consideration of the first line of the Table shows that out of a total number of real trapezia, the primary stars of which are of O-B2 spectral type, 79% belong to associations and 62% - to galactic clusters. Accordingly it is clear that certain part of trapezia belong to these two types of objects simultaneously.

Examination of the other lines shows that among the trapezia with their primary stars of B3-B9 spectral class and of an unknown spectral type there is a measurable number of trapezia belonging to associations and the quantity of those ones entering the clusters decreased very much.

"Star Clusters and Associations"
Publ. Astron. Dep. Eotvos Univ.
No. 10, Budapest (1990)

Table II lists the results of the Trapezium type multiple stars search in 13 associations [2,3] .

TABLE II. Number of Trapezia Entering Selected T-Associations

Name of associations	Number of trapezia	Name of association	Number of trapezia
Ori T1	9	Tau T3	8
Ori T2	54	Tau T4	2
Ori T3	16	Aur T1	2
Ori T4	14	Cep T2	1
Tau T1	4	Oph T1	2
Tau T2	1	Sco T1	7

Though it was established long ago that Trapezium type stellar systems are the objects of great interest in our Galaxy, there exist scarce observational data on these systems from the standpoint of dynamics as well as stellar evolution. At present there are very little data on the colors and spectral classes of the trapezia stars.

Only two papers of the Mexican scientists [4,5] , who study the Trapezia purposefully deal with the results of UBVRI for stars making 68 Trapezium type systems from V.A. Ambartsumian's list [6] .

Lately X.Abt [7] , with the 2.1 m telescope of the National Observatory at Kitt Peak, performed spectral observations of 120 stars forming 31 trapezia from an unpublished list of S.Allen et al.

Paper [8] deals with the results of photoelectric measurements of the components of 20 young multiple systems. Among them there are five trapezia from Ambartsumian's Catalogue [9] .

Individual estimations of magnitudes and spectral classes of the trapezia components, mainly of the primary stars, are scattered in references and therefore it is difficult to use them. Evidently such a situation will be changed in the near future. In 1987 at Belgium Colloquium, devoted to wide double and multiple stars, E.Oblak reported on his compilation of a photometric catalogue of double and multiple systems. The catalogue will contain the results of photometric observations of 11713 stellar system components in UBV, UVBy and the Geneva photometric systems [10] .

The present work aims at reporting of the first results of photoelectric observations of the components of Trapezium type multiple systems in uvbyβ . The color indices (b-y), m_1, c_1 and β were estimated in order the spectral classes to have been established, the absolute magnitudes, effective temperatures and gravity on the stellar surface to have been estimated.

Trapezium type multiple systems were picked out of the Catalogue by Salukvadze [9] . 41 stars forming the following systems of AAO, were observed: 2, 34, 48, 51, 313, 316, 348, 356, 359, 363, 387, 396. The 125-cm automatically computer controlled mirror telescope equipped with a one-channel photometer based on photon counting with 10" and 20" diaphragms was used. The exposure time was changed depending on the stellar light with the interval of 10-80 sec. At each night we tried to perform three observational cycles. Each cycle involved an observation of the comparison star, a background near the star, all components of the system, again the background and the comparison star.

The telescope is described in the paper [11]. The light-filters used and reduction of the instrumental photometric system to a standard one is described in the paper [12].

The comparison stars are selected from the paper [13].

Altogether 425 cycles were fulfilled for 41 stars.

The observations were treated according to the program composed at the computer bureau of the observatory.

The procedure of obtaining the unwidened indices and astrophysical parameters is thoroughly described in the paper [14].

After the spectral intervals have been determined (Table III) it was found that out of 41 components of the observed trapezia, 30 ones are of "B" spectral type (O-B9 spectral classes), 8 objects - of AF spectral type (A4-GO spectral classes) and the rest - of late K-M spectral classes.

The final results of the determination of absolute magnitudes, effective temperatures, gravitational forces and Fe/H are given in Table III.

TABLE III. Results of Photometric Spectral Types Determined for the Trapezia Components, Absolute Magnitudes, Effective Temperatures and Gravitational Forces

AAO Numb.	Compo-nent	Spectrs. Interv.	M_v	log T_{eff}	log g	[Fe/H]
2	A	B	-3.92	4.49	4.37	-
	B	B	-1.17	4.30	4.12	-
	C	B	0.00	4.12	3.62	-
	D	AF	3.70	3.89	-	-
34	A	B	-4.82	4.48	-	-
	D	B	-2.08	4.37	-	-
	C	B	-2.04	4.37	-	-
48	A	B	-4.02	4.48	4.48	-
	B	B	-0.74	4.33	4.45	-
	C	B	-0.69	4.12	4.04	-
51	A	B	-2.83	4.48	4.60	-
	B	B	-4.44	4.43	3.88	-
	D	B	-0.49	4.22	3.92	-
	E	B	-0.10	4.14	3.64	-
313	AB	B	-	4.45	3.53	-
	C	B	-3.26	4.40	4.01	-
	D	B	-2.18	4.20	3.22	-
316	B	B	-1.85	4.31	3.69	-
	D	B	-4.02	4.39	3.76	-
	E	B	-1.85	4.29	3.81	-
	F	B	-6.31	4.46	3.54	-
348	A	B	-	4.43	-	-
	B	AF	-3.17	4.07	3.90	-
	C	AF	5.72	4.26	2.85	0.17
356	A	B	-	4.36	-	-
	B	AF	5.39	4.25	3.78	-0.07
	C	K-M	-	-	-	-
359	A	B	-	4.47	2.77	-
	B	AF	3.40	3.81	3.18	-
	C	K-M	-	-	-	-
363	A	B	-4.94	4.52	4.43	-
	D	B	-2.83	4.47	4.52	-
	C	B	-2.83	4.45	4.44	-
387	A	B	-3.82	4.37	3.71	-
	B	B	-1.12	4.32	4.26	-
	C	AF	-	-	3.11	-
396	A	B	-2.75	4.33	3.78	-
	B	AF	3.99	4.13	3.75	-
	C	AF	3.35	4.16	3.30	-0.03

Besides the above-mentioned trapezia the observational data were collected for 13 trapezia with their primaries of O-B2 spectral classes and the treatment is under way. The trapezia with their primary stars of M class were

observed as well. The results and discussion will be published in the nearest future.

May, 1989.

REFERENCES

1. Salukvadze G.N. Astrophysica, 15, 311, 1979.
2. Salukvadze G.N. Astrophysica, 16, 505, 1980.
3. Salukvadze G.N. Astrophysica, 16, 687, 1980.
4. Warman I. and Echevarria I. Rev.Mex.Astron.Astroph. 3, 133, 1977.
5. Echevarria I., Roth M. amd Warman I. Rev.Mex.Astron. Astroph.4, 287, 1979.
6. Ambartsumian V.A. Bull.Bjurakan Astroph.Obs. 15, 1, 1954.
7. Abt H.A. Ap.J.304, 688, 1986.
8. Burnichon M.L. and Garniez R. Astron.Astroph.Suppl. 24, 89, 1976.
9. Salukvadze G.N. Bull.Abastum.Astroph.Obs. 49, 39, 1978.
10. Oblak K. Astron.Astroph.Suppl. 34, 453, 1978.
11. Salukvadze G.N., Snezhko L.I. Bull.Abastum.Astroph.Obs. 53, 191, 1980.
12. Alania I.Ph., Abuladze O.P. Bull.Abastum.Astroph.Obs. 61, 15, 1980.
13. Hauck B. and Mermillion M. Astron.Astroph.Suppl.Ser. 40, 1, 1980.
14. Salukvadze G.N. Bull.Abastum.Astroph.Obs. No.66.

ON THE ORIGIN OF THE UV CETI TYPE STARS

L.V. Mirzoyan
Byurakan Astrophysical Observatory
Armenia
USSR

ABSTRACT. Observational data on flare stars in star clusters and associations of various ages and on UV Ceti stars of solar vicinity confirm that:

- All of them have the same physical nature and constitute one common class of objects possessing flare activity, the UV Ceti stars being very old.
- UV Ceti stars were formed in stellar systems (associations and clusters) which disintegrated long ago.
- UV Ceti stars represent a population of general galactic field.
- The total number of UV Ceti stars in the Galaxy is of the order of 2×10^{10}.

At present there is no doubt that star formation in our Galaxy is going on continuously already billions of years. The stars are formed in stellar associations (physical systems of very young stars of a new type). They are now expanding and will disintegrate in a relatively short time of the order of only 10^7 years. This new conception of stellar evolution has been developed by Ambartsumian after his discovery of stellar associations (see, for example, /1-4/).

What is the origin of the UV Ceti type stars in frames of this conception?

The problem is whether the system (systems) where the UV Ceti stars were formed still exists or not. There are two points of view on this problem.

According to the first point of view suggested by Ambartsumian /5/ the UV Ceti stars constitute a physical system around the sun. It means that all UV Ceti stars are members of the existing stellar system (clus-

"Star Clusters and Associations"
Publ. Astron. Dep. Eotvos Univ.
No.10, Budapest (1990)

ter) in the solar vicinity. This point of view was developed further by Oskanian /6/, Haro and Chavira /7/, Arakelian /8/ and Garibjanian /9/ who have brought some evidences supporting it.

The opposite point of view on this problem has been expressed by Herbig /10/ who considered that the UV Ceti stars of the solar vicinity were formed in systems which were already disintegrated. Herbig's explanation allowed to assume that the UV Ceti stars belonged to the population of general galactic field.

The statistical study of flare stars /11-13/ carried out at Byurakan has shown that present observational data on the flare stars in star clusters and associations and in the solar vicinity are in better agreement with Herbig's point of view.

Really, the existing data show that flare stars in star clusters and associations of various ages and UV Ceti stars in the solar vicinity are of the same physical nature and constitute one common class of objects showing flare activity. All differences observed between them can be explained by differences in their ages, the UV Ceti stars being very old /11/.

The UV Ceti stars of the solar vicinity have very low luminosities. Owing to low luminosities these flare stars kept the flare activity.

This important observational fact has its natural interpretation. In spite of the general idea that the evolutionary stage of flare activity is one of the early stages in the evolution of red dwarf stars (see, for example, /14/) stars of low enough luminosities can stay in this stage hundreds of millions and more years (see, for example /15/). This is a consequence of the well-known relation between stellar mass (or indirectly luminosity) and evolutionary rate.

At last, the observational data on UV Ceti stars are in agreement with the assumption that their space distribution is practically uniform in the solar vicinity /12/. It is likely that the distribution is uniform in the whole Galaxy as well. This can be understood assuming that the UV Ceti stars were formed in stellar systems (associations and clusters) which disintegrated long ago. The UV Ceti stars survived their parent systems due to very low luminosities.

Thus, there are enough grounds to assume that the UV Ceti type flare stars represent a population of general galactic field and that their space distribution in the Galaxy is approximately uniform. In this case the estimated total number of UV Ceti stars in the Galaxy is about 2×10^{10} /13/.

The detailed consideration of the above-mentioned problem was given in papers /11-13/.

REFERENCES

1. V.A. Ambartsumian: Stellar Evolution and Astrophysics, Ac. Sci. Armenian SSR, Yerevan, 1947.
2. V.A. Ambartsumian: Scientific Works, vol.1-3, Ac. Sci. Armenian SSR, Yerevan, 1960, 1988.
3. V.A. Ambartsumian, L.V. Mirzoyan: Probleme der Modernen Kosmogonie, Bd.1 und 2, Birkhäuser Verlag, Basel - Stuttgart, 1976.
4. L.V. Mirzoyan: Stellar Instability and Evolution, Ac. Sci. Armenian SSR, Yerevan, 1981.
5. V.A. Ambartsumian: Non-Stable Stars, ed. by M.A. Arakelian, Ac. Sci. Armenian SSR, Yerevan, 1957, p.9.
6. V.S. Oskanian: Publ. Astron. Obs. Beograd, No. 10, 1964.
7. G. Haro, E. Chavira: Vistas in Astronomy, 8, 89, 1966.
8. M.A. Arakelian: Non-Periodic Phenomena in Variable Stars, IAU Coll. No. 4, ed. by L. Detre, Academic Press, Budapest, 1969, p.161.
9. A.T. Garibjanian: Comm. Byurakan Obs. 49, 63, 1976.
10. G.H. Herbig: Symposium on Stellar Evolution, ed. by J. Sahade, La Plata, 1962, p. 45.
11. L.V. Mirzoyan, V.V. Hambarian: Astrofizika, 28, 375, 1988.
12. L.V. Mirzoyan, V.V. Hambarian, A.T. Garibjanian, A.L. Mirzoyan: Astrofizika, 29, 44, 1988.
13. _____: Astrofizika, 29, 531, 1988.
14. V.A. Ambartsumian, L.V. Mirzoyan: New Directions and New Frontiers in Variable Star Research, IAU Coll. No. 15, Veröff. Bamberg, 9, Nr. 100, 98, 1971.
15. W. Kunkel: Variable Stars and Stellar Evolution, IAU Symp. No. 67, eds. W. Sherwood, L. Plaut, Reidel, Dordrecht, 1975, p. 15.

THE USE OF CCD DETECTORS IN H-ALPHA EMISSION STUDIES OF FLARE STARS

Gábor Szécsényi-Nagy
Roland Eötvös University, Department of Astronomy
Budapest, Kun Béla tér 2.
H-1083
Hungary

ABSTRACT. Photoelectric and photographic UBV photometry of solar neighbourhood and cluster member flare stars yielded a large amount of data about the apparent brightness and colour of these objects. In many cases it was possible to determine the absolute brightness as well and the position of the star on the HRD could be marked. It was found that points representing late type flare stars are not arranged along the main sequence but preferably scatter in a wide brightness range when they are plotted against their (B-V) colour index or their spectral type if the latter is available. This large scatter can not be caused by classification or measuring errors. It just reflects true brightness differences of dwarf stars of the same spectral subclasses. In order to have a better knowledge of these objects and that phenomenon a new physical parameter should be introduced into the method of classification.

As the majority - if not all - of the late type (dM) flare stars are emission-line (dMe) objects, hydrogen Balmer emission seems to be suitable to characterize these stars. The red H-alpha line is the most prominent of the Balmer series but photographic methods are not sensitive enough at its wavelength-range to record the necessary number of photons of these intrinsically faint and mostly distant sources. Up-to-date solid state photon detectors are much more sensitive in the 600-700 nm band and can offer ideal solution to this problem. The use of charge coupled devices (CCDs) is suggested.

The method described in the paper is based on CCD-photometry of the flare stars through two different colour filters. One of these is a narrow-band (practically monochromatic) filter transparent only in the H-alpha line while the other has a considerably wider passband. Brightness measurements of the program stars are done through both of the filters and the results are compared. The parameter defined as the ratio of the two intensity measurements seems to be useful when the studies are aimed at discriminating between flare stars of the same colour but of different intrinsic brightness.

The method was successfully tested by observing flare stars of some subfields of the Pleiades region with a Photometrics CCD camera mounted on the 40 inch reflector of the Stockholm Observatory erected at Saltsjöbaden.

"Star Clusters and Associations"
Publ. Astron. Dep. Eötvös Univ.
No.10, Budapest (1990)

1. INTRODUCTION

During the fourth 'Star Clusters and Associations' symposium two papers were read which gave at least an impression of the position of flare-active red dwarf stars in the HRD. Figure 1. of Parsamian's contribution (Parsamian 1986) clearly demonstrates that flare stars discovered in the Eta Tauri fields and especially those which belong to the nearby Pleiades cluster are not restricted to a narrow band of the m_V - spectral type diagram of these objects. Hottest members of this group can be found in the K2-K6 spectral range where the band is about 1-1.5 mag. wide. But the majority of the flare stars discovered in the M45 region have lower surface temperatures and later - mainly M - spectral types. In this range of the diagram dots representing active red dwarf stars are spread over a much broader area. Faintest and brightest members of the same spectral subclasses may differ 3.5-4.5 mag. in their visual brightness. In magnitudes the patch occupied by flare stars is the most extended from M0 to M3 but later decimal classes are probably underrepresented because their absolute weakness.

These results agree perfectly with the fact found decades earlier by Ahmed et al. (1965) and by Chavushian and Gharibjanian (1975) that flare stars of the Pleiades can be found both above and below the MS.

The other HRD of that volume (Figure 2. of Szécsényi-Nagy 1986a) shows an absolute visual magnitude - spectral type plot of stars of the solar neighbourhood. It contains the reddest objects from M0 to M6.5 and both flare-active and quiet stars are represented in the diagram.

Although this plot is not limited to flare stars the main sequence defined by red dwarfs of the solar vicinity (which have more precise distance data than those of M45) is broadened too. In this case magnitude differences of stars of the same spectral subclasses range from 1.5 to 2.5 mag. without any explicit dependence upon spectral type. Unfortunately the M5-M6.5 range is so much underpopulated that no definitive conclusion can be drawn from that part of the graph.

In the same paper the author tried to define the lower main sequence of stars in the K0-M6.5 spectral range. This job had been done more or less successfully but at the cost of compromise only. The

adopted mean absolute visual magnitudes of dM0-dM6.5 stars differ 0.1-0.4 mag. from values given by others in both directions (Szécsényi-Nagy 1986a and references cited therein). This also indicates that the scatter of absolute brightness values of red dwarfs is a physical phenomenon and can not be explained as the consequence of inaccuracies of photometric measurements. Therefore it is a justified claim to search for a new physical parameter which could contribute to the termination of this degeneracy.

2. H-ALPHA EMISSION IN SPECTRA OF FLARE STARS

2.1. H-alpha Emission in Minimum Light

H-alpha emission is a common feature of late type dwarf stars (Joy and Abt 1974). Amongst solar neighbourhood dM stars at least 60% and very likely 80% are dMe objects (Szécsényi-Nagy 1990a). It is practically impossible to determine whether any of these objects are stable or all of them are active since defined limits of variability always rely on the available measuring techniques. For the moment it seems highly probable that each dMe star is able to produce more or less powerful outbursts. Of course to discover these phenomena and identify their sources as flare stars the amount of observing time allocated to flare patrol programs should be multiplied which is hardly to be expected.

For these reasons it is useless to divide these objects artificially and study them as members of independent subclasses. To start with consider all the dM stars of the solar vicinity which were marked in the above-mentioned Figure 2. By good fortune normal (absorption) and hydrogen Balmer-emission dwarfs were plotted by different symbols and can easily be discerned. This distribution chart suggests that irrespective of their possible flares the absolute majority of stars later than M2 and very likely all of those later than M4.5-M5 are hydrogen emission line stars. This means that they also emit H-alpha photons continuously. The absolute visual brightnesses of these stars may differ too raising the question of the possible existence of a luminosity - H-alpha-emissivity relation.

2.2. Intensity Variations of the H-alpha Line in Spectra of Flare Stars

It is well known from spectral investigation of solar vicinity flare stars that emission Balmer-lines (which are probably the most sensitive flare indicators) are often enhanced over their quiescent values already at the onset of a flare. This usually happens before the flare continuum begins to rise in the outburst. Then the continuum flux will be dominating the spectrum and the emission lines will become practically unobservable for minutes or more. With the fading of the continuum line emission goes from strength to strength and reaches its maximum flux definitely after the peak of the continuous radiation. Some other important emission lines like those of CaII, MgII and HeI show similar behaviour but are delayed compared to the Balmer-lines (Pettersen 1989).

Evidently the dM stars show the most dramatic line-intensity changes as their normal absorption features have to turn into emission. Regrettably enough only the short term variations of spectral characteristics of flare stars have been extensively investigated up to now although significant long term (or solar-like) activity changes were reported on one Hyades and more Pleiades member stars too (Szécsényi-Nagy 1986b and 1989).

On the basis of all these a much more detailed analysis of the time-dependence of H-alpha emissivity of these objects seems to be a program of great promise. Unfortunately the methods used to collect the necessary spectral information are not able to provide meticulously comparable data because the most preferred photographic spectroscopy can be standardized to a cetrain extent only. This immediately brings up the imperative need for a more strictly defined and hopefully more sensitive spectrophotometric technique which - I think - has to be based on solid-state light detectors.

3. A COMPARISON BETWEEN PHOTOGRAPHIC AND CCD-PHOTOMETRY

3.1. Fundamentals

Photometric and spectroscopic observations have necessarily been based

on photographic techniques for decades. As these chemical processes offered the very first opportunity to objectively record astronomical events in the last century they have been extensively used in optical observatories since then. Consequently all astronomers are supposed to be more or less familiar with astrophotography and it is not needed here to give a detailed description of its methods.

Quite the contrary the use of solid-state devices in astrophysical research is a real novelty in COMECON countries. For that reason a genuine comparison of these two techniques requires the brief presentation of the latter.

Solid-state photon detectors are usually fabricated of semiconductor materials. From an astronomer's point of view we can classify these devices into two groups. Some of them are only able to detect the collective effect of the photons reaching the sensitive area of the device and give an integrated signal which is proportional to the apparent brightness of a cosmic object (a star, a galaxy or a planet) e.g. These devices can not be used for imaging purposes because they have exactly one light-sensor which defines one picture element (pixel) only. In order to receive one- or two-dimensional 'images' of any light source an arrangement of the formers is the most suitable. For spectroscopic studies e.g. linear arrays of tiny light detectors (photodiodes) are used and spectra of cosmic sources are projected in a way that photons of neighbouring sections of the spectra fall on adjacent pixels. In order to simultaneously record the spectrum of the night sky too the receiver can be built out of two identical arrays or a twin array which is also offered by manufacturers of photoelectric detectors. The most 'flexible' of these solid-state devices are able to collect and deliver spatial information too and can directly be compared with photographic materials. Of these two-dimensional semiconductor light detectors astronomers have a preference for Charge Coupled Devices (CCDs) - tiny silicon chips containing 10^4-10^6 independent pixels arranged in a matrix. CCDs and photographic plates are in many respect very like and it is straightforward to compare their most characteristic features.

3.2. Spectral Sensitivity and Quantum Efficiency

3.2.1. Spectral Sensitivities of Photographic Emulsions

The photographic sensitivity of any emulsion is defined as the reciprocal of the exposure required to produce a fixed response. It shows a definite dependence on the wavelength of illuminating radiation (Fig.1.) The natural sensitivity of the photographic emulsion is to blue and ultraviolet light (curve A) but it can be extended towards the red by the addition of dye sensitizers (B and C) as Mees suggested in 1912 (Miller 1987).

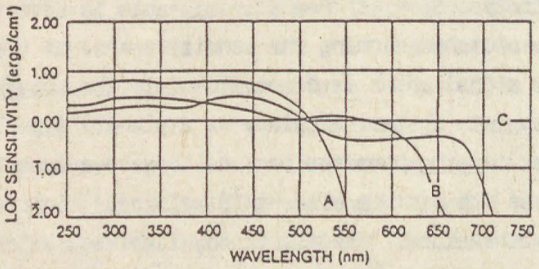

Figure 1. Typical spectral sensitivity curves of three different photographic emulsions. Curve A demonstrates the ultraviolet-blue sensitivity of unsensitized emulsions. The spectral sensitivity of a panchromatic material is given by curve B and that of a specially extended red-sensitive emulsion by C.

These curves illustrate clearly that the color-sensitizing dyes necessarily reduce sensitivity to photons of the shorter wavelength ranges while extend the sensitivity of the emulsion to longer wavelengths.

Nevertheless there are some astronomical emulsions which have maximum sensitivity to yellow, orange or red lights. Eastman Kodak Co. e.g. has developed a wide variety of photographic materials for specialized applications and recommends the use of E, F and TP 2145 emulsions in recording H-alpha light. These plates and films have extended-red sensitivity and have been successfully used in survey programs as well as in more detailed studies concentrated upon individual H-alpha emission objects.

3.2.2. Spectral Sensitivities of CCDs

The spectral response of semiconductor devices made of silicon is just the opposite. These detectors are absolutely unsensitive to ultraviolet photons and have very low sensitivity to photons of the violet and blue spectral ranges (Fig.2.). However in return for that they are extremely sensitive to orange and red lights and are able to detect infrared photons too. The three panels of Fig.2. show detailed spectral sensitivity curves of different CCDs offered by various manufacturers (Thomson CSF, Eastman Kodak and Photometrics Ltd. respectively). These graphs clearly demonstrate that CCDs of all makes have their peak sensitivity somewhere in the 600÷700 nm range thus offering an almost perfect solution to our problem of measuring the H-alpha emissivity of red dwarfs near to the 656.28 nm laboratory wavelength of this Balmer-line.

Likewise the spectral sensitivity of photographic emulsions that of silicon photodetectors can be extended too. But in this case the extension must be connected to the violet wing of the sensitivity range in order to make these devices usable in the astrophysically very interesting ultraviolet band as well. Curve C of Fig.2. demonstrates the effect of a special sensitizing layer patented under the name METACHROME II by Photometrics Ltd. (compare the two branches - 'coated' and 'uncoated' - of the curve between 250 nm and 450 nm).

3.2.3. Comparison of the Quantum Efficiencies

The quantum efficiency (QE) of photoelectric or photoelectronic detectors is usually defined as the ratio of the number of electrons produced by photoelectric processes to the number of photons absorbed by the detector during the measurement. It is customarily to express the QE as a percentage. Sometimes it is called absolute quantum efficiency (AQE) in order to be distinguishable from an other important quantity, the detective quantum efficiency which is often used too in characterizing the efficiency of a device in detecting photons.

The detective quantum efficiency (DQE) is most generally used to

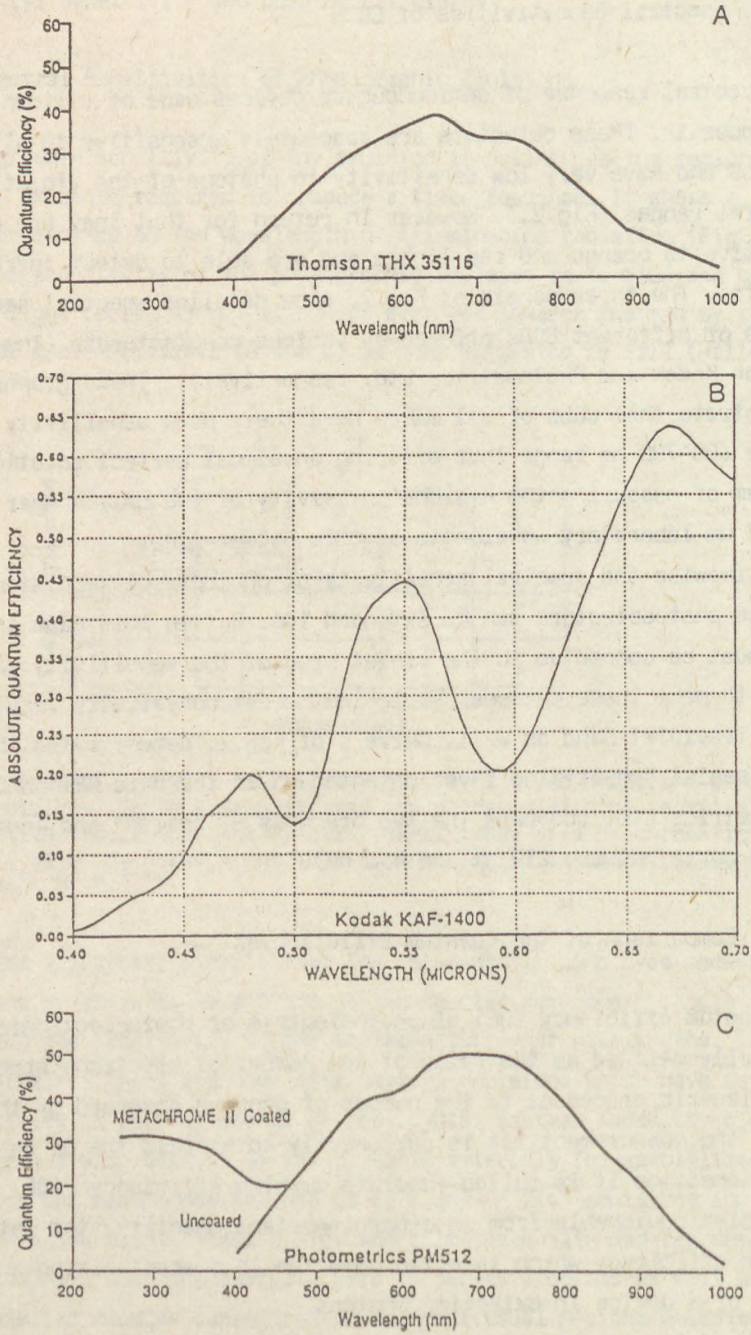

Figure 2. Typical CCD quantum efficiency versus wavelength curves

give information about a complete measuring system (e.g. the detector, the amplifier and the counter etc.) because it takes into account any loss of detected photons and the quantum efficiency of each component of the complex device. Consequently the DQE of a single stage loss-free system is the same as its QE. The DQE of a detector can also be expressed in terms of the signal-to-noise (S/N) characteristics of the output signals and that of the input ones as the ratio:

$$DQE = (S/N)^2_{out} / (S/N)^2_{in}$$

Most often it is expressed as a percentage too and will never exceed 100%. Because of this flexible definition DQE is very useful in comparing different types of light-detectors.

But let us compare first the QE of photographic emulsions and that of CCDs. This comparison is to inform us about the relative 'speed' of the twoo detectors. To determine the QE of some typical CCDs it is enough to have a look at the plots of Fig.2. Although it is well known that QE varies from CCD to CCD - sometimes from pixel to pixel too - and from lot to lot these curves published by manufacturers may convince us of the reasonably high (25-50 %) QE of these devices in the yellow-infrared spectral range. (In this respect Kodak's full-frame imager with its 60% AQE at the wavelength of H-alpha /curve B/ is the most promising.)

It is much more difficult to determine the QE of photographic emulsions since the number of detected photons (or that of the liberated electrons) can not be measured. There are some indirect methods to calculate the probable number of photons having caused the birth of developable silver grains and they suggest a QE inferior to 1% (Weigert and Zimmermann 1977). This peak efficiency is reached by the most sensitive emulsions and in the ultraviolet-blue range only. At the wavelength of the H-alpha line the QE of photographic materials is more than two orders of magnitude lower than that of CCDs. This can be demonstrated more spectacularly by comparing photographs of H-alpha clouds taken by telescopes with an exposure of an hour and CCD frames taken by the same telescopes and with an exposure of a minute or less. (It is a pity that this volume

of papers is not provided with an appendix of plates). The detecting speed of the best charge coupled devices incredibly surpasses the photographic speed of the most sensitive astronomical emulsions.

Finally let us compare the detective quantum efficiencies of these two kinds of light-detectors. According to Eccles et al. (1983) even the best emulsions have a peak DQE of only 4%. This value represents the awful degradation of the signal during the process of photographic detection (c.f. the formula on the previous page). Furthermore emulsions having peak DQE of this order are considerably less sensitive and slower than those cited by Weigert and Zimmermann (ibid). But even this overestimated 4% shrinks into insignificance beside the typical DQE of CCDs which ranges between 40% and 60%.

Consequently both their high QE and definitely superior DQE argue in favour of using silicon-based charge coupled devices especially for the photometric study of faint H-alpha sources.

3.3. Linearity and Uniformity

The photographic response of any emulsion is best characterized by the well known H&D (Hurter and Driffield or 'characteristic') curve of the material which is not at all a straight line. Although it may have a linear section in most cases (especially when the program stars are red dwarfs) the exposure level does not reach that portion. The non-linearity of the curve in this region gives rise to persistent problems in the photometric calibration of astronomical plates and often prevents us from collecting the necessary data of acceptable quality. In order to present a basis for comparison the largeness of exposure corresponding to the linear section of H&D curves of astronomical emulsions is always inferior to 100 and rarely exceeds even 20.

Quite the contrary charge coupled devices like many other kinds of photoelectric detectors have a very extended linear response which starts immediately at the noise level. This surprisingly wide range of linearity is usually called dynamic range and is defined as the ratio of full well capacity of the individual pixels to the RMS readout noise.

The full well capacity of a picture element mainly depends on the effective volume of the pixel and is proportional to its surface. It is given as the maximum number of electric charges that may be collected in a picture element. The CCD Selection Chart shown as Table 1. which informs us of the most important characteristics of some widely used charge coupled devices demonstrates that typical full well capacity of these detectors' pixels ranges from 45000 to 700000 electrons. Other manufacturers who integrate the most sophisticated CCDs into their cameras report even higher saturation levels reaching 1000000 charges per image cell.

From these values and the typical RMS readout noise which is - depending on the scanning frequency - between 7 and 25 charges per readout the dynamic range of the devices can be calculated. While the dynamic range of CCDs is always superior to 10^3 and most typically equals 10^4 in some special cases it can reach 10^5 (e.g. the Astromed CCD 2200, Astromed Limited, 1989) over which the device is perfectly linear. And what is more this dynamic range is offered in a single exposure. Using different exposure times from milliseconds to many hours this range can be extended to 10^{11} - 10^{12} which corresponds to the absolute illuminance range from 10^{-11} lux to 10 lux.

The effective detection of ultra low light level images is made possible by the use of high performance thermo-electric or Liquid Nitrogen coolers giving CCD operating temperatures of 190K and 105K. The thermal dark current has been measured at about 0.01 events per second per pixel at the higher temperature and was undetectable at the lower one. This practically means that using the LN cooler there is no upper limit to exposure time set by the dark current of the device.

Our last point is a brief comparison of the uniformity of photographic emulsions and CCDs. Although the uniformity of spectral and overall sensitivity of astronomical emulsions over the wide area of a photographic plate is often criticised the fact that repeated use of these detectors is absolutely impossible makes the settlement of the disputed question difficult. Photographic tests made in specially equipped laboratories demonstrated that the sensitivity of good emulsions only seldom differs more than 1-2 per cent from the average on

TABLE 1. The most important characteristics of six charge coupled devices offered by Photometrics Ltd. for integration into very low light level astronomical cameras

CCD SELECTION CHART

		Thomson CSF 7882	Photometrics PM 512	Texas Instruments TC 215	Kodak Megapixel	Tektronix TK512M-011	Tektronix TK512M-012
Format		384 x 576	512 x 512	1024x1024	1320 x 1035	512 x 512	512 x 512
Pixel Size (μ)		23 x 23	20 x 20	12 x 12	6.8 x 6.8	27 x 27	27 x 27
Full Well (e-)		500 K	250 K	60 K	45 K	700 K	700 K
Typical Read Noise (e-) at ( ) kHz		10 (50)	10 (50)	12 (200)	15 (200)	12 (50)	12 (50)
% QE at -40°C	300 nm	less than 1*	less than 1*	37	less than 1*	less than 1*	less than 5*
	500 nm	25	27	32	21	(TBD)	(TBD)
	700 nm	40	50	47	33	(TBD)	(TBD)
	900 nm	13	30	20	9	(TBD)	(TBD)

* Device may be coated with MetaChrome-2 for ultraviolet-response enhancement

scales of 10 cm but these are not the same plates which we intend to use to record the light of cosmic objects of course. Unfortunately there is no way to correct our astronomical images for photographic non-uniformity simply because of the uniqueness of the whole photographic procedure.

On the other hand pixel to pixel sensitivity variations (see 3.2.3) of CCDs are common and in some cases reach incredibly high values. The most widely known examples are offered by the so called dead pixels and hot spots. The dead pixels have very low QE and reduced transfer efficiency too while hot spots are completely saturated pixels filled by thermally generated electrons even in effectively cooled devices. But these discrete pixel defects can be mapped and following well elaborated procedures their disturbing effects can be minimized or eliminated. These defects usually originate from manufacturing processes and most of the imperfect chips can be rejected during preselection of the detectors. In fact the most sophisticated CCD cameras practically never contain defected chips and their minor sensitivity variations are always correctable.

The dimensional stability and rigidity of solid-state devices is practically the same as that of astronomical plates and of course is much better than that of photographic films. To summarize the most important results of our comparison are the following: CCDs are definitely more sensitive to H-alpha light than photographic emulsions, their DQE is at least 10 times and their QE is at least 100 times higher. CCDs have much larger dynamic range and have absolutely linear response over it. Although sometimes their uniformity is inferior to that of astronomical plates proper computational methods and reference frames taken after or before the detection of program objects make the necessary corrections always possible.

3.4. Imaging Area and Resolution

The light sensitive area of a typical astronomical plate is in the 10^3 mm^2 - 10^5 mm^2 range and the largest ones (used at Las Campanas Observatory) are 500 mm by 500 mm squares. In comparison the area of solid-

state photon detectors only seldom exceeds 10^2 mm^2 (Table 1.) The largest astronomical CCD is a 2048 by 2048 pixel chip made by Tektronix while those in regular use at the best equipped observatories measure 1024 by 1024 pixel. The record holder however is the 4096 by 4096 pixel device which has an imaging area somewhat greater than 10^3 mm^2. This giant CCD developed by Ford Aerospace Corp. is currently the highest-resolution electronic imager made which needs about 700 seconds to be read out completely and produces nearly 32 megabytes of data per frame. Actually these huge images are too big to be displayed as even the greatest CRT screens are unable to show larger area than the quarter of the new Ford Aerospace chip.

As a consequence of the significant differences between the dimensions of photographic plates and CCDs the formers are more suitable for photometric or spectroscopic studies of objects of larger fields while the use of the latters is more advantageous when the cosmic sources to be investigated are densely condensed into compact clusters or limited sky fields.

The resolutions offered by these two kinds of detectors do not differ significantly. Of course first CCDs gave more rugged images than the best astronomical emulsions which are able to reach a resolution of 200 line-pairs per mm. But the resolution of recently released CCDs is comparable to that of the most sensitive astro-plates (about 75 line-pairs per mm).

Consequently it is obvious that the use of CCDs in detecting the orange/red radiation of faint cosmic sources especially of those which are condensed into compact groupings is preferable to the use of photographic materials.

4. THE METHOD

Let us summarize now the most important points of the new photometric method. It was introduced to help the detailed photometric classification of (more or less flare active) red dwarf stars. The goal of the

study is to characterize the H-alpha emissivity of these objects relative to their continuous light emission. In order to establish a really effective procedure only two new photometric passbands were defined. One of them (the narrower) was set to involve as many H-alpha photons as possible while rejecting the majority of photons arriving in the neighbouring spectral regions. The other one was intended to check the mean level of the object's continuous radiation in the red region of the spectrum. The idea of the measurements is to collect enough photons to reach a preselected S/N value and then determine the apparent intensity of the star's light in both spectral bands. Having received the intensity values they are to be compared and their ratio is to characterize the H-alpha emissivity of the object.

4.1. Definition of the Photometric Bands

The shapes of the photometric response curves of the system are defined by the spectral sensitivity curve of the detector (since the same device detects the photons in both spectral bands) and the spectral transmission characteristics of the filters. As far as the chip is concerned there was no problem of choice at all since the LN cooled Photometrics CCD camera used for the preliminary test measurements incorporates a scientific grade Tektronix device absolutely free from defects. This sort of chip has a considerably smooth spectral response (see Fig. 3.) which eliminates any difficulties related to the fitting of narrow- and medium-band color filters.

The selection of the two passband filters is somewhat more complicated. The narrower filter is intended to transmit all H-alpha photons arriving in a practically symmetric spectral window. According to flare models of Cram and Mullan (1979) an H-alpha profile typical of a dMe star can exceed a spectral width of 0.6 nm. Assuming a reasonable relative velocity limit of $\pm$ 100 kms^{-1} the width of the spectral window defined by the narrower H-alpha filter must be increased to about 1.04 nm and taking into account the thermal sensitivity of interference filters it seems wise to choose a spectral window of 1.3 nm centered on the 656.3 nm H-alpha line. The next step is to find a filter which is satisfactory to

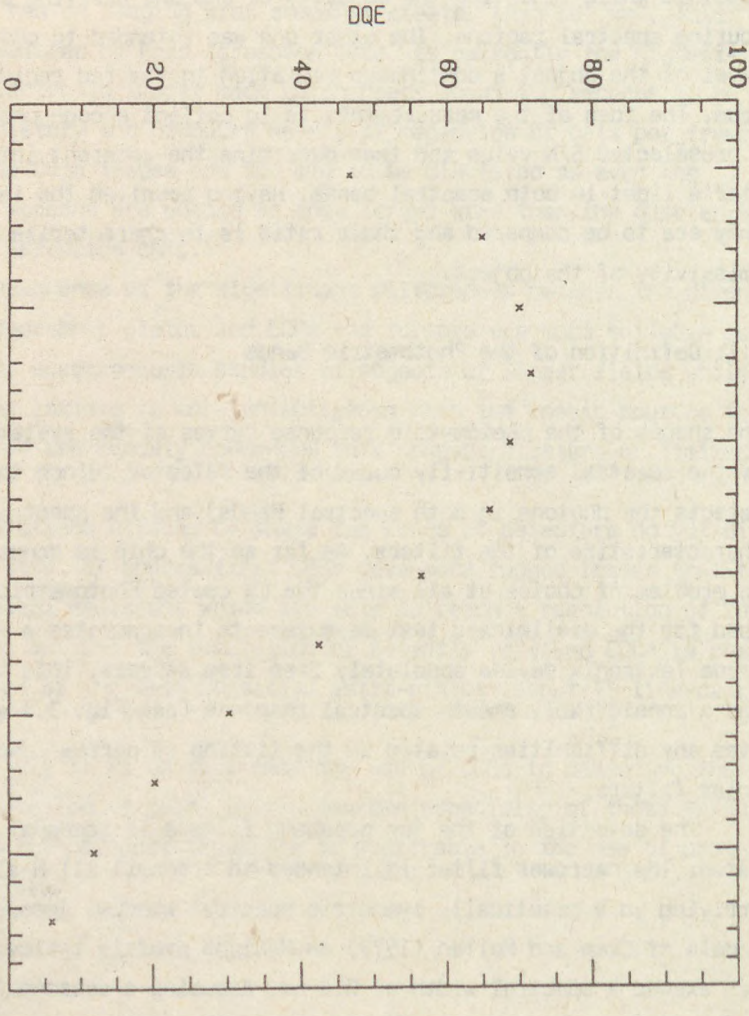

Figure 3. The spectral response of the CCD chip used to test the method

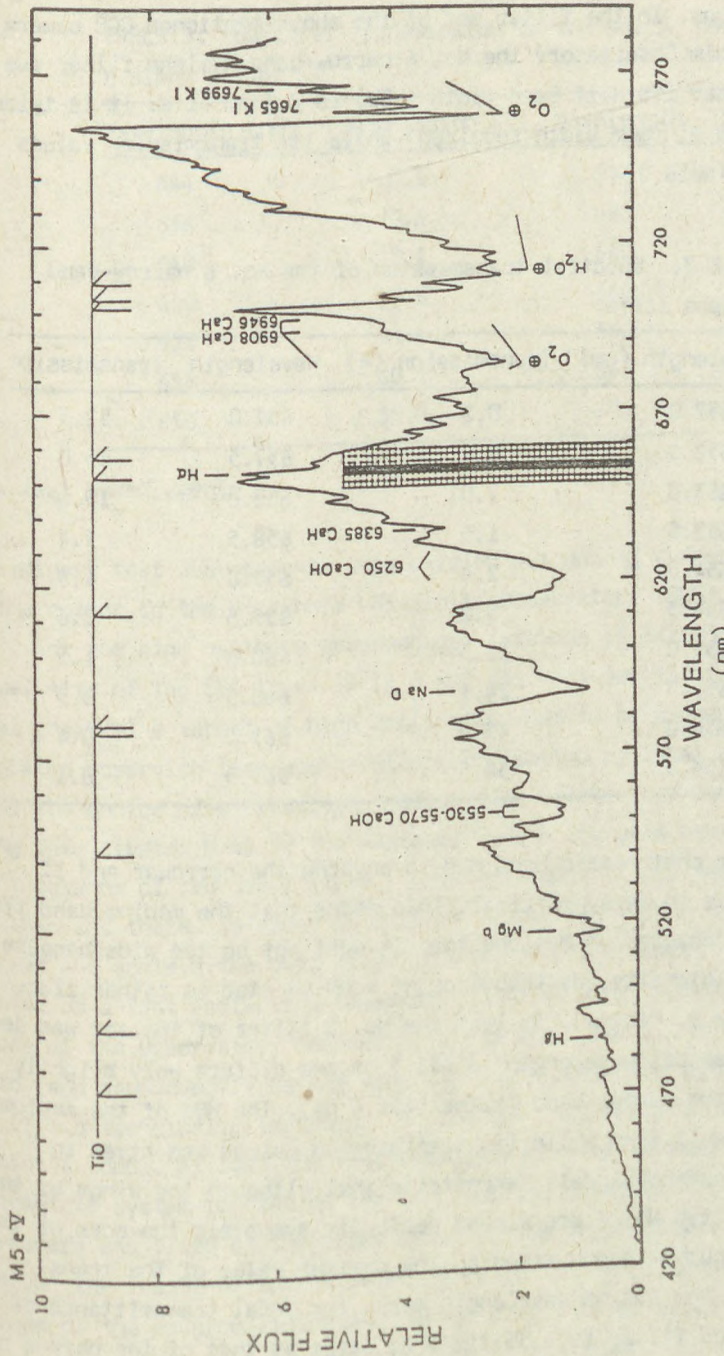

Figure 4. Schematic optical spectrum of the dwarf red variable IX Ari with the passbands of the two filters proposed to characterize the H-alpha emissivity of flare stars (after Turnshek et al. 1985)

these conditions. In the filter set of the above-mentioned CCD camera of the Stockholm Observatory the No. 6 narrow-band H-alpha filter was the best choice. Its Half Band Width (HBW) is 2.6 nm (i.e. it is twice as wide as the minimum width required) while its transmission values are given in Table 2.

TABLE 2. Spectral transmission of the No. 6 narrow-band H-alpha filter

Wavelength (nm)	Transmission (%)	Wavelength	Transmission
652.0	0.2	657.0	52.3
652.5	0.5	657.5	45.0
653.0	1.0	658.0	19.6
653.5	1.5	658.5	9.4
654.0	2.6	659.0	4.9
654.5	5.2	659.5	2.6
655.0	11.5	660.0	1.5
655.5	24.1	660.5	0.9
656.0	42.0	661.0	0.4
656.5	50.5	661.5	0.1

The other photometric band has to environ the narrower and if possible it has to be symmetrical. This means that the medium band filter is to be centered on H-alpha too. It must not be too wide because the spectral intensity distribution of a dM(e) star is rather fluctuating (see e.g. Fig.4.). At last the No. 5 filter of the set was selected. Its central wavelength is 656.5 nm and differs only slightly from that of the narrow-band filter (656.6 nm). The HBW of the medium band filter is 11.4 nm while its transmission values are given in Table 3. The numerical data demonstrate that although the wings of the profile of filter No. 5 are almost perfectly symmetric the core of the transmission curve is one-sided as the maximum value of the transmission is at the 654 nm wavelength mark. The total transmittance of the medium band filter is 4.35 times as large as that of the narrow one.

TABLE 3. Spectral transmission of the No. 5. medium band H-alpha filter

Wavelength (nm)	Transmission (%)	Wavelength	Transmission
644	0.1	658	59.0
646	0.6	660	58.7
648	3.1	662	37.2
650	17.6	664	11.3
652	34.8	666	2.8
654	60.1	668	0.7
656	59.9	670	0.2

4.2. Test Measurements

Preliminary test measurements were carried out during a short study trip of the author to the Stockholm University Observatory (SUO) in October 1987. For the high northern geographical latitude of Saltsjöbaden (the actual site of the SUO is at $59^{o}16'$) and its very low altitude above sea level (h=55 m) a target of high declination had to be chosen. As the anticipated observing time was considerably limited by local weather conditions the choice of a relatively nearby star cluster was favoured. The young open cluster M 45 or the Pleiades (which contains many hundreds if not thousands of red dwarf stars - Szécsényi-Nagy 1990b) was high in the sky then and there. In order to collect enough light from these faint sources and achieve the best possible S/N ratio the camera had to be mounted on a fast reflecting telescope. I would have chosen the Schmidt-camera of the Observatory because of its shorter focal length and larger field (and consequently having more dMe stars projected onto the CCD-chip) but it was technically impossible to fix the Photometrics camera at the Schmidt's focus. At last the test measurements were carried out with the photometric system mounted on the 40" (102 cm) parabolic reflector. The CCD-camera was fixed at the prime focus of the instrument (f=500 cm) and recorded the images of approximately 8 by 10 $arcmin^2$ fields. By tricky choices of the program fields an average of 2-3 flare stars per field was attainable and a kind of calibration of the frames could also be done.

This was the only way to collect enough data during the short clear hours of the four usable nights. In most cases the CCD was exposed to starlight from 400 to 1000 seconds. These long exposures, the stability and the extremely low noise level of the device due to the perfect LN-cooling resulted an RMS error inferior to 1% for the brighter objects while for the faintest but measurable stars the error slightly exceeded the 2% level.

5. PRELIMINARY RESULTS

Insufficient observing time and abruptly changeable weather prevented us from collecting enough photometric data for a really detailed and serious

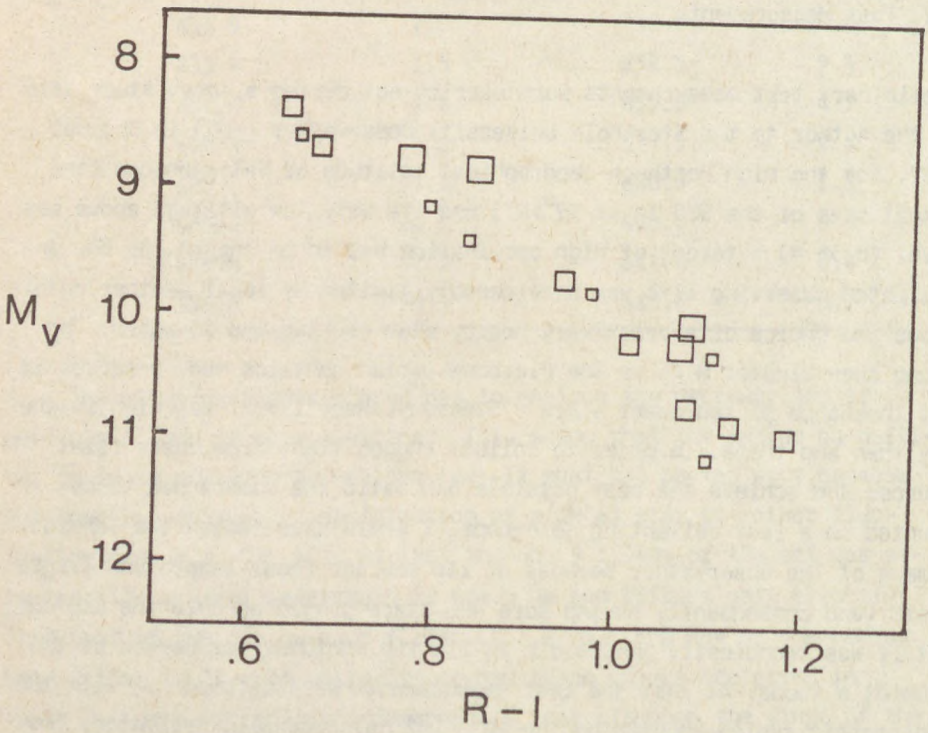

Figure 5. Absolute visual brightness versus red colour index plot for 17 flare-active dwarf stars of the Eta Tauri fields. M_V was calculated assuming a distance modulus of $5^m.5$ (that of the Pleiades). Areas of the squares are proportional to the relative H-alpha emissivity of the stars.

study of the H-alpha emissivity of flare-active red dwarf stars. But the results are promising and allow some preliminary conclusions.

The apparent brightness of 17 flare stars of the Eta Tauri fields was determined in two red photometric bands namely in the narrow H-alpha (H_N) and in the medium H-alpha (H_M) band. Both of these are practically centered on this hydrogen line. The measured brightness values of each star were compared and the intensity ratio $R_{NM}=H_N/H_M$ was computed. As there was no way to receive any kind of absolute calibration during the above observational run these relative H-alpha emissivity parameters of the stars had to be analyzed. Although the investigation resulted various R_{NM} values these might be classified into three groups. Relative emissivity values of 7 objects seemed to be similar and were spread in a narrow band around $\overline{R}_{NM}$ (an average which was chosen as an arbitrary reference level). Stars emitting stronger in H-alpha were less numerous in this sample. Only 4 red dwarfs produced significantly (practically by a factor of 2) higher R_{NM} values, while 6 were definitely fainter than the reference mean. Members of these three groups can easily be distinguished on the colour-magnitude diagram shown as Figure 5. However the squares representing the observed dMe stars are not ordered into perfect branches it seems highly probable that from flare stars of the same colour the stronger H-alpha emitters tend to be absolutely brighter in the visual range too.

For the importance of this relation in the explanation of the energy budget of atmospheres of dMe stars this kind of studies have to be repeated in the Pleiades amidst better weather conditions and carried out in other sky fields rich in flare-active dMe stars too.

6. CONCLUSIONS

The method developed to measure and characterize the H-alpha emissivity of red dwarf stars is ideally suited for doing that. The LN-cooled CCD-camera is sensitive enough at this very low light level and is a highly useful tool for photometric measurements especially in the orange/red spectral range. The two filters defining the system seem to work better than those suggested by Herbst and Layden (1987). Theirs have bandwidths of 3 and 15 nm respectively being a bit too large. Having seen the tendency it is very

likely that the optimal HBWs of the filters are below 2 and 10 nm resp.

REFERENCES

Ahmed, F., Lawrence, L.C., Reddish, V.C.: 1965, Publ. Edinburgh Obs. 3, 182.

Astromed Limited : 1989, CCD 2200 LN Cooled Camera, Cambridge, GB.

Chavushian, H.S. and Gharibdjanian, A.T.: 1975, Astrofizika 11, 565.

Cram, L.E. and Mullan, D.J.: 1979, Ap. J., 234, 579.

Eccles, M.J., Sim, M. Elizabeth, Tritton, K.P.: 1983, Low light level detectors in astronomy, Cambridge University Press, Cambridge, GB.

Herbst, W. and Layden, A.C.: 1987, Astron. J., 94, 150.

Joy, A.H. and Abt, H.A.: 1974, Ap. J. Suppl., 28, 1.

Miller, W.C.: 1987, in Scientific Imaging with KODAK Films and Plates, Eastman Kodak Company, Rochester, USA, p. 5.

Parsamian, E.S.: 1986, in B.A. Balázs and G. Szécsényi-Nagy (eds.), Star Clusters and Associations, Budapest, p. 115.

Pettersen, B.R.: 1989, Solar Physics 121, 299.

Szécsényi-Nagy, G.: 1986a, in B.A. Balázs and G. Szécsényi-Nagy (eds.) Star Clusters and Associations, Budapest, p. 101.

Szécsényi-Nagy, G.: 1986b, in L. Szabados (ed.), Eruptive Phenomena in Stars, Budapest, p. 425.

Szécsényi-Nagy, G.: 1989, in B.M. Haisch and M. Rodonó (eds.), Solar and Stellar Flares, Catania, p. 143.

Szécsényi-Nagy, G.: 1990a, in S. Bowyer and Ch. Leinert (eds.), Galactic and Extragalactic Background Radiation - Optical, Ultraviolet and Infrared Components, Kluwer Academic Publishers, Dordrecht, in press.

Szécsényi-Nagy, G.: 1990b, Astrophysics and Space Science, in press.

Turnshek, D.E., Turnshek, D.A., Craine, E.R. and Boeshaar, P.C.: 1985, An Atlas of Digital Spectra of Cool Stars (Types G, K, M, S and C), Western Research Company, Tucson, USA.

Weigert, A. and Zimmermann, H.: 1977, Brockhaus ABC Astronomie, VEB F.A. Brockhaus Verlag, Leipzig, p. 277.

AGE CALIBRATION FOR OPEN STAR CLUSTERS ON THE BASIS OF INTEGRATED COLOURS AND MAGNITUDES

Béla A. Balázs
Roland Eötvös University, Department of Astronomy
Budapest, Kun Béla tér 2.
H-1083
Hungary

ABSTRACT. Making use of the age dependence of integrated colours and luminosities of open clusters a new "age index" is defined. Ages based on this index turn out to be in good agreement with the customary turn-off point ages and the new method is applicable even in those cases when only an integrated two-colour photometry is possible or available.

Integrated colours and luminosities of star clusters are of outstanding importance in a number of astronomical investigations. (See e.g. Gray, 1965; Piskunov, 1974; Searle at al., 1980; Barbaro, 1981; Sagar at al., 1983; Chiosi at al., 1986; Baev and Spassova, 1986; Balázs, 1986; Chiosi at al., 1988.)

The age dependence of the integrated magnitudes and colours of open clusters was discussed by Gray as long ago as 1965 and later primarily by Searle at al. (1980), Barkhatova and Pylskaya (1983), Sagar and co-workers (1983), Elson and Fall (1985), Chiosi at al. (1986) and Balázs (1986).

Searle, Wilkinson and Banguolo (1980) have classified the rich clusters in the Magellanic Clouds into seven types on the basis of two reddening free parameters derived from integrated ugvr four-colour photometry. The SWB types form a one-dimensional sequence, which the authors interpret in terms of increasing age and decreasing metal abundance . An essentially equivalent sequence appeares in a plot of U-B against B-V intrinsic colours (Frenk and Fall, 1982).

Elson and Fall (1985) presented a more finely partitioned cali-

"Star Clusters and Associations"
Publ. Astron. Dep. Eötvös Univ.
No.10, Budapest (1990)

bration of the SWB sequence using a larger number of LMC and SMC clusters and new age determinetions. They have drawn a smooth middle line along the sequence of LMC clusters in the two-colour diagram and have divided the section into 51 intervals of equal length and have assigned a value of s to each cluster by projecting it normally onto the curve. The age calibration of s was made using clusters with known ages.

Chiosi and co-workers (1986) re-calibrated the age sequence using novel isochrones from models with convective overshooting and got the following relation:

$$\lg \tau = 0.062\, s + 6.99 \quad . \qquad (1)$$

Fig. 1 presents you the summary in the $(B-V)_0$ versus lg age plane showing theoretical curves by Chiosi at al. based on synthetic HR diagrams and integrated colours of model star clusters with two different metallicity.

Unfortunately a large spread in the integrated colours of real clusters exists as a consequence of random fluctuations in the mass distribution of cluster stars. Since the colour dispersion is mostly caused by the presence of very evolved stars via stochastic effects in the IMF, ages based on the turn-off luminosity ought to be preferred, as stochastic variations there should be less of a problem.

However only a small number of clusters out of the large sample for wich integrated colours have been measured possesses all the information required to date them on the basis of customary colour-magnitude diagrams (using turn-off and main sequence termination luminosities, red giant clump luminosity, etc.). On the other hand, it is certainly worth of interest to rank clusters as a function of the age even in those (far more numerous) cases, in which only integrated colours and magnitudes are available.

On the basis of our own data (Balázs, 1986), which includes 66 clusters up to an age of 10^8 years, we obtained the following linear relation between the integrated magnitude and logaritmic age of a cluster:

$$I(M_V) = (1.45 \pm 0.27) \lg \tau + (-14.95 \pm 2.68) \quad , \qquad (2)$$

which is -- concerning the slope -- in good agreement with Gray's result:

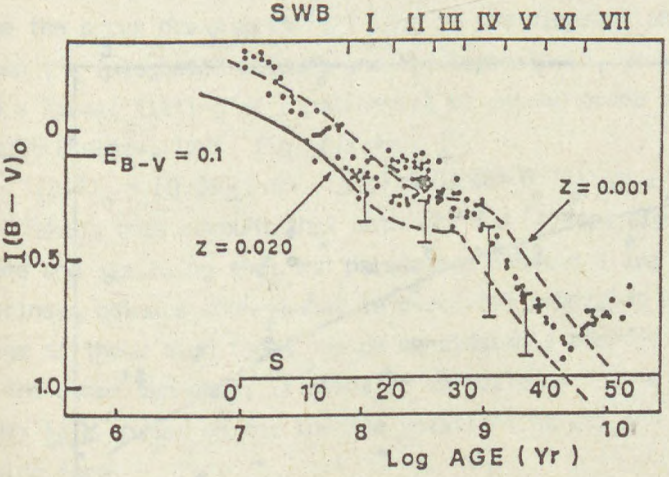

Fig. 1. The summary $(B-V)_o$ versus log age plane. The correspondence between the SWB type and age, and between the parameter s and age are shown on separate scales. The vertical bars visualize the dispersion in the colours given by stochastic effects in the IMF, limited to the case of Z = 0.020. The full dots are clusters from van den Bergh's compilation (1981), whose age has been derived with the aid of the relation s(t). A mean colour excess E(B-V) = 0.10 has been adopted to correct the apparent colours (Chiosi at al., 1986).

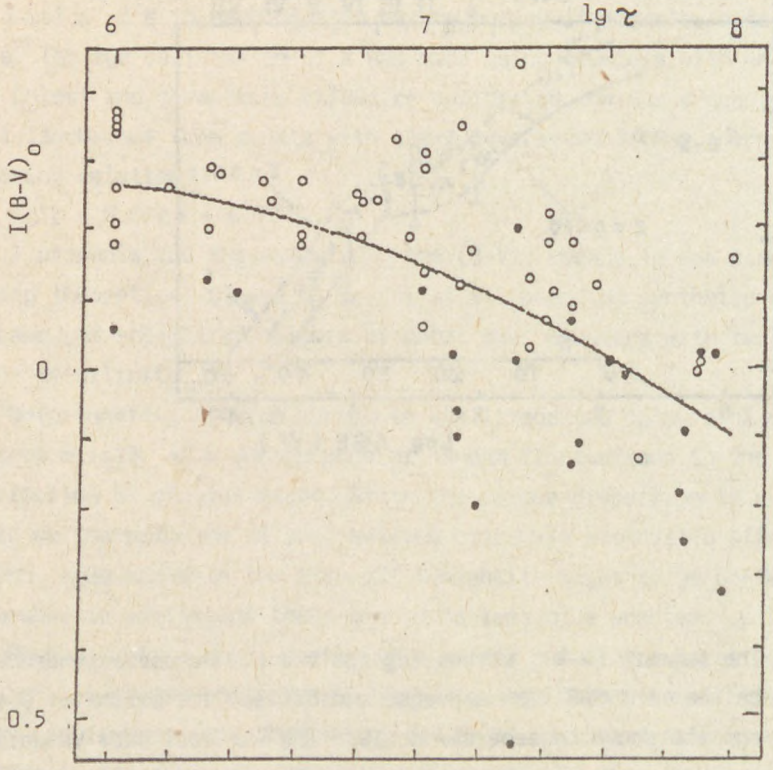

Fig. 2. The age dependence of the $I(B-V)_0$ colours according to Balázs (1986). The curve is the best fit given by the relation (4).

$$I(M_V) = 1.46 \lg\tau - 15.7 \qquad (3)$$

and the deviation at the zero point is simply a consequence of the different distance scales.

In conformity with the theoretical results of Chiosi at al. (1986) (see the curve drawn with full line in the diagram) the relation between the integrated colours and the logarithmic age is not linear, and a formal fitting of a polinomial of second order gave the following result (Balázs, 1986, fig. 2):

$$I(B-V)_o = (0.06 \pm 0.05)(\lg\tau)^2 - (0.68 \pm 0.72)\lg\tau + (1.61 \pm 6.23) \; . \qquad (4)$$

Taking into account that both (2) and (4) are significant relations and realizing that the parameters SWB and s are using only the intrinsic colours and -- what is even more important -- the effective range of the U magnitudes can be considerably shorter than the reach of the other two ones; it seems to me quite useful to define an age index $\lg\tau'$ based on the inverse relations of (2) and (4) in the following form:

$$\lg\tau' = a\, I(M_V) + b(I(B-V)_o)^2 + c\, I(B-V)_o + d \; . \qquad (5)$$

A formal curve-fitting to our 66 clusters gave us the following parameter values:

$$a = 0.124; \; b = -2.85; \; c = 1.56 \text{ and } d = 7.91 \; .$$

Let's stop here for a moment. Why to use this more complicated relation than the relation (4) between the integrated $(B-V)_o$ colour and the age? As it was pointed out earlier, the absolute magnitude of the brightest member stars is a decreasing linear function of the cluster age on a logarithmic scale. So if we are using only the colours, we simply give away this information.

Fig. 3 shows the customary turn-off point ages against the new age index (for our 66 clusters). The correlation is quite acceptable. A formal linear regression gives the following result:

$$\lg\tau = 1.09 \lg\tau' - 0.628 \qquad (6)$$

with a root-main-square scatter of 0.387, which corresponds to an uncertainty of a factor of 2.4 in the ages of individual clusters. This is comparable with the errors claimed for the previous methods of age determination, but the age index method is applicable even in those

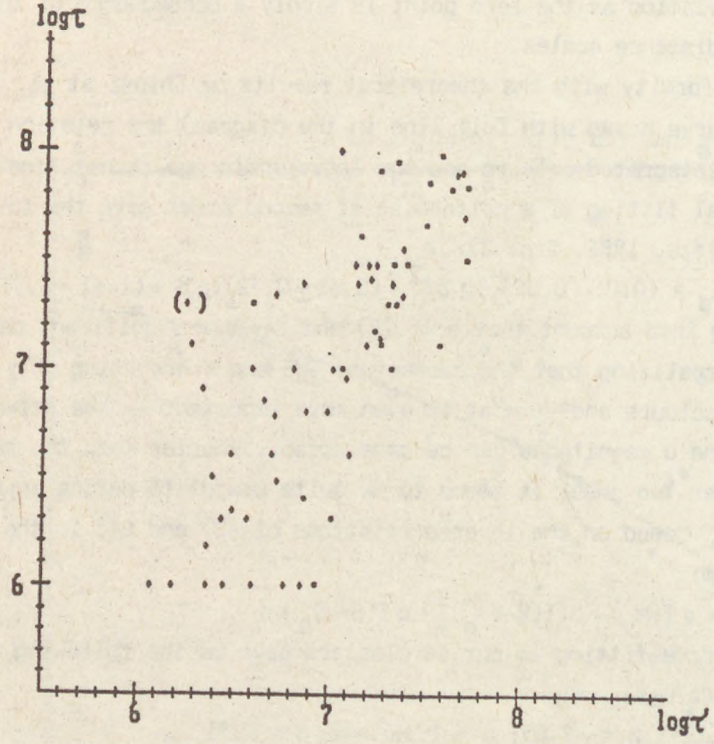

Fig. 3. Calibration of the age index ($\lg \tau'$) with the aid of customary turn-off point ages (for 66 clusters).

cases when only an integrated two-colour photometry is possible or available.

REFERENCES

Baev, P.V., Spassova, N.M.: 1986, Publ. Astron. Dept. Eötvös Univ. No. 8, 35.

Balázs, B.A.: 1986, Publ. Astron. Dept. Eötvös Univ. No. 8, 41.

Barbaro, G.: 1981, Astrophys. Space Sci. 77, 23.

Barkhatova, K.A., Pylskaya, O.P.: 1983, Publ. Astron. Inst. Czech. Akad. Sci. No. 56, 14.

Chiosi, C., Bertelli, G., Bressan, A.: 1986, Mem. Soc. Astron. Ital. 57, No. 3, 507.

Chiosi, C., Bertelli, G., Bressan, A.: 1988, Astron. Astrophys. 196, 84.

Elson, R.A.W., Fall, S.M.: 1985, Astrophys. J. 299, 211.

Frenk, C.S., Fall, S.M.: 1982, M.N.R.A.S. 199, 565.

Gray, D.F.: 1965, Astron. J. 70, 362.

Piskunov, A.E.: 1974, Nauch. Inf. Astr. Counc. USSR, 33, 101.

Sagar, R., Joshi, U.C., Sinvahl, S.D.: 1983, Bull. Astron. Soc. India, 11, 44.

Van den Bergh, S.: 1981, Astron. Astrophys. Suppl. Ser. 46, 79.

KINEMATICS OF STAR FORMING REGIONS IN OUR GALAXY

Jan Palouš
Astronomical Institute of the Czechoslovak
Academy of Sciences
Budečská 6
120 23 Prague 2
Czechoslovakia

ABSTRACT. Radial velocities of star forming regions from our Galaxy are analyzed. The possibility that their motion is due to the circular flow is assessed and we show that a sharp hump and/or noncircular motions are present near the Sun. The complexes of star forming regions are also detected and we review briefly how they may be formed in galaxies.

1. INTRODUCTION

A kinematical sample of radial velocities of 218 Star Forming Regions / SFR / from our Galaxy has been studied statistically by Avedisova and Palouš / 1989 - Paper I /. We discovered several complexes of SFR's sharing a common motion different from circular streaming.

In Paper I, a flat rotation curve with the linear velocity of rotation 220 km s^{-1} has been used. How far is our conclusion concerning complexes of SFR's influenced by this particular choice of the rotation curve? This is the question we address in the present contribution.

The distribution of SFR's in the galactic plane and the deviations from the circular motion are shown in Fig. 1. Our approach is the following:

1. We omit from the sample the SFR's deviating strongly from the circular streaming, e.g. complexes P1 and P2 specified in Paper I and in Fig. 1.
2. We use the condition equation from Paper I, where we removed all terms reflecting only noncircular streaming. The other terms partly reflect the circular flow and we discuss if the results are compatible with any rotation curve.
3. We analyze the distortions of the velocity field and we also discuss where the star forming complexes come from.

"Star Clusters and Associations"
Publ. Astron. Dep. Eötvös Univ.
No.10, Budapest (1990)

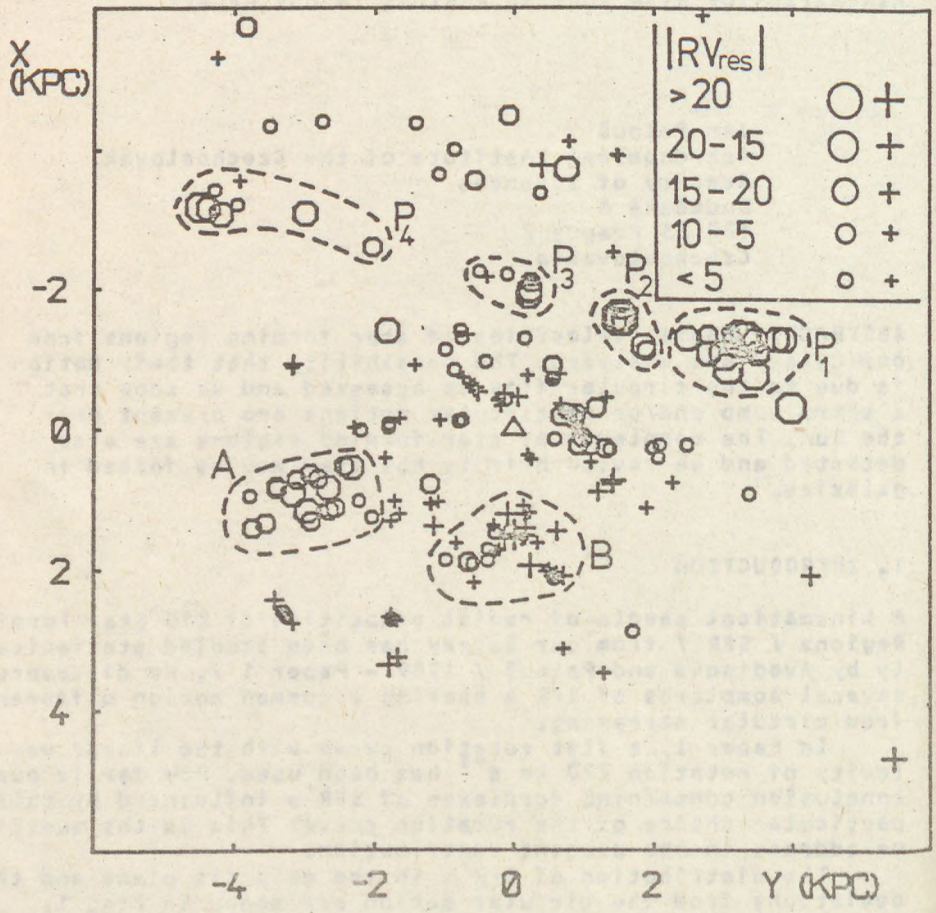

Fig. 1. The distribution of SFR's in the galactic plane. The /X, Y/ coordinates are centered on the Sun / the triangle /. X axis points towards the galactic centre and Y axis in the direction of galactic rotation. The departures of individual SFR's from circular streaming are also shown: /+/ or /o/ represent the positive or negative departure, the size of the symbol shows the value of the departure. The dashed lines define the complexes of SFR's.

2. THE ROTATION CURVE

The exact derivation of the condition equation describing the general velocity field in the galactic plane is given in the Appendix of Paper I. Omitting all terms originating strictly in noncircular streaming in the Galaxy the equ. 1 of Paper I reduces to

$$V_{r,LSR} = A\, r \cos^2 b \sin 2l + r^2 \cos^3 b\,(a_1 \sin l + a_3 \sin 3l) + r^3 \cos^4 b\,(b_2 \sin 2l + b_4 \sin 4l) \qquad /1/$$

r is the distance from the Sun in kpc and (l, b) are the galactic coordinates. The coefficients in /1/ partly originate from the rotation curve and its derivatives at the position of the Sun. For these parts we may write / see Paper I /

$$\begin{aligned}
A_{rc} &= 1/2\,(\theta/R - d\theta/dR)_o \\
a_{1,rc} &= 1/8\,(d^2\theta/dR^2 + d\theta/dR - \theta/R^2)_o \\
a_{3,rc} &= 1/8\,(d^2\theta/dR^2 - 3\,d\theta/dR\;1/R + 3\theta/R^2)_o \\
b_{2,rc} &= 1/8\,(1/3\,d^3\theta/dR^3 + d\theta/dR\;1/R^2 + \theta/R^3)_o \\
b_{4,rc} &= 1/16\,(1/3\,d^3\theta/dR^3 + 2\,d^2\theta/dR^2\;1/R - \\
&\quad - 5\,d\theta/dR\;1/R^2 + 3\,\theta/R^3)_o\ ,
\end{aligned} \qquad /2/$$

where R is the galactocentric distance in kpc and $\theta = \theta(R)$ is the linear rotation curve in km s^{-1}. The subscript /o/ means the position of the Sun.

What are the expected values for the coefficients /2/ ? Let us assume that the rotation curve is smoothly rising or falling by less than ± 20 km s^{-1} kpc^{-1}. These are very broad limits, but we also assume that there are no sharp humps on the rotation curve, which could cause that the second and third derivatives of it are large. Then, the expected values for /2/ are

$$\begin{aligned}
3 &< A_{rc} < 23 && \text{km s}^{-1}\text{kpc}^{-1} \\
-0.7 &< a_{1,rc} < -0.1 && \text{km s}^{-1}\text{kpc}^{-2} \\
0.3 &< a_{3,rc} < 2.0 && \text{km s}^{-1}\text{kpc}^{-2} \\
0.01 &< b_{2,rc} < 0.08 && \text{km s}^{-1}\text{kpc}^{-3} \\
-0.02 &< b_{4,rc} < 0.15 && \text{km s}^{-1}\text{kpc}^{-3}
\end{aligned} \qquad /3/$$

The fit of equation /1/ with our SFR's yields

$$A = 13.2 \pm 0.4 \text{ km s}^{-1}\text{kpc}^{-1}$$
$$a_1 = -0.26 \pm 0.07 \text{ km s}^{-1}\text{kpc}^{-2}$$
$$a_3 = 0.79 \pm 0.07 \text{ km s}^{-1}\text{kpc}^{-2} \qquad /4/$$
$$b_2 = -0.08 \pm 0.01 \text{ km s}^{-1}\text{kpc}^{-3}$$
$$b_4 = 0.07 \pm 0.01 \text{ km s}^{-1}\text{kpc}^{-3} \ .$$

Values /3/ and /4/ are compatible except the value of b_2, which is significantly off. There are two possible explanations of this unconfortable situation:

a. there is a sharp hump in the circular streaming not very far from the Sun,
b. the motion is noncircular and dominated by groups or complexes of SFR's.

In this paper, we discuss the second possibility, since it is similar to the conclusion of Paper I and some complexes are clearly distinguished in Fig. 1. However, the first interpretation is also possible and we postpone this discussion to another paper.

3. THE COMPLEXES OF SFR'S

The star forming regions in complexes of 1 - 2 kpc in size share a common motion and they probably dominate the velocity field around the Sun. In our opinion, this is only another evidence of the fact that the star formation operates in disks of spiral galaxies coherently on scales of one kiloparsec or more. The complexes of young O and B stars / Efremov, 1989, see also the review by Efremov in this volume /, coeval open star clusters or stellar moving groups yield further evidence for the statement above.

The star formation on such large scales is probably connected with some process propagating in the galactic disk. We assume that a self-regulating cycle between star formation, supershells and molecular clouds operates in galaxies / Tenorio-Tagle and Bodenheimer, 1988 /: stars are formed in clumps inside the molecular clouds. But the parent cloud is quickly disrupted due to the large amount of energy released from newly born massive stars. The ionizing photons, stellar winds and supernovae inject in total some 10^{53} erg over 10^7 years and disrupt the cloud forming an expanding supershell. The supershell accumulates the ambient medium and after certain time the new molecular clouds are created. They may become the sites of next generation of star formation.

In differentially rotating disks the supershells may form molecular clouds on their tips and we assume that this is the mechanism propagating the star formation within the galactic disk. This mechanism has been described

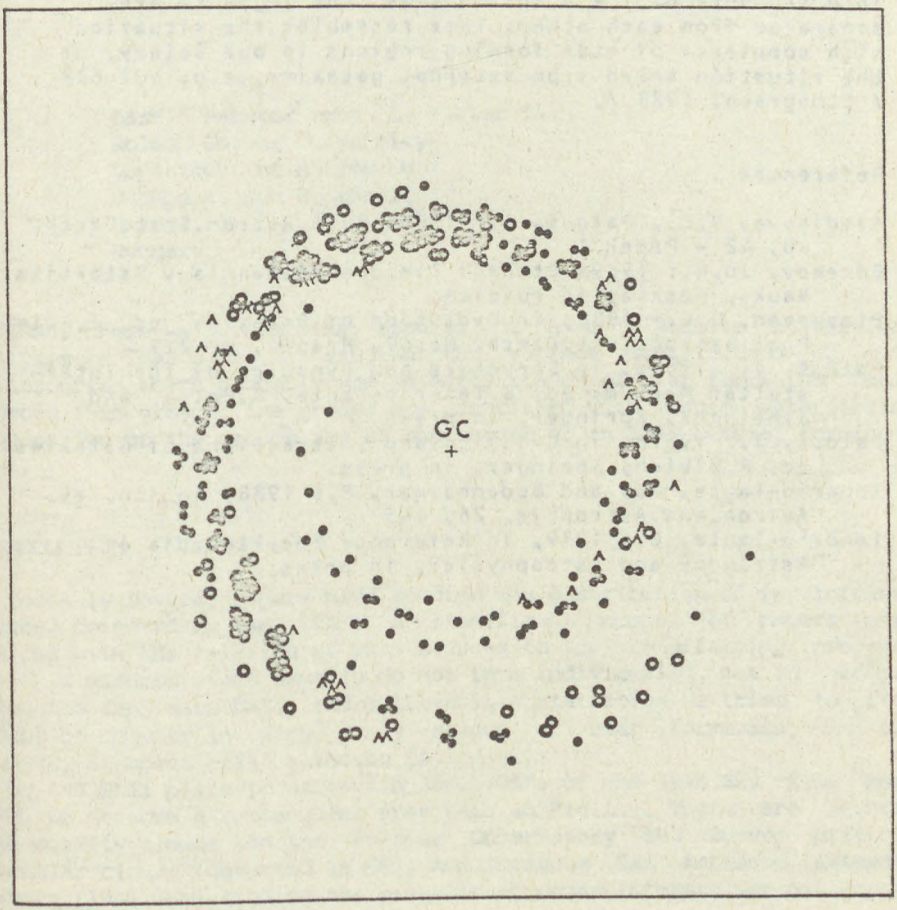

Fig. 2. The distribution of atomic /o/ and molecular clouds /•/ and SFR's /^/ after 0.5 Gyr of propagation. The side of the box is 32 kpc long.

elsewhere / Palouš, 1989a, b, Tenorio-Tagle, 1989 /.

We like to demonstrate only / see Fig. 2. / that after some time of propagation the multistructured arms are created. The star forming regions are concentrated into segments of 1 - 4 kpc in size, the segments are separated from each other. This resembles the situation with complexes of star forming regions in our Galaxy, or the situation known from external galaxies, e.g. NGC 628 / Elmegreen, 1988 /.

References

Avedisova, V.S., Palouš, J.: 1989, Bull.Astron.Inst.Czech. 40, 42 - Paper I

Efremov, Ju.N.: 1989, Otchagi Zvezdoobrazovania v Galaktikach, Nauka, Moskva, in russian

Elmegreen, B.G.: 1988, in Evolution of Galaxies, ed. J.Palouš, Publ.Astron.Inst.Czech. No.69, Prague, p. 219

Palouš, J.: 1989a, in Structure and Dynamics of the Interstellar Medium, eds G.Tenorio-Tagle, M.Moles, and J.Melnick, Springer, in press

Palouš, J.: 1989b, in Dynamics and Interactions of Galaxies, ed. R.Wielen, Springer, in press

Tenorio-Tagle, G., and Bodenheimer, P.: 1988, in Ann.Rev. Astron.and Astrophys. 26, 145

Tenorio-Tagle, G.: 1989, in Reference Encyklopedia of Astronomy and Astrophysics, in press.

AN IRAS BASED STUDY OF YOUNG OBJECTS IN A CEPHEUS REGION

László Pásztor and L. Viktor Tóth
Roland Eötvös University
Department of Astronomy
Budapest, Kun B. tér 2.
H-1083
Hungary

ABSTRACT. Here we present the results of a multivariate statistical analysis on IRAS data. We studied the surface distribution of cold pointsources which probably are in early stages of star formation. These objects form groups, the groups are associated with dense interstellar clouds. Two of the groups are at the border of an IRAS bubble, forming a shell.

INTRODUCTION

Recently several papers have studied the distribution of far infrared sources detected by the IRAS. A significant number of papers were dealing with the relation of IRAS sources to the starforming process. As it is assumed stars usually do not form individually, but in groups. Using the IRAS data base, and multivariate statistics we tried to find groups of objects in very early stages of star formation, in the Cepheus, at about b=15° galactic latitude.

On the PL11 plate (centre: 21h 30m, +75°) of the IRAS Sky Flux Maps (SFM) we seleced a rectangular area (see on Fig.1.). There are several high opacity clouds (on the Palomar Observatory Sky Survey prints), molecular clouds (detected in CO), and luminous far infrared extended sources (IRAS SFM) signing the presence of dense interstellar matter. We listed these objects in Table 1..

The large scale CO mapping of Lebrun (Lebrun 1986) revealed, the Cepheus giant molecular cloud complex (Cepheus GMCC) at $100° < l < 120°$,and $10° < b < 20°$ and at a distance of about 400 pc. Observational results on outflows and embedded sources, show a widely extended star formation in this area (Snell 1981., Schwartz et al. 1988., Mayers et al. 1988., Parker et al. 1988., Sato and Fukui 1989.).These objects are situated in and/or around Lynds dark clouds (Lynds 1962), together with H alpha emission stars found by Kun (1982).

On the 100 micron IRAS map (Fig. 1.) one can see that the Lynds dark nebulosities and the CO clouds usually are connected with little IR clumps in the giant molecular cloud complex.

"Star Clusters and Associations"
Publ. Astron. Dep. Eötvös Univ.
No.10, Budapest (1990)

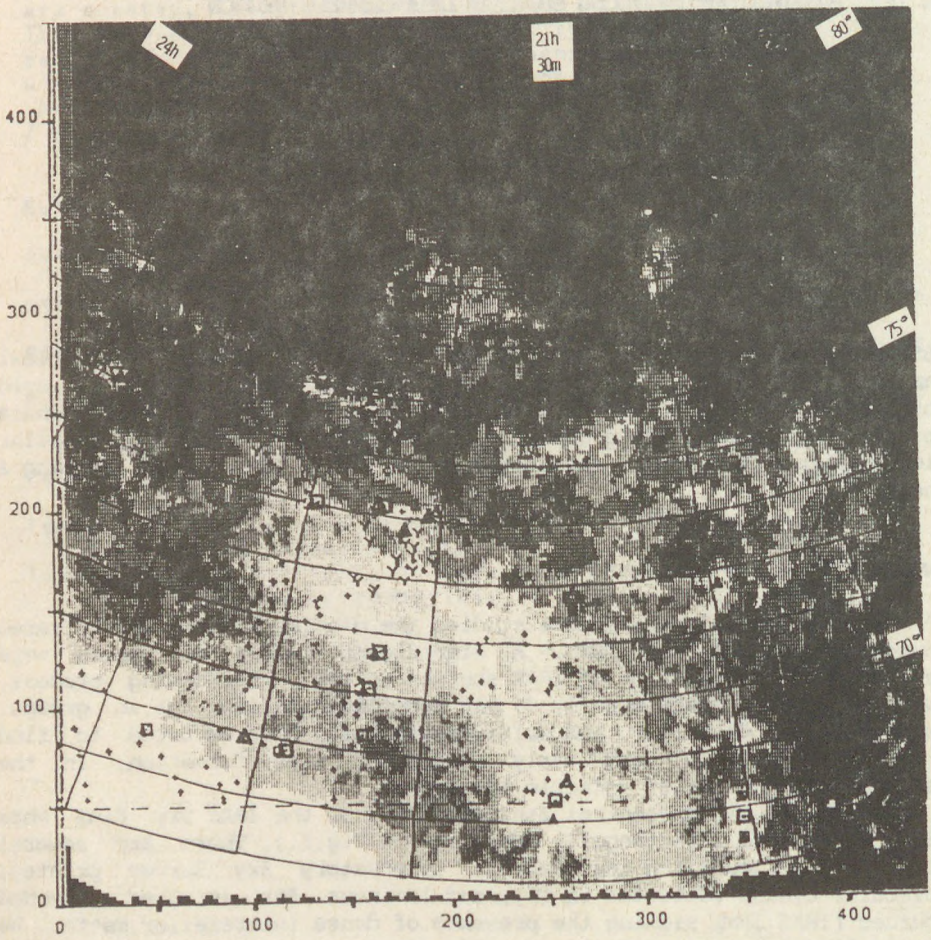

Fig.1 The surface distribution of the interstellar matter in the studied area. The cold IRAS pointsources (+) and the interstellar clouds regardless of their size: optically selected dark clouds:(⊡) Lynds (1962) and Barnard (1927), and the others: (Δ) (Taylor et. al. 1987., Desert et. al. 1988. and Magnani et. al. 1985.) centres overlayed on the PL11 100 micron IRAS SFM (centre: 250; 250= 21h 36m +75° 00').

The (Y) signe the H alpha sources found by Kun (1982) in the region. The dotted line shows the squere in which we investigated the IR sources, the solid lined net gives an orientation showing a grid of the equatorial coordinates on the SFM.

Table 1. The interstellar clouds in the studied area.
(The names; equatorial; and plate coordinates; and the references.)

CLOUDS	RA	DEC	SM	XL
	h m	° '	pixel	pixel
LDN1172 TDS392	21 01	67 47	349	39
LDN1199 TDS398	21 35	68 20	252	49
LDN1217 TDS410	22 12	70 04	157	108
LDN1219 TDS414	22 11	70 40	163	126
LDN1221 TDS416	22 26	68 49	114	77
LDN1228 MBM162 DBB149	21 00	77 20	309	324
LDN1235 TDS426	22 14	73 08	167	200
LDN1242	22 30	73 00	132	203
LDN1243 TDS428	22 13	75 14	179	262
LDN1247 TDS430	22 21	75 00	163	258
LDN1251 TDS431	22 35	75 00	136	264
LDN1259 TDS446	23 21	74 00	38	267
LDN1261 TDS448	23 25	74 00	31	270
LDN1262 TDS447	23 23	74 00	35	269
TDS417	22 34	68 55	93	85
TDS420	22 04	73 04	189	195
TDS421	22 09	72 48	177	188
TDS452	23 35	74 57	26	306
MBM161 DBB149	20 53	81 15	299	442
MBM164 DBB154	21 57	80 35	224	419
MBM165 DBB154	21 59	80 35	221	419
MBM166	22 01	82 15	224	470
DBB142	21 33	68 41	258	59
BARNARD175	22 11	69 19	157	85

BARNARD: BARNARD (1927)
DBB: DESERT ET AL. (1988)
LDN: LYNDS (1962)
MBM: MAGNANI ET AL. (1985)
TDS: TAYLOR ET AL. (1987)

We have studied the distribution of the cold pointlike IRAS sources of the area selected in order to answer the following questions:

1. Do the sources form groups or have a random distribution in the region?
2. Is there any connection between the distribution of the sources (groups) and the interstellar matter?

THE DATA ANALYSIS

We have obtained the sample of IRAS sources for the analysis on the following way: We have started with the total number of IRAS sources listed in the PSC within the 300x300 pixels squere signed on Fig. 1.. We used the selection criteria:

I., have a non-stellar like IRAS spectra ($F12 < F25$, if their flux qualities are good).

II.,have at least 90% pointlike feature in longer wavelengths (derived from the 25, 60, 100 micron point source correlation coefficients according to Beichmann et al. 1984). The 192 sources fulfilling these criteria have a non-random surface distribution. We controlled this fact by the next neighbours method. The mean separations of the first, second, ..., tenth neighbours (Table 2.) are clearly less than in random samples (gained by Monte Carlo simulations) due to the large number of couples with close separation in the real sample.

Table 2. Separations of the pointsources in the 300x300 pixels area.

	MEAN	STD DEV	MIN	MAX		MEAN	STD DEV	MIN	MAX
SEP 1	10.13	6.68	1.00	34.21	SEP 6	29.53	14.57	7.07	100.57
SEP 2	15.45	8.93	3.00	56.94	SEP 7	31.88	14.93	8.60	105.23
SEP 3	20.04	10.72	5.39	62.03	SEP 8	33.99	15.54	9.43	108.24
SEP 4	23.50	12.02	6.00	75.58	SEP 9	35.82	15.82	11.05	109.42
SEP 5	26.76	13.11	6.00	90.38	SEP 10	37.64	15.94	11.18	110.64

NUMBER OF CASES IS 192

We checked the significance of the variance by statistical tests (Kolmogorov-Smirnov Goodness of Fit Test, Chi-Square Test) comparing the separations' frequency distributions of the real sample with ones expected theoretically.

Since the probability that the i-th neighbour is just within a distance of s from a certain object in the case of randomly, non-correlatedly scattered points is:

$$p_i(s)=[2(N\pi/A)^i/(i-1)!]\,s^{(2i-1)}\exp(-Ns^2\pi/A)ds,$$

Where N is the number of points scattered in a field with an area of A.

The statistical tests revealed that the difference of the frequency distributions can be considered significant almost with 100% probability. Thus we may say that the our cold IRAS pointsources form groups in this region.

To obtain the groups at first we dropped away the sources which had less than 7 neighbours (other cold pointsources) within a circle of a radius of 28 pixels (50 arcmin), and which had not a next neighbour closer than 10 pixels (18 arcmin).

Fig 2. shows the remainder 61 IRAS objects. We derived 7 groups by a K-means clustering. Table 3. cointains the equatorial and SFM coordinates of the cluster centres, the number of the members and the identification of the associated clouds as well as the distance between the centre of the group and the associated clouds.

DESCRIPTION OF THE GROUPS

For the 61 group-member objects we derived the Tdust(60/100), the 60/100 micron dust temperature using the model of Leene (1988) of $\alpha=1$. We also derived the type of the IRAS sources according to Emerson's classification (Emerson, 1988). Here below we give a short description of our groups.

1: Group of faint, cold sources, near to the CO peak intensity on Lebrun's map. On the SFM the objects are located in an extended luminous region. The point sources may be cores of this dense part of the GMC. One of them which is near to the centre of the group has a comparable higher Tdust(60/100) of 37 K. This IRAS 21498+7053 object shows embedded source-like IRAS spectrum and has not associated, catalogized source on 2 micron (Gezari et. al. 1984).

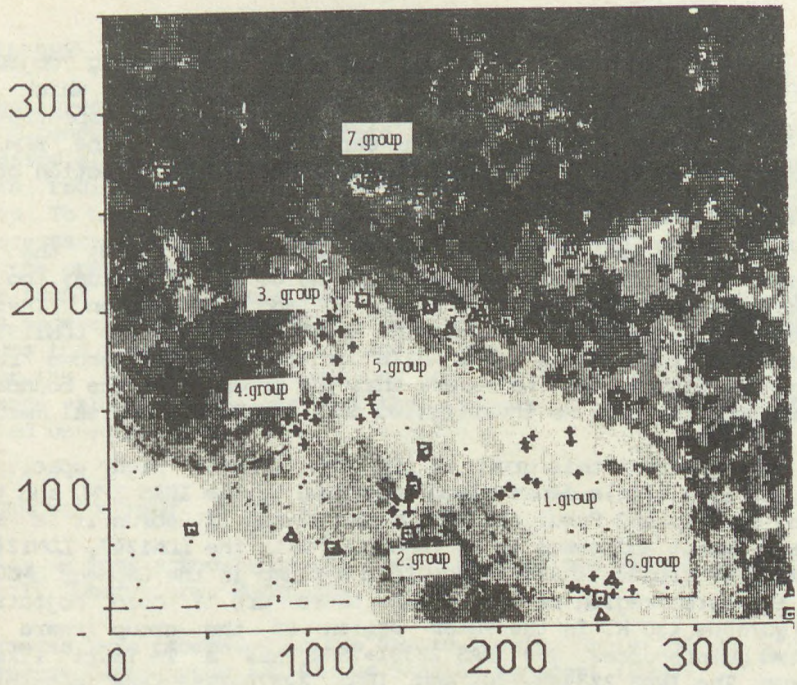

Fig 2. The 7 groups of the selected IRAS pointsources (+) and the contour of the buble overlayed on the investigated part of Fig. 1..

2: The group is associated with the Barard175 cloud (Barnard 1927) which shows strong absorption on the POSS. The sources are situated along a rim containing TDS417, LDN1221, LDN1217, LDN1219 clouds, which appears on the 100 micron SFM, too. Two sources: IRAS 22122+7000 and IRAS 22129+7000 are associated with the VdB.66N 152 very bright nebula (Van den Bergh 1966) and with the CED201 bright dense nebula which is considered as a product of a small isolated molecular cloud (Witt et. al. 1987). These two point sources have an IRAS spectrum like star forming areas according to Emerson's classification.

3 and 4: These sources appear in 60 and 100 micron only. They form a shell projected on the edge of a bubble-like structure on the SFM found by cluster analysis on 25, 60, 100 micron channels of PL11 SFM plate (Tóth 1988). The projection of the bubble on the SFM has a radius of about 90 minutes of arc, which corresponds to 5-6 pc assuming a distance of 4-500 pc in the line of sight, the same as one of the GMC according to Lebrun. The estimated coordinates of the centre of the bubble are: RA(1950)=23 h ; DECL(1950)=+71 deg 30 min.

5: It is a low populated, compact group containing objects of Tdust(60/100) of about 20 K except IRAS 22256+7102, which has a Tdust(60/100) of about 40 K and show a T Tauri-like IRAS spectrum. The group is not associated with known dark clouds but the SFM shows intensive far IR emission signing dense matter in the direction of this group.

6: This group is associated with the LDN1199 dark cloud, the DBB142 molecular cirrus cloud which appears on the CO map of Lebrun, too. These sources have good IRAS fluxes only in 60 and 100 micron. These are probably cold cores in the cloud. The southern part of the LDN1199 cloud is a place of known young stars while our 6th group may shows recently forming protostars. Here we remark that the group is at the boundary of the studied area thus we investigated only a part of the real members.

7: The center of this group is in the LDN1251 high opacity dark cloud. It is a little dense cloud according to the IRAS SFM, and the CO mapping of Sato and Fukui (1989). On the CO map of Lebrun it is a peak intensity point and seems to be connected with the LDN1247, LDN1243 and LDN1241 dark clouds. These clouds form a clump in the Cepheus GMCC.

In the outer region of the group there are 7 cold objects with Tdust(60/100) <30 K. In the inner region of the group there are 3 selected pointsources. The IRAS 22331+7502 has a T Tauri like IRAS spectrum. The IRAS 223443+7501 and IRAS 22376+7455 are possible the driving sources of molecular outflows detected in CO (Sato and Fukui 1989). Here are also a few H alpha emission stars in and around the LDN1251 (Kun 1982). We think that the star forming occurs here in a larger volume than the LDN1251 cloud.

Table 3. The main data of the 7 groups: the equatorial coordinates of the centers; the number of members; the name of the associated clouds and the distance between the group and cloud centers in arcmin.

NO	RA h	RA m	DEC °	DEC '	N	ASSOCIATED CLOUDS	DISTANCES '	REMARKS
1	21	47	70	39	10	LEBRUN CO-PEAK	38	LOOSE GROUP
2	22	13	69	41	14	BARNARD175	23	ADVANCED STAR FORMATION
						LDN1217 TDS410	23	
3	22	35	72	19	6			BUBBLE
4	22	36	71	00	9			BUBBLE
5	22	25	71	15	5			EXTENDED IR EMISSION
6	21	35	68	34	7	LND1199 TDS398	14	PART OF A LARGER GROUP
						DBB142	11	
7	22	36	75	01	10	LDN1251 TDS431	4	ADVANCED STAR FORMATION

SUMMARY

The investigated sample of IRAS sources shows concentrations in and around dense parts of the interstellar matter. We assume that we found pre-associations which signe that in the Cepheus Flare GMC there are several regions of recent star formation with different ages, and masses. To have a correct estimating for the starforming efficiency it is necessary to find the other members (more evolved, more faint, etc. than the presented objects) of the groups.

We found a new evidence for the existence of a bubble like structure. It is necessary to have a more extensive CO mapping than Lebrun's, to discuss the real structure and age of the bubble.

For the further investigations one have to obtain good enough distance values for the parts of the Cepheus Flare GMC and for the related objects.

ACKNOWLEDGEMENT

Finally we must acknowledge the useful discussions with Lajos G. Balázs (Konkoly Observatory, Budapest).

The images were processed in the Remote Sensing Center of the Institute of Geodesy Cartography and Remote Sensing Budapest (FÖMI).
We have got additional valuable help from András Holl (Konkoly Obs.).

REFERENCES

Barnard, E. E., 1927, Carnegi Institute of Washington Publ. No.247.
Beichmann, C. A. et. al., 1975, IRAS Catalogues and Atlases Explanatory Supplement (U.S. GPO, Washington, DC)
Desert, F. X., Bazell, D., Boulanger, F., 1988, Ap.J. Vol.334, p.815.
Emerson, J. P., 1988, in Formation and Evolution of Low Mass Stars, Kluwer, 1988, p. 193.
Gezari, D. Y., Schmitz, M., Schmitz, M., and Mead, J. M., 1984, Catalog of Infrared Observations, NASA Ref. Publ. 1118.
Joint IRAS Science Working Group, 1985., IRAS Point Source Catalogue (U.S. GPO, Washington, DC)
Kun, M., 1982, Astrofizika, 18, p.63.
Leene, A., 1988, IRAS Studies of the Nature of Interstellar Dust and Planetary Nebulae, Thesis (manuscript)
Lebrun, F., 1986, Ap.J. Vol.306. p.16.
Lynds, B., 1962, Ap.J. Suppl. Ser. Vol.64. p.1.
Magniani, L., Blitz, L., and Mundy, L., 1985, Ap.J. Vol.295. p.402.
Myers, P.C., Heyer, M., Snell, R. L., and Goldsmith, P. F., 1988, Ap.J. Vol.324. p.907.
Parker, N. D., Padman, R., Scott, P. F., and Hills, R.E., 1988, M.N.R.A.S., 234, p.67.
Pásztor, L., 1989. Thesis (manuscript in Hungarian)
Sato, F., and Fukui, Y., 1989, submitted to A.J.

Snell, R.L., 1981, Ap.J. Suppl. Ser. Vol.45. p.121.
Schwartz, P.R., Gee, G., and Huang, Y. L., 1988, Ap.J., Vol.327. p.350.
Taylor, D. K.., Dickmann, R. L., and Scoville, N., 1987, Ap.J. Vol.315. p.104.
Tóth, L. V., 1988., Star Formation in Molecular Clouds, Thesis (manuscript in Hungarian)
Van den Bergh, S., 1966. A.J. Vol.71. No.10.
Witt, A. N., Bohlin, R. C., Stechler, T. P., Graff, S. M., 1987, Ap.J. Vol.321, p.912.

SOME CONSIDERATIONS ON DATA BASES AND CATALOGS

C. JASCHEK
CDS, Strasbourg, France

Traditionally catalogs were the product of a scientist near retirement age, who published his private files (i.e. his private data base) for public use. That was the way of Aitken for the double star catalog, and of Wilson for the stellar radial velocity catalog. Obviously such a practice does not favor a re-edition of the catalog in a near future. Since then things have changed, at least in two aspects. Data bases and catalogs are now often the result of a team work, like for instance the photometric catalogs of the Lausanne group headed by Hauck; secondly the very large inflow of data requires re-editions at short time intervals. As a good example consider the *"Bright Star Catalog"*. The third edition came out in 1964, the forth in 1982 and we have already a fifth on tape since 1987. This example is instructive because we are dealing with a number of stars which is constant ($N \sim 9200$) in which only the amount of information for each object is increasing. If one looks at catalogs in which the number of object varies but the information content is the same, we may quote the case of the UBV catalogs. Johnson and Morgan (1953) provided data for 2,9 $x10^2$ stars; Blanco et al (1968) for 2,4 x 10^4; Mermilliod & Nicolet (1977) for 5,3 x 10^4, Mermilliod (1984) for 7,2 x 10^4 and Mermilliod (1987) for 8,7 x 10^4 stars. This represents an exponential growth in which the number doubles every eight years.

Such a rapid data growth obliges to issue re-editions as soon as possible, and this in turn poses new problems. First of all consider the time elapsed since the final date for data collection and the day the catalog can be mailed. Secondly, on what support should the catalog be printed.

With regard to the first point one has to consider two different delays. The first one is the time elapsed between the closing date of the catalog or the data base ("literature up to 1980.0 was included") to the date the printer gets a manuscript. The second step is the time elapsed between the presentation of the manuscript to the printer and its apparition in print.

The first delay is deadly when hand-written cards have to be transcribed, but -happily- it reduces to almost zero when the information is stored in a computer. With regard to the second delay, we all know that a magazine takes about one year to publish a catalog whereas a (book) editor takes two years to get a book printed. If one puts the two steps together one finds himself confronted with the fact that a catalog printed in book form from hand-written cards has a handicap of at least three and up to five or six years: it is out-dated even before published.

"Star Clusters and Associations"
Publ. Astron. Dep. Eötvös Univ.
No.10, Budapest (1990)

How should catalogs then be presented to overcome this time delay? The traditional printing on paper has the advantage of being permanent (permanent meaning "at least one century") but as we have seen, it is a rather slow procedure. The second possibility is the magnetic tape, which in principle permits re-edition at any moment. Tapes have however a limited life (less than ten years), unless precautions are taken. It also requires a computer to read it. But it has definite advantages over the printed catalog: one can perform all kinds of operations on it, re-arrange it, sample it, combine it with other catalogs and so on. For all this we must produce computer readable version of all catalogs, even of the ones which are printed. In second place, catalogs on tape are cheaper to produce and to distribute than books: there is no problem of producing one more copy of the tape, whereas when one miscalculated the number of exemplars to be printed, a re-issuing is (almost) out of question. Let us mention in by-passing that from the tapes one can also produce print-outs, microfiches and even laser-printed books. So it seems that all data bases have now to be computerized from the start, so that issuing a catalog becomes a relatively simple thing. Often scientists assume that essentially all necessary information exists already on tape at the astronomical data centers around the world (USSR, GDR, France, USA, China, Japan) This is however a flagrant exaggeration because as I have shown in my book *"Data in Astronomy"* (Jaschek, 1989) there are whole chapters of astronomy without catalogs (either on tape or printed). I shall provide just a few examples. Radiodata surely exist on tape, but are very difficult to get, a fact which is paradoxical and prevents further use. Catalogs of associations do exist, but no catalog of association members. The catalog of interstellar polarization is badly outdated, and a similar remark applies to the catalog of MK spectral types. Photoelectric observations of variable stars are currently made in huge quantities and are sometimes even published, but no one has put them in a data base. As far as galaxies are concerned, we can quote the case of M31. This galaxy has been observed often, but we have neither a cross-identification of all the objects observed, nor a comprehensive catalog of positions. Besides M31 there are at least half a dozen other galaxies who merit similar treatment. (Up to now such a catalog exists only for the Small Magellanic Cloud (Bischoff, et al., 1988). The list of examples could be prolongated without much effort and shows how much is still to be done.

Let me simply mention a last point, namely why it is important to set up catalogs or data bases. The justification lies in the fact that modern science is broken up in many small fields of specialization. If we go outside our own narrow field, we must rely upon the data of other specialists, because even if we would attempt to study the literature to know which is value of the datum we need, we lack the necessary expertise. Conversely other specialists expect from us that we collect and summarize the data of our field of specialization for them. If we do not do it we fail as responsible scientists: we are expecting others to provide us with data, but we do not provide anything in return.

Bibliography

Bischoff, M., Florsch, A., Florsch, J. and Marcout, J.: 1988, "Catalogue of the Objects in the Direction of the Small Magellanic Cloud", Publ. Observatoire de Strasbourg, France

Blanco, V.M., Demers, S., Douglass, G.C., FitzGerald, M.P. (1968) "Photoelectric Catalogue: Magnitude and Colours of Stars in the UBV and UcBV Systems", *Publ. U.S. Naval Observatory* 2nd Ser., vol. 21, Washington

Jaschek, C. (1989) "Data in Astronomy" Cambridge University Press

Johnson, H.L. and Morgan, W.W. (1953) *Astrophys. J.* 117, 313

Mermilliod, J.Cl. and Nicolet, B. (1977) *Astron. Astrophys. Suppl.* 29, 259

Mermilliod, J.Cl. (1984) *Bull. Inform. CDS* 26, 3

Mermilliod, J.Cl. (1987) *Astron. Astrophys. Suppl.* 71, 413

INVESTIGATIONS BASED ON "CATALOGUE OF STAR CLUSTERS AND ASSOCIATIONS" DATA

O.P.Pyl´skaya
Astronomical Observatory, Ural State University
620083 Sverdlovsk, USSR

ABSTRACT. We present an information on preparation of Supplements to "Catalogue of Star Clusters and Association" (G.Alter et al., 1970, Budapest) (CSCA) in the Ural State University. This work is carrying out in collaboration with collegues from Czechoslovakia and Hungary. We shortly review integral parameters of open clusters and discuss metallicity distribution of open clusters determined from different scales.

The observational data for complex star clusters investigations including the determination of their dynamic, kinematic, photometric parameters, age characteristics and chemical composition of cluster stars must be as homogeneous as possible. It is often necessary to transform the characteristics determined with different calibrations to the uniform system.

This is especially important for the investigation of star cluster complexes, determination of genetical connections between different age open clusters, exploration of Galaxy evolution and gradients of chemical composition.

"The Catalogue of Star Clusters and Associations" (CSCA) is being systematically supplemented with new data on the stellar groups investigations.

Since 1981 this work is being performed in collaboration with scientists from Czechoslovakia and Hungary. In 1987, the Ural State University was intitled by conference of participants of the Project III "Creation and Processing Astronomical Catalogues on Computers" (Potsdam,

"Star Clusters and Associations"
Publ. Astron. Dep. Eotvos Univ.
No.10, Budapest (1990)

1987, Nov.30-Dec.5, Subcomission No.6 "Star Clusters and Associations") to review the main part of soviet and foreign literature concerning the topic. Information from more than a hundred of periodic astronomy editions issued in different countries within 1981-1988 has been collected in Supplement III of CSCA. About 20 thousands of records in English including new data on cluster physical parameters are put down on magnetic tape and sent to Czechoslovakia for editing.

At latter decades, the analysis of CSCA and Supplements led us to some interesting conclusions about the Galaxy structure and dynamics. New methods of observation and statistical processing of stellar group data have also been stimulated in the Ural State University. Particular attention was paid to the exception of errors due to selection effects and data unhomogeneousness.

So, the main parameters for 28 open clusters of different ages were determined and luminosity functions were derived using the method of uniform three-colour (UBV) photometry in a system of hundreds of thousands stars. Using the statistic criteria we have demonstrated also that the initial luminosity function universality hypothesis can not be expected because the open clusters luminosity functions of all four selected age groups have only eccidental differences. The star formation period calculation method using luminosity functions was applied for some open clusters (OCL). The duration of star formation appeared to be 10^7-10^8 (Zakharova 1987, 1989).

Theoretical and experimental problems need homogeneous data. They are: investigations on OCL dynamic evolution character, initial stages of cluster evolution after the OCL stars formation in the molecular clouds nuclei, etc. A new statistical method for estimation of diameters, number of stars and OCL reality was elaborated at the Ural State University. This method is based on the star quantity functions N(R) comparison in different radius R circles for clusters and for wide background field areas (Danilov, Matkin, Pyl'skaya 1985). The method allows to study in details the star background and to estimate the errors of the determined values. For cluster dimension estimations (LD) we used not only the mean photometric distances, calculated according to many CSCA authors data but also the clusters distances determined at the Ural State University (Barkhatova, Pyl'skaya 1980) with the help of Kholopov's ZAMS (Kholopov 1978). The parameters of a hundred open clusters have been determined by now (Danilov, et al. 1987, 1989). More clusters being analysed by the new tech-

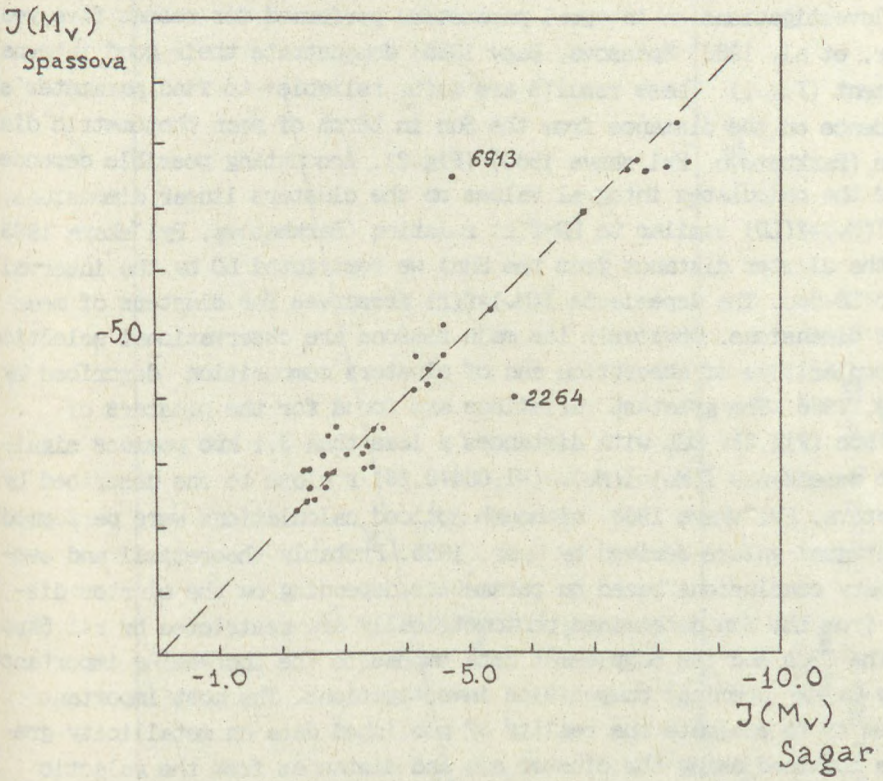

Fig.1. Comparison of the integral OCL parameters according to Sagar et.al. 1983; Spassova 1985.

nique, more accuracy of different mass clusters space distribution will be obtained. It will clear the reasons of some paradoxical dependences for OCL subsystem described by Barkhatova, Pyl´skaya 1983.

Investigations on integral parameters performed for recent five years (Sagar, et al. 1983, Spassova, Baev 1985) demonstrate their good internal agreement (Fig.1). These results are quite reliable to find parameter´s dependence on the distance from the Sun in terms of mean photometric distances (Barkhatova, Pyl´skaya 1980) (Fig.2). Accounting possible dependence of the calculated integral values on the clusters linear dimensions, i.e. $I(M_v)=f(LD)$ similar to $LD=f(r)$ relation (Barkhatova, Pyl´skaya 1983) (r - the cluster distance from the Sun) we restricted LD by the interval of $3pc<LD<5pc$. The dependence $I(M_v)=f(r)$ preserves for clusters of mean linear dimensions. Obviously its main reasons are observational selection and pecularities of absorbtion and of clusters composition described by Balazs, 1986. The greatest variations are found for the clusters of $r>1.5$ kpc (Fig.2). OCL with distances r less than 3.1 kpc possess significant dependence $I(M_v)=I(M_v)_o+(-1.084+0.28)\cdot r$ close to one described by Barkhatova, Pyl´skaya 1983, although noticed calculations were performed for integral values derived by Gray, 1965. Probably theoretical and evolutionary conclusions bazed on parameters depending on the cluster distance from the Sun determined photometrically are restricted by $r<1.5$kpc.

The CSCA and its Supplement data emphasize the increasing importance of the Galaxy chemical composition investigations. The most important problem is to estimate the reality of published data on metallicity gradients obtained using the cluster age and distances from the galactic centre and galactic plane.

The metallicity values are determined with essential errors even for individual cluster stars. Thus authors (Claria, Lapasset, 1985) report that the value [Fe/H] changes from -0.09 to -0.60 for the star No.58 of the cluster NGC 5822 according to different metallicity indices.

Different metallicity systems (Janes 1979; Jennens, Heller 1975; Cameron 1985 a, b; Lynga 1987) of OCL have been compared (Pyl´skaya 1988) and the published values of metallicity have been reduced to a homogeneous system similar to Lynga´s 1987 one. The cluster metallicity function is presented at Fig.3. This function is like already published [Fe/H]-distributions of red giants and G-dwarfs of field (Marsakov, Suchkov 1985). Distribution bimodality and its centre pit remain also after the addition of [Fe/H]-values from Panagia, Tosi 1981; Strobel 1987 papers (the shaded part of hystogramm, Fig.3). Probably this similarity

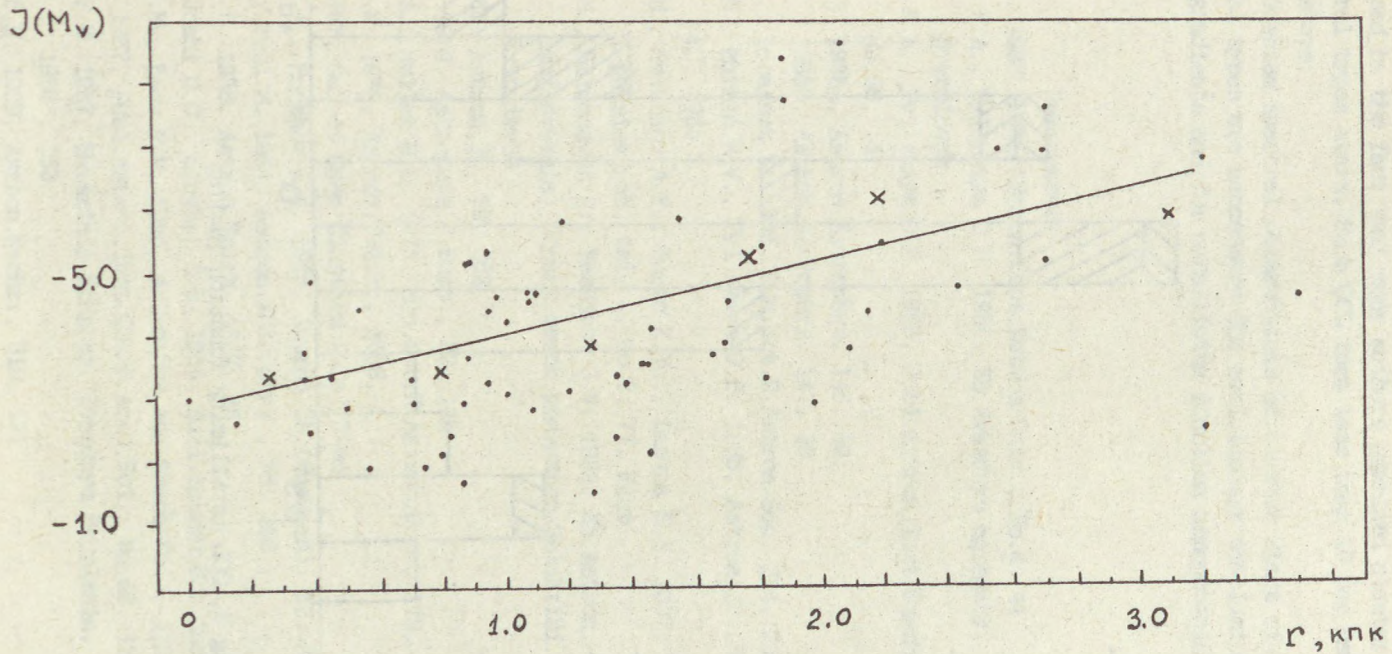

Fig.2. I(Mv) from r(kpc) dependence:

$I(M_v)=I(M_v)_o+(-1.08+0.28)\cdot r$, $0.18<r<3.2$, N=112

$I(M_v)=I(M_v)_o+(-0.41+0.33)\cdot r$, $r<1.5$, N=65

$I(M_v)=I(M_v)_o+(-0.09+0.30)\cdot r$, $r<0.5$, N=19

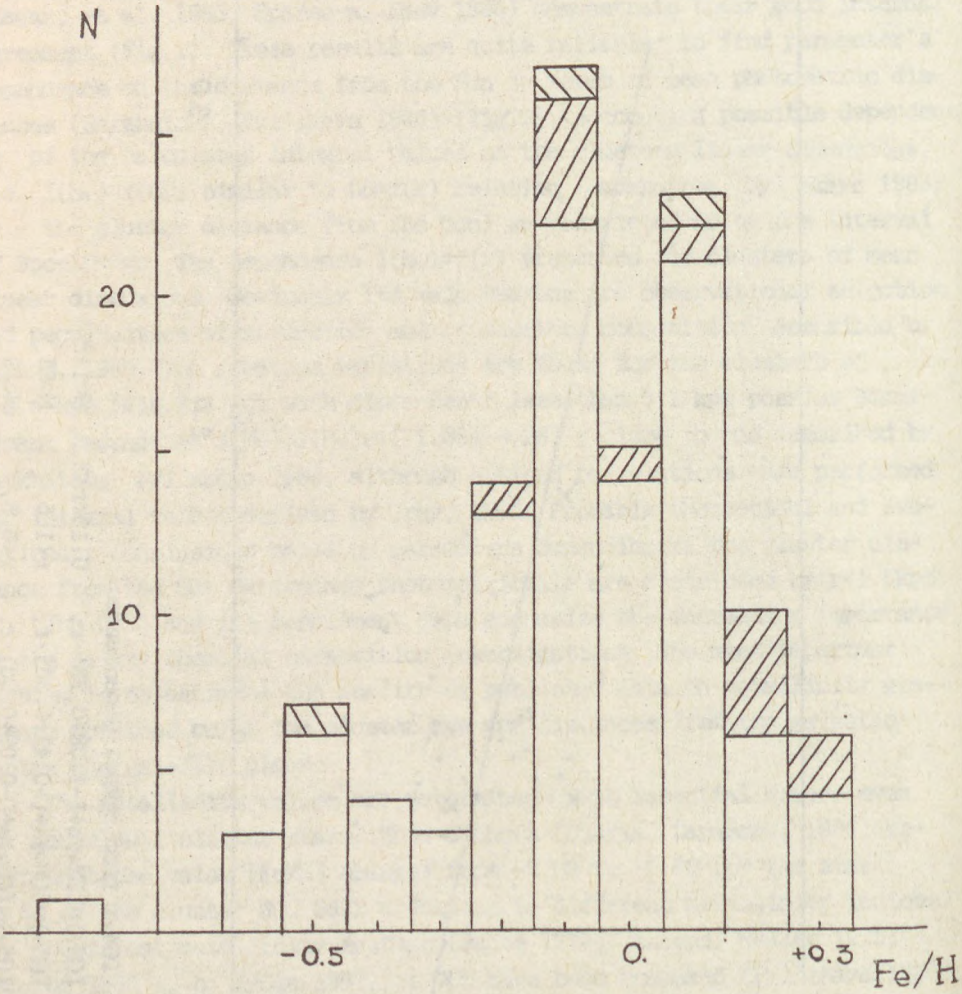

Fig.3. OCL metallicity function (N=114)

may be caused by the fact that many authors examined clusters containing late spectral types stars. Such OCL form less than 10 per cent of all Galaxy clusters.

More precise spectral observations of cluster stars of wider interval spectral types are neccessary for evolutionary conclusions about abundance gradients and for metallicity function nomonotonicity estimation.

References

Balazs B.A. 1986, Publ.Astron.Dept.Eotvos Univ., No.8, 41
Barkhatova K.A., Pyl'skaya O.P. 1980, Sb.Zvezdnye agregaty, 26, Sverdlovsk
Barkhatova K.A., Pyl'skaya O.P. 1983, Publ.Astron.Inst.Czech.Acad.Sci., No.56, 14
Cameron L.M. 1985a, Astron.Astrophys. 146, 59;
1985b, Astron.Astrophys. 147, 39
Claria J.J., Lapasset E. 1985, Mon.Not.R.Astron.Soc. 214, 229
Danilov V.M., Matkin N.V., Pyl'skaya O.P. 1985, Astron.Zh.(Russian), 62, 1065
Danilov V.M., Seleznev A.F., Gurto E.Yu., Lapina E.A. 1987, Kinematika i physica neb. tel, 3, No.6, 77, Kiev
Danilow V.M., Seleznev A.F., Beshenov G.V. 1989, Sb.Astron.-Geodezich. Issledovania; Struct.ossob.podsystem Galaktiki, 8, Sverdlovsk
Gray D. 1965, Astron.J., 70, 362
Janes K.A. 1979, Astrophys.J.Supp., 39, 135
Jennens P.A., Heller H.L. 1975, Mon.Not.R.Astron.Soc., 179, 681
Kholopov P.N. 1978, Astron.Tsirk., 1006, 1
Lynga G. 1987, Cat.of Open Clusters Data, 5-ed
Marsakov V.A., Suchkov A.A. 1985, Astron.Zh.(Russian), 62, 847
Panagia N., Tosi M. 1981, Astron.Astrophys., 96, 306
Pylskaya O.P. 1988, Astron.Tsirk. 1527, 25
Sagar R., Joshi U.C., Sinvhal S.D. 1983, Bull.Astron.Soc.India, 11, 41
Spassova N.M., Baev P.V. 1985, Astrophys.and Space Sci., 112, 111
Strobel A. 1987, Publ.Astron.Inst.Czech.Acad.Sci., No.69, 129
Zakharova P.E. 1987, Materialy Konpher."Zvezdnye Skoplenia, Sverdlovsk, 1986", 153
Zakharova P.E. 1989, Astron.Nachr., 310, 127

SOME INFORMATION ON THE BIBLIOGRAPHIC CATALOGUE OF VARIABLE STARS

SIEGFRIED RÖSSIGER
Central Institute of Astrophysics
Sonneberg Observatory
PF. 55-27/28
Sonneberg - 6400
G. D. R.

ABSTRACT. The paper reports briefly on the development and structure of the Sonneberg bibliographic card file catalogue of variable stars, and shows how this catalogue became the starting point of the Bibliographic Catalogue of Variable Stars and the Bibliographic Catalogue of Suspected Variable Stars at the Strasbourg Stellar Data Centre. Information is given on the up-to-dateness of those catalogues.

HISTORICAL BACKGROUND

Sonneberg Observatory is one of the most important research centres for variable stars. This can already be seen from the fact that nearly one third of all known variable stars have been detected at Sonneberg, mostly by C. Hoffmeister. For investigating variable stars a bibliographic catalogue is an almost indispensable aid in avoiding repetition of research work or simply answering the question whether a variable star newly detected at Sonneberg has been known before. Therefore in the first years after the Second World War the so-called "Sonneberger Zettelkatalog" was established. This is an extensive card file containing all attainable references for variable and suspected variable stars, with each star having one or more cards (depending on the amount of literature referring to it), and the cards being sorted according to the customary rules of nomenclature. It was a lucky chance that just at that time H. Schneller had been working for some years at Sonneberg Observatory. He was, after R. Prager, the author of the second edition of the publication "Geschichte und Literatur des Lichtwechsels der Veränderlichen Sterne" (GuL). By copying Schneller's file the foundation for the Sonneberg card file catalogue was laid. In this respect one can consider the Sonneberg bibliographic catalogue to be the continuation of the GuL. It is absolutely necessary to mention

"Star Clusters and Associations"
Publ. Astron. Dep. Eotvos Univ.
No.10, Budapest (1990)

the work of H. Huth in this connection, who directed this catalogue during more than 4 decades. Since his death in April 1988 the work on the bibliographic catalogue has been continued under my direction.

STRUCTURE OF THE SONNEBERG BIBLIOGRAPHIC CARD FILE

Since the late fourties the Sonneberg bibliographic card files has increased considerably. Continually all attainable literature on variable stars is being looked over and references are being excerpted and entered into the cards. Each of these entries generally consists of the name of the author, the year of the publication, the name of the publication, volume and page number, and one or a few key words characterising the contents of the publication. A total of nearly 47 000 objects is being supervised in this way. Most of them are named variable stars. The fourth edition of the General Catalogue of Variable Stars contains 28 457 stars. Since its appearance the stars of name-lists no. 67, 68, and 69 (published in IBVS 2681, 3058, and 3323, respectively) have been added, so that we have now 30 099 named variable stars. By the way, there exists a card file of the unnamed, so-called suspected variable stars in the order of the numbers used in the New Catalogue of Suspected Variable Stars (NSV). This catalogue contains a total of 14 811 objects. Since however 499 of them have been named in the meantime, there remain 14 312 in the card file. Moreover we have a special card file concerning about 2 700 very different objects with conspicuous physical properties, for example unnamed novae, X-ray sources, infrared sources, emission-line objects, unnamed variable stars detected at Sonneberg and so on. This card file has also proved to be very useful in our work. If a star of this file happens to be given a final variable star designation, the corresponding cards, which often contain a large number of entries, can be transferred into the card file of named variable stars.

THE BIBLIOGRAPHIC CATALOGUE OF VARIABLE STARS AT THE CDS

The Sonneberg bibliographic card files had been mainly intented for internal use. It became however more and more desirable to make this catalogue available to all observatories and interested astronomers. This is nothing but a natural consequence of the fact that the Sonneberg bibliographic catalogue was regarded as the continuation of the GuL. Therefore in 1973, after an arrangement with the Strasbourg Stellar Data Centre (CDS), at Sonneberg the storing of the contents of the card file for the named variable stars on electronic data carrier was started. At

intervals the material is sent to the Astrophysics Computing Centre in Potsdam-Babelsberg. There it is put in order and examined for errors by computer, and then transferred to the CDS for further processing and storage. The so resulting Bibliographic Catalogue of Variable Stars (BCVS) has been available on microfiches already for some years under the number 6022. The Astrophysics Computing Centre in Potsdam-Babelsberg acts as the sub-centre of the CDS and is also in a position to provide data from this catalogue. Those interested should pay attention to the remark in IBVS no. 2353. A detailed description of the BCVS you can find in the Information Bulletin of the CDS, no. 20, p. 131. At present this catalogue embraces the literature up to the year 1981 inclusive. We are kept busy correcting errors and inconsistencies still being found in the catalogue. Unfortunately, according to an agreement with C. Jaschek from the CDS in the early seventies, the above-mentioned key words have not been taken over into the BCVS. This is undoubtedly a handicap for the user, considering that there are several stars with more than 500 entries each. How can he know which of the references are relevant for his investigation? We therefore plan in future to add the key words to the references.

THE BIBLIOGRAPHIC CATALOGUE OF SUSPECTED VARIABLE STARS

In the meantime by the same procedure as for the named variable stars the contents of the Sonneberg card file for the NSV catalogue stars has been transferred to the CDS, and the Bibliographic Catalogue of Suspected Variable Stars (BCSVS) established. Closing date is the end of 1986. Included are all NSV objects with the exception of those stars that got a final designation in the name-lists no. 65 (IBVS 1921), no. 66 (IBVS 2042), and no. 67 (IBVS 2681) from NSV no. 5384 onwards. The stars of the name-lists 65 and 66 are included in the BCVS, the quoted stars of the name-list 67 will first appear in a supplementary edition of the BCVS, and the stars of the name-lists 68 and 69 (IBVS 3058 and 3323) are, under their NSV number, still included in the BCSVS, although a final designation has been given to them in the meantime. An inconvenience of this kind can never be avoided completely.

To save labour we have omitted the references from those journals that are extracted anyway by the CDS for the purposes of its Bibliographic Star Index (BSI; CDS Catalogue no. 6002). For completeness the BSI and/or SIMBAD data bases should therefore be consulted too. Experience shows that this is absolutely necessary for the brighter suspected variable stars because they are chiefly treated in the common journals, whereas frequently the fainter stars (say below 10^m) are only dealt with by papers in spe-

cialized publications, and mainly with those latter ones has been our concern. In future - that is, concerning the literature of 1987 and onwards - this unfortunate restriction will be removed. - More detailed information on the BCSVS you can look up in the Information Bulletin of the CDS, no. 35, p. 137.

CONCLUSION

To conclude I would like to say something about our further work on the bibliographic catalogue. Up to now we enter all references into the cards by hand. Inspecting arriving literature and entering the references into the cards has been two half-time jobs; putting the data on tape, another half job. Owing to the worldwide dramatically increasing publication rate the amount of work is fast growing beyond the limits of one and a half jobs, and we have to look after a more efficient procedure. We are planning to start, in course of this year, to excerpt and feed the new data directly into a computer. From there we can deliver the data immediately to the CDS sub-centre in Potsdam. The cards for our internal use then are to be printed from time to time by the computer. This promises to safe a lot of time and, moreover diminishes the rate of errors. We also hope for keeping the references quoted in the BCVS and BCSVS more closely up-to-date on the new publications.

Finally I should like to appeal to all colleagues interested in variable stars to send preprints and reprints of their papers to Sonneberg Observatory to guarantee proper inclusion of the titles in the BCVS.

LARGE VOIDS OF RICH CLUSTERS OF GALAXIES

K. Y. Stavrev
Department of Astronomy and National Astronomical Observatory
72 Lenin Blvd., 1784 Sofia
Bulgaria

ABSTRACT. The data in the machine-readable catalogue of clusters of galaxies with published redshifts, compiled by Lebedev and Lebedeva (1986), is used to search for large voids in the spatial distribution of rich clusters of galaxies in the north galactic hemisphere. A statistically homogeneous sample of 220 rich Abell clusters, defined by a limiting redshift $z \leq 0.14$ and galactic latitude $b \geq 30^{o}$, which is relatively complete for $z \leq 0.08$, has been processed. The void-searching procedure is based on the calculation of the distances from the nodes of a cubic grid, built in the investigated space, to the nearest neighbouring cluster of galaxies. Some 19 regions devoid of rich clusters of galaxies (12 "closed" voids and 7 "open" voids) have been detected, assuming minimal dimension of 80 Mpc for the selected voids (for Hubble constant $H_0 = 100$ km s^{-1} Mpc^{-1}). A list with data for the void parameters (coordinates of center, distance, dimensions, etc.) is given.

1. INTRODUCTION

The advance in our knowlidge of the large-scale structure of the Universe in the past decade is due mainly to the accumulation of more and more data for the redshifts of galaxies and clusters of galaxies. At present more than 20000 galaxies and about 2000 clusters and groups of galaxies have measured redshifts.

The studies of the spatial distribution of galaxies, based on these data, have shown clearly the existence of large regions with dimensions 20-60 Mpc (a Hubble constant $H_0 = 100$ km s^{-1} Mpc^{-1} is used in this paper), devoid of galaxies (Gregory and Thompson 1978; Kirshner et al. 1981; de Lapparent et al. 1986). If the clusters of galaxies are used as tracers of the large-scale distribution of galaxies, then the search for voids may be carried out in larger spatial volumes, to larger distances. Bahcall and Soneira (1982a, b) were the first to find out large voids in the distribution of clusters of galaxies. Later Schmidt (1983) and Batuski and Burns (1985) used extensive cluster surveys and discovered more

"Star Clusters and Associations"
Publ. Astron. Dep. Eötvös Univ.
No.10, Budapest (1990)

voids.

The purpose of the present paper is to determine on the basis of the increased amount of available redshift data the locations of the large voids in the distribution of clusters of galaxies, using a statistically homogeneous and relatively complete sample of rich clusters of galaxies. Unlike Batuski and Burns (1985), who use measured as well as estimated cluster redshifts, we have included in our sample only clusters with measured redshifts, avoiding in this way possible large errors in the distances to the clusters.

The volume occupied by the sample of rich clusters contains also a large number of poor clusters and groups of galaxies, which do not constitute a homogeneous and complete sample. Nevertheless, they may provide valuable information for the voids. The results from the processing of such a sample of rich and poor clusters will be given elsewhere (Stavrev 1989).

2. OBSERVATIONAL DATA

The search for large voids in the distribution of clusters of galaxies is based on the data in the catalogue of clusters of galaxies with published redshifts, compiled by Lebedev and Lebedeva (1986). Updated in 1988, it contains 1702 clusters and groups of galaxies from nearly 100 sources.

The preliminary analysis of the catalogue data has shown that it is highly inhomogeneous and incomplete in respect to the sky coverage, as well as in respect to the depth. Statistically homogeneous samples, which are complete to larger distances, can be formed only for the rich (richness class $R \geq 1$) Abell clusters (Abell 1958). Further on we present results from the processing of a sample of rich clusters in the north galactic hemisphere, which is more uniformly covered by the cluster surveys than the south galactic hemisphere.

The north galactic hemisphere contains 1110 clusters and groups of galaxies with measured redshifts. Out of them 427 are rich Abell clusters. The completeness limits of the sample of rich clusters by galactic latitude and redshift are defined from the distributions of the number density of clusters as a function of galactic latitude and redshift, given in Figures 1 and 2, respectively. It is seen from Figure 1 that the effects of galactic obscuration are not significant for $b > 40^{\circ}$. This value is chosen as completeness limit of the sample of $R \geq 1$ clusters. In order to avoid boundary effects near $b = 40^{\circ}$ the investigated volume is enlarged to $b \geq 30^{\circ}$.

Figure 2 shows that the spatial density of rich clusters does not decrease significantly to $z \leq 0.08$, which is the completeness limit of the sample of $R \geq 1$ clusters. Here we enlarge the volume to $z \leq 0.14$ in order to avoid boundary effects, and because of the large number of clusters in the redshift range 0.08–0.14. Thus, a sample of 220 rich clusters with $b \geq 30^{\circ}$ and $z \leq 0.14$ is formed, which is complete for $b \geq 40^{\circ}$ and $z \leq 0.08$ (80 clusters).

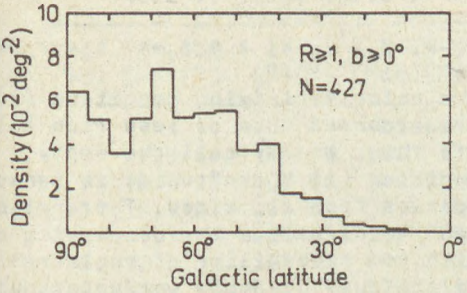

Fig. 1. Surface number density of rich clusters as a function of galactic latitude b for 427 clusters with $b \geq 0^{\circ}$.

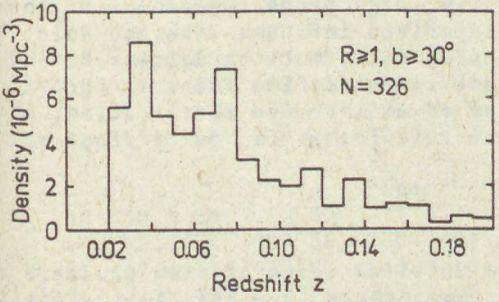

Fig. 2. Spatial number density of rich clusters as a function of redshift z for 326 clusters with $b \geq 30^{\circ}$ and $z \leq 0.20$.

3. THE VOID-SEARCHING PROCEDURE

The search for voids of clusters is based on the computation of the distances from the nodes of a cubic grid, built in the investigated volume, to the nearest neighbouring cluster of galaxies. Similar technics have been applied in studies of the voids in the distribution of galaxies by Aarseth and Saslaw (1982), and by Ryden and Turner (1984).

To construct the grid we use a 3-D Cartesian coordinate system, centered in our galaxy, with x axis directed to $l = 0^{\circ}$ and $b = 0^{\circ}$, y axis to $l = 90^{\circ}$ and $b = 0^{\circ}$, and z axis to the north galactic pole. The grid constant is $k = 20$ Mpc. The distances to the clusters are computed from the Hubble law with $H_0 = 100$ km s^{-1} Mpc^{-1}.

By computing the distances from every grid node to the nearest neighbouring cluster the investigated sample space is transformed into a discrete 3-D field $d(x, y, z)$, where d is the distance from the node with coordinates (x, y, z) to the nearest neighbouring cluster. The local minima in this field indicate the regions of the clusters and the superclusters, and the local maxima indicate the central regions of the voids of clusters.

The following criterion for the selection of large voids is adopted: large void of clusters is an empty region, indicated by a local maximum $d(x_v, y_v, z_v)$ in the field of nearest-neighbour distances $d(x, y, z)$, which satisfies the conditions

(i) $d(x_v, y_v, z_v) \geq d(x, y, z)$, and

(ii) $d(x_v, y_v, z_v) \geq 40$ Mpc,

where $x = x_v-k,\ x_v,\ x_v+k$; $y = y_v-k,\ y_v,\ y_v+k$; $z = z_v-k,\ z_v,\ z_v+k$ (k is the grid constant).

For convenience, we call the voids satisfying condition (i) "closed" voids because they are surrounded more or less from all sides by clusters. In contrary to this, we may call the empty regions which do not satisfy condition (i) "open" voids in sense that they have not defined boundaries from all sides. The application of the criterion for "closed" voids allows the processing of incomplete samples of objects with low probability of registration as voids of empty regions, which are due to sample incompleteness.

The maximal distance $d(x_v, y_v, z_v)$ gives the radius of the largest sphere, which can be inscribed into the detected void. The void itself may have a complicated form, but the void-searching procedure in its present variant cannot define forms different from spherical. The elaboration of an improved modification, which will permit to define arbitrary void forms, is now in progress.

4. RESULTS AND DISCUSSION

Table I contains a list of the detected voids of rich clusters of galaxies in the north galactic hemisphere ($b \geq 30^o$) to the limiting distance of 420 Mpc ($z \leq 0.14$). The first part of the table includes 12 "closed" voids. We have added to them 7 "open" voids. Only such "open" voids, which nearly satisfy the criterion for "closed" voids, are included in the list (i.e. 1-2 of the 26 neighbouring nodes of the central node (x_v, y_v, z_v) may have distances to the nearest neighbouring cluster $> d(x_v, y_v, z_v)$).

The following data for the voids is given in Table I: equatorial and galactic coordinates of the void center in columns 2-5, distance to the void center in column 6, diameter of the void (i.e. of the largest sphere, inscribed into the void) in column 7, angular dimension in column 8, indication for the position of the void center in the investigated volume in column 9: "1" means that the void is in the nearer $b \geq 40^o$ and $z \leq 0.08$ part of the volume, where the analysed sample is complete, and "2" is for the rest of the volume. Column 10 contains identifications with voids, detected by Bahcall and Soneira (1982a, b) and Batuski and Burns (1985).

From examination of different cross-sections of the field d(x, y, z) one can see that many of the detected voids overlap each other, or they are connected by "tunnels", forming in this way larger voids, or "multiple" voids.

The voids which are in the nearer, $b \geq 40^o$ and $z \leq 0.08$, part of the investigated space have higher probability of being real voids. There are 6 such "closed" voids in Table I.

Figures 3 and 4 show two cross-sections of d(x, y, z), the first one perpendicular to the galactic plain (y = 0 Mpc), and the second one parallel to it (z = 200 Mpc). The voids, whose centers lie in these cross-sections, are shown by the largest spheres inscribed in them. Two "open" voids are seen in Figure 3 (No. 15 and 19 from Table I), and 5 "closed" and "open" voids in Figure 4 (No.No. 8, 11, 12, 14, 16 from Table I).

TABLE I. Large voids of rich clusters of galaxies.

Void No.	RA (h)	DEC (°)	l (°)	b (°)	R (Mpc)	D (Mpc)	A (°)	C	Identifications
					"Closed" voids				
1	9.3	55	162	43	262	176	37	2	BS VOID, BB 9
2	10.8	29	202	64	245	96	22	2	
3	10.9	27	207	64	201	106	29	1	
4	11.1	15	236	63	157	88	31	1	
5	12.2	39	153	76	185	88	27	1	(BB 16)
6	13.0	15	315	77	123	116	51	1	
7	14.5	50	90	60	161	100	35	1	BOOTES VOID, BB 18
8	14.6	37	63	66	219	86	22	1	
9	16.0	58	90	45	368	164	25	2	
10	16.1	43	68	48	322	154	27	2	
11	16.4	47	73	44	289	142	28	2	(BB 24)
12	16.9	64	94	37	329	172	29	2	
					"Open" voids				
13	10.3	54	159	52	279	154	31	2	
14	12.3	-4	288	58	237	84	20	1	BB 14, (BB 15)
15	12.4	31	180	83	161	88	31	1	BB 16
16	12.7	63	124	54	247	86	20	2	BB 21?
17	13.2	35	90	81	122	98	44	1	(BB 18)
18	13.6	46	101	69	279	130	26	2	
19	14.4	10	0	61	206	90	25	1	

Notes: BS = Bahcall and Soneira (1982b)
BB = Batuski and Burns (1985)
Brackets in last column mean "partly".

The distribution of the 12 "closed" voids of rich clusters of galaxies on the sky is shown in Figure 5 in Lambert equal-area projection. The voids, given with their angular dimensions, are superimposed on the surface distribution of all rich Abell clusters with measured redshifts in the north galactic hemisphere. As it is seen from figure 5, most of the voids coinside with voids in the surface distribution of rich clusters with measured redshifts.

Some of the detected voids of rich clusters of galaxies can be identified with voids, known from previous investigations. Void No. 7 (Table I) is the well known void in Bootes (Kirshner et al. 1981; Bahcall and Soneira 1982a). Void No. 1, which is the largest void in our list (176 Mpc), is part of the 300 Mpc void, discovered by Bahcall and Soneira (1982b). We have identified also more or less surely 8 voids from Table I with voids from the list of Batuski and Burns (1985).

It has been already pointed out, that the voids of rich clusters percolate considerably, and this makes the determination of their dimensions and forms uncertain. However, if we assume that the largest spheres, inscribed into the voids, approximate well their real dimensions and form, then we may conclude from the data in Table I that the large voids of rich clusters have dimens-

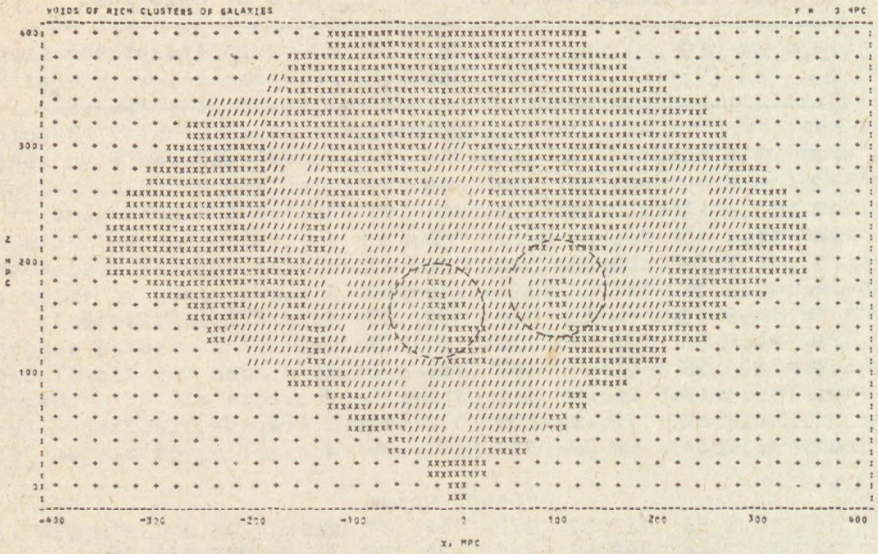

Fig. 3. The central cross-section (y = 0 Mpc) of the field of nearest-neighbour distances d(x, y, z). The coordinate system is centered in our galaxy with x axis directed to $l = 0^{o}$ and $b = 0^{o}$, the y axis to $l = 90^{o}$ and $b = 0^{o}$, and z axis to the north galactic pole. The grid nodes are shown only outside of the investigated volume by symbol "+". The blank squares (regions) inside the investigated volume indicate 20 Mpc elementary cubes, containing one or more clusters of galaxies. Symbols "/" and "X" mark the regions, devoid of clusters, where the grid nodes have distances to the neares neighbouring cluster $d < 40$ Mpc, and $d \geq 40$ Mpc, respectively. The voids, whose centers lie in this cross-section, are shown by the largest spheres, inscribed in them (voids No. 15 and 19 from Table I).

ions in the range 100-200 Mpc. Most reliable are the estimates of the dimensions of the "closed" voids, situated in volume 1 ($b \geq 40^{o}$ and $z \leq 0.08$; see column 9 in Table I). The mean diameter of these voids is 97 Mpc, while the mean diameter of the "closed" voids in volume 2 is 151 Mpc, i.e. about 50% larger. This is obviously due to the incompleteness of the sample of rich clusters in volume 2.

5. CONCLUSIONS

Rich clusters of galaxies with measured redshifts may be used as

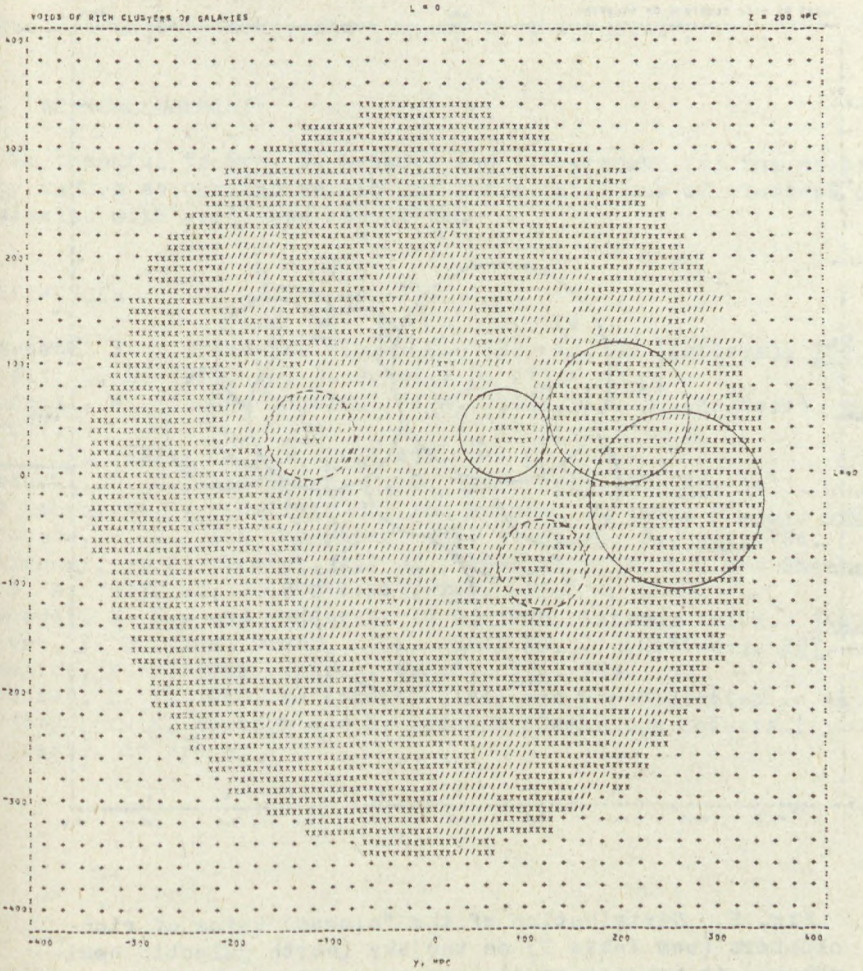

Fig. 4. Same as in Figure 3 for a cross-section, parallel to the galactic plain, corresponding to z = 200 Mpc. The "closed" and "open" voids (No.No. 8, 11, 12, 14 and 16 from Table I) with centers in this cross-section are indicated by solid-line circles and dashed-line circles, respectively.

tracers of the large-scale distribution of luminous matter in the Universe to determine the location in space of large regions, which are probably devoid of galaxies. About 20 such regions, candidates for real voids, are detected in the north galactic hemisphere to a limiting distance of about 400 Mpc, some of them

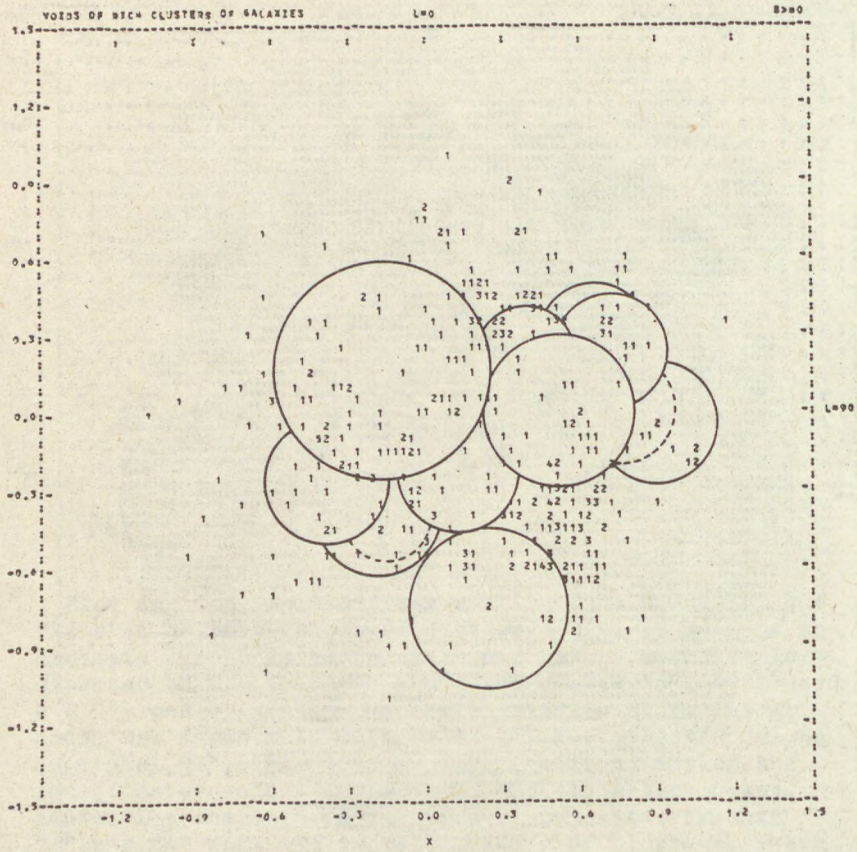

Fig. 5. Distribution of the "closed" voids of rich clusters (see Table I) on the sky (north galactic hemisphere) in Lambert equal-area projection, superimposed on the distribution of all $b \geq 0^{o}$ rich clusters of galaxies with measured redshifts (427 clusters). The coordinate system is centered in the north galactic pole with x axis along $l = 90^{o}$ and y axis along $l = 0^{o}$. The circles indicate the angular diameters of the largest spheres, inscribed into the voids. The more distant voids are plotted "hidden" behind the nearer ones. The numbers indicate the positions of the clusters.

known from previous investigations. The dimensions of the voids of rich clusters are of the order of 100-150 Mpc. They percolate and may form larger voids. The reality of the detected voids of rich clusters (as well as their dimensions and form) has to be verified by further measurements of the distances to all unmeasured

clusters in the background regions of the voids.

6. ACKNOWLEDGEMENTS

I am thankful to Drs. V. Lebedev and I. Lebedeva for the possibility to use an updated version of their catalogue of clusters of galaxies with published redshifts.

REFERENCES

Aarseth, S. J., and Saslaw, W. C. 1982, Ap. J. (Letters), 258, L7.
Abell, G. O. 1958, Ap. J. Suppl., 3, 211.
Bahcall, N. A., and Soneira, R. M. 1982a, Ap. J. (Letters), 258, L17.
_____. 1982b, Ap. J., 262, 419.
Batuski, D. J., and Burns, J. O. 1985, Astr. J., 90, 1413.
de Lapparent, V., Geller, M., and Huchra, J. 1986, Ap. J., 302,L1.
Gregory, S. A., and Thompson, L. A. 1978, Ap. J., 222, 784.
Kirshner, R. P., Oemler, A., Jr., Schechter, P. L., and Shectman, S. A. 1981, Ap. J. (Letters), 248, L57.
Lebedev, V. S., and Lebedeva, I. A. 1986, Astron. Tsirk., 1469, 4.
Ryden, B. S., and Turner, E. L. 1984, Ap. J. (Letters), 287, L59.
Schmidt, K.-H. 1983, Astron. Nachr., 304, 201.
Stavrev, K. Y. 1989, in Errors, Bias, and Uncertainties in Astronomy, ed. F. Murtagh and C. Jaschek (Cambridge University Press), in press.

A CATALOGUE OF BLUE STARS IN M33

G. R. Ivanov

Department of Astronomy, Sofia University,

Anton Ivanov Street 5. 1126 Sofia, Bulgaria

Abstract. A catalogue of blue stars was used to examine their distribution in M33. More than 5600 blue stars were detected and 1156 of them are candidate O stars. The slope of the luminosity function is derived. The maximum of stellar density occurs at the center of M33. The candidate O stars predominate in the central region and in the southern spiral arm. The radial distribution of blue stars is briefly discussed.

1. Introduction

Humphreys and Sandage (1980) studied bright blue and red stars in M33. They published BV photometry of 488 blue stars and the spectra of the brightest stars. Extensive photographic and CCD survey of M33 has been undertaken by Freedman (1984) using the 3.6 CFHT. Freedman (1985) has pointed that U-V criterion is an extremely useful discriminator against foreground contamination. She obtained the luminosity function (LF) and spatial distribution of 7778 blue stars in M33.

In the present study we added UBV photographic photometry of about 2000 blue stars in the associations and in the central region of M33. We obtained LF of the blue stars. Then we discuss the radial distribution of blue stars in M33.

2. Observational data.

The present study is based on data described by Freedman (1984) and on a photometry of the 2m Rozhen telescope at the Bulgarian Academy of Sciences. Freedman scanned plates taken with 3.6 m CFHT on automatic plate scanning machine (APM) in Cambridge, England. She was obtained U,B and V magnitudes and positions of stars. W. Freedman very kindly put at my disposal the computer catalogue which contains a stellar file with 20032 objects and another file with 45000 objects classified as nonstellar; many of them are unresolved stars with overlapping images, clusters, HII regions ect. The stellar file was used in the present study. Most of the

"Star Clusters and Associations"
Publ. Astron. Dep. Eötvös Univ.
No.10, Budapest (1990)

stars in this file are not members of M33. A large contamination from the dwarf stars of our galaxy is seen on the colour-magnitude diagram of Freedman (1985). If we accept Freedman's criterion U-V < 0, it is possible to eliminate the galactic foreground contamination. We selected 3705 stars with U-V and U-B < 0 from the stellar file and called them blue stars. The completeness of this photometry is V = 20 mag.

Photographic photometry was made independently on the 2 m Rozhen telescope. The plates 30x30 cm giving a field 1 x 1^{o} cover M33 entirely. The conventional iris photometry was not suitable for very crowded regions in the associations and near the center of M33. We used the photometer with an average constant slit 30 x 30 mk. The maximum density of star image was measured related to the mean background around it. A calibration curve was constructed for each plate. We used the photoelectric sequences of Sandage and Johnson (1974) and photoelectric data of Humphreys and Sandage (1980). The photoelectric observations of Hubble's comparison stars made by Sandage (1983) were used to check the accuracy of our photometry. The mean dispersion of our calibrations is less than 0.1 mag. The stars were measured at least on two plates. A comparison of the magnitudes V, B and U obtained from different plates are accurate to 0.1 mag for isolated stars but the errors increase to 0.3 mag in the crowded fields and in the center of M33 . The photometry of objects in OB84 = NGC 604 was not possible. Their magnitudes were evaluated by eye compared to the photoelectric standards. Most of the stars measured on Rozhen plates are in stellar associations. Photographic U, B and V photometry of 2500 stars was made. It was used for examination of the stellar associations in M33 (Ivanov, 1987). There are some differences between the two photometries which we discuss in the next section.

Freedman (1985) has shown that nearly all stars with U-V < 0 are members of M33. This criterion is apparent the from colour - magnitude diagrams presented by Freedman. In the present study we selected 5603 stars with U-V < 0 and U-B < 0 using APM and Rozhen photometry. Hereafter we call them blue stars.

3. Luminosity function.

A comparison of the luminosity functions obtained by APM and Rozhen photometries is shown in Figure 1 and in Table 1. It is clear that APM photometry is an incomplete set of bright blue stars which predominate in the stellar associations. The machine did not measure crowded regions. The level of APM incompleteness increases approaching both OB associations and the center (Figure 2). The combination of

Table 1. Luminosity functions of Freedman's (1984) and Rozhen photometries

V	15.2	15.8	16.2	16.8	17.2	17.8	18.2	18.8	19.2	19.8	20.0
N(F)	0	1	3	6	15	51	97	203	393	670	1082
N(R)	2	1	18	35	55	102	244	471	705	322	13

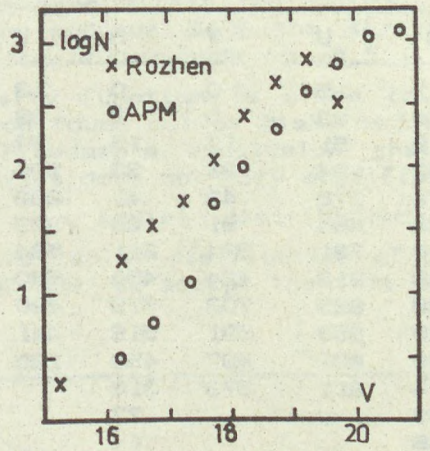

Figure 1. Luminosity functions according to APM and Rozhen photometries.

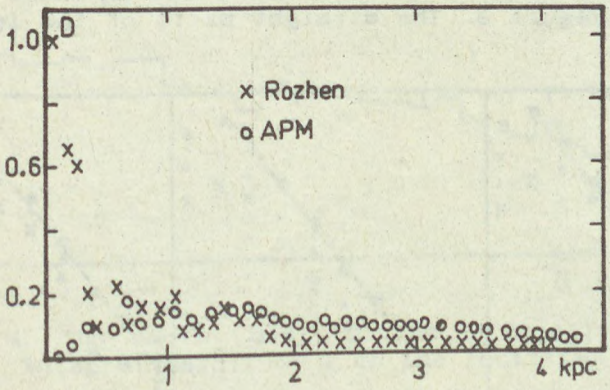

Figure 2. Radial distribution of blue stars. The APM photometry is incomplete approaching the center of M33. The number of Rozhen stars at radius R > 2 kpc is smaller than APM stars due to incompleteness down 19.5 mag.

APM and Rozhen sets is complete up to 19.5 mag. The number of blue stars in 0.5 interval bins is listed in Table 2. We

consider three U-V criteria as follows: blue stars with U-V < 0, candidate OB stars - U-V < -0.6 and candidate O stars - U-V < -0.9. The luminosity functions based on these criteria are shown in Figure 3. The straight parts of the luminosity

Table 2. Luminosity functions based on different colour intervals

Mag.	U-V < 0			U-V <-0.6			U-V <-0.9		
	V	B	U	V	B	U	V	B	U
15.25	2	1	15	0	0	13	0	0	9
15.75	2	4	32	0	2	29	0	1	14
16.25	21	19	51	17	15	38	8	6	17
16.75	41	42	124	26	33	100	9	15	66
17.25	70	72	278	42	41	232	13	16	157
17.75	153	148	484	91	106	389	44	64	236
18.25	341	310	781	224	211	584	121	113	278
18.75	674	649	913	424	452	560	203	254	176
19.25	1098	1026	825	702	679	420	311	289	121
19.75	922	850	953	531	519	441	202	203	81
20.25	1095	860	835	497	458	120	139	122	
20.75	1184	914	311	373	316		106	57	
21.25		538			77			7	
21.75		148			14			6	
22.25		21			3			2	

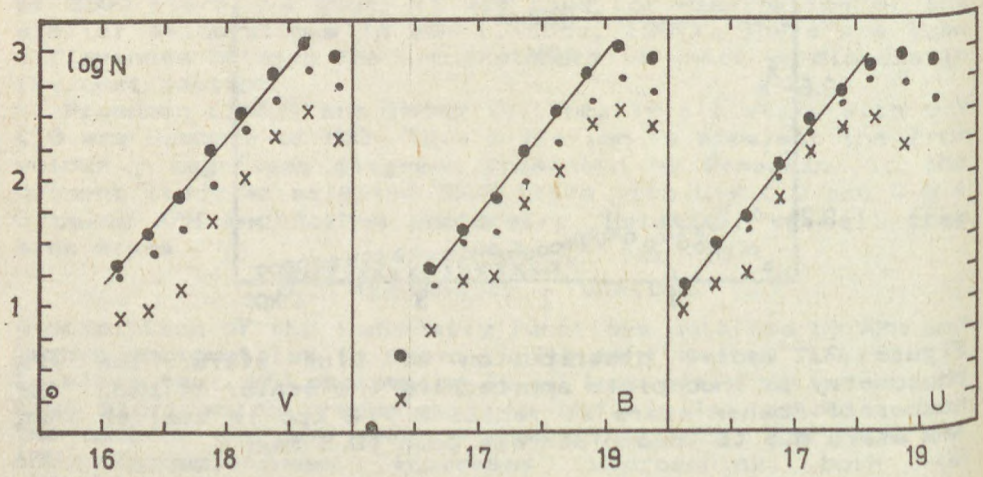

Figure 3. The luminosity functions based on three different U-V criteria.

functions are in 16 < V < 19.5 mag. interval. A least square fits the slopes d(log N)/d mag = 0.60 + 0.02 for blue stars where N is the number of stars in the 0.5 mag interval bins. This slope is appropriate for different U-V criteria. It seems that U-V < 0 is a good criterion against the foreground contamination stars. For each U-V colour criterion the slopes of the luminosity functions in U, B and V are nearly the same within the errors. If we accept an apparent distance modulus 24.8 the straight part of the luminosity function corresponds to $-8.5 < M_V < -5.5$. Our slope of luminosity function is close to the one for the solar neighborhood found out by Blaha and Humphreys (1988). We agree with Freedman's conclusion that the luminosity function of galaxies does not vary significantly.

4. Radial distribution

Figure 4 shows the radial distribution of blue stars on the rectified plot of M33. We accept the tilt angle i = 57 , the

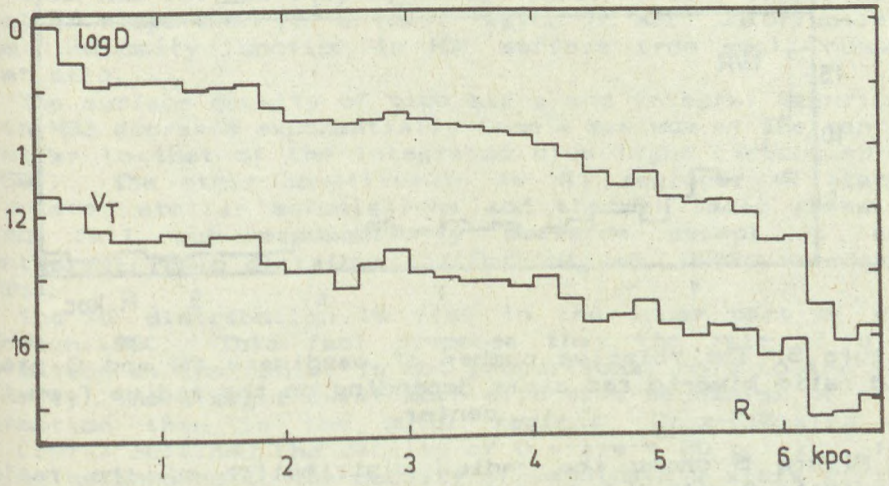

Figure 4. The radial distribution of stellar density and integral magnitude V on the rectified plot.

position of major axis = 22° and the true distance modulus = 24.2. The distribution shows a peak around the nucleus. The maximum of stellar density within the radius of 0.2 kpc is 406 stars per kpc^2. This value is accepted to be equal to the unit in Figure 4. Candidate O stars and B supergiantnts predominate there. The radius 0.3 < R < 2.0 kpc corresponds to the inner part of the two main spiral arms where the value of star density is lower than that the center.

Multiarm spiral features correspond to 2 < R < 4.4 kpc while the outer diffuse disk of the galaxy 4.4 < R < 7 kpc. The distribution of the integral magnitude V is also shown in Figure 4. It is similar to star density distribution.

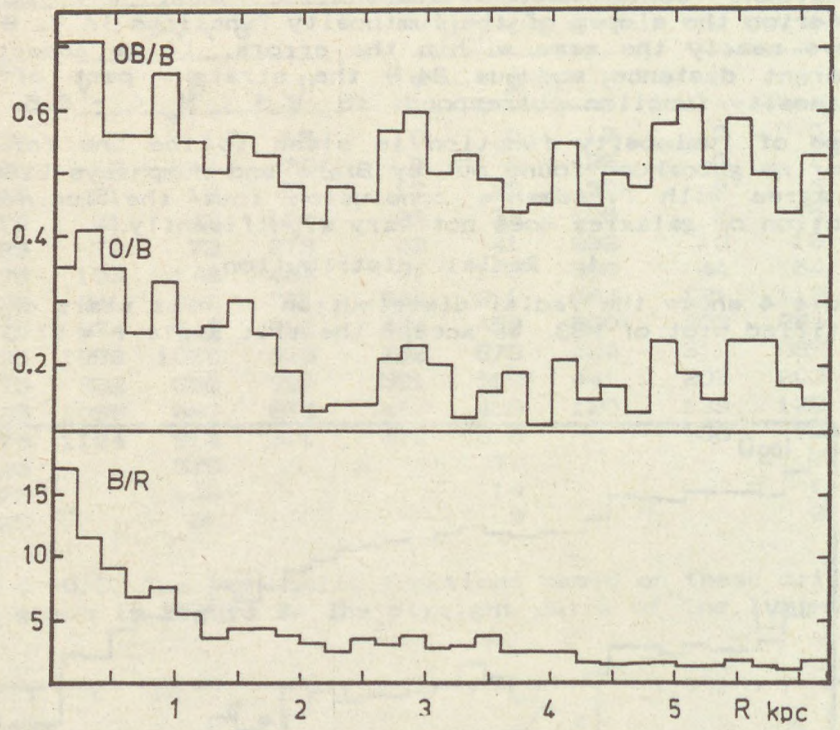

Figure 5. The relative number of candidate OB and O stars a..d ratio blue-to red stars depending on the radius from the center.

Figure 5 shows the radial .distribution of the ratios candidate O with U-B < -0.9 to blue stars O/B and candidate OB with U-B < -0.6 to blue stars OB/B. The main sequence O stars dominate in the latter sample while the OB sample is a mixture of O stars and B supergiants. The number of O and OB stars increases to the center of M33.

There are more stars in the southern region than in the northern. The ratio south/north is 1.39 for blue and OB stars and 1.58 for O stars. There is an additionally population of luminous blue stars with V < 17 mag in the southern region (65%) and 35 % in the north as could be seen in Table 3. It is clear that there is a deficiency of OB and

O stars in the north. A similar asymmetry has been noted by Berkhuijsen (1983) and Freedman (1984).

5. Discussion

We used three different U-V criteria to obtain the slope of the luminosity function. It does not differ for the three samples. The mixture of O stars, B and A supergiants in the first sample has nearly the same slope as the upper main sequence O stars in the latter sample. Consequently the slope of the luminosity function does not depend on a fraction of evolved B and A supergiants. Berkhuijsen and Humphreys (1988) obtained flatter luminosity function for the sample of B and A supergiants than that of O stars. Probably the fraction of the evolved stars in M31 is larger than in M33. Our value 0.60 is close to the average slope of the luminosity functions (0.67) found out by Freedman (1985). On the other hand, Blaha and Humphreys found out a slope of the luminosity function in U = 0.62 for the solar neighborhood 0.62. This value is nearly the same as our slope. Berkhuijsen and Humphreys (1988) obtained a slope = 0.72 in M31 for the O stars. Hodge et al. (1988) suggested a flatter slope 0.53 for a small region in M31. Unfortunately the luminosity function in M31 suffers from small number statistic.

The surface density of blue stars and integral magnitude V in M33 decrease exponentially from a maximum at the center similar to that of the integrated blue light (Vaucouleurs, 1959). The other constituents as HII regions, WR stars, clusters, stellar associations and thermal radio emission also fall out exponentially outwards except HI and nonthermal radio distribution (Berkhuijsen, 1983; Freedman, 1984).

The HI distribution is flat in the inner part of M33 (Newton,1980). This fact proposes that the rate of star formation at the center is not proportional only to the gas density. There might exist more effective mechanism of star formation than in the outer regions. Gruz-Conzalez et al.(1974) obtained the density of O stars = 20 per kpc^2 for solar neighborhood. The density of candidate O stars at the center of M33 is ten times higher. It is evident that the fastest rate of star formation is in the nucleus region of M33.

The maximums of O stars at 1 - 1.5 kpc in Figure 5 is due to the southern spiral arm. They outline a band about 100 pc wide and 2 kpc long at the inner border of S1. The first observational evidences for spiral wave density theory were provided by Dubout-Crillon (1977). Our data support this suggestion. However, the distribution of the most luminous blue stars does not support this theory. The blue stars with $M_v < -7$ outline a diffuse and wide spiral arm without any

age gradient. It seems that the star formation of the most massive stars begins beyond the front of the wave density.

It is clear now that a Sc galaxy as M33 is richer of bright blue supergiants, O stars and stellar associations than a Sb-type galaxy as M31. In the present study we confirm the conclusion that the brightest stars in M31 are fewer and fainter than those in M33 (Berkhuijsen and Humphreys, 1988 and Nedialkov et al., 1989).

Table 3. The brightest blue stars in M33.

R.A.	D	V	B-V	U-B	REM.
1 31 17.8	30 34 56.2	15.00	0.40	-0.40	Q8
1 30 45.8	30 20 39.3	15.20	0.30	-0.40	var C
1 31 6.5	30 30 9.3	15.20	0.00	-0.20	B324,M
1 30 50.8	30 13 24.3	15.87	0.42	-0.66	
1 31 1.0	30 23 13.7	15.90	0.00	-0.20	b246
1 30 21.9	30 29 54.3	16.10	-0.40	-0.70	ns
1 30 56.8	30 21 32.5	16.10	0.00	0.00	TU,M
1 31 50.8	30 30 41.7	16.10	0.00	-0.70	B552,M
1 30 52.0	30 7 14.3	16.10	0.10	-0.90	110A,D
1 31 8.8	30 17 47.9	16.20	-0.10	-0.90	5A,M,A3Ia
1 30 59.8	30 36 31.5	16.20	0.00	-0.80	B255,ns
1 30 13.8	29 55 58.6	16.20	0.20	-0.90	
1 31 17.1	30 26 26.5	16.30	-0.30	-0.60	B416,M
1 30 46.8	30 46 13.5	16.30	-0.10	-0.40	B158
1 31 9.3	30 20 5.8	16.40	0.10	-1.20	B457,M
1 31 26.9	30 36 34.1	16.40	0.00	-1.30	n,M
1 30 50.6	30 23 5.7	16.40	-0.10	-0.30	M
1 30 22.7	30 23 31.9	16.40	0.00	-1.00	b287
1 31 44.0	30 31 44.9	16.40	0.00	-1.60	n
1 31 10.6	30 7 38.2	16.40	0.10	-0.70	1
1 30 22.0	30 33 35.4	16.40	0.00	-0.60	B92a
1 31 1.6	30 22 58.5	16.40	0.20	-0.90	
1 30 59.9	30 22 48.5	16.40	-0.40	-0.20	varB
1 31 27.3	30 16 5.2	16.40	0.30	-0.70	
1 30 59.6	30 26 59.7	16.46	0.54	-0.89	
1 31 21.5	30 19 16.8	16.46	0.26	-1.17	
1 31 28.9	30 23 16.2	16.48	0.20	-1.25	
1 30 22.7	30 19 0.1	16.50	0.00	0.00	B57,D
1 30 39.6	30 32 22.9	16.50	0.00	-0.70	B133
1 30 23.4	30 24 54.2	16.50	0.00	-0.20	TI
1 30 44.4	30 26 10.5	16.50	0.10	-0.50	B167a
1 31 18.9	30 23 41.7	16.50	-0.20	-0.30	96A=HS05
1 31 28.9	30 23 16.2	16.50	0.20	-1.30	var2
1 31 21.5	30 19 16.8	16.50	0.20	-1.10	
1 31 10.6	30 18 33.9	16.60	0.00	-0.90	B466,M
1 31 8.9	30 17 59.9	16.60	0.00	-0.40	D
1 31 8.5	30 17 41.7	16.60	0.10	-0.30	B475

Table 3 (continued).

R.A.	D	V	B-V	U-B	REM.
1 29 53.7	30 23 24.2	16.60	-0.30	-0.50	
1 31 0.7	30 26 5.1	16.60	0.00	-1.00	
1 31 21.1	30 30 28.1	16.60	0.20	-0.60	
1 31 10.2	30 7 48.6	16.60	0.20	-0.50	
1 30 11.1	30 7 59.5	16.60	-0.20	0.10	117A
1 31 1.4	30 23 14.2	16.60	-0.40	-0.40	
1 30 7.2	30 23 22.3	16.62	-0.74	-0.10	
1 30 23.4	30 24 54.2	16.67	0.02	-0.24	
1 30 7.2	30 23 22.3	16.70	0.20	-1.10	B26
1 30 44.9	30 26 15.1	16.70	-0.20	-0.70	B170
1 30 44.2	30 26 10.5	16.70	0.10	-1.00	Q1
1 31 43.5	30 31 39.3	16.70	-0.10	-0.60	
1 31 26.7	30 18 24.1	16.70	0.00	-0.90	B526
1 30 27.1	30 37 28.1	16.70	0.70	-0.90	B103
1 31 3.0	30 23 39.3	16.70	-0.70	0.30	
1 30 53.8	30 23 46.3	16.70	-0.10	-0.80	

The designation of blue stars of Humphreys and Sandage (1980) was used. The letters ns, n and M correspond to objects suspected as nonstellar, nebulous and multiple.

References:

Berkhuijsen, E.M.: 1983, Astron. Astrophys. 127, 385.

Berkhuijsen, E.M., and Humphreys, R.M.: 1988, Astron. Astrophys., in press.

Blaha, C. and Humphreys, R.M.: 1988, preprint.

de Vaucouleurs, G.: 1959. Astrophys. J. 130, 728.

Dubout-Crillon, R.: 1977, Astron. Astrophys. 56, 293.

Freedman, W.L.: 1985, Thesis, University of Toronto.

Freedman, W.L.: 1985, Astrophys. J. 299, 74.

Gruz-Conzalez,C., Recillas, E., Costero, R., Peimbert,M and Peimbert, S.: 1974, Rev. Mex. Astron. Astrofis. 1, 211.

Hodge, P.W., Lee, M.G., and Mateo, M.: 1988, Astrophys. J. 324, 172.

Humphreys, R.M. and Sandage, A.: 1980, Astrophys. J. Suppl. 44, 319.

Ivanov, G.R.: 1987, Astrophys. Space Sci. 136, 113.

Nedialkov, P.L., Kourtev, R.G. and Ivanov, G.R.: 1989, Astrophys. Space Sci., in press.

Newton, K.: 1980, Monthly Notices Roy. Astron. Soc. 190, 689.

Sandage, A.:1983, Astron. J. 88, 1108.

Sandage, A. and Johnson, H.L.: 1974, Astrophys. J. 191, 63.

ASSOCIATIONS IN M31 AND M33

N. S. NIKOLOV
University of Sofia
Faculty of Physics
Department of Astronomy
Anton Ivanov Street 5
1126 SOFIA, Bulgaria

ABSTRACT. A review of the studies of groups of luminous stars in the nearby galaxies M31 in Andromeda and M33 in Triangulum on the basis of a photographic observational material taken by the 2-meter Ritchey-Chrétien telescope of the Bulgarian Academy of Sciences is made.

One of the important points discussed is about the nature of the groups of bright stars in M31 and M33. Efremov et al. (1987) came to the conclusion that the recognized by van den Bergh (1964) on the Tautenburg Schmidt plates associations in M31 are not associations but mostly star complexes. The by Efremov et al. newly recognized associations in M31 show a size distribution which resembles that of the Large Magellanic Cloud. Their mean diameter is near to the mean diameter of the associations in the Small and Large Clouds, as well as that of our Galaxy. Such a revision of the distinguished by Humphreys and Sandage (1980) associations in M31 was made by Ivanov (1987), who came to analogous results.

Photometric measurements of the bright stars inside and outside of the groups of young stars mainly in M31 are used for the construction of colour-magnitude diagrams of those groups. Some characteristics of the associations, obtained from these diagrams show different behaviour in different spiral arms. For the arm S4 that behaviour agrees with the predictions of the density wave theory.

INTRODUCTION: One of the projects carried out by means of the 2-meter Ritchey-Chrétien (RC) telescope of the National Observatory of the Bulgarian Academy of Sciences is the investigation of nearby galaxies. One of the most important objects in these galaxies are the associations of young luminous stars because of the allowance they give to study the structure of the galaxies and some aspects of star formation in them. The limiting magnitude ($\approx 20.5^m$ in U and V and $\approx 21.5^m$ in B) and the plate scale (12.8" mm^{-1} on 30x30 cm plates for $1^o x 1^o$ field) of the RC telescope are very

"Star Clusters and Associations"
Publ. Astron. Dep. Eötvös Univ.
No.10, Budapest (1990)

appropriate to discern the groups of the bright stars in the galaxies M31 in Andromedae and M33 in Triangulum and to construct the uppermost parts of the main sequences of the colour-magnitude diagrams.

In M31 van den Bergh (1964) recognized on plates of the 2-meter Tautenburg Schmidt (scale 54" mm^{-1}) 188 vast groups of bright stars he called OB-associations. Humphreys and Sandage (1980) on plates of the 5-meter Hale reflector (11.06" mm^{-1}) distinguished 143 such groups in M33 also called by them associations.

The U-plates of the 2-meter RC telescope allowed to separate 54 new associations in M33 (Kunchev and Ivanov, 1984). An attempt in this direction for M31 revealed not only new associations (Efremov, 1982a; Efremov et al., 1985) but gave the possibility to distinguish in more details different groups of stars with high temperature and brightness.

Groups of high temperature luminous stars in M31. Nearly 20 years ago Hodge and Lucke (1970), comparing the size of catalogued by them 122 associations in LMC (Lucke and Hodge, 1970) with the size of the 188 van den Bergh's associations in M31, which are on an average more than about five times larger than that in the LMC, stated that "selection effects may also explain the differences between the size distribution of stellar associations in M31 and that for the LMC. The vast majority of the LMC associations are smaller than 150 pc, whereas almost all of the M31 associations are larger than this. Possibly because of the limitation of resolution and because of a different set of rules of discrimination, the M31 survey did not include many associations that may exist with diameters smaller than this limit". Later on discussing the same matter Sharov (1982) pointed out that with the term "associations" one may name

different objects and that "when they compare the associations in different galaxies it is necessary to be sure that they deal with one and the same kind of objects". After a more detailed study Hodge (1985) concluded that "the differences in the published characteristics of the samples arise from the use of different observational material and selection criteria" and that "the difference is probably not real". Bearing in mind the above cited inferences and taking into account Efremov's (1982b) suggestion that most of van den Bergh's associations in M31 are star complexes, he terms thus very large groups of young stars, which may contain star clusters and associations (Efremov, 1978, 1979), as well as cepheids, as important indicators (Efremov, 1978, Efremov et al., 1981), a new search of groups of bright stars in M31 was undertaken using the more appropriate for this aim observational material from the 2-meter Bulgarian telescope. Before that an attempt to define more precisely the criteria for discriminating an association on a photograph of a nearby galaxy as M31 was made (Zlatev and Ivanov, 1985). The main results are as follows (Efremov et al., 1987).

On U-plates were distinguished 210 groups of bright stars, which in majority appear as subclusterings of the van den Bergh's associations (only 15 are outside the boundaries of them), which are considered as just OB-associations. We find thirteen of them in the list of the open clusters by Hodge (1979). The normalized distribution of the measured along the major axis of M31 diameters of the thus newly discriminated associations is almost the same as for the LMC associations (Fig. 1.).

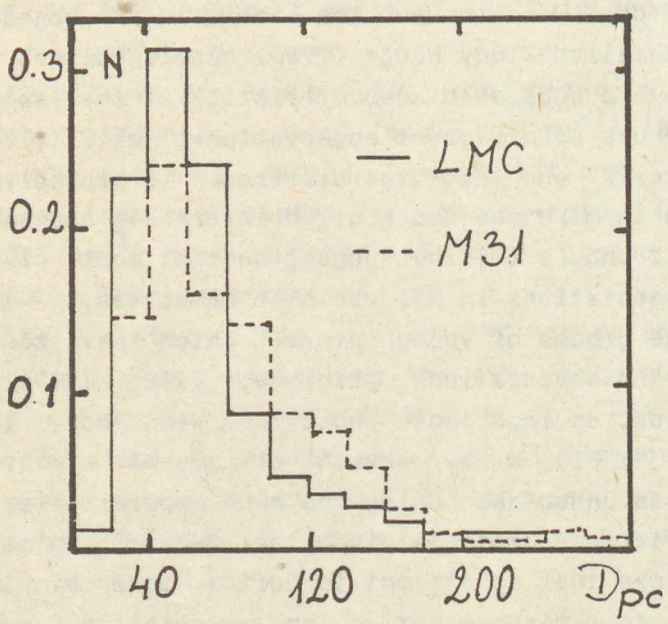

Fig. 1.

As for van den Bergh's associations we consider the majority of them as star complexes. An independent delineation of star complexes taking into account not only the surface density of the resolved on our B-plates stars, but the other considerations connected with the physical means of the term star complex divorces many of van den Bergh's associations on two or more complexes. The mean diameter of these complexes (measured along the major axis of M31) is 650 pc, close to but greater than the mean diameter of star groups denoted by van den Bergh, as associations, which is 480 pc.

After the paper by Efremov et al. (1987) they may conclude that the sizes of the associations in the Galaxy, the LMC and SMC (Hodge, 1985), as well as in M31 are very close one to the other. Their mean diameter is about 80 pc. Only the associations in M33 appeared to be larger with a mean diameter of about 200 pc after Humphreys and Sandage (1980). This situation was revised by Ivanov (1987). He inspected plates taken with the 2-meter RC telescope of the Bulgarian National Observatory and succeeded to distinguish about 460 - the smallest resolved star groups. Their size distributions, as their mean size, resemble those of the LMC and M31 and this fact shows that these star groups are identical with the associations in the other nearby galaxies. Often 2 or 3 associations in M33 form larger groups and such groups are named associations by Humphreys and Sandage (1980). Ivanov estimated the mean size of these larger groups as 250 pc. Moreover Ivanov (1987) reecognized 55 star complexes with a mean size along the major axis of M33 of 570 pc, which is near to the mean size of the star complexes in M31.

The paper by Ivanov (1987) together with the other papers, which show the sizes of the different groups of luminous stars in the nearby galaxies arise once more the question whether the obvious discrimination of sizes - roughly 100, 200, 600 pc - is by chance or the cause of this feature is the star formation mechanism (see Efremov et al., 1987).

Colour magnitude diagrams. The photographic photometry of the separate stars belonging to a group in a nearby galaxy allows the construction of the uppermost parts of its colour-magnitude (CM) diagram. Even only such a part of the diagram with a great dispersion in addition gives the possibility to obtaine some important characteristics of the measured group, although with great uncertainties. These characteristics for a number of associations, situated in a

part of the galaxy, give the possibility to receive some idea about structural and evolutionary features of this part.

With the above mentioned considerations in mind the group at the Department of Astronomy of the University of Sofia, studying nearby galaxies, constructed the colour-magnitude diagrams for a number of groups of bright stars mainly in M31. In M33 up to now have been investigated only a few groups.

M33 associations. About ten years ago Humphreys and Sandage (1980) were the first to construct the CM diagrams for six of the associations, recognized by them in M33. Using the turnoff points, as well as the calculated evolutionary tracks, they estimated the ages of the six associations to be about 5×10^6 years. Although with an error of about 0.5 mag they determined the turnoff points and estimated its ages to be in a range of $(4\text{-}6) \times 10^6$ years, independently of their situation along and across the spiral arms of the galaxy.

Few years ago Kunchev and Nikolov (1986) investigated photometrically three fields, situated in the southern region of M33 - namely the associations 110 and 112 from the list of Humphreys and Sandage (1980) plus a star-field (SA) situated in proximity of the associations covered uniformly with relatively faint stars. A preliminary announcement for the photometry of OB 112 has appeared earlier (Kunchev and Ivanov, 1985). More than 60 stars in OB 110, 90 in OB 112 and 50 in Na were photometried in UBV and CM and two-colour diagrams were formed. Using the constructed by Hodge (1983) calibration between the age and the absolute magnitude M_V of the brightest mainsequence star of star clusters it was determined that the age of OB 110 is 4.2×10^6 years, whereas of OB 112 it is 6.5×10^6 in agreement with the ages of other associations in M33.

M31 associations. The modern study of the CM diagrams of groups of bright stars in other galaxies began with the paper by Baade and Swope (1963), in which a CM diagram of the brightest stars in Baade's Field IV in the Andromeda nebula is given, as well as the CM diagram of the so called by them "Big Association", listed later on with number 184 by van den Bergh (1964). The CM diagram of van den Bergh's richest OB 78 association was obtained by van den Bergh (1966) on the plates taken with the 84" Kitt Peak telescope. Once more Baade's Field IV was studied photomerically and the CM diagram of OB 184 was obtained by Racine (1967) and somewhat later on by Humphreys (1979) with CM diagrams of OB 184 and OB 185 as a result.

So it is evident that when they began to study M31 by means of the 2-meter RC only few papers, devoted to the photomerty of the bright stars in the Andromeda galaxy existed. The first one who used the observational material of the 2-meter RC together with such a material taken with the 1-meter reflector of the Institute of Astrophysics of the Tadzhik Academy of Sciences and obtained preliminary CM diagrams for 4 associations in M31 was Efremov (1982a).

Using observational material from the 2-meter RC telescope Ivanov and Kunchev (1985) concentrated their attention on the CM diagrams of the associations in the spiral arm S4 of M31. Obtaining the ages of the associations using Hodge's calibration they found out a pronounced age gradient not only across, but also along the spiral arm S4.

An extensive photometry of nearly 700 stars in the UBV in the spiral arm S4 was carried out by Ivanov (1985 a, b) mainly to obtain the behaviour of some characteristics of the associations across the arm. The main results are that the number of stars, as well as their mean magnitudes and colours decreases from the inner to the outher edge of S4 which agree with the earlier results obtained by Efremov and Ivanov (1982), whereas the age increases toward the outer

edge, which is in agreement with the density wave theory too. Another prediction of this theory was confirmed by a study of the absorption across the arm S4, which shows a cocentration of the absorbing matter at the inner edge of the arm (Ivanov and Golev, 1984).

An investigation of the surface brightness behaviour in UBV across not only the arm S4, but other spiral arms of M31 as well was carried out on the plates taken with the 50-cm Schmidt telescope of the National Observatory by Georgiev and Ivanov (1985). The results are that the surface bightness increases toward the inner edges of the arms 3, 4 and 5, whereas for the arms 6 and 7 the maximum of the surface brightness is around their middles.

A photometric study of the bright stars in the associations OB 54 and OB 56 in the spral arm N4 shows that the luminosity, as well as the surface density of the stars increases toward the inner edge of this arm, which agrees with the density wave theory too (Ivanov, Nedyalkov and Kunchev, 1986). But since the gardient of luminosity is not so pronounced as in S4, the authors supposed that in different groups of stars, especially in OB 54, there are different star formation mechanisms.

More than 1000 bright stars inside and outside the associations in the spiral arm S5 of M31 were photometrically studied using UBV plates recently by Nikolov and Tasheva (1989) by continuing the photometry of the same arm carried out by Kurtev (1985) and Kurtev and Ivanov (1986). The CM and the colour-colour diagrams for about twenty associations were constructed. The behaviour of the derived colour excesses E_{B-V} twelve of these associations containing about 20 and more stars show an increase of the obscured matter in the southern edge of S5 in comparison with its other parts. Along S5 the absorption increases though not so steeply as in S4 after Ivanov (1985) and Ivanov and Kunchev (1985). The ages of the studied

associations, obtained by means of Hodge's (1983) calibration, do not show either an increase along the arm S5, or across it, which is quite different with the association age behaviour in the arm S4 (Ivanov and Kunchev, 1985). The ages of the associations in the arm S5 are from 0.9×10^7 to about 1.7×10^7 years. In general the ages for the associations in M31 are greater than those in M33 which may be in agreement with the conception that M33 as an Sc galaxy is younger than M31 as an Sb galaxy.

The ratio of the blue to red supegiants B/R in the associations of S5 does not decrease along the arm S5. The main value of this ratio for the associations of S5 is about 4, as it was derived by Kurtev and Ivanov (1986). If we accept the mean ratio for S4 from the paper by Efremov (1982a), which is about 15, and for S6 from Baade and Swope (1963), we can conclude that the ratio of the blue to red supergiants increases with the distance from the center of M31, as was concluded earlier by Efremov (1982a) and Kurtev and Ivanov (1986). But it is necessary to take into account that the criteria for the selection of red supergiants in the different papers are different. So we think that such a conclusion is yet rather hasty. A conclusion that on an average the ratio B/R is smaller for M33 (Humphreys and Sandage, 1980) appears more reliable, which may be interpreted as an inference that M33 is younger than M31.

The most luminous stars. The comparison of the photometric characteristics of the stars in some investigated nearby galaxies with those of the Milky Way shows similarity. So Kunchev and Nikolov (1986) show that the integral absolute magnitudes of the association OB 110 and OB 112 in M33 are comparable with the integral absolute magnitude of the groups of bright stars in our Galaxy and M31. The same conclusions are drawn by Nikolov and Tasheva (1989). These authors concluded that the brightest stars in M31 are as bright as those in M33 and our Galaxy in

agreement with the analogous conclusion by Kunchev and Ivanov (1986), who added also the Magellanic Clouds. Efremov and Ivanov (1987) show that the absolute magnitude of the brightest red supergiants in M31 is $M_V \approx -8^m$. Sandage and Tammann (1974) obtained $M_V = -7.9 \pm 0.1$ mag for the red supergiants in galaxies with various luminosities, as it was obtained by Humphreys (1983) too. The recept result of Sandage (1985) is that M_V of the red supergiants ranges from ≈ -7 to ≈ -9 mag, when the luminosities of parent galaxies range from ≈ -13 to ≈ -22 mag. As for the blue supergiants Sandage (1985) obtained M_B from about -6.5 to about -10 mag for the same range of the luminosities of parent galaxies. These results are in connection with the use of the brightest stars as distance indicator. The recent result obtained by Golev, Ivanov and Kunchev (1987), who applied a noise-reduction followed by an image enhancement technique and showed that some of the brightest blue stars in M33 are not stars but stellar groups - double or multiple stars or even star clusters - brings difficulties in the practical use of the brightest stars in other galaxies as indicators of its distances.

CONCLUSION: The reviewed investigations of the brightest luminous stars in the two nearby galaxies M31 and M33 allowed the drawing of some interesting conclusions on the existence of different groups of bright stars in the studied galaxies, on some features of the stars in some arms of M31, which agree with the predictions of the density wave theory and with some age characteristics of the stellar groups and the galaxies themselves.

The obtained results show the good opportunities provided by the 2-meter Ritchey-Chrétien telescope of the Bulgarian National Observatory. Perhaps the most important result is that all that is achieved provides a reliable basis for future investigations.

REFERENCES

Baade, W. and Swope H., 1963, Astron. J. 68, 435.
Bergh, S. van den, 1964, Astrophys. J. Suppl., 9, 65.
Bergh, S. van den, 1966, Astron. J., 71, 219.
Efremov, Yu. N., 1978, Astron. Zh., Letters, 4, 125.
Efremov, Yu. N., 1979, Astron. Zh., Letters, 5, 21.
Efremov, Yu. N., 1982a, Astron. Zh., Letters, 8, 585.
Efremov, Yu. N., 1982b, Aston. Zh., Letters, 8, 663.
Efremov, Yu. N., Ivanov, G. R. and Nikolov, N. S., 1981, Astrophys. Space Sci., 75, 407.
Efremov, Yu. N. and Ivanov, G. R., 1982, Astrophys. Space Sci., 86, 117.
Efremov, Yu. N. and Ivanov, G. R., 1987, Astrophys. Space Sci., 129, 39.
Efremov, Yu. N., Ivanov, G. R. and Nikolov, N. S., 1985, IAU Symp. No. 116 "Luminous Stars and Associations in Galaxies", De Loore C. W. H. et al. (eds.), Domdrecht, Reidl, p. 389.
Efremov, Yu. N., Ivanov, G. R. and Nikolov, N. S., 1987, Astrophys. Space Sci., 135, 119.
Georgiev, Ts. B. and Ivanov, G. R., 1985, Astron. Zh. Letters, 11, 178.
Golev, V. K., Ivanov, G. R. and Kunchev, P. Z., 1987, Astrophys. Space Sci., 135, 301.
Hodge, P. W., 1979, Astron. J., 84, 744.
Hodge, P. W., 1983, Astrophys. J., 264, 470.
Hodge, P. W., 1985, IAU Symp. No. 116, De Loore, C. W. H. et al. (eds.), Dordrecht, Reidel, p. 369.
Hodge, P. and Lucke, P., 1970, Astron. J., 75, 933.
Humphreys, R. M., 1979, Astrophys. J., 234, 854.
Humphreys, R. M., 1983, Astrophys. J., 269, 335.
Humphreys, R. M. and Sandage, A., 1980, Astrophys. J. Suppl., 44, 319.
Ivanov, G. R., 1985b, Astrophys. Space Sci., 110, 357.

Ivanov, G. R., 1985a, C. R. Bulgarian Ac. Sci., 38, 819.
Ivanov, G. R., 1987. Astrophys. Space Sci., 136, 113.
Ivanov, G. R. and Golev, V. K.,
1984, Astron. Tsirculiar No. 1352.
Ivanov, G. R. and Kunchev, P. Z.,
1985, Astron. Zh. Letters, 11, 737.
Ivanov, G., Nedyalkov, P. and Kunchev, P.,
1986, Astron. Tsirkuliar No. 1435.
Kunchev, P. Z. and Ivanov, G. R.,
1984, Astrophys. Space Sci., 106, 371.
Kunchev, P. and Ivanov, G.,
1986a, Astron. Tsirculiar No. 1386.
Kunchev, P. Z. and Ivanov, G. R.,
1986b, R. Acad. Bulg. Sci., 39, 5.
Kunchev, P. Z. and Nikolov, N. S.,
1986, Astrophys. Space Sci., 127, 327.
Kurtev, R. G., 1985, Master Degree Thesis, Univ. of Sofia.
Kurtev, R. G. and Ivanov, G. R.,
1986, Astron. Tsirkuliar No. 1435.
Lucke, P. and Hodge, P. W., 1970, Astron. J., 75, 171.
Nikolov, N. S. and Tasheva, R. P.,
1989, Astrophys. Space Sci.,152, 239.
Racine, R., 1967, Astron. J., 72, 65.
Sandage, A., 1985, IAU Symp. No. 116, De Loore et al.
(eds.) Dordrecht, Reidel, p. 31.
Sandage, A. and Tammann, G. A.,
1974, Astrophys. J., 191, 603.
Sharov, A. S., 1982, "The Andromeda Galaxy", (Moscow: Nauka), p. 149, 151.
Zlatev, S. S. and Ivanov, G. R.,
1985, C. R. Acad. Bulg. Sci., 38, 822.

BRIGHT ASSOCIATIONS IN M33

G. R. Ivanov

Department of Astronomy, Sofia University,

Anton Ivanov Street 5, 1126 Sofia, Bulgaria

Abstract. Bright stellar associations in M33 were selected. Their coordinates, integral properties, sizes, the number of blue member stars and HII regions are tabulated. The questions related to their star content, ages, distribution and star formation are briefly discussed. The stellar associations are compared to similar samples in nearby galaxies.

1. Introduction

Associations indicate the sites of active massive star formation. A typical bright association in the Galaxy is Ori OB1. It contains four subgroups. The diameter of the oldest group is 50 pc and of the youngest (Trapezium cluster) - 0.05 pc. Blaauw (1964) obtained the difference in ages of subgroups in Ori OB1 3×10^6 yr. The Ori OB1 is the best examined group in the Galaxy and it is a good example for a young stellar association.

The aim of the present paper is to define the bright associations in M33 similar to Ori OB1.

2. Observational data

We compiled a computer catalogue of 2485 bright stars in M33 which contains the stellar coordinates their UBV magnitudes. The photographic photometry was made on 2m RCC Rozhen telescope. The catalogue is complete up to V = 19.5. We selected 1968 stars with U-V < 0. Hereafter we call them blue stars. Freedman (1985) has shown that this criterion eliminates the foreground stars. We accepted an apparent distance modulus of M33 $(m-M)_{AV}$ = 24.5. From that follow that OB stars and blue supergiants brighter than M_V = - 5 dominate in our sample. They are the main constituents of stellar associations.

3. Criteria for selection of bright associations

We accepted a distance of M33 700 kpc. Table 1 gives some integral properties of four subgroups of Ori OB1 if they

"Star Clusters and Associations"
Publ. Astron. Dep. Eötvös Univ
No.10, Budapest (1990)

were in M33 based on Humphreys' (1980) data. The oldest subgroup could not be detected on our plates. The two younger subgroups b and c could be observed as cores with 5 and 3 stars.

Table 1. Observational properties of subgroups Ori OB1 at 700 kpc based on Humphreys'(1980) data.

Subgroup	a	b	c	Trapezium
Size	15"	8"	5"	0.1"
No	0	5	3	1
Age 10^6yr	8	5	4	0.5

Trapezium cluster with HII region (2 pc) would look as peculiar star-like image < 1". Ori OB1 would be observed as an association with two subgroups and one nonstellar object (Trapezium) with V = 18.5. OB associations in M33 contain about 60 candidate objects similar to Trapezium cluster. We call them multiple stars. The gradient mask analysis of the nine brightest blue stars in M33 suggests that they are compact group of star images (Golev et al.,1987). The brightest blue stars with M_v < -6.5 and U-B < -0.6 are candidate multiple stars. All these objects are within the brightest cores of OB associations. Probably the multiple stars are massive tight young clusters.

Table 2. Integral properties of Ori OB1 at distance 700 kpc

V_T	SIZE	No	BR/B	O/B	HII	Multiple
14.1	30"	8	0.33	0.62	YES	1

V_T is the integral magnitude per arcmin^2.

SIZE - mean size of Ori OB1 in arcmin, No - number of blue stars.

BR/B - ratio of the bright stars with M_v < - 7 to the blue ones.

O/B - ratio of the candidate O stars (U-V < -0.9) to the blue stars.

Table 2 contains the main integral properties of Ori OB1 at 700 kpc. We included only the stars with M_v < -5 because this sample is complete in our catalogue. We conclude that a region of active star formation should look as OB association with size 30". This association contains two or more subgroups, a HII region and a multiple star. The integral magnitude V_T is a measure of blue star concentration. The young associations in the Galaxy contain a small subgroups while the blue stars are distributed at random in the older associations. Compact associations in

M33 with a core structure and small size should be younger than associations with large dimensions and without cores . Assuming an expansion velocity of 5 km/sec, we obtain that the ages of associations with sizes 10 and 100 pc are equal to 2×10^6 and 2×10^7. We used the ratios O/B and BR/B as additional criteria. The candidate O stars in our catalogue $M_v < -5$ and $U-V < -0.9$ are younger than $\simeq 4 \times 10^6$. The concentration of O stars is a good indicator of the association's youth. According to evolution theory they have to predominate in younger OB associations. The blue luminous stars ($M_v < -7$ and $U-V < 0$) are younger than 7×10^6. Other young star formation indicators are HII regions and WR stars. WR stars are luminous young objects with masses > $40 M_\odot$. Finally we accepted seven criteria: $V_T < 14.1$, size < 100 pc, BR/B > 0.3, O/B > 0.5, No > 3, presence of a HII region and a WR star or a multiple star. If an association has five properties coinciding with these criteria we consider it as a bright association.

4. Results

Table 3. The integral properties of bright blue associations.

	RA(1950)	D(1950)	V	SIZE	BR/B	O/B	No	ASS	HII	REM
1	31 12.1	30 21 7	14.4	95	0.33	0.44	9	1a*	100	M
1	31 12.4	30 20 38	14.3	57	0.00	0.67	6	1b*	1	WR
1	31 8.7	30 20 7	14.3	102	0.25	0.25	8	2a	4,5	WR
1	31 4.4	30 20 8	12.6	36	0.14	0.71	7	3a	10	M
1	31 9.4	30 19 00	13.6	82	0.24	0.71	17	4a*	Z1A	WR
1	31 6.8	30 18 55	14.6	60	0.00	0.50	4	4b*	11	WR
1	31 9.5	30 18 34	13.3	68	0.22	0.67	9	4c*	8A	WR
1	31 8.4	30 17 59	11.5	38	0.67	0.33	6	5a	-	WR
1	31 8.7	30 17 45	12.2	50	0.38	0.38	8	5b	703?	M
1	31 4.9	30 17 50	13.1	41	0.50	0.25	4	6a	13	M
1	30 57.8	30 17 37	14.2	77	0.29	0.71	7	8a*	17	
1	30 53.1	30 17 37	12.0	20	0.00	0.75	4	9c*	Z10	WR
1	30 55.0	30 16 47	13.7	51	0.40	0.20	5	10a	1502	
1	30 54.1	30 16 25	13.7	52	0.40	0.60	5	10b	1502	
1	30 50.1	30 17 11	14.1	45	0.00	0.60	5	11a*	200	
1	30 50.6	30 15 58	14.4	190	0.29	0.62	21	12a	204	WR
1	30 45.6	30 16 51	14.7	59	0.00	1.00	4	13a*	208	WR
1	30 45.0	30 18 31	11.8	26	0.20	0.80	5	14a*	209,Z132	M
1	30 40.8	30 16 25	10.7	12	0.67	0.67	3	15a*	211	WR
1	30 26.8	30 16 44	12.9	53	0.80	0.40	5	17c	Z123A	
1	30 25.8	30 17 8	13.9	35	0.00	1.00	3	17d*	215	WR
1	30 22.0	30 18 51	13.4	57	0.20	0.40	5	18a	Z116	WR
1	30 12.1	30 18 42	13.8	61	0.67	0.00	3	20a	230	
1	30 10.6	30 18 15	13.5	37	0.33	0.67	3	20b	Z77	
1	30 6.7	30 20 9	12.3	28	0.50	0.75	4	21d	234	
1	29 56.2	30 19 34	12.2	46	0.33	0.67	3	22a*	238	M

Table 3 (continued).

RA(1950)	D(1950)	V	SIZE	BR/B	O/B	No	ASS	HII	REM
1 29 56.4	30 23 36	11.5	27	0.60	0.80	5	27a*	280	M
1 30 18.0	30 27 14	13.0	23	0.00	1.00	3	28b*	288	
1 30 25.9	30 29 38	16.0	170	0.00	0.78	9	29a*	Z196	WR
1 30 40.1	30 32 24	12.5	39	0.50	0.00	4	31a	609	M
1 30 47.4	30 35 10	13.6	44	0.00	0.67	6	33a	629	
1 31 00.0	30 36 26	11.4	23	0.33	0.67	3	34b*	632	M
1 31 27.8	30 36 32	14.1	91	0.33	0.67	6	38a*	691	M
1 31 23.2	30 37 17	14.0	76	0.09	0.45	11	39a*	667	
1 31 37.3	30 37 43	15.1	114	0.11	0.44	9	40a	664	M
1 31 42.2	30 42 9	14.4	40	0.00	1.00	3	44b*	Z378	M
1 31 43.8	30 45 7	14.8	95	0.11	0.44	9	45a*	650	
1 32 0.5	30 39 30	13.9	66	0.00	0.50	6	47a*	657	
1 30 57.0	30 21 24	15.2	62	0.00	0.50	4	48a*	27	WR
1 30 55.8	30 21 6	13.3	92	0.40	0.30	10	48b*	25	WR
1 30 55.3	30 20 36	13.1	28	0.00	0.25	4	48c	26	M
1 30 56.7	30 19 28	13.0	34	0.00	0.50	4	49b	-	WR
1 30 42.9	30 20 16	12.5	36	0.40	0.60	5	52a	-	M
1 30 49.9	30 23 2	12.5	45	0.50	0.50	4	55a*	35	
1 30 50.5	30 22 47	13.5	48	0.00	0.67	6	55b	36	M
1 30 46.2	30 23 12	13.6	91	0.30	0.40	10	56a	1008	
1 30 38.3	30 23 21	14.6	70	0.00	0.33	6	58a*	1007,	Z85A
1 30 21.4	30 23 21	13.0	43	0.67	0.00	3	59a*	277	M
1 30 23.1	30 23 28	12.6	61	0.40	0.60	10	59b*	277	WR
1 30 40.1	30 25 3	11.3	17	0.00	0.75	4	61d*	45	
1 30 43.7	30 26 13	13.1	71	0.43	0.57	7	62b*	49	WR
1 31 0.9	30 26 7	12.5	35	0.25	0.75	4	64a*	64	
1 31 0.6	30 25 38	12.8	8	0.75	0.00	4	64b	Z140	
1 31 2.0	30 25 35	13.4	45	0.17	0.67	6	64c*	66	
1 31 2.4	30 27 56	13.1	37	0.00	0.50	6	65b	-	M
1 31 2.9	30 28 29	13.4	30	0.00	0.75	4	65f	65	WR
1 30 57.0	30 27 19	14.7	62	0.00	0.67	6	65h*	60	
1 30 58.1	30 29 27	14.2	44	0.00	0.75	4	66b	-	
1 30 55.5	30 29 25	11.2	12	0.00	0.75	4	66d*	62	
1 30 54.7	30 29 11	14.4	60	0.00	0.50	4	66e*	62	WR
1 31 7.2	30 29 56	14.2	151	0.60	0.80	5	67a*	301	M
1 31 17.5	30 32 4	14.4	108	0.25	0.50	8	71b*	302	
1 31 19.4	30 31 38	13.9	50	0.20	0.40	5	75a	-	
1 31 19.0	30 31 12	13.3	58	0.11	0.00	9	75b	689	M
1 31 21.4	30 31 22	13.7	78	0.07	0.40	15	75c*	688	M
1 31 43.0	30 31 44	13.6	152	0.44	0.40	25	84a*	680	WR
1 31 51.4	30 30 42	14.1	112	0.33	0.11	9	85b	-	M
1 31 49.4	30 28 43	13.3	34	0.00	0.60	5	87a*	749	M
1 32 12.2	30 26 35	13.5	33	0.33	0.67	3	88a	-	
1 32 8.9	30 26 23	15.0	97	0.00	0.14	7	88b	753	WR
1 32 17.3	30 26 32	12.3	22	0.00	0.67	3	89a*	756	
1 32 16.5	30 25 48	13.5	53	0.33	0.67	6	89b*	Z366	WR
1 31 49.8	30 26 14	15.6	161	0.25	0.63	8	90a*	740	M
1 31 40.6	30 25 25	12.1	30	0.00	0.67	6	93a*	734	

Table 3 (continued).

RA(1950)	D(1950)	V	SIZE	BR/B	O/B	No	ASS	HII	REM
1 31 16.9	30 26 26	12.0	34	0.25	0.50	4	94b*	77	M
1 31 21.6	30 24 40	13.8	49	0.00	0.40	5	95a	732?	
1 31 19.8	30 23 49	13.7	81	0.57	0.71	7	96a*	83	M
1 31 17.7	30 24 2	13.7	43	0.00	0.29	7	96b	85	
1 31 29.4	30 22 44	13.7	45	0.00	0.50	4	100b	-	
1 31 26.8	30 22 10	14.0	46	0.00	0.57	7	100c	-	WR
1 31 26.2	30 21 50	12.2	34	0.25	1.00	4	100e*	88	WR
1 31 28.1	30 18 15	12.4	33	0.67	0.67	3	101a*	711	WR
1 31 26.4	30 18 22	11.4	21	0.25	0.25	4	101b	-	M
1 31 24.5	30 18 25	13.2	31	0.00	0.60	5	101c*	710	
1 31 26.3	30 18 44	13.6	45	0.14	0.14	7	101e	714?	WR
1 31 25.2	30 19 36	14.5	51	0.00	0.50	4	101k*	714	
1 31 23.8	30 12 19	14.2	45	0.00	0.50	4	105b	Z325	
1 30 50.4	30 7 8	14.5	154	0.11	0.44	9	110c*	246	M
1 30 54.8	30 6 15	13.9	87	0.43	0.43	7	112a	248?	
1 30 49.3	30 5 32	14.8	131	0.08	0.54	13	112c*	249?	WR
1 30 49.8	30 4 57	12.2	38	0.40	0.00	5	112d	250?	M
1 30 35.5	30 10 7	11.3	11	0.00	0.75	4	113a*	222	M
1 30 33.2	30 10 46	13.5	32	0.00	0.50	4	114a	Z37	M
1 30 21.6	30 12 2	14.8	80	0.00	0.57	7	115a*	220	WR
1 30 22.4	30 8 2	11.9	19	0.33	0.33	3	116b*	256	M
1 30 10.8	30 7 57	13.4	63	0.25	0.25	4	117a	Z19	M
1 29 52.2	30 7 5	12.9	31	0.25	0.00	4	119a	264	M
1 29 54.6	30 8 36	12.7	18	0.00	0.67	3	120a	265	
1 30 7.3	30 12 12	11.3	17	0.33	0.00	3	122a	243	WR
1 29 44.9	30 11 45	11.8	17	0.00	0.50	4	123c*	Z6	
1 30 25.4	30 14 25	13.3	56	0.33	0.50	6	127a*	Z23	WR
1 30 22.7	30 14 28	13.6	57	0.17	0.67	6	127b*	216	M
1 30 20.1	30 14 29	13.3	57	0.33	0.17	6	127d*	217	WR
1 30 15.2	30 15 36	13.8	67	0.67	0.33	3	128a	-	WR
1 30 11.7	30 15 28	11.9	35	0.40	0.60	5	128b*	218	
1 30 7.6	30 16 25	14.8	88	0.20	0.20	5	129a	Z74	WR
1 29 48.6	30 24 45	12.2	27	0.17	1.00	6	132a*	281	WR
1 30 22.6	30 33 27	13.2	49	0.33	0.00	3	135a	Z101	WR
1 30 26.2	30 37 42	12.2	17	0.00	0.33	3	137b	624?	M
1 30 25.9	30 37 59	13.2	45	0.40	0.00	5	137c	624	
1 30 25.9	30 38 14	12.9	32	0.20	0.20	5	137d	625	
1 30 38.8	30 46 7	14.3	73	0.25	0.75	4	139	629?	
1 30 46.6	30 46 20	12.4	42	0.29	0.71	7	140*	640	M
1 31 3.1	30 23 56	13.4	75	0.40	0.80	5	142a*	93	M
1 31 2.3	30 23 35	13.4	139	0.17	0.31	36	142b*	99	WR
1 31 2.3	30 22 57	14.8	183	0.13	0.53	15	142e	20	WR
1 31 2.8	30 24 45	14.5	96	0.07	0.21	14	147a*	71	M
1 31 1.2	30 24 26	14.8	130	0.00	0.47	17	147b*	69	
1 31 5.2	30 25 11	13.3	44	0.00	0.89	9	148*	66	
1 31 8.3	30 26 53	13.0	31	0.00	0.80	5	149a*	74	
1 31 11.1	30 25 27	15.4	68	0.00	0.50	4	150a*	79	
1 30 52.2	30 26 20	11.7	27	0.25	0.25	4	152d	56	WR

Table 3 (continued).

RA(1950)	D(1950)	V	SIZE	BR/B	O/B	No	ASS	HII	REM
1 31 12.4	30 22 29	14.8	124	0.14	0.50	14	156a	89B	
1 31 11.7	30 21 57	12.9	33	0.00	0.50	4	156c*	97	
1 31 11.8	30 23 35	14.4	93	0.09	0.55	11	159d*	87	
1 30 13.8	29 55 57	10.0	16	0.50	0.25	4	173a	HII	M
1 30 13.3	29 56 9	12.0	13	0.00	0.50	4	173b	HII	

Columns 1 and 2 give the coordinates of the center of associations for 1950. The coordinates were obtained using the positions of 5 stars in SAO catalogue, 20 star clusters of Christian and Schoommer (1982) and three WR stars of Massey et al. (1987). We estimated that the positions are accurate to $\mp$ 1.5 arcsec.

Column 3 gives the integral V magnitude of the associations per arcmin^2.

Column 4 gives the size of associations along the major axis in parsecs.

Column 5 gives the ratio candidate O stars (U-V < -0.9) to blue stars (U-V < 0).

Column 6 gives the ratio bright stars (M_v < -7) to blue stars.

Column 7 gives the number of blue stars in an association.

Column 8 gives the number of associations. The numbers are identical with Ivanov (1987). The asterisk marks very young associations coinciding with the bright dense HII regions of Courtes et al.(1987).

Column 9 gives number of HII regions in the catalogue of Courtes et al. identical with the associations.

Column 10 contains some remarks. "M" means a multiple star within an association. These are bright blue stars with peculiarities of the image resembling Trapezium. "WR" means identification with the WR stars according to the charts of Massey et al. (1987).

The OB associations in Table 3 superimposed on a B plate are shown on Figure 1. Most of them fall in the spiral arms marked by Humphrey and Sandage (1980) or Ivanov and Kunchev (1985). The spiral arms S1, N1 and S3 are well outlined. Figure 1 shows that the bright associations give better evidence for the spiral structure than low luminosity associations. The highest concentration of associations occurs in the spiral arm S1 and there is a similar concentration at the center. Most of the associations (91%) coincide with HII regions. This correlation is natural because O stars in them contribute mainly to the ionization of the interstellar gas. 9% of associations outside HII regions without doubt are older but rich in massive stars. They have high values of O/B, BR/B and WR stars. The distribution of bright associations is similar to that of WR

Figure 1. The bright associations superimposed on a B plate.

stars. About 60% of associations in Table 3 contain WR or multiple stars. We conclude that all indicators of active star formation fall in the region defined by the associations selected in Table 3.

5. Discussion

a) Observational evidences for the evolution of OB associations

We accepted seven criteria for the selection of 127 bright associations in Section 3. However these associations differ by their ages. It should be emphasized that van den Bergh (1964) suggested the size of associations in M31 as a good criterion for age estimation. There is a well defined difference in the size of the associations in Table 3 ranging from 10 to 200 pc. The other properties in Table 3 do not show any correlation with the size of the associations. For instance ratio O/B does not differ considerably for associations with various sizes. The O stars in the associations must vanish by 5×10^6 yr. If the dimension of the associations depend on the age (as supposed van den Bergh, 1964) we may expect a correlation between the size and the ratio O/B. However the data in Table 3 do not show such correlation. A mixture of O stars and B supergiants may exist in an older association but the ratio BR/B does not correlate with the size too. The star content, the size and the other integral properties in Table 3 depend on the age, peculiar motion of each star and the rate of star formation in the associations. Which is the best criterion for the age of association? Humphreys and Sandage (1980) estimated the ages of the associations in M33 using the CM diagrams. They obtained the resulting ages for associations 10, 12, 17, 127, 131 and 137 $t = 5.5 \times 10^6$. The criterion of van den Bergh (1965) suggests quite different ages from 3×10^6 to 4×10^7 for the same associations. We found that the ages of M31 associations obtained by the CM diagrams coincide with van den Bergh's criteria (Ivanov, 1984). Our data do not show a similar coincidence for M33 associations. The luminosity of the brightest candidate O stars in the association does not depend on its size. We explain the disagreement between M31 and M33 associations with the different kind of star formation in the associations in the two galaxies. An older association in M33 may contain second or third generation of O stars. The brightest OB main sequence stars may indicate the age of the association suppose there is only one generation of star formation and an universal initial mass function.

Almost every association in Table 3 contains a HII region. The HII region is a direct evidence for the existence of O stars. It is quite possible the stellar wind of O stars to create an expanded HII region. Courtes et al. (1987) found 30 - 40 ring like structure around the associations in M33. Rosa (1980) defined P Cyg type profile

of spectral lines of NGC 604, the greatest HII regions in M33. Probably the expansion velocity of HII regions due to stellar wind of early O, WR stars and supernova explosions. There are observational evidences in the Galaxy for expanding nebulae which surround the young OB stars. The expansion velocity $\simeq 10 - 20$ km s^{-1}. It is clear that HII regions around associations are dynamically unstable and their sizes give some information on the age. We accepted that the bright associations with dense HII regions belong to the youngest generation of M33.

The bright, compact and well defined HII regions of Courtes et al. (1987) with a mean size of 40 pc were identified with the stellar associations in Table 3. The O stars almost entirely provide the ionization of the interstellar gas. The stellar wind of O stars may create expanding HII regions at the edge of associations. The young newborn associations with $t \simeq 3 \times 10^6$ yr. consist of about three O stars without B supergiants. Probably they are connected with the bright, compact HII regions. The stellar wind of O stars would impart mechanical energy $> 10^{50}$ ergs during the main sequence phase. A typical OB association with three O stars can create an expanding HII region $\simeq 80$ pc for a $t \simeq 5 \times 10^6$. (Weaver et al., 1977). The older stellar associations with $t \simeq 2 \times 10^7$ should be connected with ring-like or extended HII regions with size of 200 pc before a supernova has occurred. The star content of such associations must be a mixture of young O stars and blue and red supergiants. The older associations without O stars are not able to ionize gas. In this case HII regions must vanished. It is possible for old associations to be more extended groups with diameter about 100 pc because the stars are not bound and migrate with $v = 5$ km s^{-1}.

We conclude that the young associations are compact groups of O stars connected with dense HII regions. The luminosity of the brightest candidate O star in the association does not depend on its age or size. The older association may contain O stars of the second generation but we may recognize them by their extended or ring-like HII regions.

b) Morphology of the arm S1

The inner part of the arm is well outlined by associations with diameter from 10 to 50 pc. They are disposed at the inner part of the arm. We evaluated their expansion ages from 2×10^6 to 10^7. The size of the associations increases toward the outer edge of the arm $t \simeq 2 - 4 \times 10^7$. We estimated the velocity of propagating star formation across the arm to 40 km s^{-1}. The chart of Courtes et al. (1987) shows ten bright, condensed and clearly outlined HII regions at the inner part of S1 coinciding with the associations. Their mean size is 40 pc. The brightness of HII regions decreases while their size increases across the arm. The most extended

HII regions are observed at the outer part of the arm. The first observational evidences of density wave in M33 were provided by Courtes and Dubout-Crillon (1971). Dubout-Crillon (1977) found out that the dust, HII regions and O stars are concentrated at the inner border of S1. Newton (1980) indicated a good correlation between the dust patches and the HI peak along the inner part of S1. Usually HI clouds are extended north - south but two clouds are elongated along the arm S1 (Newton,1980). The dust patches are located in front of S1 (Humphreys and Sandage (1980). It seems that dust and HI clouds indicate the front of the spiral shock wave in S1.

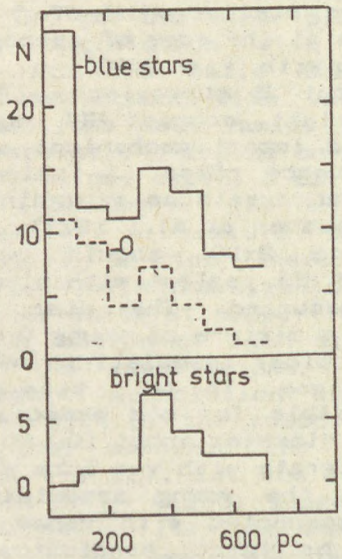

Figure 2. Distribution of the blue stars, candidate O stars and bright blue stars with $M_v < -7$ across the spiral arm S1.

Figure 2 shows the distribution of the blue stars across the spiral arm S1. A concentration of blue stars occurs at the inner part of the arm. A band of young stars (100 pc wide and 2 kpc long) clearly outlines the inner border of the arm. The distribution of O stars in Figure 2 gives the best evidence for the propagation of star formation across S1. The highest rate of star formation occurs at the inner edge. So we found out the following observational evidences for the density wave theory: (1) dust patches and dense HI clouds along the inner edge of the arm (2) well defined tight spiral arm by O stars, young associations and HII regions, (3) the propagating star formation across the arm, (4) the four brightest confirmed M supergiants occur at the outer edge of the arm.

The ratio O/B does not vary considerably across S1. The four associations 9c, 11a, 13 and 15a with O/B > 0.5 and M_v $\simeq$ -5 form a chain along the inner part of the arm. We have discussed the criterion for the age estimation in Section 5a and accepted that these four associations are the youngest because of their small diameter and coincidence with dense HII regions. Figure 2 suggests the highest rate of star formation there. The spiral arm is 700 pc wide. It is possible to observe the stellar evolution effects across it. Some associations at the outer edge of the arm (10b and 12a) are older but the ratio O/B > 0.5. However the ratio BR/B of luminous stars is also higher there. Figure 2 shows that the maximum in the distribution of luminous stars is at the middle of the arm. The massive stars evolve rapidly and the concentration of luminous and candidate O stars there may due to an evolution effect in the stellar associations. For instance, a mixture of evolved stars and young stars of the second generation occur at the outer border of S1.

The morphological structure of S1 gives the best observational evidences for the density wave theory. However the morphology of the symmetrical spiral arm N1 does not show similar signs of shock wave except HI clouds of Newton (1980) and dust patches in the Figure 26 of Humphreys and Sandage (1980). However the dust patches and HI clouds are located behind N1.

c) Size distribution

Hodge (1985 a) describe the problem on the differences between the sizes of stellar associations in the Magellanic clouds and M31. Efremov et al. (1987) and Ivanov (1987) concluded that identification criteria are the cause of this difference. It was found out that the mean size of the associations is $\simeq$ 80 pc in the Galaxy, Magellanic clouds, M31 and M33 is $\simeq$ 80 pc. Hodge (1985 b) determined the mean size of the stellar associations in NGC 2403 $\simeq$ 270 pc. This result is not surprising as the distance to this galaxy is 3.3 Mpc. Hodge (1985 a) has shown that the mean size of associations depends on the plate sale and distance to the galaxy.

Figure 3 is a plot of the size distribution of the associations in M33 compared to that of HII regions of Boulesteix et al. (1974). The mean size of associations is 60 pc. The two distributions look quite similar. The mean dimensions are also similar. We conclude that the mean size does not depend on the galaxy type. This size may be an universal unit of massive star formation. The identification criterion in the present paper may explain the slightly lower mean size (60 pc) of associations than in the previous paper (Ivanov, 1987). In the present paper we used a more strong criterion.

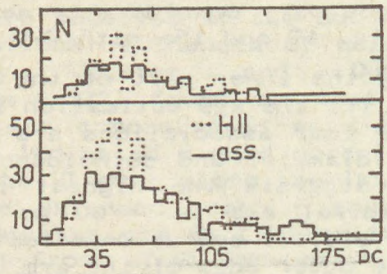

Figure 3. Size distributions of: (a) bright associations and HII regions, (b) all of them.

d) Constituents of the associations.

About 90 % of the associations are connected with HII regions, 30 % contain WR and 30% multiple stars. The associations selected in Table 3 consist of O stars or other indicators of massive star formation as WR, blue luminous or blue multiple stars. Probably the associations selected in Table 3 are rich in massive stars.

The spectroscopic confirmed M supergiants fall in the associations rarely. Most of associations do not contain candidate M supergiants with B-V > 1.9. They are absent both in the young associations and in the older associations. The latter fact is surprising because the older associations with ring-like and extended HII regions must have M supergiants. The blue-to-red ratio is higher in the associations than in the field of M33. This fact may explain the radial gradient of blue-to-red ratio in M33 obtained by Humphreys and Sandage (1980). This ratio is highest in the center of M33 due to the high density of associations. Humphreys and Davidson (1979) suggest that the most massive stars (M > 40 M_o) do not evolve into red supergiants. It is also possible the deficiency of red supergiants is due to the flatter initial mass function.

We used the charts of Hubble (1926), Sandage (1983) and Sandage and Carlson (1983) to compare the distributions of the cepheids to the stellar associations. It is interesting to note that most of the associations do not contain cepheids. It is well known that B2V - A0V main sequence stars evolve to cepheids. The initial mass function of such stars is $dN/d(\log M) \simeq M^{-\beta}$, where $\beta \simeq 1.0 - 1.7$ (Garmany et al., 1982). Adopting $\beta = 1.0$, we estimate that an association should produce about nine stars in the range of B2V - B3V. If we use period-age relation $\log t = 8.26 - 0.78 \log P$, obtained by cluster cepheids in the Galaxy, then the periods > 20 days correspond to the ages $t \simeq 2.10^7$. These cepheids should be met in the older M33 associations. Actually there is a deficiency of cepheids in the two main

spiral arms and in the association rich in luminous or WR stars ($M_v < -7$) with masses > 40 M_o. The cepheids occur in associations or star complexes without massive stars. A concentration of cepheids is observed in the central region of M33. It is possible that the high rate of mass loss of stars to limit their evolution to red supergiants. There exists another possibility that these associations in M33 to be poor in less massive stars (B2V - B3V). Ambartsumian (1949) suggested that associations are poor in stars with small masses. It seems that associations in M33 rich in massive stars (M > 40 M_o) possess a lower density of stars with the masses < 12 M_o. Unfortunately forty years after Ambartsumian's hypothesis there are not direct observational evidences for the luminosity functions in the associations. We conclude that the associations with active massive star formation have a deficiency of cepheids.

e) A comparison of stellar associations in the nearby galaxies

About 90 % of associations selected in the present work are connected with HII regions while the full catalogue of 272 stellar associations in M33 gives 73 %. In this sense M33 is similar to the LMC, NGC 2403 and NGC 6822 for which these values are 79 %, 85 % and 62 %, respectively while in the SMC and IC 1613 only 30 % of associations contain HII regions. This problem was discussed by Hodge (1985 b). We agree with him that the older associations predominate in the latter galaxies.

The SMC and M31 are poor in WR, massive stars and stellar associations. On the other hand they are rich in cepheids. For M33 and NGC 2403 it is quite the opposite. They are rich in massive stars and HII regions and poor in cepheids. At the same time the two galaxies show a quite similar radial distribution of the stellar associations and HII regions. The Galaxy and LMC are rich both in WR stars and cepheids. These differences may due to the ages, IMFs, metallicity, rate of star formation and other factors. Freedman (1985) has shown that the Luminosity Functions (LFs) of different galaxies have indistinguishable slopes. This conclusion does not apply to the stellar associations. Some associations in M33 as OB15 are poor in stars with masses < 12 M_o. The IMF is one of the factors which may explain the peculiarities of M33 associations. The IMFs may be flatter for associations rich in massive stars than those rich in cepheids. Recently Elson et al. (1988) found that IMFs for six young clusters in LMC are flatter than Salpeter IMF. We conclude that M33 and NGC 2403 are similar to the main observational characteristics. They are rich in massive and poor in less massive stars.

6. Summary

The present study is an attempt to give the main properties of the bright stellar associations in M33. The ages of M33 associations obtained by the gap of the CM diagrams is nearly the same in the interval of $4 - 6 \times 10^6$ while their expansion ages are from 3×10^6 to 4×10^7. HII regions are the most dynamic objects in the associations. If we accept an expansion velocity of 10 km s^{-1} the age of the ring-like and extended HII region is about $2 - 3 \times 10^7$. This difference could be explained if there exist two or more generations of star formation.

We found out a gradient of star formation across the arm S1. This is a good proof for the wave density theory.

The LF seems to be universal for the entire surface of galaxies but the flatter slope of the LF in M33 associations could explain the high frequency of massive stars > 40 $M_\odot$ and deficiency of the less massive stars The stellar associations in NGC 2403 are similar to those of M33.

References

Ambartsumian, V.A.: 1955, Observatory 75, 72.
Blaauw, A.: 1964, Annual Rev. Astron. Astrophys. 2, 213.
Boulesteix, J., Courtes, G., Laval, A., Monnet, G. and Petit, H.: 1974, Astron. Astrophys. 37, 33.
Courtes, G and Dubout-Crillon, R.: 1971, Astron. Astrophys. 11, 468.
Courtes, G., Petit, H., Sivan, J.-P., Dodonov, S. and Petit, M.: 1987, Astron. Astrophys. 174, 28.
Christian, C.A. and Schoommer, R.A.: 1982, Astrophys. J. Suppl. 49, 405.
Dubout-Crillon, R.: 1977, Astron. Astrophys. 56, 293.
Efremov, Yu.N., Ivanov, G.R., Nikolov, N.S.: 1987, Astrophys. Space Sci. 135, 119.
Elson, R.A.W., Fall, S.M. and Freeman, K.C.: 1988, Preprint No 292, Space Telescope Science Institute.
Freedman, W.L.: 1985, Astron. J. 299, 74.
Garmany, C.D., Conti, P.S., and Chiosi, C.: 1982, Astrophys. J. 263, 777.
Golev, V.K., Ivanov, G.R., Kunchev, P.Z.: 1987, Astrophys. Space Sci. 135, 301.
Ivanov, G.R.: 1984, Astrophys. Space Sci. 110, 357.
Ivanov, G.R. and Kunchev, P.Z.: 1985, Astrophys. Space Sci. 116, 341.
Ivanov, G.R.: 1987, Astrophys. Space Sci. 136, 113.
Hubble, E.: 1926, Astrophys. J. 63, 236.
Humphreys, R.M.: 1978, Astrophys. J. Suppl. 38, 309.
Humphreys, R.M. and Davidson, : 1978, Astrophys. J. 232, 409.
Humphreys, R.M. and Sandage, A.: 1978, Astrophys. J. Suppl. 44, 319.

Massey, P, Conti, P.S., Moffat, A.F.J. and Shara, M.M.: 1987, Publ. Astron. Soc. Pacific 99, 816.
Rosa, M.: 1980, Astron. Astrophys. 85, L21.
Sandage, A.:1983, Astron. J 88, 1108.
Sandage, A. and Carlson, G.: Astrophys. J.267, L25.
van den Bergh, S.: 1964, Astrophys. J. Suppl. 9, 65.
Weaver, R., Castor, J., McCray, R., Shapiro, P. and Moore, R.: 1977, Astrophys. J. 218, 377.

THE STRUCTURE OF STELLAR ASSOCIATION N 104 (LUCKE AND HODGE) IN THE LARGE MAGELLANIC CLOUD

P.E. ZAKHAROVA
Astronomical Observatory, Ural State University
620083 Sverdlovsk, USSR

ABSTRACT. There is investigated the structure of association N 104 in LMC. The linear diameter of association is 76 pc. Stellar density distribution in association is compared with that of open cluster of our Galaxy NGC 1960.

The investigation of structure of stellar associations is necessary for the understanding of galactic structure and physics of star formation process.

We have performed the investigation of the structure of one stellar association in LMC, namely N 104 association from Lucke and Hodge list [1]. It is situated at $\alpha=5^h\ 40^m.3$, $\delta=-69^\circ\ 25'$ (1975.0).

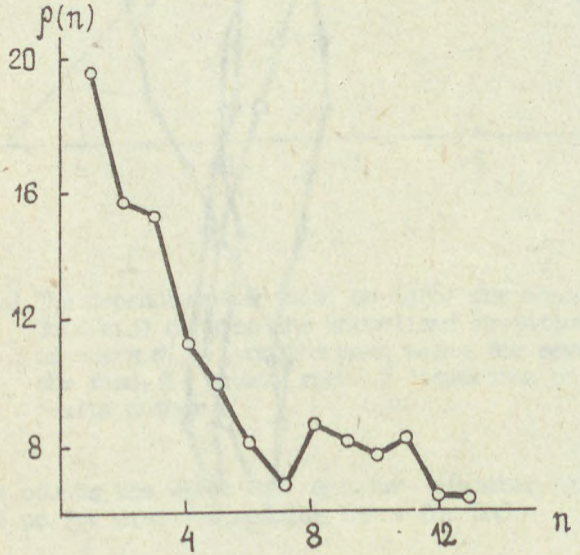

Fig.1 Radial distribution curve for apparent stellar density in association N 104

"Star Clusters and Associations"
Publ. Astron. Dep. Eötvös Univ.
No.10, Budapest (1990)

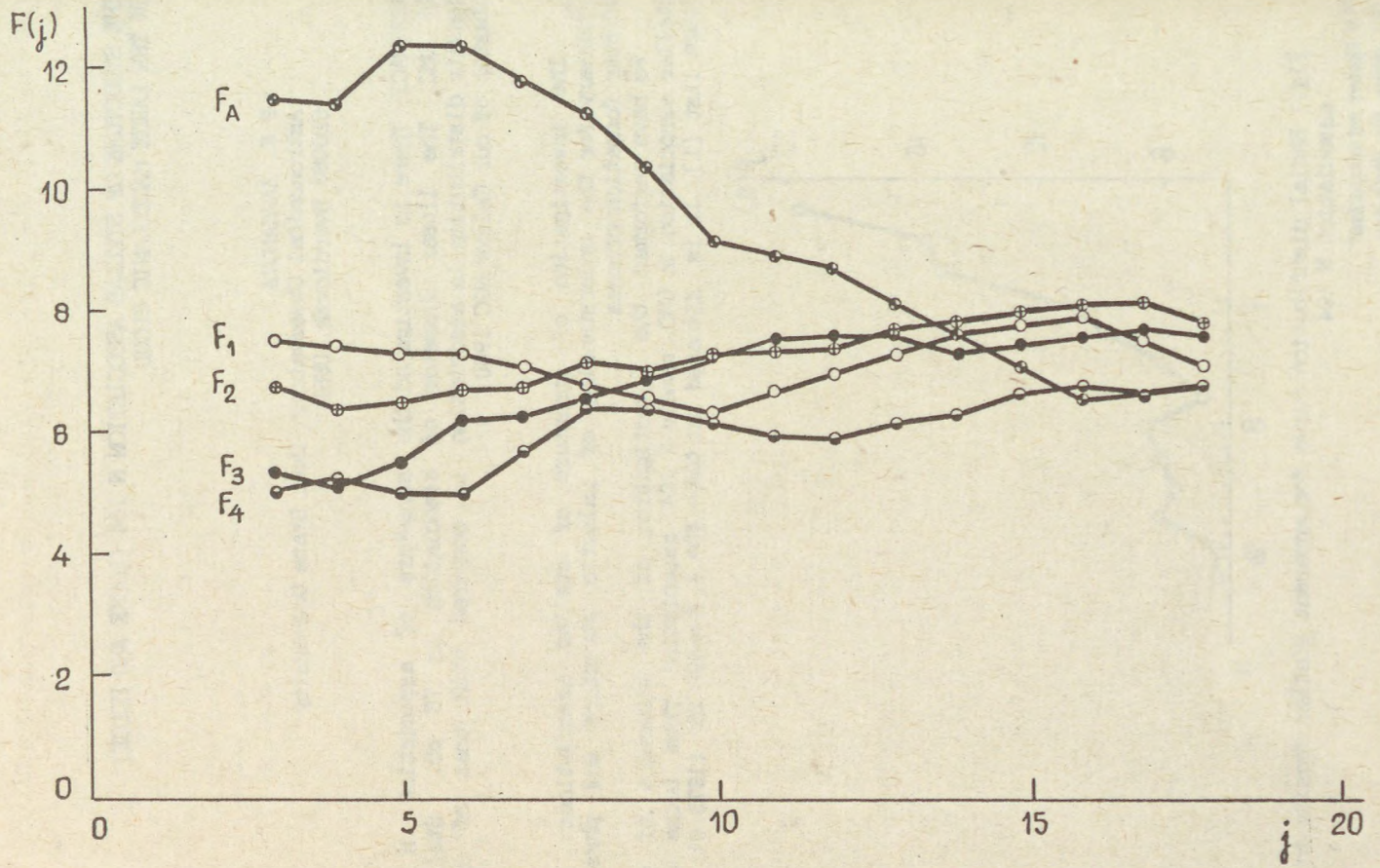

Fig.2 Apparent stellar density distributions F(j) for association N 104 and surrounding background areas

The plates for that investigation are taken in V-band of UBV system on 70-sm menisk telescope of Pulkovo observatory in Chile. The plates scale is 100 "/mm. On these plates we have performed the stellar counts, for which the field of association is devided on 20 concentric zones, centered on association, and 6 sectors. The mean stellar density curve is showned on Fig.1. One can see from the figure, that stellar density in association field really exceeds that of surrounding regions.

The same conclusion (fig.2 and 3) is got from the counts, made by Danilov et al. method [2], which is proposed for open clusters.

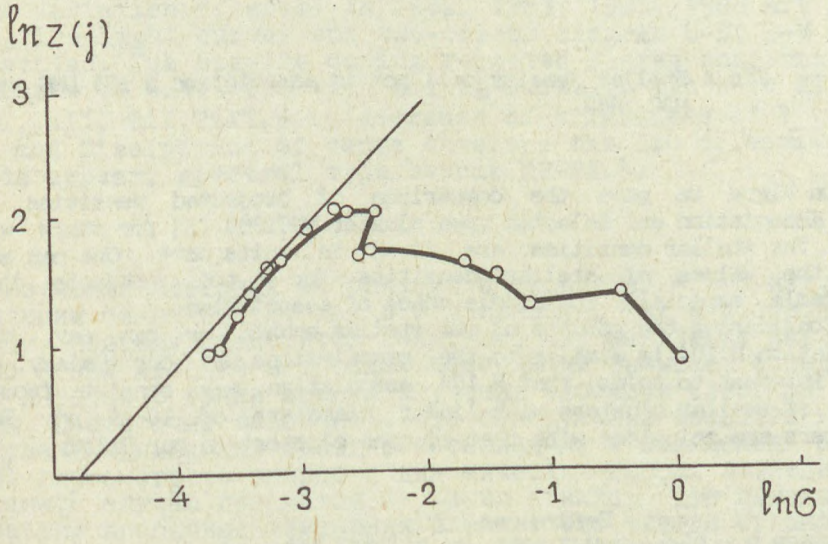

Fig.3 The dependance of ln(z) on ln(σ) for association N 104. Here z(j) denotes the normalized deviation of number of stars N(j) from the mean value for several areas of the fied, σ - square root of dispersion of stellar density number

From these counts the value of angular diameter of association is 5'.5 or 76 pc for distance modulus $18^m.4$ for LMC.

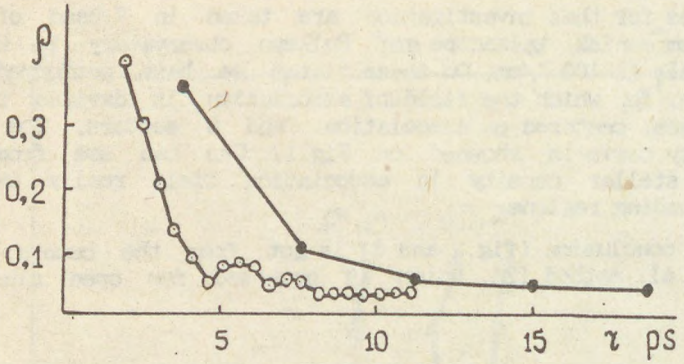

Fig.4 Stellar density on 1 pc^2 in association N 104 LMC and NGC 1960

On Fig.4 we give the comparison of projected densities for N 104 association and Galactic open cluster NGC1960 [3] for stars with $M<+1^m$. The stellar densities are given in units pc^{-2}. One can see, that the values of stellar densities for two objects are comparable, especially for middle zones of association.

Considering the results of our stellar counts we can say, that association N 104 is similar to the associations of our Galaxy. It is of interest to point, that N 104 association may consist from a number of stellar clusters with linear diameters of 10-15 pc. Such diameters are coinsides with that of open clusters in our Galaxy.

References

1. Lucke P.B., Hodge P.W., 1970, A. J., 75, 171
2. Danilov W.M., Matkin N.V., Pyl´skaya O.P. 1985, Astron. Zh., 62,1065
3. Barkhatova K.A., Zakharova P.E., Shashkina L.P., Orekhova L.K., Astron. Zh., 1985, 62, 854

ФУОРООБРАЗНЫЕ ПЕРЕМЕННЫЕ В АССОЦИАЦИИ ОРИОНА

К.Г.Гаспарян, А.С.Мелконян, Г.Б.Оганян,
Э.С.Парсамян
Бюраканская астрофизическая
обсерватория АН Арм.ССР, 378433,СССР

ABSTRACT. Observational data on two stars V 1143 Ori = object Sugano and MSV 2229 Ori = object Shanal during fuor-like variation (flares) in 1982, 1983, 1986, 1988 are given. The light curves and two-colour diagram U-B, B-V are presented. The spectra during repeated flares confirms appearance of envelopes with strong emission lines of HI,FeI, FeII,CaII, TiI,TiII.With decrease of brightness of V 1143 Ori and Dissipation of dense envelope the TiO molecular bands appear, spectral type become M2-M2.5.

Изучение звездных ассоциаций и скоплений - это изучение эволюции самих звезд, как в отдельности, так и в совокупности. Поэтому становится понятным, что появление каких-либо новых явлений в звездах ассоциаций вызывает определенный интерес с точки зрения изучения эволюции звездной системы. Достаточно вспомнить, что обнаружение большого количества вспыхивающих звезд в ассоциациях и скоплениях заставило пересмотреть вопрос о динамических массах последних. В данном случае предметом изучения явились две звезды, показавшие необычные изменения блеска. Это звезда Сугано = V1143 Ori = Аб 24 [1,2] и звезда Шанала = NSV 2229 = Аб 17 [3]. Наблюдения показали, что за последние 7 лет эти звезды демонстрировали изменения блеска, напоминающие фуоры (звезды типа FU Ori), но в меньшем масштабе, из-за чего были названы субфуорами [4].

I. Звезда Сугано. Значение блеска звезды в минимуме [2, 4-6]:

U	B	V
I7.8 ÷ I8.5	I7.8 ÷ I8.6	I7.2 ÷ I7.6

Повышение блеска звезды до максимума в 1982 году продолжалось около 3.5 месяца, после чего звезда более чем четыре месяца находилась в максимуме, испытывая при этом колебания порядка $0^m.3 \div 0^m.5$. Затухание блеска до нормального минимума

"Star Clusters and Associations"
Publ. Astron. Dep. Eötvös Univ.
No.10, Budapest (1990)

продолжалось два года и четыре месяца. Показатели цвета и амплитуда вспышки во время максимума I9.I0.I983г. имели следующие значения [4] :

U - B	B - V	V	Δm_U	Δm_B	Δm_V
-0.7	0.3	I4.6	~4	2.9	2.6

На рис.I приводится кривая изменения блеска звезды VI143 Ori во время вспышки I982 года [4] .

На рис.2 приводится диаграмма зависимости U-B и B-V где показано изменение положения звезды V I143 Ori в течение вспышки. Для сравнения приведены аналогичные значения для родственных объектов: фуоров и звезды DR Tau .

На рис.3 приводится кривая блеска звезды Сугано в лучах U , B , V .

В конце I985 г. и в начале I986 г. V I143 Ori оставалась в минимуме блеска или около него. В конце I986 г. было обнаружено второе повышение блеска V I143 Ori в Бюраканской обсерватории [7] . 4 ноября I986 года амплитуда вспышки (или повышения) в лучах U равнялась 4 звездным величинам, а блеск звезды равнялся:

U	B	U - B
I4.6	I5.9	-0.49

Данных о длительности подъема и стояния в максимуме у нас нет. Затухание длилось около 4-х месяцев.

Третье повышение началось в феврале-марте I988 г. , а уже 7 апреля I988 г. достигла значения B ~ I5.5 [8] .

Спектральные наблюдения, проведенные во время первой вспышки[5,9,I0] показали, что у звезды наблюдаются сильные эмиссионные линии HI, Fe II, CaII, FeI, [FeII], Ti II , Cr II , свидетельствующие о появлении оболочки у звезды. Спектр по мнению наблюдателей похож на спектр звезд типа T Тельца. Спектральный тип оценивался как K7-M0 [5] . В течение второй вспышки уже на спаде нами был получен спектр V I143 Ori на 6 м телескопе САО АН СССР на спектрографе СП-I24 со сканером в диапазоне 3800-7000 ÅÅ, D = I.8 Å/канал, разрешающая сила ~ 4 Å(рис.4).

Спектр показал, что у звезды снова появилась мощная оболочка с эмиссионными линиями и уже через месяц в спектре наряду с эмиссионными линиями появились полосы поглощения TiO. Спектральный тип ~ M2 (рис.5).

2. Звезда Шанала. Вспышка произошла в I983 г. [3] . Блеск звезды в минимуме B ~ I8.4, V ~ I7.0. Во время вспышки звезда имела следующие значения блеска, показатели цвета и амплитуды:

U	B	V	U-B	B-V	Δm_U	Δm_B	Δm_V
I3.9	I4.8	I3.8	-0.8	I.0	~4	3.6	3.2

О времени подъема звезды до максимума в I982 г. у нас

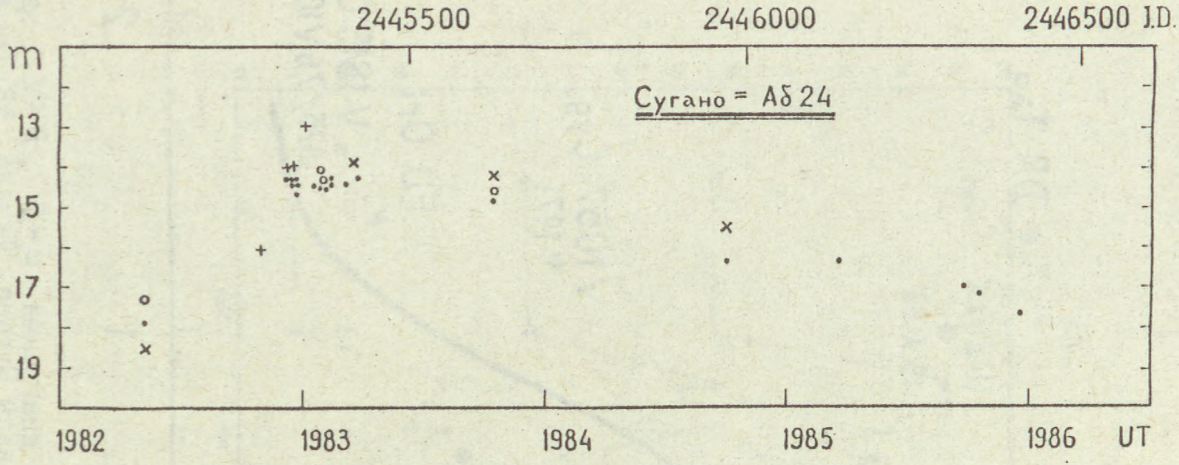

Рис. I Кривая блеска VII43 Ori , + - в лучах λλ3000-6700 ÅÅ (пленка Tri -X), x - U , •• - B , o - V

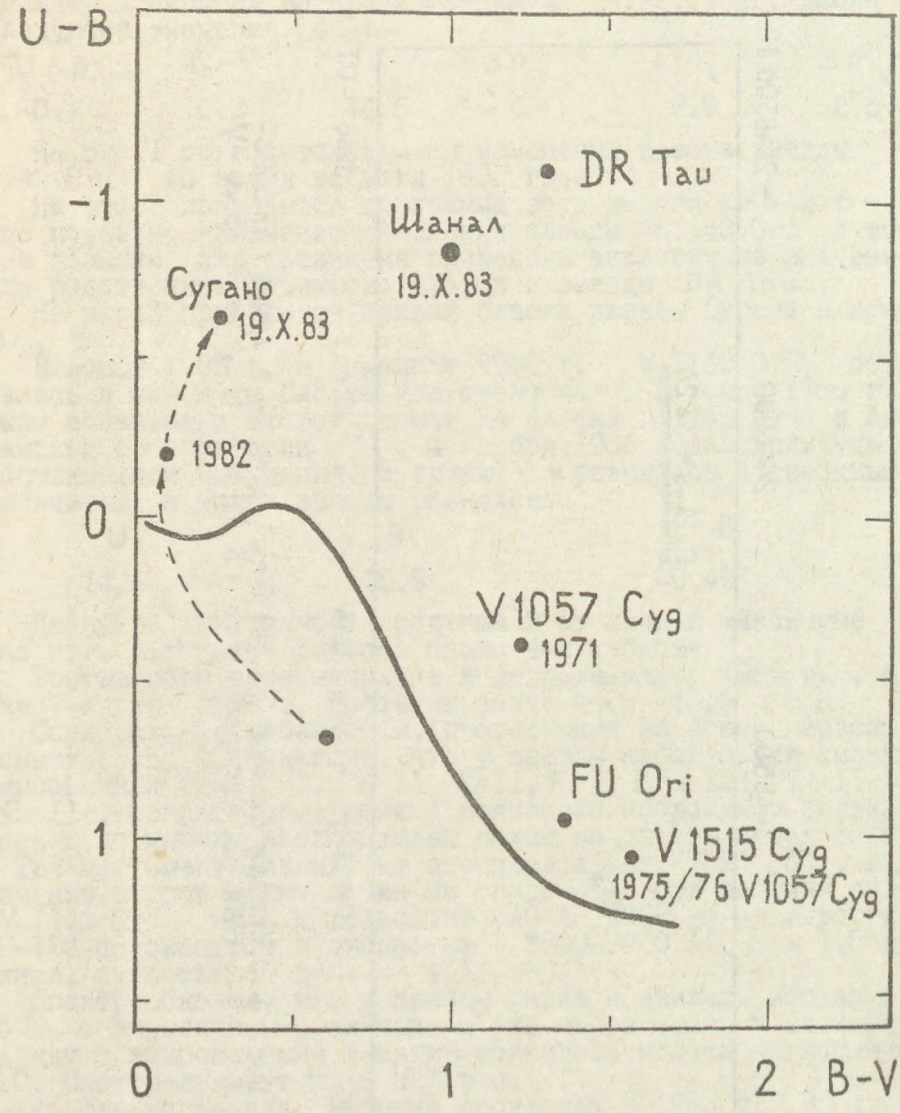

Рис. 2 Двухцветная диаграмма U-B , B-V , на которой нанесены звезды Сугано, Шанала, DR Tau во время вспышки, а также фуоры V1057 Cyg , FU Ori , V 1515 Cyg.

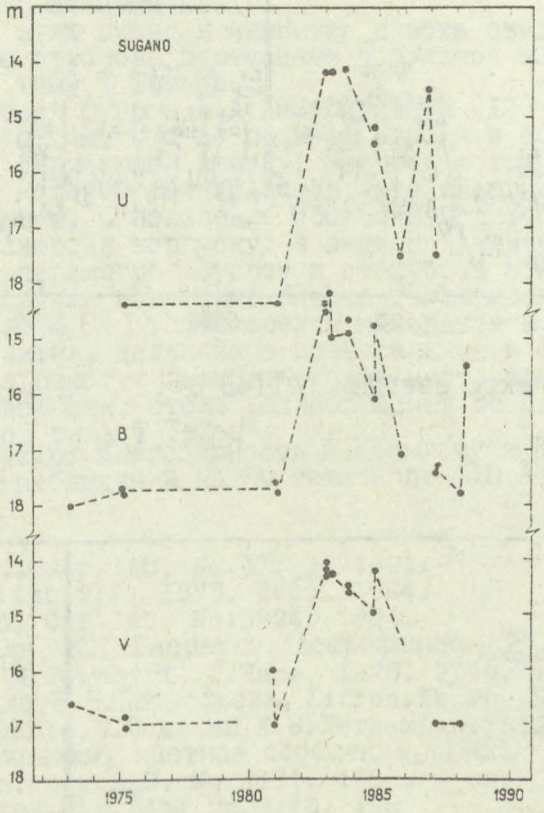

Рис. 3 Кривая блеска звезды V 1143 Ori в лучах U , B , V .

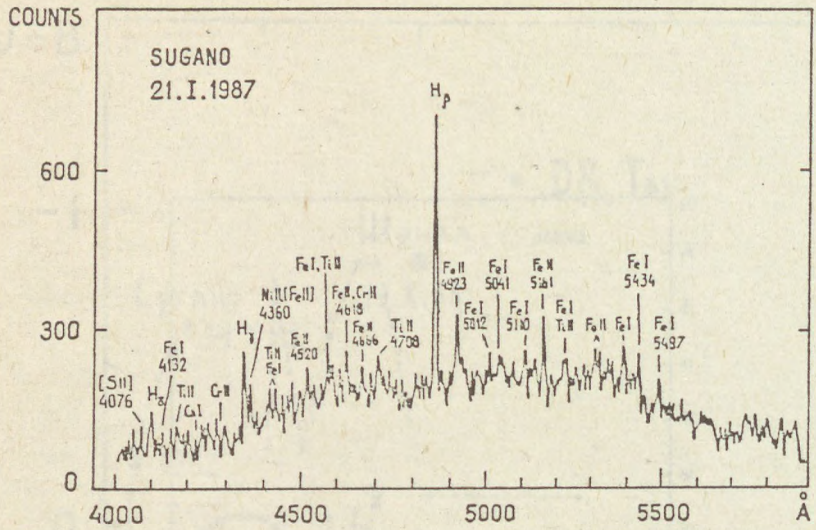

Рис. 4 Спектр звезды V II43 Ori , 2I.0I.I987 г.

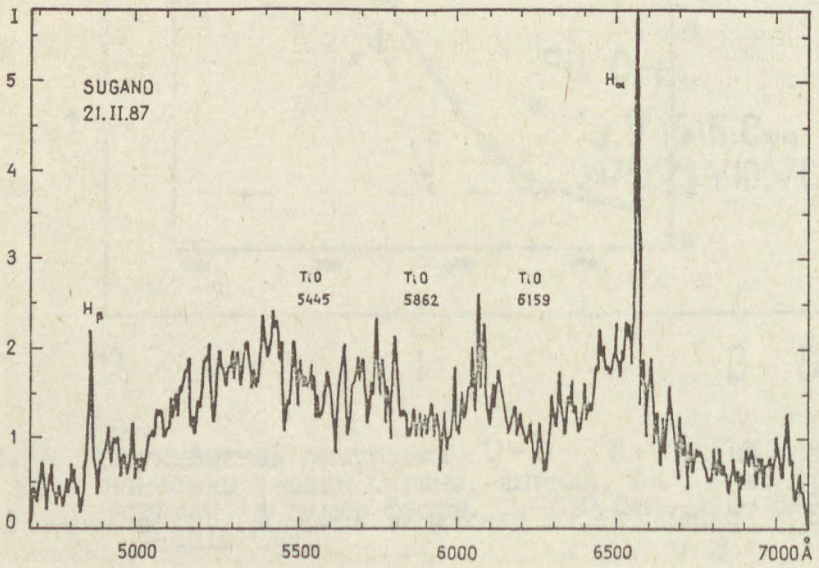

Рис. 5 Спектр звезды VII43 Ori, 2I.02.I987 г.

данных нет. В максимуме она находилась 4 месяца, затухание длилось 12 месяцев. В декабре 1988 г. в Бюраканской обсерватории был обнаружен вторичный подъем блеска звезды [11].

1 февраля 1989 года блеск звезды в фотографических лучах достиг 13.8, амплитуда $\Delta m_{pg} \geq 4.6$.

Спектр звезды, полученный нами на 6 м телескопе САО АН СССР и 2.6 м телескопе Бюраканской обсерватории, эмиссионный, с сильными линиями HI.

Наблюдения этих звезд в минимуме блеска свидетельствуют о том, что это орионовы переменные в большой вероятностью принадлежат к типу Т Тельца.

Для объяснения фуоров В.А.Амбарцумяном [12] была выдвинута гипотеза о том, что до подъема блеска в области, непосредственно окружающей звезду, имеются источники энергии, большая часть которой выделяется в виде энергии корпускулярного излучения. С появление оболочки большого радиуса, происходит конверсия корпускул в видимое излучение. Сравнение некоторых параметров фуоров и субфуоров показывает, что в данном случае повышение блеска также можно объяснить тем же механизмом [4]. Обе звезды находятся в активной фазе своего развития, дальнейшие спектральные и фотометрические наблюдения помогут выяснить какое место занимает фаза субфуоров в эволюции, столь разнообразных по своим характеристикам, звезд типа Т Тельца.

Авторы выражают благодарность И.Копылову и Н.Борисову за осуществление наблюдений на 6м телескопе САО АН СССР.

ЛИТЕРАТУРА

1. B.G.Marsden, Cir.IAU, No.37, 3, 1983.
2. R.Sh.Hatsvlishvili, IBVS, 2665, 1984.
3. B.G.Marsden, Cir.IAU, No.3924, 1984.
4. Э.С.Парсамян, К.Г.Гаспарян, Астрофизика, 27, 447, 1987.
5. E.Chavira, M.Peimbert, G.Haro, IBVS, 2746, 1985.
6. Е.П.Павленко, В.В.Прокофьева, Astron.Tsirk., No.1530, 1989.
7. K.G.Gasparian, G.B.Ohanian, E.S.Parsamian, IBVS, No.3024, 1987
8. Р.Ш.Натцвлишвили, частное сообщение, 1988.
9. B.G.Marsden, Cir.IAU, No.3771, 1983.
10. B.G.Marsden, Cir.IAU, No.3778, 1983.
11. K.G.Gasparian, G.B.Ohanian, IBVS, No.3327, 1989
12. В.А.Амбарцумян, Астрофизика, 16, 231, 1980.

AP AND AM STARS IN YOUNG STELLAR GROUPS

Tsvetanka Radoslavova
Department of Astronomy, Bulgarian Acad.of Sciences
72, Lenin Blvd., 1784 Sofia
Bulgaria

ABSTRACT. Nearly two hundred new Ap and Am stars were discovered in the course of objective-prism spectral classification work in five galactic fields centered at the associations Vulpecula OB4, Cygnus OB4, Cepheus-Lacerta OBI, Cassiopeia OB9 and Cassiopeia OBI4. The main line-features for identifying the Ap and Am stars on low-dispersion spectrograms are discussed. The surface distribution of these types of stars compared to that of the normal B and A-stars in the considered regions has shown to be similar. The proportion of the Ap and Am stars in the total number of stars of the same spectral type is estimated to 2-3%, and is almost equal in the five surveyed fields.

I. Introduction.

The use of objective prisms and, respectively, low-dispersion spectra in modern astrophysics is a very effective tool. It is important not only as a search method in spectroscopy - its proper role in a great number of classification projects has to be highly estimated, too (McCarthy, 1984). General classification projects with objective prisms are usually carried out on blue sensitive plates and cover the range from

"Star Clusters and Associations"
Publ. Astron. Dep. Eötvös Univ.
No.10, Budapest (1990)

3800 to 4800 Å at dispersions from about 150 Å/mm to 250 Å/mm at H_γ. Such surveys have opened the possibility to classify stars of all spectral types to a rather faint limiting magnitude and have much contributed to our knowledge about the distribution of stars, and herefrom - about the structure of our Galaxy.

Further, a great benefit of these surveys is that they lead to the discovery of a large number of interesting stars, namely, stars of the types WR, Ap, Am, Ba, S, H_α-emission, composite, etc.; and, of course, also of various, mainly extragalactic, objects like quasars and nebulae which will not be discussed here since their detection is connected with the use of much lower dispersions.

2. Observational Material.

In the course of our work on mass spectral classification, carried out by means of objective-prism techniques, many peculiar objects have been recognized; and here attention will be paid on the newly discovered Ap and Am stars. The plates on which they were identified, were taken with the 70-cm meniscus telescope of the Abastumani Astrophysical Observatory by means of an 8^o-objective prism. The dispersion of the spectra is 166 Å/mm at H_γ, their extent being from H_β up to 3500 Å. The spectrograms were widened to 0.4 mm. Well-exposed images were obtained for stars from about 8 to 11 photographic stellar magnitude, in five galactic fields in the surroundings of the OB-associations Vulpecula OB4, Cygnus OB4, Cepheus-Lacerta OB1, Cassiopeia OB9 and Cassiopeia OB14. Each field covers about 70 square degrees. In Table I the limits in α and δ (for epoch 1950.0) of the surveyed galactic fields are indicated.

TABLE I. Designation of the OB-associations and coordinates of the surveyed fields.

Fd.No.	Ass.No.	Designation	α(1950.0)	δ(1950.0)
I	Ass I4	Vul OB4	19^h24^m - 20^h02^m	$20^\circ30'$ - $29^\circ30'$
II	Ass 22	Cyg OB4	20^h52^m - 21^h32^m	33° - $42^\circ30'$
III	Ass 26	Cep-Lac OBI	21^h46^m - 22^h42^m	$49^\circ30'$ - $58^\circ30'$
IV	Ass 32	Cas OB9	23^h06^m - 00^h04^m	$54^\circ30'$ - $63^\circ30'$
V	Ass 37	Cas OBI4	00^h06^m - 01^h02^m	$58^\circ30'$ - $68^\circ30'$

3. Methods and Results.

In the five fields a total of I96 new Ap and Am stars were recognized. Their numbers for each field are given in Table 2; by semicolon the doubtful Ap and Am stars are indicated. Identification lists of the newly discovered Ap and Am stars have been published earlier (Radoslavova, I978, I985, I986), accompanied by short information about their spectral characteristics as seen on the objective-prism plates. For every star more than one - often 3 or 4 - spectrograms were studied visually. It should be pointed out that this method is most effective for such kind of work. The automatic objective-prism classification techniques proved to be unsufficient when peculiar objects are concerned. The reason is that these techniques are generally based on measurements of separate lines or groups of lines; this involves the possibility of omitting some peculiarities in the spectra. There is nothing but the human eye which is able to distinguish even rather subtle nuances in the spectral images. And when these nuances have to be searched for on low-dispersion spectrograms, the visual estimates are the most plausible. On the other hand, one should not forget that, as a matter

of fact, the visual objective-prism spectroscopy is subjective, depending strongly not only on the quality of the spectra but also on the personal perception of the astronomer who does the work as well as on his experience and conscientiousness. Consequently it may happen that stars announced as peculiar, after examining at higher dispersion prove not to be such.

TABLE 2. Numbers and types of the newly discovered peculiar stars in each of the fields.

Fd.No.	Ap	Ap:	Am	Am:	FOp
I	6	2	7	4	I
II	I3	22	2I	I8	2
III	I4	I4	9	9	2
IV	I5	I0	5	4	I
V	I0	2	3	I	I

Here we shall briefly discuss some characteristic line-features of the peculiar stars on Abastumani objective-prism spectrograms (Kharadze, Bartaya, I973). First of all, it should be emphasized that, because of the low resolution, it is not always possible to assign the observed peculiar lines to a particular chemical element. For instance, the lines in the range λλ4I28-4I3I Å merge in a blend and it is impossible to precise whether they are connected with the Eu or with the Si. Therefore it is difficult to draw a unambiguous conclusion about the type of the revealed Ap star - and we have not done that. Other lines, observed on Abastumani spectrograms in the case of Ap stars, are these of Sr λ4077 Å, Mn λλ4030-4033 Å

and Cr λ4171 Å.

As to the Am stars, they are discerned by the extreme sharpness of their hydrogen lines; although, a more prominent feature is the line of Sr λ4077 Å. This one is specific for supergiants too, but only when the star is later than spectral type A5. Therefore, in the case of a star earlier than A5 which shows a strong λ4077 Å line, one can be sure that it is an Am star.

When the star is of spectral type A2-A3 (the spectral class determination being performed according to the intensity ratio $(H+H_{Ca})/K_{Ca}$), it is often difficult to decide between the Ap and Am-phenomenon. Here the risk to be in error is rather high; and it may happen that some stars, classified as Ap, are in fact Am, or vice versa.

Most of the detected by us peculiar stars are of classical varieties; but those, indicated as FOp, with strong line at λ4077 Å, may represent something untypical, since they do not seem to be associated with the well-known strontium stars. On Abastumani spectra the FOp stars are characterized by the very strong line λ4077 Å and the blend λλ4128-4131 Å , which stand out on both sides of the line H_δ. Their intensity ratio to H_δ is I:3, sometimes even I:2.

4. Discussion.

All revealed Ap and Am stars were examined with respect to their surface distribution, taking into consideration also the stars found by other authors in the same galactic fields. The point is that such a consideration could provide valuable information concerning the evolutionary status of the Ap/Am stars. It is of significance to know whether these stars do or do not show a preference to particular stellar groups. As the fields in question comprise OB-associations - which

means that they have a greater content of early-type stars than the normal - it was important to verify whether there exists some specificity in the distribution of the Ap/Am stars as compared to that of the normal B and A stars. The examination of this point showed a similarity in the behaviour of the Ap/Am stars to that of the normal stars of the same spectral type - which corresponds to the results obtained by other authors (Renson, 1971).

Some statistics was also attempted with the purpose of correlating the number of the Ap/Am stars with the total number of early stars of similar spectral types. Almost the same results were obtained for the five fields in consideration, the proportion of the Ap and Am stars being calculated to vary from about 2 to about 3%.

It seems rather important to study the membership of the revealed Ap and Am stars to the respective OB-associations, but for this purpose more information is needed than we actually have at our disposal.

Obviously, a higher-resolution study of the Ap and Am stars discovered by means of objective-prism techniques is very desirable. Meaningful results could be expected only if closer reports between the objective-prism spectroscopists, slit spectroscopists and photometrists are established.

REFERENCES

Kharadze, E.K. and Bartaya, R.A. 1973, IAU Symp. 50, p.91.
McCarthy, M. 1984, Astronomy with Schmidt-Type Telescopes, Reidel Publ.Comp., p.37-52.
Radoslavova, Ts. 1978, Astron.Zirk., No.979, p.5.
Radoslavova, Ts. 1985, IBVS, No.2679.
Radoslavova, Ts. 1986, IBVS, No.2845.
Renson, P.1971, Astron.Astrophys., 13, p.130-135.

Interstellar extinction observed in spectra of B_e stars

Walter Wegner[1], Jacek Papaj[2] and Jacek Krełowski[2]

[1] Institute of Mathematics, Pedagogical University, ul. Chodkiewicza 30, Pl-85-064 Bydgoszcz, Poland

[2] Institute of Astronomy, N. Copernicus University ul. Chopina 12/18, Pl-87-100 Toruń, Poland

Abstract. Evident differences between extinction laws observed in spectra of "normal" B type and B_e stars are shown. The latter do not contain in many cases the prominent feature of the extinction curve - the 2200A bump. The results are derived both from multicolour (including the ultraviolet ANS) photometry and from TD-1 UV spectra. It is suggested that the observed peculiarities are originated in circumstellar shells which add their contributions to the interstellar reddening.

1. Introduction

Recent results on interstellar extinction have shown reliably that the extinction law may change from cloud to cloud (Wegner and Krełowski 1989). The variability is certainly caused by the differences in physical properties of the dust grains contained in these clouds. It has been suggested in early forties (van de Hulst 1986) that dust particles may evolve in the interstellar medium and thus their sizes, shapes and chemical composition may vary as well as their crystalline structure. An evolutionary track of interstellar grains has been recently discussed by Greenberg (1984).

The evolution of grains may be boosted in close vicinities of newly formed stars, particularly - hot stars emitting a lot of energetic UV quanta. Absorbed UV radiation may trigger some chemical reactions in grain mantles - the latter growing in cold, dense protostellar clouds. Thus the evolutionary effects should take place mostly in close vicinities of massive, young stars - still immersed in remnants of their parent clouds (which very recently passed a very cold and dense phase). These remnants are now strongly irradiated by the stellar radiation. In cases of massive stars a substantial part of the stellar energy is

"Star Clusters and Associations"
Publ. Astron. Dep. Eötvös Univ.
No.10, Budapest (1990)

expelled in the form of far-UV radiation. It seems to be of basic importance to know whether the evolving grains in vicinities of hot stars produce the extinction differing or not from that observed in the truly interstellar medium.

2. Description of the method

B_e stars are well known objects closely related to some circumstellar matter - possibly remnants of their parent clouds. Very peculiar extinction curves derived from spectra of at least some of them (Wegner and Krełowski 1989) make a more systematic investigation really attractive. Let's select a sample of B_e stars of nearly the same spectral type and luminosity class. A difference in the extinction law should be most easy to detect in the UV spectral range, particularly around the famous 2200A bump. Thus an analysis of possible peculiarities of extinction in B_e stars should start from a consideration of this prominent feature.

The spectral type and luminosity class most frequently observed from astronomical satellites is B2V. Thus we have selected the sample of these stars from the ANS Catalogue (Wesselius et al 1982). The colour index between the ANS 2200A band and the V band was correlated with the B-V in the selected set of normal B and B_e stars. The result is shown in Fig. 1. The observed differences between colour indices of different stars within the sample of the same Sp/L should result only from different reddenings. We observe here different slopes of the two-colour relations for normal B2 and $B2_e$ stars. This fact, as shown by Krełowski and Strobel (1987) indicates for different extinction laws towards the stars of both samples. The 2200A extinction bump is apparently stronger in relation to E_{B-V} when observed in spectra of normal B2 stars. Let's emphasize that the scatter observed in Fig. 1 is also greater in the case of B_e stars. Thus the sample of B_e stars is probably much less homogeneous - reflecting different stages of the evolution of circumstellar grains.

The most interesting cases are, however, these for very low reddenings. In such cases we may expect that extinction effects are caused by single clouds or solely by circumstellar shells in the case of B_e stars. Thus a comparison of extinction curves characterizing single clouds (such as "sigma" or "zeta" types introduced by Wegner and Krełowski 1989) with those derived from spectra of slightly reddened B_e stars may be very interesting. In spectra of heavily reddened B_e stars the truly interstellar effects become more and more important and thus their extinction curves get more and more similar to "normal" ones.

Fig. 1 Two-colour diagram relating the colour index between the 2200A ANS band and V band to B-V. Normal B2V stars - triangles; B2Ve - open circles. Note the different slopes of the mean relations - they intersect close to the assumed $(B-V)_o$ indicating that stars of both samples are intrinsically identical.

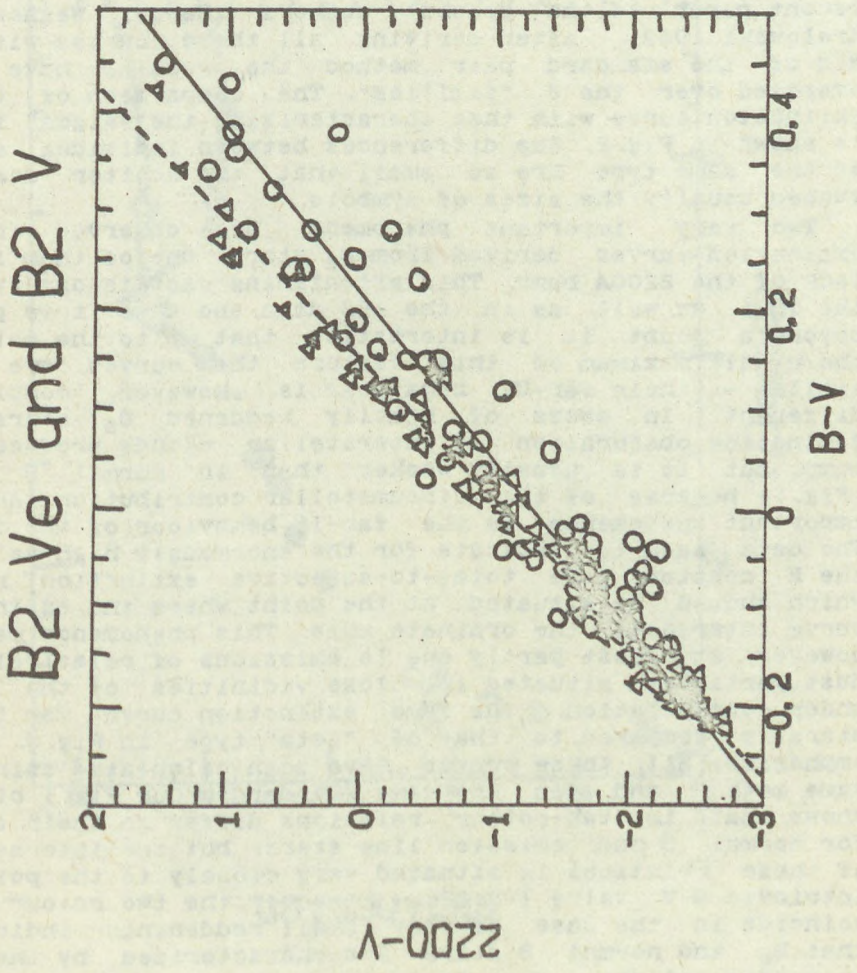

The stars selected for this purpose are listed in the Table. They are divided into the objects showing "sigma" or "zeta" extinction curves and the B_e stars of relatively low reddening. The another criterion of selecting these objects was the availability of their photometric data from far infrared (Gezari et al. 1984) together with the UBV data and the ANS photometry as well as of the TD-1 spectra (Jamar et al, 1976, Macau-Hercot et al. 1978). All these data allow to construct extinction curves in a very broad wavelength range and, moreover, one of the data sets may be a kind of the check of results obtained with the aid of another.

The individual extinction curves of the chosen stars have been calculated using the standards recommended in the recent paper of the present authors (Papaj, Wegner and Krełowski 1989). After deriving all these curves with the aid of the standard pair method the results have been averaged over the 3 "families". The comparison of the B_e extinction curve with that characterizing the "sigma" family is shown in Fig. 2. The differences between individual curves of the same type are so small that the scatter does not exceed usually the sizes of symbols.

Two very important phenomena are observed in the extinction curves derived from B_e stars. One of them is the lack of the 2200A bump. This astonishing fact is observed in the TD-1 as well as in the ANS data and thus it is proved beyond a doubt. It is interesting that up to the point of the usual maximum of this feature the curves are very similar - their far-UV behaviour is, however, completely different. In cases of heavily reddened B_e stars the dominating obscuration of interstellar clouds produces the bump, but it is usually weaker than in normal B stars (Fig. 1) because of the circumstellar contribution. Another important phenomenon is the far-IR behaviour of the curve. The data seem to indicate for the enormously high value of the R constant (the total-to-selective extinction ratio) which should be situated at the point where the extinction curve intersects the ordinate axis. This phenomenon may be, however, at least partly due to emissions of relatively hot dust particles situated in close vicinities of the stars under consideration. The same extinction curve for the B_e stars is compared to that of "zeta" type in Fig. 3. Let's emphasize: all these curves have been calculated using the same method and even the same standards. Our Fig. 1 clearly shows that the two-colour relations differ in their slopes for normal B and emission line stars, but the intersection of these relations is situated very closely to the point of intrinsic B-V value (-0.22). Moreover the two colour plots coincide in the case of very small reddenings indicating that B_e and normal B stars are characterized by the same intrinsic colours. This fact makes the results completely reliable.

Fig. 2 The comparison of the extinction curves averaged over the samples listed in the Table. Dots - B2Ve, open circles - "sigma" type extinction law. The segments calculated from TD-1 spectra are added in both cases.

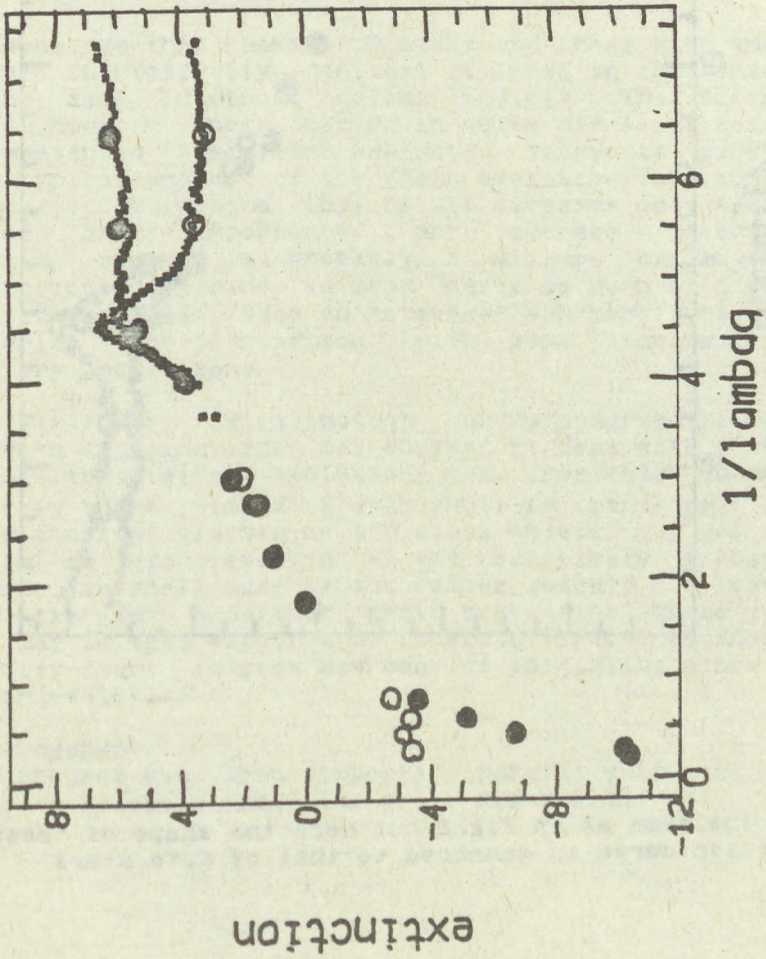

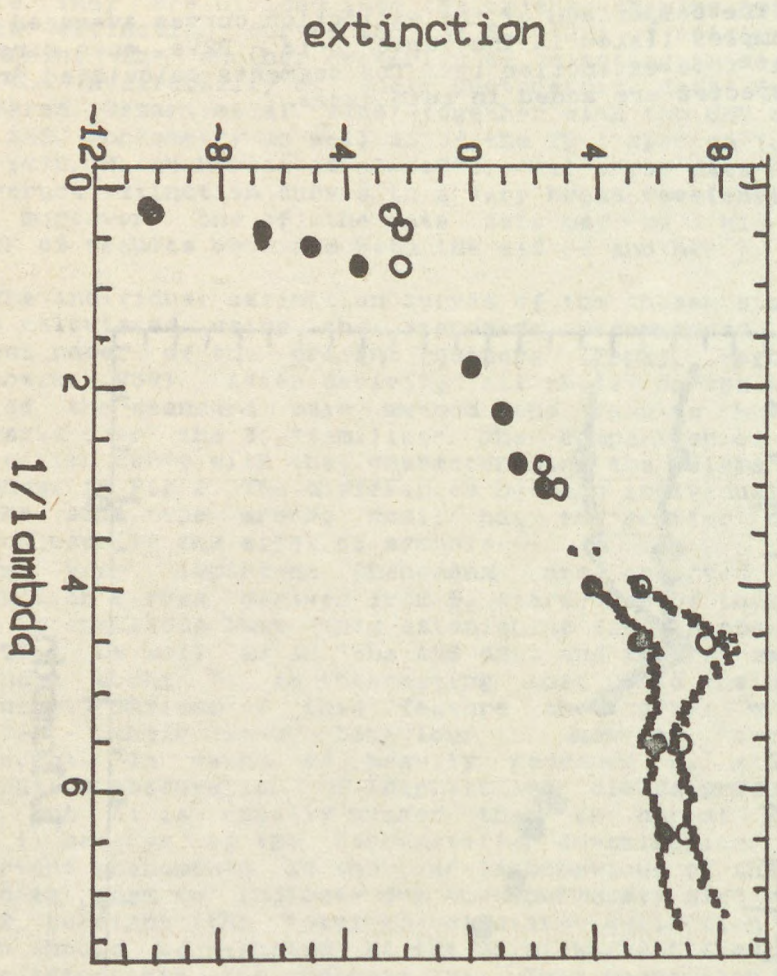

Fig. 3 The same as in Fig. 2 but here the shape of "zeta" mean extinction curve is compared to that of B2Ve stars.

3. Discussion and conclusions

Our analysis shows clearly that the extinction originating in close vicinities of hot, newly formed stars is "peculiar" in the above described sense. This peculiarity is probably related to certain stages of evolution of the grains that remained in the remnants of the parent clouds of the observed stars. We may hardly say anything certain about the geometry of the obscuring clouds. They may occur in the form of disks or more or less spherical shells - our analysis can hardly distinguish such cases; taken together they produce probably the scatter observed in our Fig. 1.

We conclude that "normal" B stars and those with emission lines are intrinsically identical at least in the sense they have the same intrinsic colour indices. The extinction modifies however their spectra in quite different ways. The above presented "peculiar" extinction curve is probably a rather typical product of the grain evolution in vicinity of a source of UV quanta. This result stresses once again the fact of basic importance: any "average interstellar extinction curve" is probably a mixture of individual contributions differing in many cases as much as the above presented examples. Such an "average" can hardly be used as a material for comparison with some theoretical or laboratory predictions.

The similarity of extinction curves observed in many B stars with emission lines may suggest we deal with a certain phase of the stellar evolution too. Possibly through a relatively short time a B star shell is transparent enough to make the star visible as a B class object. The grains are probably so far evolved - the relatively transparent circumstellar shell must expand rather quickly not leaving a lot of time for a further grain processing. These evolved grains may be thus captured by interstellar clouds when they eventually start to grow new mantles initiating a new phase of their evolution.

Acknowledgement.
This project has been supported partially by the Polish Academy of Sciences under the grant RPB-R 1.11.

HD number	Star name	Sp/L	V	B-V	E(B-V)
		Be stars			
20336		B2.5 Ven	4.84	-0.15	0.05
32343	11 Cam	B2.5 Ve	5.08	-0.08	0.12
44458		B1 Vpe	5.64	-0.02	0.19
57150		B2 V + B3 IVne	4.66	-0.10	0.10
60606		B3 Vne	5.54	-0.06	0.12
65875		B2.5 Ve	6.51	-0.07	0.13
88661		B2 IVpne	5.72	-0.08	0.13
202904	66 Cyg	B2 Vne	4.43	-0.11	0.10
		"sigma" family			
34989		B1 V	5.80	-0.13	0.10
144217	β^1 Sco	B1 V	2.62	-0.07	0.16
144470	ω^1 Sco	B1 V	3.96	-0.04	0.19
147933	ρ Oph	B2 IV	5.02	0.24	0.45
148605	22 Sco	B2 V	4.79	-0.11	0.10
		"zeta" family			
3901	19 Cas	B2 V	4.80	-0.11	0.10
35149	23 Ori	B1 V	5.00	-0.15	0.08
60325		B1 V	6.21	-0.04	0.19

References

Gezari, D. Y., Schmitz, M., and Mead J. M. 1984. Catalog of Infrared Observations. NASA Ref. Publ. 1118.

Greenberg, J. M., 1984. In: *Laboratory & Observational Infrared Spectra of Interstellar Dust*, p. 1, eds Wolstencroft, R. D. and Greenberg J. M., Royal Observatory Edinburgh, Edinburgh.

van de Hulst 1986 in *Light on dark matter*, F. P. Israel (ed.), D. Reidel, Dordrecht 1986, p. 161.

Jamar, C., Macau-Hercot, D., Monfils, A., Thompson, G. I., Houziaux, L. and Wilson, R., 1976. *Ultraviolet Bright Star Spectrophotometric Catalogue.* ESA SR-27.

Krełowski, J. and Strobel, A., 1987. *Astr. Astrophys.* 175, 186.

Macau-Hercot, D., Jamar, C., Monfils, A., Thompson, G. I., Houziaux, L. and Wilson, R., 1978. *Supplement to the Ultraviolet Bright Star Spectrophotometric Catalogue.* ESA SR-28.

Papaj, Wegner and Krełowski 1989. Mon. Not. R. astr. Soc. (submitted)

Wegner, W. and Krełowski, J., 1989. *Astr. Nachr.*, in press.

Wesselius, P. R., van Duinen, R. J., de Jonge A. R. W., Aalders, J. W. G., Luinge, W., Wildeman, K. J. 1982. Astron. Astrophys. Suppl. 49, 427.

MULTIDIMENSIONAL STATISTICAL ANALYSIS OF STAR CLUSTERS AND COMPLEXES

A.M.Ejgenson and O.S.Yatsyk
Lvov University Astronomical Observatory
Lomonosov St. 8
Lvov 290005
USSR

ABSTRACT. Taxonomical analysis used for study of galactic distribution of open clusters, OB-associations and cepheids shows about 2/3 of these objects to enter non-random condensations with characteristic dimensions of some hundred parsecs. Classification of star clusters leads to conclusion that in process of their formation there has been no substantial gaps. Variety of clusters' properties is determined mainly by two factors. Prognostication of X-ray radiation from globular clusters is made.

We report here some results of application of multidimensional statistical analysis (MSA) to the study of star clusters and complexes as it relates to understanding of structure and evolution of Galaxy. MSA consists of three branches: taxonomical analysis, factor analysis and, finally, pattern recognition. In taxonomical analysis groups of objects similar in some sense are distinguished. In factor analysis one finds number and nature of independent factors determining an observational variety of objects' properties. Finally in pattern recognition according to properties of object we classify it to one of several groups.

Taxonomical analysis was used for two different aims: 1) the study of space distribution of open clusters, OB-associations and cepheids, and 2) classification of star clusters. The results are the following.

1) Galactic distribution of 361 open clusters, 53 OB-associations and 300 cepheids was considered by hierarchial clumping method. It is shown that about 2/3 of these objects enter non-random condensations (taxons) with characteristic dimensions of some hundred parsecs. In some cases it is possible to join neighbouring taxons into systems with dimensions of about 1 kps or more. Traces of common origin are preserved sometimes for more than 10^9

"Star Clusters and Associations"
Publ. Astron. Dep. Eötvös Univ.
No.10, Budapest (1990)

years. We composed the list of 53 taxons and 32 pairs of objects.

2) Distribution of open and globular clusters was considered in spaces of basic physical parameters. Several variants of classification are proposed. Open clusters form a linear consequence by age. For globular ones the role of "free parameter" plays the distance from Galaxy centre. Common consideration of clusters of both types confirmes these dependences. The conclusion is made that in clusters' formation process possibly there where no substantial gaps.

3) Variety of globular clusters' properties is shown to be determined by two factors. The first factor is associated with metallicity and/or the distance from Galaxy centre, while the second is connected with "richness" and/or concentration of clusters. Most observational parameters are determined by preferential action of one of these factors, while geometrical dimensions of cluster are dependent on both factors simultaneuosly.

For open clusters the role of the first factor plays an age and/or a distance from galactic plane.

4) One of pattern recognition methods is used to find the deciding rule for separating X-ray globulars from non-X-ray ones. It is used for prognostication such radiation from clusters being unresearched in this sense.

Some results of this study are given in details in our papers (Ejgenson and Yatsyk, 1986; 1987a; 1987b; 1988; 1989; Ejgenson,Yatsyk and Khomik, 1988; Ejgenson,Yatsyk and Chernogyl, 1988).

References

Ejgenson A.M.,Yatsyk O.S.:1986,Astron.Zh. 63, 659.
Ejgenson A.M.,Yatsyk O.S.:1987a,Astron.Zh. 64, 965.
Ejgenson A.M.,Yatsyk O.S.:1987b,Pisma v Astron.Zh.13, 481.
Ejgenson A.M.,Yatsyk O.S.:1988,Astron.Zh. 65, 330.
Ejgenson A.M.,Yatsyk O.S.,Khomik S.I.:1988,Astron.Zh. 65, 730.
Ejgenson A.M.,Yatsyk O.S.,Chernogyl P.M.:1988,Astron.Zh. 65, 1244.
Ejgenson A.M.,Yatsyk O.S.:1989,Pisma v Astron.Zh. 15, 223.

DYNAMICAL MASSES OF GALACTIC GLOBULAR CLUSTERS

N. Spassova[1], *G. Mandushev*[2] *and A. Staneva*[2]

[1]Department of Astronomy, Bulgarian Academy of Science, 72 Lenin St, 1784 Sofia, Bulgaria

[2]Department of Astronomy, University of Sofia. University Astonomical Observatory, 1504 Sofia, P.O.Box 36, Bulgaria.

ABSTRACT. Dynamical masses of 146 galactic globular clusters have been determined using single mass isotropic King's models, and high quality observational data of the clusters central velocity dispersion. The typical value of a globular clusters mass is 1.1 10^5 $m_\odot$, and the mean mass-to-light ratio is 1.37 ± 0.43.

1. INTRODUCTION

The first determinations of the individual masses of the richest globular clusters ω Cen (*Dickens and Woolley* 1967), M92 (*Wilson and Coffeen* 1954; *Schwarzschild and Bernstein* 1955) and 47 Tuc (*Feast and Thackeray* 1960) have been based on the knowledge of the velocity dispersion derived from radial velocity measurements for individual giants from low-dispersion spectra. The mass of M3 has also been estimated from the luminosity function (*Sandage* 1957). In both cases the masses are fairly uncertain. In 1976 dynamical masses have been determined for 10 southern globular clusters (*Illingworth* 1976). In this case the central velocity dispersions determined from high-dispersion coude spectra of the integrated light were incorporated into King's (1966) single mass star cluster models to calculate the cluster masses.

2. MASS DETERMINATION METHODS

Reasonably good dynamical constreints - surface brightness profile and central value of the velocity dispersion - are available now for 39 galactic globular clusters. In the present study all these observations of the velocity dispersion will be converted into mass, according to King's (1966) single - mass model formula $M = \rho_c^3 \mu$, reduced by

"Star Clusters and Associations"
Publ. Astron. Dep. Eötvös Univ.
No.10, Budapest (1990)

Illingworth (1976) to

$$\mathcal{M} = 167\, r_c \mu \langle V_r^2 \rangle_o \qquad (1).$$

Here r_c is the core radius derived from the fit of the observed surface brightness profile to King's models, and tabulated in Webbink's catalogue (1985) of the structure parameters of galactic globular clusters; μ is interpolated using King's Table II (1966). (The concentration parameter $c = \lg (r_t/r_c)$ was calculated on the bases of the values of r_t and r_c, quoted in the Webbink's catalogue, 1985); $\langle V_r \rangle_\sigma$ is the central velocity dispersion obtained by different authors from integrated light spectra (ILS) or from high-quality radial velocities (RV) of cluster's members.

Table I represents the following parameters for the thirty nine clusters: the mean observational velocity dispersion $\langle \overline{V_r} \rangle_o$ derived by data obtained from several authors; the method of its determination; the total masses of the clusters $\mathcal{M}$ (in solar units) calculated with formula (1); the visual mass-to-light ratio $\mathcal{M}/L_v$, and references. The visual integrated luminocity L_v (in solar units) was determined, taking $M(V)_\odot = 4.83$ (*Allen* 1973), and using the Webbink's data (1985) for the absolute integrated magnitudes M(V) of the corresponding clusters.

Table I. Masses determined with Eq. (1)

NGC	$\langle \overline{V_r} \rangle_o$ [km/s]	method	$\mathcal{M}_{tot}$ [$10^6 m_\odot$]	$\mathcal{M}/L_v$ [$\odot$ units]	references
104	11.32	RV, ILS	0.68	1.13	5, 8
288	2.90	RV	0.06	1.59	10
362	8.63	RV, ILS	0.21	1.09	2, 5
1851	8.18	ILS	0.17	0.95	5
2808	14.76	ILS	0.92	1.76	5
3201	4.30	RV	0.12	1.44	2
4147	2.80	RV	0.03	1.30	10
4372	3.55	RV	0.10	1.08	2
4833	5.59	RV	0.17	1.46	2
5139	14.33	RV	2.18	1.76	8
5272	6.02	RV	0.39	0.99	2, 4
5466	1.85	RV	0.07	1.14	9, 10
6093	12.88	ILS	0.33	2.73	5
6121	3.90	RV	0.05	0.92	9
6171	2.90	RV	0.04	0.87	10
6205	7.10	RV	0.35	1.40	6
6218	3.70	RV	0.06	0.73	10
6266	13.91	RV, ILS	0.40	1.60	2, 5
6273	10.60	RV	0.74	1.22	2
6341	7.00	RV	0.19	1.27	2, 7
6356	7.68	RV	0.38	1.25	2

Table I. - continue

NGC	$\langle \overline{V_r} \rangle_o$ [km/s]	method	$\mathcal{M}_{tot}$ [$10^6 m_\odot$]	$\mathcal{M}/L_v$ [$\odot$ units]	references
6362	3.97	RV	0.11	1.71	2
6388	19.65	ILS	1.30	1.65	5
6397	3.10	RV	0.03	0.71	1
6441	18.30	ILS	0.90	1.99	5
6624	5.40	RV	0.07	0.85	10
6626	8.90	RV	0.23	1.48	10
6637	6.97	RV	0.19	1.37	2
6652	6.12	RV	0.13	1.75	2
6656	8.94	RV	0.32	1.46	2, 9
6681	6.10	RV	0.10	1.73	2, 10
6712	4.00	RV	0.05	0.70	3
6715	14.83	ILS	0.98	1.75	5
6723	5.37	RV	0.16	1.56	2
6809	4.06	RV	0.08	1.04	2, 10
6838	2.80	RV	0.02	1.23	9
6864	10.72	ILS	0.37	2.03	5
7078	7.97	RV	0.37	0.84	2
7089	10.40	RV	0.66	1.80	10

References correspond as follows:

(1) *Da Costa et al.* (1977)
(2) *Geyer et al.* (1983)
(3) *Grindlay et al.* (1987)
(4) *Gunn and Griffin* (1979)
(5) *Illingworth* (1976)
(6) *Lupton and Gunn* (1987)
(7) *Lupton et al.* (1985)
(8) *Meylan* (1987)
(9) *Peterson and Latham* (1986)
(10) *Pryor et al.* (1987)

The mean formal error of the estimated masses is probably about 20% and results primarily from the uncertainty of the velocity dispersion, and from the fitting error for $r_c \mu$. It is necessary to emphasize, that as far as the King's models make assumption which simplifies the real dynamical situation in globular clusters, the basic uncertainty of the thus masses derived is a result mainly from the limitations of the model. The masses of the above mentioned 39 globular clusters, calculated with formula (1) have been used to calibrate the function $\mathcal{M}(M_v)$:

$$\lg \mathcal{M} = -(0.44 \pm 0.02) M_v + (1.76 \pm 0.16) \qquad (2)$$

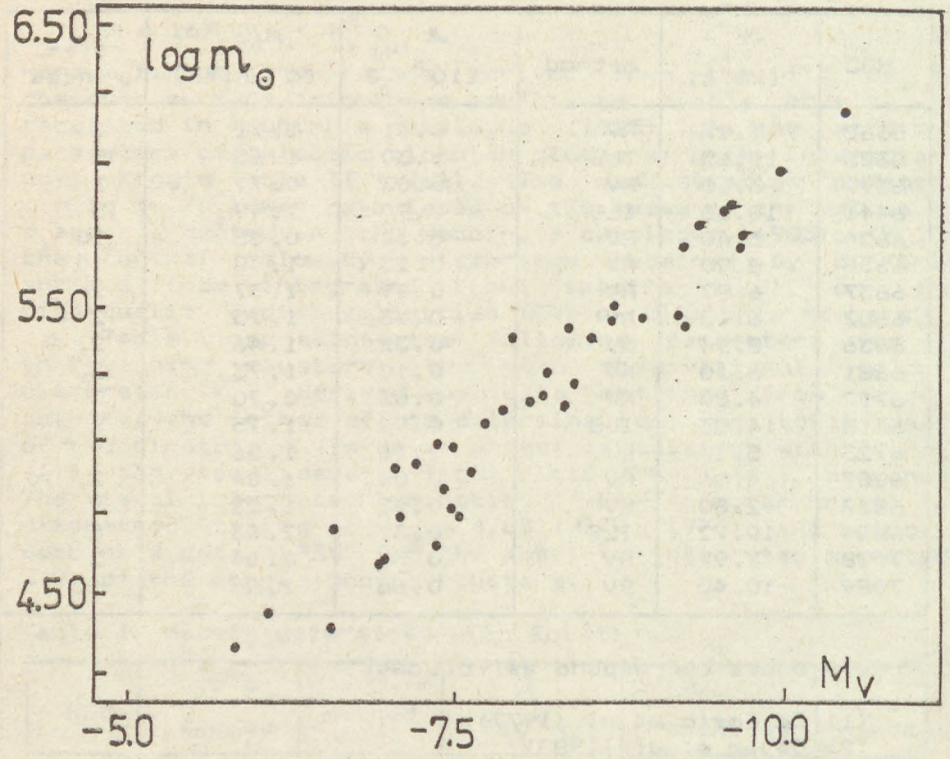

Fig.1. For thirty nine clusters, masses $\mathcal{M}$ as a function of the absolute magnitude M_v.

The calibration curve (2) is deduced for $-5^m.82 \leq M_v \leq -10^m.4$ and it has been used for calculating the masses of another 84 clusters which absolute magnitudes M_v are larger than $M_v = 5^m.8$ and are given in Webbink's catalogue. There are 23 known globular clusters with absolute magnitudes $-1^m.7 \leq M_v \leq -5^m.8$. The extrapolation of the calibration curve (2) to $M_v = -1^m.70$ leads to unusually small masses of the weakest clusters (AM-1, $\mathcal{M} \simeq 317\ m_\odot$!). In this case the mass-to-ligt ratio $\mathcal{M}/L_v$ for thirty nine clusters, which masses have been determined directly from their velocity dispersion (see Eq. 1) have been used. The typical one was find to be $\mathcal{M}/L_v = 1.37 \pm 0.24$.

The values of masses of globular clusters calculated by the calibration curve (2) and by the mass - to - light ratio = 1.37 are given in Table IIa and IIb, respectively.

Table IIa. Masses determined with Eq. (2)

object	$\mathcal{M}_{tot}$ [$10^5 m_\odot$]	$\mathcal{M}/L_v$ [$\odot$ units]	object	$\mathcal{M}_{tot}$ [$10^5 m_\odot$]	$\mathcal{M}/L_v$ [$\odot$ units]
N1261	1.37	1.27	N6355	0.59	1.19
N1466	1.11	1.25	Ter 4	0.59	1.18
Ret	0.21	1.09	HP 1	1.65	1.29
Pal 2	0.84	1.22	Gri 1	1.69	1.29
N1841	0.94	1.23	N6366	0.29	1.12
N1904	1.42	1.27	N6380	0.31	1.13
N2298	0.35	1.14	Pal 6	0.61	1.19
N2419	8.56	1.47	N6401	0.83	1.22
Pal 3	0.23	1.10	N6402	6.66	1.44
ESO 093	0.58	1.18	N6426	0.31	1.13
Rup 106	0.64	1.19	Ter 5	0.83	1.22
N4499	1.21	1.26	N6440	3.72	1.38
N4590	0.84	1.22	N6453	0.89	1.23
N5024	4.16	1.39	Ter 6	0.34	1.13
N5053	0.26	1.11	UKS 1	1.19	1.26
N5286	2.67	1.34	N6496	0.20	1.08
N5634	1.39	1.27	N6517	0.71	1.20
N5694	3.30	1.36	Ter 10	0.35	1.14
N5824	8.39	1.47	N6522	0.87	1.22
N5897	0.71	1.20	N6528	0.45	1.16
N5904	3.99	1.38	N6539	0.30	1.12
N5927	1.90	1.30	N6541	2.96	1.35
N5946	0.73	1.20	N6544	0.33	1.13
BH 176	1.76	1.30	N6553	2.35	1.33
N5986	2.67	1.34	N6558	0.31	1.13
N6101	0.64	1.19	Pal 7	1.13	1.25
N6139	1.74	1.30	N6569	1.42	1.27
Ter 3	0.29	1.12	N6584	1.14	1.25
N6144	0.55	1.18	N6638	0.31	1.13
N6229	2.02	1.31	Pal 8	0.75	1.21
N6235	0.44	1.16	N6717	0.22	1.09
N6254	1.06	1.24	N6749	0.28	1.11
N6256	0.32	1.13	N6752	1.33	1.27
N6284	0.71	1.20	N6760	0.54	1.18
N6287	0.44	1.16	Ter 7	0.24	1.10
N6293	0.95	1.23	N6779	0.91	1.23
N6304	0.78	1.21	Ter 8	0.35	1.14
N6316	2.76	1.35	Pal 11	0.63	1.19
N6325	0.27	1.11	N6934	1.06	1.24
N6333	1.56	1.29	N6981	0.60	1.19
N6342	0.62	1.19	N7006	1.25	1.26
N6352	0.36	1.14	N7099	0.76	1.21

Table IIb. Masses determined with mean $\mathcal{M}/L_v = 1.35$

object	$\mathcal{M}_{tot}$ [$10^3 m_\odot$]	object	$\mathcal{M}_{tot}$ [$10^3 m_\odot$]	object	$\mathcal{M}_{tot}$ [$10^3 m_\odot$]
Pal 1	1.20	Pal 14	9.60	Ter 11	18.30
AM 1	7.22	ESO 452	4.86	N6842	18.98
Eri	10.92	Pal 15	16.68	Pal 10	19.69
E 3	5.53	Ter 2	5.04	Arp 2	15.36
UKS 2	5.28	Ter 1	10.60	Pal 12	9.51
Pal 4	21.00	Ton 2	16.08	Pal 13	2.41
AM 4	0.56	Ter 9	3.49	N7492	11.23
Pal 5	11.54	N6535	9.34		

The distribution of the calculated masses for the sample of 146 galactic globular clusters and the mass - to - light ratios distribution for the galactic globular clusters are given in Figure 2.

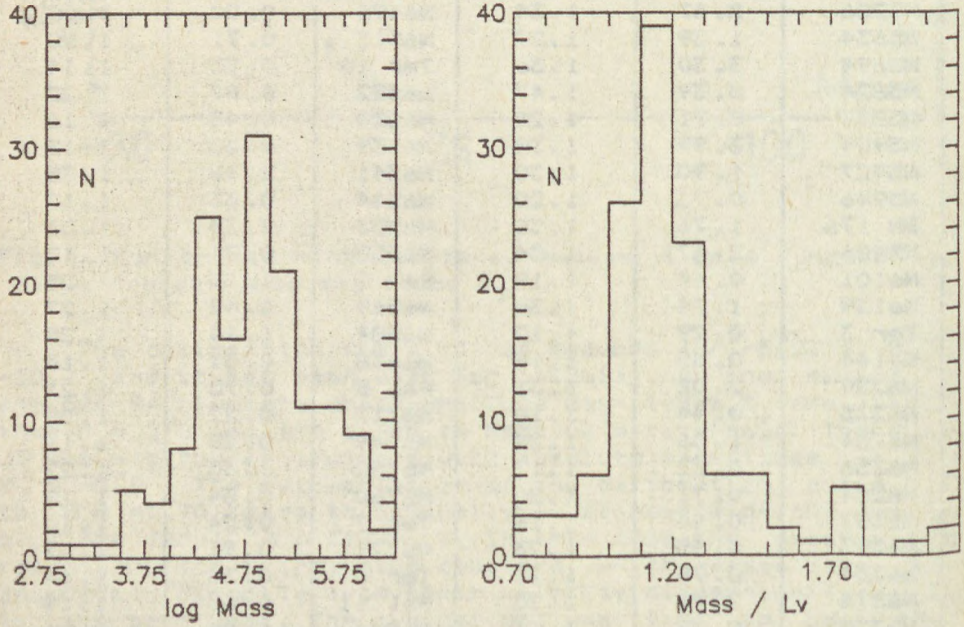

Fig.2. Mass and mass - to - light ratio distribution for globular clusters in our Galaxy.

It can be seen that about 82% of all globular clusters have masses between $1\ 10^4 \div 5\ 10^5\ m_\odot$ with typical value $1.12\ 10^5 m_\odot$. The distribution of the mass-to-light ratio for the clusters is shown on the same Figure.

Recently, a high-quality observational data allowing the investigation of the internal cluster structure are acquired only for six clusters. The total mass and the value of $\mathcal{M}/L_v$ for these clusters have been obtained from different authors, using multi-mass anisotropic King-Michie's dynamical models, and are summarized by Meylan (1987).

A comparison between $\mathcal{M}$ and $\mathcal{M}/L_v$ values, calculated according to single - mass models (Eq. 1), and those multicomponent models mentioned above for six clusters is shown in Table III. It must be noted that masses and $\mathcal{M}/L_v$ values given in columns 2 and 3 respectively are calculated with Eq.(1), using data for r_t, r_c, $\langle V_r \rangle_0$ and M_v, taken from Meylan's Table 2 (1987). Thus the differences $\Delta\mathcal{M}$ is due only to the difference of the models used (between col. 2 and 4).

Table III. Comparison between different model masses

NGC	single-mass model		multi-mass model		single-mass model-this study	
	$\mathcal{M}$ $[10^6 m_\odot]$	$\mathcal{M}/L_v$	$\mathcal{M}$ $[10^6 m_\odot]$	$\mathcal{M}/L_v$	$\mathcal{M}$ $[10^6 m_\odot]$	$\mathcal{M}/L_v$
(1)	(2)	(3)	(4)	(5)	(6)	(7)
104	0.7	1.8	0.7	1.8	0.7	1.1
5139	3.3	2.5	3.9	2.9	2.2	1.8
5272	0.5	1.8	0.6	2.2	0.4	1.0
6205	0.2	1.0	0.7	3.6	0.35	1.4
6341	0.2	1.2	0.4	2.4	0.2	1.3
7089	0.6	1.8	0.9	2.7	0.7	1.8

It is worth mentioning, that a clear correlation, displayed in Fig.3 appears between the $\Delta\mathcal{M}$ and the concentration parameter $c = lg\ r_t / r_c$ of the considered clusters. This close correlation is interesting but since only six points are deduced we are not in a possition to make generalized conclusion. Bearing in mind this fact we can note that only the mass estimations of the high-concentration clusters are not greatly influenced by the type of the model. The absolute comparison of the masses of the six clusters (columns 4 and 6) of the Table III shows that the masses of the clusters with $c \leq 2.0$, calculated by single-mass model are about 26 - 50 % smaller than those, calculated by multi-mass models.

It is evident that mass determination largely depends

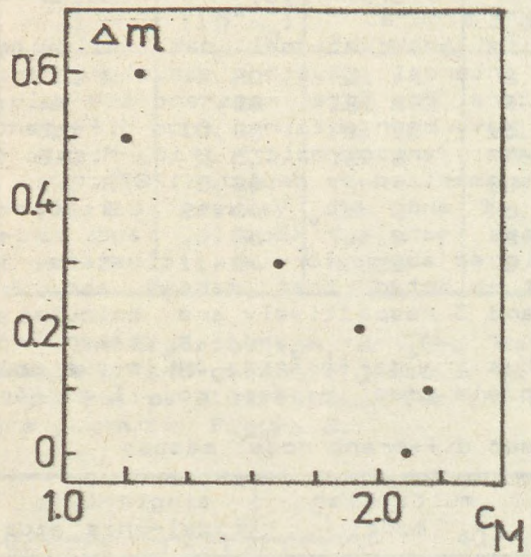

Fig.3. Correlation between the concentration parameter c and the mass difference. ΔM is the difference in masses, determined by multi-mass and single - mass star cluster models.

on the model used and on the quality of the observational data. Taking into account the limitations in the self - consistent star clusters dynamical model (*King* 1966) that we have used in this study, the mass estimates should be considered fairly uncertain and taken as a lower limit of the expected actual masses of the globular clusters in our Galaxy.

3. CONCLUSIONS

1. The masses of 146 globular clusters were determined from:

i) their central velocity dispersion, using the King's (1966) single-mass globular cluster models (for 39 objects).

ii) the calibration curve (eq.2), deduced from the values of masses, calculated according to (*i*), and the corresponding absolute magnitudes M_v (for 84 clusters).

iii) the mean mass-to-light ratio $M/L_v = 1.37$ from (*i*) (for 23 clusters).

2. The masses range from $5.6\ 10^2 m_\odot$ (AM-1) to $2.2\ 10^6 m_\odot$ (ω Cen) with a typical value $1.1\ 10^5 m_\odot$.

3. The values of the mass - to - light ratio M/L_v are located between 0.70 to 2.73.

REFERENCES

Allen, C.W. 1973, *Astrophysical Quantities* - 3rd ed., London, Athlone press.
Da Costa, G.S., Freeman, K.C., Kalnaj A.J., Rodgers, A.W., Stapinski, T.E. 1977, *Astron. J.*, 82, 810.
Dickens, R.J., and Wooley, R.v.d.R., 1967, *R.O.B.*, 128.
Feast, M.W., and Thackeray, A.D. 1960, *M.N.R.A.S.*, 120, 463.
Geyer, E.H., Hopp, U., and Nelles, B. 1983, *Astron. Astrophys.*, 125, 359.
Grindlay, J.E., and Philip, A.G.D. 1987, *The Harlow Shapley Symposium on Globular Cluster Systems in Galaxies*, IAU Symp. 126, Eds. J.Grindlay and D.Philip, Reidel, p.659.
Gun, J.E., and Griffin, R.F. 1979, *Astron. J.*, 84, 752.
Illingworth, G. 1976, *Astrophys. J.*, 204, 73.
King, I.R. 1966, *Astron. J.*, 71, 64.
Lupton, R., Gunn, J.E., and Griffin, R.F. 1985, *Dynamics of Star Clusters* IAU Symp. 113, Eds. J.Goodman and P.Hut, Reidel, p.19.
Lupton, R., and Gunn, J.E. 1987, *Astron. J.*, 93, 1106.
Meylan, G. 1987, *ESO Preprint* No.530.
Peterson, R.C., and Latham, D.W. 1986, *Harvard-Smithsonian Center for Astrophysics Preprint* No.2233.
Pryor, C., Mc Clure, R.D., Fletcher, J.M., Hartwick, F.D.A., and Kormendy, J. 1986, *Astron.J.*, 91, 546.
Pryor, C., Mc Clure R.D., Fletcher J.M., Hesser, J. 1987, *The Harlow Shapley Symposium on Globular Cluster Systems in Galaxies*, IAU Symp. 126, Eds. J.Grindlay and D.Philip, Reidel, p.661.
Sandage, A. 1957, *Astrophys. J.*, 125, 422.
Schwarzschild, M., and Bernstein, S. 1955, *Astrophys. J.*, 122, 200.
Webbink, R.F. 1985, *Dynamics of Star Clusters*, IAU Symp.113, Eds. J.Goodman and P.Hut, Reidel, p.541.
Wilson, O.C., and Cofeen, M.F. 1954, *Astrophys. J.*, 119, 197.

THE "COCIA", A CATALOGUE OF OPEN CLUSTER AGES
Experiences in Data Handling, and Presentation of the Catalogue

Maria Luise Roth-Höppner
Hamburger Sternwarte, Hamburg University
Private Address:
Hansastrasse 1
D - 2054 Geesthacht

ABSTRACT. The COCIA is a compilation of published age and turn-off mass determinations of galactic open clusters. Besides the age values, however, it contains also information and references on all the assumptions and quantities on which the respective age determination is based. The present version of the catalogue contains 1260 entries referring to 250 galactic clusters. A special chapter of the catalogue gives a short description (in tabular form) of the most widely used age calibration curves. In the following, Section 1 shows the need for this kind of catalogue, Section 2 describes the way used for data compiling and analysing, the layout of the catalogue is described in Sections 3, and Section 4 gives some statistics.

1. Motivation for preparing a catalogue of cluster ages

1.1 What is needed?

In many fields of astronomical research a homogeneous set of reliable cluster ages comprising as many clusters as possible would be strongly needed.

1.2 What is available in the Literature ?

When searching the Literature for cluster age determinations one finds:
a) Papers that contain age values of single clusters;
b) Age catalogues that are old, the age values thus superseded;
c) Modern age catalogues containing a limited number of clusters.

To get the desired set of cluster ages for "as many clusters as possible" one has to combine age values taken from all these sources. To combine the results of different authors, however, requires to correct the different age values. A laborious task! It does not only require to follow step by step the whole chain of arguments that led to the resultant age, but moreover, it requires a painstaking inspection of all assumptions that entered the respective age determination - from the criteria of selection of cluster members to the calibration of photometric data and up to the smallest details of stellar evolutionary calculations.

1.3 What kind of catalogue could help ?

This would be a catalogue that fulfils two conditions:
a) To give for each cluster a complete compilation of all age values published in the Literature. (This would dispense the user from a time consuming search).
b) To give informations and references, for each of these age values, on all the assumptions and quantities on which the corresponding age determination has been based. (This would help the user to discard erroneous or superseded age values, and would also help with the attempted homogenisation of age values taken from different sources).

"Star Clusters and Associations"
Publ. Astron. Dep. Eötvös Univ.
No.10, Budapest (1990)

The catalogue "COCIA", presented in the following, tries to fulfil these two conditions.

2. Working concept

The original concept of data compiling was the following:

a) Systematical literature search;
b) Writing of circular letters to the authors of the papers in which we found one (or more) age determination(s). In these letters we would have asked the authors to specify all data and assumptions on which the age determination relies, giving them also the chance to revise published data or to send us additional, still unpublished, data.

This way of data compiling was conceived in 1982. At that time we were 2 to 3 persons working on the project, and financial support from our institute, the Hamburger Sternwarte, was assured. Since 1984, however, the COCIA project has not been supported any more by our Institute. As a consequence, from that time I had to do all COCIA work alone and on a privately financed basis. So, to my great regret, I had to change the working concept. I renounced the circular letters and did the compiling only from the Literature.

2.1 Compiling and analysing of COCIA data

The operations I carried out for bringing one entry into the COCIA are sketched in Figure 1. Some remarks to the Figure:

"Main Reference Paper" (step 2) means the paper in which the age value has been published to which the entry in the COCIA refers. All papers referenced in the Main Reference Paper in connection with the age determination are called "Secondary Reference Papers" (step 4). The auxiliary files FCC, FEv and FPh mentioned in the Figure contain informations concerning often used age calibration curves, stellar evolutionary calculations and photometric studies. To save computer storage most of the information I type into my computer (an Victor AT with a harddisk storage of 20 MB) is in coded form. The amount of data for different files (shown in the Figure) refers to the present version of the COCIA. The figures in parantheses shown in the boxes labelled "authors", "journals" and "references" give the present number of entries in the corresponding files. "Computer's work" is done by a FORTRAN program which provides the printed form of the COCIA Table. Its principal functions are: the decodation of data, the arrangement of data into tabular form, and the arrangement of the references into sorted lists.

2.2 Additional information

All COCIA data stored in the computer files are also recorded in printed forms. This paper version of the COCIA contains some more data than the computer version as well as detailed additional remarks. This additional information may be send to the COCIA users on request. It may also help for a, possibly changed, second version of the catalogue, if the users will suggest that other data than those given in the first catalogue version would be of more interest.

3. Description of the COCIA

3.1 Data content and organisation of the catalogue

Due to the lack of colaborators, as explained in Section 2, I was forced to restrict the catalogue to *galactic open* clusters only. For the same reason the first version of the COCIA that shortly will be published together with the second supplement of the Catalogue of Star Clusters and Associations is not a complete compilation of cluster ages but only gives selected data. As shown in the boxes at the bottom of Figure 1 the COCIA consists of five parts. To facilitate the orientation of the user

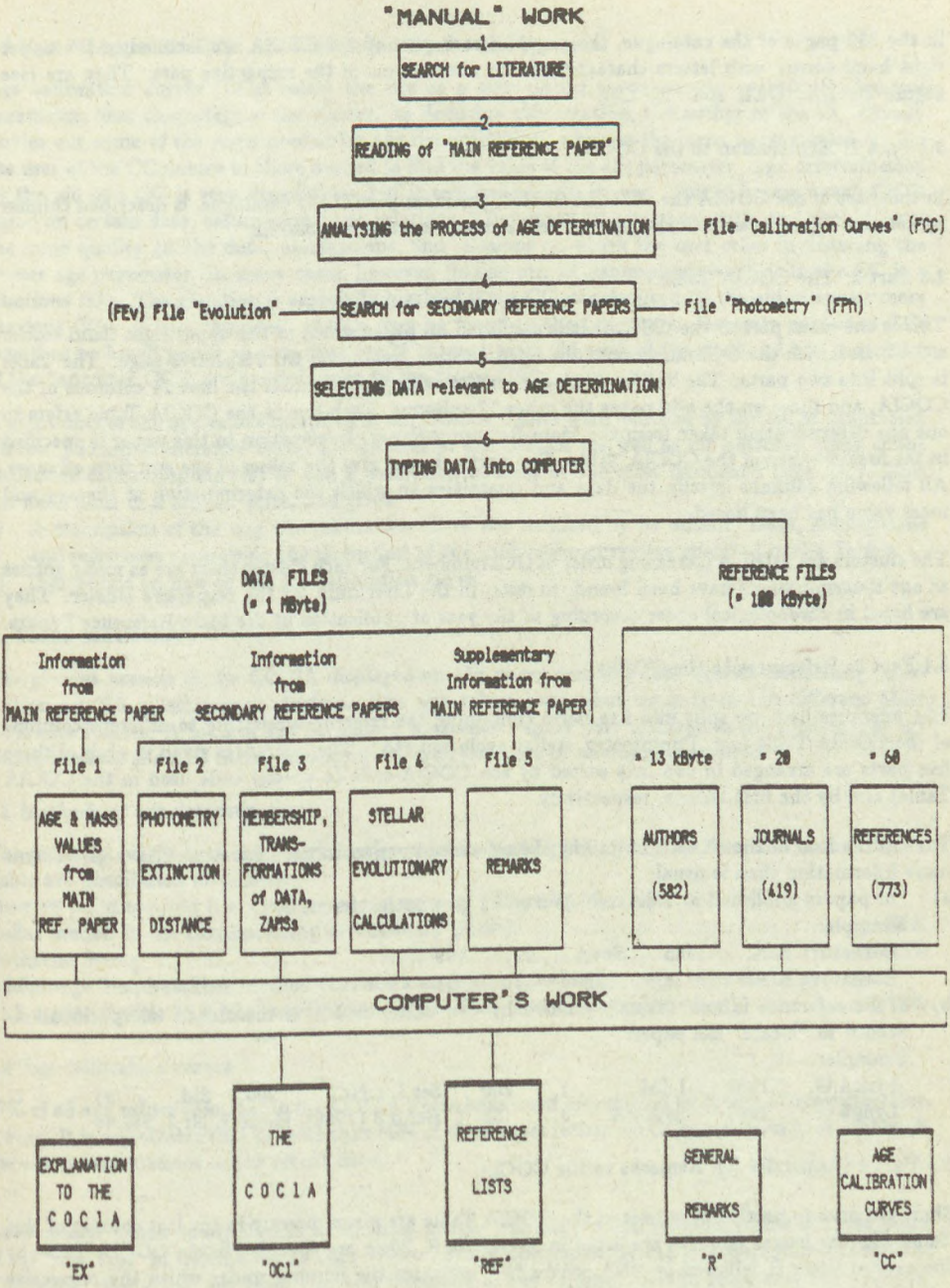
"MANUAL" WORK
1
SEARCH for LITERATURE
2
READING of "MAIN REFERENCE PAPER"
3
ANALYSING the PROCESS of AGE DETERMINATION
File "Calibration Curves" (FCC)
4
(FEv) File "Evolution"
SEARCH for SECONDARY REFERENCE PAPERS
File "Photometry" (FPh)
5
SELECTING DATA relevant to AGE DETERMINATION
6
TYPING DATA into COMPUTER
DATA FILES
(≈ 1 MByte)
REFERENCE FILES
(≈ 100 kByte)
Information from MAIN REFERENCE PAPER
Information from SECONDARY REFERENCE PAPERS
Supplementary Information from MAIN REFERENCE PAPER
File 1
File 2
File 3
File 4
File 5
≈ 13 kByte
≈ 20
≈ 60
AGE & MASS VALUES from MAIN REF. PAPER
PHOTOMETRY EXTINCTION DISTANCE
MEMBERSHIP, TRANS-FORMATIONS of DATA, ZAMSs
STELLAR EVOLUTIONARY CALCULATIONS
REMARKS
AUTHORS (582)
JOURNALS (419)
REFERENCES (773)
COMPUTER'S WORK
EXPLANATION TO THE COCIA
"EX"
THE COCIA
"OCI"
REFERENCE LISTS
"REF"
GENERAL REMARKS
"R"
AGE CALIBRATION CURVES
"CC"

Figure 1

in the 330 pages of the catalogue, the pages of each part of the COCIA are labelled in the upper right hand corner with letters characteristic for the content of the respective part. They are (see Figure 1): EX, OCl, Ref, R, CC.

3.2 Part 1: Explanation to the COCIA

In this part of the COCIA the "COCIA Table", the main part of the catalogue, is described column by column. Many examples are given to make things as clear as possible.

3.3 Part 2: The COCIA Table

This is the main part of the COCIA. It is displayed on pages which in the upper right hand corner are labelled with the OCl-numbers of the open clusters treated on the respective page. The Table is split into two parts: The Tables displayed on the even pages contain the first 24 columns of the COCIA, and those on the odd pages the other 17 columns. Each line in the COCIA Table refers to one age determination taken from the Main Reference Paper. Information to this paper is specified in the first columns of the COCIA Table. The next columns give the values of age and turn-off mass. All following columns specify the data and quantities on which the determination of the age and mass value has been based.

The clusters are listed in increasing order of OCl-numbers. For each cluster there are as many entries as age determinations have been found, to date, in the Literature for the respective cluster. They are listed in chronological order according to the year of publication of the Main Reference Papers.

3.4 Part 3: References to the COCIA

The reference lists are split into five parts containing the references referring to different columns of the COCIA Table (e.g. Photometry, stellar evolution etc.). The references given in each of these five parts are arranged in two lists sorted by the COCIA-code (a special code used in the COCIA Table) and by the first author, respectively.

To help the user of the COCIA in finding the referenced papers in the Literature I have given some more information than is usual:

a) For papers published in 2 different journals I give both references.
   Example:

Barhatova K.A.	1985	SovA	29,	499
Barhatova K.A.	1985	AZh	62,	854

b) If the reference is not uniquely defined by two numbers I have mentioned all specifications needed to "locate" the paper.
   Example:

Lyngå G.	1962	LdM	1,	200	Ser.I,	Nr.	200,	Sid. 65
Lyngå G.	1962	SvArkA	3,	65	Band 3 (1966), Häfte 1, Nr.8, Sid.65			

3.5 Part 4 (Appendix R): Remarks to the COCIA

Short remarks to particular entries of the COCIA Table are given directly in the last column of this Table whereas longer remarks are listed in Appendix R. They are specified in the COCIA Table by the capital letter R followed by "N", where "N" indicates the number under which the respective remark is to be found in Appendix R. This Appendix gives - on 50 pages - details to special methods of age determination, to the photometric system used in the course of age determination, clarifies misprints or other errors found in the Main Reference Papers etc., etc.

3.6 Part 5 (Appendix CC): Age Calibration Curves and Formulæ.

Age calibration curves (CCs) relate the age of a star cluster to one single quantity, called age parameter, that characterizes the cluster. In deducing this relation, the author of the CC already carries out some of the steps needed for age determination, whereas the steps to be carried out by the user of the CC reduce to those needed to find the value of the age parameter. Age determination by the aid of a CC is very expeditious, but it requires care in its use. This is because each CC is based on certain data, assumptions, and relations. They must be consistent with, and should be of the same quality as, the data, assumptions, and relations on which the user relies in deducing the cluster age parameter. In many cases, however, finding out all assumptions implicit in the CC is a laborious task. The situation is especially involved if the CC was deduced by the aid of one or more previous CCs. Whole "families" of CCs may be found in the Literature. Recently published CCs may thus be based partly on data that are 20 or more years old, and all the good and bad properties of the "ancestor CCs" are handed down to the "issue CC".

A great deal of the age values compiled in the COCIA Tables were deduced by the aid of calibration curves. I found it therefore useful for the user of the COCIA (as well as for potential users of the respective calibration curves) to add a desciption of some of the most frequently used CCs. This has been done in a tabular form, and gives

a) A description of the way the calibration curve was deduced by its author. Data, assumptions and references concerning the deduction of the calibration curve are specified in the Tables.
b) Indications on how to use the calibration curve.

4. Some statistics

The present version of the COCIA displayed on 174 pages contains 1260 entries comprising information on 250 galactic open clusters. The age values have been taken from 112 different Main Reference Papers. A total of 525 Secondary Reference Papers were involved in the processes of age determination. Most of them - namely 315 - are references to photometric studies.

4.1 Methods of age determinations

The principal methods of age determination used for getting the age values compiled in the COCIA Table are distributed as follows:

Turn-off point method (i.e. cluster stars at turn-off point identified with stellar models in the corresponding evolutionary phase): 50%
Isochrone fitting: 25%
Schönberg-Chandrasekhar method (i.e. stars at cluster termination point identified with stellar models at Schönberg-Chandrasekhar limit (homologous evolution)): 20%

4.2 Age calibration curves

50% of all age values compiled in the COCIA Table have been determined by means of age calibration curves. It is regrettable that in more than 60% of these cases rather old CCs have been used, although the age determinations are of recent date.

Acknowledgements: Many thanks to all those people who helped and encouraged me in these years of my "solo run" in COCIA work: Lars Winter, Frauke Böhrnsen, Marta Burchard, Kirsten Holert-Chmielnik, and - last not least - to two members of my family: Anselm Roth and my husband Wolfgang Höppner. Special thanks are due to Dr. B. A. Balázs for accepting the COCIA to be published together with the CSCA.

SUPPLEMENT

DISTANCE CORRECTIONS FOR 203 OPEN STAR CLUSTERS AND 8 ASSOCIATIONS

Béla A. Balázs
Roland Eötvös University, Department of Astronomy
Budapest, Kun Béla tér 2.
H-1083
Hungary

Using a method described earlier |1| distance corrections were computed for 203 open star clusters and 8 associations mainly in the Orion, Carina-Sagittarius and Perseus arms. The relevant data are presented in Table I, which is taken from the D. Sc. dissertation of the author |2|.

Key to symbols and abbreviations:

OCL#, ASS# : Running number in |3| or |4|.
IAU# : Running number according to |5|.
@ : For these clusters r_n is computed by the mean relation $r_n = \bar{f} \cdot r_o$ |1|.
l,b : Galactic coordinates.
A : Interstellar absorption in magnitudes.
m - M : Apparent distance modulus.
r : Heliocentric distance.
F : $100\, r_n/r_o$ (r_n, r_o : new & old heliocentric distances).
eSp : Earliest spectral type classified by spectroscopic methods.
esp : " " " " by photometric " .
d_1' : Apparent angular diameter according to |6|.
d_2' : "Best" "--" on the basis of the whole lit. in |3|, |4| & |6|.
D_1 : Linear diameter from r_n and d_1'.
D_2 : " " from r_n and d_2'.
τ_1 : Age of the object in 10^6 yrs from the lit. in |3|, |4| & |6|.
τ_2 : "--" according to |7|
(* indicates that τ_2 is an expansion age taken from |3,4|).

"Star Clusters and Associations"
Publ. Astron. Dep. Eotvos Univ.
No.10, Budapest (1990)

TABLE I. RELEVANT DATA OF PROGRAM OBJECTS

OCL#	OBJ.	IAU#	l	b	A	a-K	r	F	eSp	esp	d_1	d_2	D_1	D_2	r_1	r_2
10 @	NGC 6520	C1800-279	2.87	-2.85	0.94	11.35	1210	71	--	b8	5	6	1.8	2.1	54	--
19	NGC 6530	C1801-243	6.13	-1.36	0.99	11.10	1050	67	O5	v	--	15	--	4.6	10	2.0
-- @	Bo 14	C1758-237	6.37	-0.50	4.86	14.42	815	71	O6	--	2	--	0.5	--	--	10
24 @	NGC 6546	C1804-233	7.31	-1.37	0.36	9.21	590	71	--	b2:	15	13	2.6	2.2	245	40
26	NGC 6531	C1801-225	7.72	-0.44	0.96	11.00	1020	77	B0	b0	15	13	4.5	3.9	16	4.6
33 @	Ma 38	C1812-190	11.99	-0.94	1.02	11.60	1305	71	B0+	--	--	2	--	0.8	--	--
34 @	Tr 33	C1821-197	12.43	-3.22	1.54	11.36	920	71	--	b5	6	7	1.6	1.9	13	13
35	Cr 469	C1813-182	12.80	-0.80	2.24	12.30	1030	70	--	b2	3	11	0.9	3.3	--	100
38	IC 4725	C1828-192	13.58	-4.48	1.50	9.86	470	78	B4	b3	30	32	4.1	4.4	52	89
40	NGC 6613	C1817-171	14.15	-1.01	1.32	11.13	915	73	B3+	b2*	5	9	1.3	2.4	30	32
54	NGC 6611	C1816-138	16.99	+0.79	2.16	12.75	1310	78	O7	v	--	7	--	2.7	10	5.5
56 @	NGC 6604	C1815-122	18.16	+1.69	3.00	13.33	1165	71	O9+	--	6	2	2.0	0.7	--	4.0
66 @	NGC 6649	C1830-104	21.64	-0.78	3.60	13.43	925	71	--	b2	6	6	1.6	1.6	25	50
67 @	NGC 6694	C1842-094	23.86	-2.92	1.97	12.01	1020	71	B8	b7	8	15	2.4	4.5	89	89
68	NGC 6664	C1834-082	23.95	-0.50	1.95	11.50	810	70	B3	b3	12	16	2.8	3.8	25	37
74	NGC 6683	C1839-063	26.28	-0.81	2.00	11.75	890	71	B4+	b2	3	11	0.8	2.8	--	100
76 @	NGC 6705	C1848-063	27.31	-2.77	1.14	11.56	1210	71	B8	b8	--	14	--	4.9	76	224
77 @	Bas 1	C1845-059	27.36	-1.93	2.01	11.89	945	71	--	b5	5	9	1.4	2.5	58	--
82	NGC 6704	C1848-052	28.23	-2.23	2.98	13.49	1270	70	--	b2	6	6	2.2	2.2	25	20
83 @	Tr 35	C1840-041	28.29	-0.01	3.60	13.51	960	71	--	b4	6	9	1.7	2.5	42	42
85	IC 4665	C1743+057	30.61	+17.08	0.50	7.57	260	79	B4	b9	70	41	4.8	2.8	49	36
96	NGC 6755	C1905+041	38.55	-1.70	3.55	13.70	1070	69	--	b0:	15	15	4.7	4.7	35	35
99 @	NGC 6756	C1906+046	39.06	-1.69	4.13	14.47	1170	71	--	b4	4	4	1.4	1.4	47	47
100 @	NGC 6709	C1849+102	42.16	+4.70	1.02	10.11	660	71	B8	b6	15	13	2.9	2.5	65	78
124	NGC 6823	C1941+231	59.41	-0.15	2.43	13.50	1640	68	O7	v	7	12	3.3	5.7	10	5.0
125 @	NGC 6830	C1948+229	60.14	-1.83	1.74	11.84	1045	71	--	b4	6	12	1.8	3.6	16:	100
134	NGC 6834	C1950+292	65.70	+1.18	1.92	12.75	1465	70	--	b3	6	5	2.6	2.1	23	79
138	Ro 4	C2002+290	66.96	-1.26	3.15	14.40	1780	61	--	b2*	6	10	3.1	5.2	10	6.3
148	NGC 6871	C2004+356	72.64	+2.08	1.23	11.50	1130	72	O9	v	30	20	9.9	6.6	10	10
152	NGC 6883	C2009+357	73.29	+1.19	1.21	11.11	955	69	B3	b0	35	15	9.7	4.2	15	15

OCL#	OBJ.	IAU#	l	b	A	m-M	r	F	eSp	esp	d1	d2	D_1	D_2	r_1	r_2
158	IC 4996	C2014+374	75.36	+1.31	2.16	12.75	1315	74	B0	b0	7	6	2.7	2.3	10	10
168	NGC 6913	C2022+383	76.92	+0.60	2.89	12.55	855	68	B0	b0	10	7	2.5	1.7	10	10
181	NGC 6910	C2021+406	78.66	+2.03	2.89	13.10	1100	70	B0	b1	10	8	3.2	2.6	10	10
208	NGC 7067	C2122+478	91.19	-1.67	2.70	15.10	3020	67	--	o	3	3	2.6	2.6	13	13
210 @	NGC 7031	C2105+506	91.32	+2.26	2.46	11.51	645	71	B5	b6	15	5	2.8	0.9	56	56
211 @	NGC 7092	C2130+482	92.46	-2.28	0.18	6.54	190	71	A0	b9	30	32	1.6	1.8	79	269
213	IC 5146	C2151+470	94.39	-5.50	2.04	11.10	650	68	B1	b1	20	9	3.8	1.7	--	4.0
214 @	NGC 7086	C2128+513	94.41	+0.20	2.09	11.75	855	71	--	b6	12	9	3.0	2.2	85	85
218	NGC 7128	C2142+534	97.35	+0.42	3.09	14.90	2300	74	B2	b1	4	3	2.7	2.0	10	10
221	NGC 7243	C2213+496	98.86	-5.55	0.55	9.74	690	79	B6	b5	30	21	5.4	3.8	26	107
222	IC 1396	C2137+572	99.29	+3.73	1.53	10.00	497	70	O6*	--	90	50	12.2	6.8	--	1.0
229	NGC 7235	C2210+570	102.72	+0.78	2.91	15.10	2740	67	B0	o	6	4	4.8	3.2	10	2.0
236	NGC 7160	C2152+623	104.02	+6.45	1.71	10.20	500	71	B2	o	5	7	0.7	1.0	10	10
237	NGC 7261	C2218+578	104.04	+0.86	2.94	14.60	2150	66	--	b1:	6	6	3.8	3.8	40	40
244	NGC 7380	C2245+578	107.08	+0.90	1.92	13.40	1975	70	O9	o9	20	12	11.5	6.9	15	3.8
254 @	K 19	C2306+602	110.57	+0.15	2.46	12.37	960	71	--	b6	5	7	1.4	2.0	40	40
256	NGC 7510	C2309+603	110.96	+0.05	3.30	14.80	1995	69	B2	o	7	4	4.1	2.3	10	10
257	Ma 50	C2313+602	111.36	-0.20	2.55	13.65	1600	75	--	b0	2	5	0.9	2.3	10	10
260 @	NGC 7654	C2322+613	112.76	+0.46	1.86	12.07	1100	71	B7	b4	16	13	5.1	4.2	35	35
275	NGC 7788	C2354+611	116.43	-0.79	0.91	12.10	1730	72	B1	b2	4	9	2.0	4.5	16	16
276	NGC 7790	C2355+609	116.59	-1.01	1.59	13.25	2150	68	--	b0	5	17	3.1	10.6	28	78
291	NGC 103	C0022+610	119.80	-1.38	1.70	13.40	2190	72	B3	b5	5	5	3.2	3.2	38	38
294	NGC 129	C0027+599	120.25	-2.54	1.72	12.29	1300	75	B3	b5	12	21	4.5	7.9	47	151
297	K 14	C0029+628	120.72	+0.36	1.80	13.00	1720	72	B2	b2	7	7	3.5	3.5	16	16
299	NGC 146	C0030+630	120.87	+0.49	2.22	13.40	1720	71	B3	b1	5	7	2.5	3.5	13	13
301 @	NGC 189	C0036+608	121.51	-1.77	1.52	10.94	770	71	A0	b9	5	3.7	1.1	0.8	20	20
320 @	NGC 436	C0112+585	126.07	-3.91	0.45	11.37	1525	71	B5	b6	5	6	2.2	2.7	79	79
321	NGC 457	C0115+580	126.56	-4.35	1.56	13.15	2080	75	B2	b1	20	13	12.1	7.9	11	25
326	NGC 581	C0129+604	128.02	-1.76	1.26	12.30	1615	66	B2	b2	6	6	2.8	2.8	10	22
328	Tr 1	C0132+610	128.22	-1.14	1.35	12.55	1740	71	B2	b2	3	4.5	1.5	2.3	--	26

OCL#	OBJ.	IAU#	l	b	A	m-M	r	F	eSp	esp	d1	d2	D_1	D_2	r_1	r_2
329	NGC 637	C0139+637	128.55	+1.70	1.20	12.03	1465	70	B0	b2	3	3.5	1.3	1.5	--	40
330	NGC 654	C0140+616	129.09	-0.35	2.61	13.80	1730	68	OB	b0	6	5	3.0	2.5	15	15
332	NGC 659	C0140+604	129.34	-1.51	1.71	12.55	1470	70	OB	b2	6	5	2.6	2.1	20	20
333	NGC 663	C0142+610	129.46	-0.94	2.40	13.50	1660	78	B1	b0	15	16	7.2	7.7	10	22
345 @	NGC 744	C0155+552	132.39	-6.16	1.20	11.37	1080	71	B7	b8	5	11	1.6	3.5	39	39
349.1	Bas 10	C0215+580	134.21	-2.64	3.25	14.81	2050	80	B2*	b2*	2	--	1.2	--	--	16
350	NGC 869	C0215+569	134.63	-3.72	1.70	12.61	1520	71	B1	b0	18	30	8.0	13.3	10	5.6
351	Ma 6	C0225+604	134.68	+0.04	1.81	9.90	415	74	B1*	b1*	6	4.5	0.7	0.5	--	25
352	IC 1805	C0228+612	134.74	+0.92	2.40	13.70	1820	75	O5*	--	20	22	10.6	11.6	--	13
353	NGC 884	C0218+568	135.08	-3.60	1.70	12.95	1780	72	B1	b0	18	30	9.3	15.4	10	3.2
357	NGC 1027	C0238+613	135.78	+1.48	1.20	10.00	575	72	B3	b7	15	20	2.5	3.3	63	347
360 @	Be 65	C0235+602	135.84	+0.27	3.39	15.25	2350	71	B2*	b2*	5	5	3.4	3.4	--	6.3
362	NGC 957	C0230+573	136.34	-2.66	2.31	13.20	1505	72	B1	b0	10	11	4.4	4.8	15	15
364	IC 1848	C0247+602	137.19	+0.09	1.80	12.80	1585	69	O7	o	18	12	8.3	5.5	--	1.0
365	Tr 2	C0233+557	137.41	-3.89	0.96	9.02	410	71	B9	b6	17	20	2.0	2.4	32	78
383	NGC 1502	C0403+622	143.65	+7.62	2.25	11.15	600	70	B0	b0	20	8	3.5	1.4	16	20
392	Mel 20	C0318+484	146.95	-7.11	0.33	5.70	120	70	B2*	b1	300	185	10.5	6.5	--	51
394	NGC 1444	C0345+525	148.16	-1.29	2.10	11.25	675	73	B0	b2	--	4	--	0.8	162	25
397 @	NGC 1528	C0411+511	152.04	+0.27	0.90	9.82	610	71	B8	b8	18	4:	3.2	0.7	95	269
411 @	NGC 1664	C0447+436	161.66	-0.44	0.84	10.67	925	71	A0	b9	--	18	--	4.8	89	302
421	M 45	C0344+239	166.56	-23.53	0.17	5.17	100	80	B5	b6	120	110	3.1	2.9	16	78
429 @	NGC 1778	C0504+369	168.88	-2.00	0.99	10.51	800	71	B7*	b7	8	7	1.9	1.6	32	158
433 @	NGC 1912	C0525+358	172.27	+0.70	0.72	10.73	1005	71	B5	b4	15	21	4.4	6.1	43	224
439	NGC 1893	C0519+333	173.59	-1.70	1.65	14.00	2950	80	O5*	o	25	11	21.5	9.4	10	1.0
445	NGC 1960	C0532+341	174.52	+1.04	0.69	10.40	865	69	B3	b3	10	12	2.5	3.1	29	25
448	K 8	C0546+336	176.40	+3.12	2.56	15.02	3105	71	B0*	b0	4	8	3.6	7.2	--	--
455	Bas 4	C0545+302	179.23	+1.20	1.97	15.06	4150	70	B2*	b2	5	8	6.0	9.7	--	13
463	NGC 1817	C0509+166	186.13	-13.13	1.05	11.65	1320	76	A0*	o	20	16	7.7	6.1	186	794
467	NGC 2129	C0558+233	186.61	+0.13	2.07	12.90	1465	78	B1	b0	6	7	2.6	3.0	16	16
-- @	Bo 1	C0622+198	192.43	+3.41	1.65	13.95	2880	71	--	o7n	--	--	--	--	--	1.0

OCL#	OBJ.	IAU#	l	b	A	m-M	r	F	eSp	esp	d_1	d_2	D_1	D_2	r_1	r_2
481	NGC 2169	C0605+139	195.63	-2.92	0.41	9.50	660	71	B1	b0	6	7	1.2	1.3	13	50
495	NGC 2264	C0638+099	202.94	+2.20	0.21	8.65	490	68	O8	σ	40	20	5.7	2.9	25	20
499	NGC 2251	C0632+084	203.60	+0.13	0.90	11.15	1120	79	--	b3	10	10	3.3	3.3	87	302
502 @	NGC 2395	C0724+136	204.62	+13.96	2.16	11.80	850	71	--	b4	15	12	3.7	3.0	50	50
515	NGC 2244	C0629+049	206.42	-2.02	1.35	11.55	1095	68	O5	σ	30	24	9.6	7.6	10	30
537 @	Do 25	C0642+003	211.94	-1.29	2.43	15.29	3730	71	--	σ*	20	24	21.7	26.0	--	1.0
-- @	Bo 2	C0646+004	212.30	-0.40	2.67	15.63	3905	71	--	σ¤	1.5	--	1.7	--	--	1.0
540 @	NGC 2301	C0649+005	212.55	+0.28	0.13	8.74	530	71	B	b7	15	12	2.3	1.9	100	107
559 @	NGC 2323	C0700-082	221.64	-1.24	0.93	10.51	825	71	B8	b4	15	16	3.6	3.8	35	78
567	NGC 2353	C0712-102	224.72	+0.38	0.30	10.10	910	70	B0	b1	18	20	4.8	5.3	13	13
596	NGC 2422	C0734-143	230.97	+3.13	0.34	8.00	340	70	B3	b2:	25	30	2.5	3.0	20	78
597 @	NGC 2287	C0644-206	231.10	-10.23	0.00	8.38	475	71	B5	b4	40	38	5.5	5.3	65	100
598	NGC 2414	C0731-153	231.41	+1.96	1.62	13.80	2730	66	B1*	b1*	6	4.0	4.8	3.2	--	6.3
601 @	NGC 2437	C0738-315	231.87	+4.07	0.30	10.66	1180	71	B9	b8	20	27	6.9	9.3	72	302
-- @	Bo 5	C0728-169	232.57	+0.69	1.89	12.95	1630	71	--	σ9¤	5	11	2.4	5.2	--	1.0
662 @	Ha 19	C0750-261	234.02	+0.52	1.49	14.94	4900	71	B0¤	--	2	1.8	2.9	2.6	--	6.3
-- @	Bo 6	C0729-193	234.77	-0.23	2.10	14.37	2840	71	--	σ¤	10	--	8.3	--	--	1.0
619	Cr 121	C0652-245	235.39	-10.40	0.06	8.65	520	69	B3+	b1	90	50	13.6	7.6	--	15
618	NGC 2384	C0722-209	235.39	-2.41	0.81	12.50	2180	66	B0*	bσ*	5	2.5	3.2	1.6	--	1.0
621	NGC 2367	C0718-218	235.65	-3.84	1.05	12.50	1950	68	B1*	b1*	5	3.5	2.8	2.0	--	1.0
626 @	NGC 2421	C0734-205	236.24	+0.08	1.41	12,03	1330	71	--	b0.5¤	8	10	3.1	3.9	--	25
633	NGC 2362	C0716-248	238.18	-5.53	0.39	10,70	1155	75	O8	b0	6	8	2.0	2.7	25	25
635	Tr 7	C0725-239	238.28	-3.38	0.87	11,25	1190	74	B1*	b1*	5	5	1.7	1.7	--	25
649 @	NGC 2447	C0742-237	240.07	+0.15	0.18	9.64	780	71	B9	b9	10	12	2.3	2.7	98	98
651 @	Ru 32a	C0742-254	241.54	-0.60	1.08	13.40	2910	71	--	b0.5¤	6	6	5.1	5.1	--	1.0
665/7@	Ha 18ab	C0750-262	243.12	+0.44	2.10	15.55	4900	71	O7¤	b0.5¤	2	1	2.9	1.4	--	1.0
668	NGC 2467	C0750-263	243.14	+0.41	1.10	12.35	1780	71	O6	--	15	16	7.8	8.3	--	1.0
677.1	NGC 2483	C0753-278	244.86	+0.28	1.29	12.70	1915	65	O9*	σ	9	10	5.0	5.6	--	10
681 @	Ru 44	C0757-284	245.77	+0.52	2.10	15.46	4690	71	O6¤	--	10	5	13.6	6.8	--	1.0
688	NGC 2439	C0738-315	246.42	-4.42	0.75	10.93	1085	70	B1	b3:	9	10	2.8	3.2	66	66

OCL#	OBJ.	IAU#	l	b	A	m-M	r	F	eSp	esp	d1	d2	D_1	D_2	r_1	r_2
695 @	NGC 2533	C0805-297	247.81	+1.29	0.90	12.43	2020	71	--	b8:	6	3.5	3.5	2.1	95	182
696	Ha 15	C0743-326	247.88	-4.17	3.48	14.69	1745	70	B2*	b2*	3	3.5	1.5	1.8	--	6.3
701	NGC 2571	C0816-295	249.11	+3.54	0.93	10.60	860	67	--	b0	7	13	1.8	3.3	50	22
708 @	NGC 2567	C0816-304	249.81	+2.98	0.47	10.98	1265	71	B7*	b8	11	10	4.0	3.7	68	68
713 @	Ru 55	C0810-324	250.69	+0.76	1.62	14.09	3120	71	--	b0a	6	17	5.4	15.4	--	1.0
725 @	Cr 185	C0820-360	254.76	+0.45	0.63	10.77	1065	71	B5*	--	7	9	2.2	2.8	79	79
726	NGC 2546	C0810-374	254.90	-1.98	0.33	9.20	595	71	B0	b0	70	41	12.1	7.1	29	42
727	NGC 2568	C0815-369	255.08	-0.74	1.55	12.31	1420	71	--	b7:	3	4.6	1.2	1.9	85	85
742 @	Cr 197	C0842-411	261.56	+0.88	1.74	11.10	745	71	B1*	b1*	25	17	5.4	3.7	--	6.3
747	Tr 10	C0846-423	262.81	+0.64	0.15	7.60	310	73	B3	b2	30	15	2.7	1.4	47	47
753 @	NGC 2547	C0804-491	264.55	-8.55	0.10	7.25	270	71	B3*	--	25	20	2.0	1.6	74	58
754	Pi 6	C0837-460	264.81	-2.87	1.20	11.20	1000	61	B2*	b2*	3	1.5	0.9	0.4	--	32
--	Bo 7	C0843-458	265.20	-1.97	2.58	15.65	4120	71	WN6	σ	20	--	24.0	--	--	--
763	IC 2395	C0839-480	266.57	-3.81	0.39	9.30	605	71	B5	b0	17	8	3.0	1.4	16	16
764 @	NGC 2670	C0843-486	267.47	-3.61	1.44	10.79	740	71	B5	b4	7	9	1.5	1.9	95	95
766	Ma 18	C0858-487	269.21	-1.85	2.26	12.40	1065	66	O*	b1*	5	2	1.5	0.6	--	1.0
767 @	IC 2391	C0838-528	270.36	-6.88	0.12	5.33	110	71	B5	b3	60	50	1.9	1.6	25	36
776 @	NGC 2516	C0757-607	273.94	-15.88	0.30	7.36	260	71	B3	b9	22	30	1.7	2.3	71	107
781 @	NGC 2910	C0928-526	275.29	-1.18	0.27	10.10	925	71	--	b8	6	5	1.6	1.3	40	40
783 @	NGC 2925	C0932-532	276.02	-1.24	0.18	8.81	530	71	--	b5	15	12	2.3	1.9	79	79
787 @	Ru 79	C0939-536	277.09	-0.80	2.46	13.22	1420	71	--	b0.5a	6	11	2.5	4.5	--	13
790	Pi 16	C0949-529	277.82	+0.66	1.80	12.70	1515	71	B1*	b1*	2	1.5	0.9	0.7	--	6.3
798	NGC 3105	C0959-545	279.92	+0.28	3.30	17.00	5495	69	--	b1a	2	2	3.2	3.2	--	13
800 @	NGC 3228	C1019-514	280.74	+4.58	0.04	7.79	355	71	B8	b7	5	18	0.5	1.9	42	42
802 @	NGC 3114	C1001-598	283.34	-3.83	0.02	8.90	595	71	B9	b4	--	35	--	6.1	51	107
806 @	NGC 3330	C1036-538	284.18	+3.83	0.54	10.51	985	71	B8*	b8	6	7	1.7	2.0	50	50
807 @	We 2	C1022-575	284.26	-0.33	5.04	17.79	3550	71	--	σa	2	1.5	2.1	1.5	--	1.0
811	IC 2581	C1025-573	284.60	+0.01	1.26	12.75	1985	72	B0	b0	5	8	2.9	4.6	--	10
816	NGC 3293	C1033-579	285.86	+0.07	0.85	12.25	1870	72	O7*	--	--	6	--	3.3	10	25

OCL#	OBJ.	IAU#	l	b	A	m-M	r	F	eSp	esp	d1	d2	D_1	D_2	r_1	r_2
819 @	NGC 3324	C1035-583	286.22	-0.17	1.35	13.19	2330	71	O6ª	--	--	6	--	4.1	--	2.2
-- @	Bo 10	C1040-588	287.03	-0.32	1.08	12.38	1820	71	OBª	b0.5ª	20	--	10.6	--	--	7.1
825	Tr 15	C1042-591	287.40	-0.36	1.58	12.00	1215	72	O*	b0	15	3	5.3	1.1	--	1.0
826	Tr 14	C1041-593	287.42	-0.58	1.55	11.89	1170	71	O	b0	--	5	--	1.8	10	10
829	Tr 16	C1043-594	287.61	-0.65	1.40	13.09	2180	74	O5	σ	--	10	--	6.3	10	10
-- @	Bo 11	C1045-598	288.03	-0.87	1.62	16.66	2555	71	OBª	b0ª	22	--	16.4	--	--	1.0
831	Tr 17	C1054-589	288.66	+0.43	2.01	12.75	1405	73	B1*	b1	5	5	2.0	2.0	35	35
833 @	Pi 17	C1059-595	289.48	+0.14	1.53	13.90	2980	71	--	b0.5ª	--	0.6	--	0.5	--	1.0
838	IC 2602	C1041-641	289.60	-4.90	0.15	5.15	100	68	B0	b1	100	50	2.9	1.5	32	36
845 @	Sk 13	C1110-586	290.52	+1.55	0.72	12.11	1895	71	B1*	b0ª	5	3	2.8	1.7	--	25
846	NGC 3572	C1108-599	290.71	+0.21	1.47	12.80	1845	69	O6*	σ	7	7	3.8	3.8	13	13
847 @	Ha 10	C1108-601	290.80	+0.10	1.38	12.35	1560	71	O6ª	--	--	3	--	1.4	--	2.0
849 @	Ha 11	C1109-601	290.89	+0.14	0.96	12.02	1630	71	--	b1ª	2	1.5	0.9	0.7	--	6.3
850	Tr 18	C1109-604	290.99	-0.14	1.05	11.15	1050	72	B3*	b1	6	12	1.8	3.7	--	25
852 @	NGC 3590	C1110-605	291.21	-0.18	0.57	11.39	1460	71	--	b3	2	4	0.8	1.7	50	50
854	NGC 3603	C1112-609	291.62	-0.52	4.11	17.88	5675	70	O5*	σ	4	2.5	6.6	4.1	--	1.0
856 @	He 105	C1117-632	292.89	-2.45	1.14	12.00	1490	71	B7*	--	5	4	2.2	1.7	59	59
860	NGC 3766	C1133-613	294.11	-0.03	0.51	11.00	1255	70	B0	b2	15	12	5.5	4.4	11	22
862	IC 2944	C1131-627	294.57	-1.37	1.02	11.70	1375	70	O6	σ	35	15	14.0	6.0	10	10
865 @	Sk 14	C1141-622	295.23	-0.63	0.78	12.10	1840	71	B2*	b0.5ª	7	4	3.7	2.1	--	6.3
871	NGC 4103	C1204-609	297.57	+1.17	0.84	12.23	1495	79	B	b2	6	7	2.6	3.0	--	22
885 @	NGC 4463	C1227-645	300.65	-2.01	1.32	11.04	880	71	B1*	b1*	6	5	1.5	1.3	--	25
891 @	Ha 15	C1240-628	302.04	-0.24	3.48	15.85	2980	71	--	b0ª	2.0	2.0	1.7	1.7	--	7.9
892 @	NGC 4755	C1250-600	303.21	+2.53	0.93	10.26	735	71	B3	b6	--	10	--	2.1	10	7.1
898	Sk 16	C1315-623	306.11	+0.14	1.59	11.78	1090	75	B8*	σ9*	20	3	6.3	1.0	--	28
913 @	NGC 5316	C1350-616	310.23	+0.12	0.54	10.04	795	71	B8	b7	15	14	3.5	3.2	51	195
916 @	Ly 2	C1420-611	313.78	-0.49	0.57	10.13	815	71	B2*	--	10	12	2.4	2.8	32	32
919 @	NGC 5617	C1426-605	314.67	-0.10	1.56	11.45	950	71	B3	b3	10	10	2.8	2.8	46	46
922	NGC 5606	C1424-594	314.84	+0.99	1.44	12.10	1355	71	B0.5*	b2	3	3	1.2	1.2	13	13
930 @	NGC 5749	C1445-543	319.50	+4.53	1.14	10.17	640	71	B8*	b5	10	8	1.9	1.5	91	91

OCL#	OBJ.	IAU#	l	b	A	m-M	r	F	eSp	esp	d1	d2	D_1	D_2	r_1	r_2
932	Pi 20	C1511-588	320.52	-1.21	3.45	13.60	1070	73	B0*	b0*	--	4.5	--	1.4	--	1.0
933	Ho 18	C1447-520	320.75	+6.43	1.59	11.00	760	65	B3	b5	5	3	1.1	0.7	--	50
948 @	NGC 6087	C1614-577	327.76	-5.40	0.48	9.58	660	71	B5	b5	15	12	2.9	2.3	41	60
951	NGC 6031	C1603-539	329.25	-1.53	1.29	13.04	2240	70	B3*	b7	3	2	2.0	1.3	22	22
953 @	NGC 6067	C1609-540	329.76	-2.20	1.10	11.96	1490	71	--	b6	15	13	6.5	5.6	15	78
975	NGC 6193	C1637-486	336.70	-1.57	1.56	11.50	975	75	O7	--	--	15	--	4.3	--	1.0
978 @	NGC 6200	C1640-473	338.00	-1.09	1.89	13.05	1705	71	--	b0	15	12	7.4	6.0	--	1.0
980	NGC 6178	C1632-455	338.40	+1.23	0.72	9.75	640	70	B1*	b1*	5	4	0.9	0.7	--	6.3
981	Ho 22	C1643-470	338.55	-1.16	1.98	13.30	1835	66	O9*	ø9*	3	1.5	1.6	0.8	--	1.0
982	NGC 6204	C1642-469	338.59	-1.08	1.53	11.35	920	70	O6	b0	6	5	1.6	1.3	13	13
990 @	NGC 6124	C1622-405	340.77	+5.96	2.16	9.87	350	71	B8	b7	40	29	4.1	3.0	51	51
991 @	NGC 6250	C1654-457	340.79	-1.83	1.14	10.29	675	71	--	b1[a]	10	8	2.0	1.6	--	14
992 @	Ly 14	C1651-452	340.88	-1.16	4.44	15.54	1660	71	--	ø9*	3	2	1.4	1.0	--	1.0
997	NGC 6231	C1650-417	343.47	+1.22	1.26	12.00	1405	79	O9	b0	--	15	--	6.1	0.1	3.2
999	Tr 24	C1653-405	344.70	+1.51	1.12	11.57	1230	77	O7*	ø	--	60	--	21.5	--	1.0
1000	NGC 6322	C1714-429	345.27	-3.07	1.65	11.25	830	74	B0	b0	5	10	1.2	2.4	10	10
1002	NGC 6268	C1658-396	346.04	+1.31	1.21	10.82	835	75	--	b2	--	6	--	1.5	--	25
--	Do 13	C1714-355	351.19	+1.37	2.64	13.04	1205	71	O7[a]	--	15	--	5.3	--	--	6.3
1015 @	Ru 127	C1734-362	352.89	-2.45	3.09	13.27	1085	71	--	b2[a]	5	8	1.6	2.5	--	6.3
1016	Pi 24	C1722-343	353.12	+0.71	5.16	16.04	1500	72	O7*	ø7*	5	4	2.2	1.7	--	1.0
1026	NGC 6383	C1731-325	355.68	+0.05	0.78	10.25	785	74	O7*	b2	20	5	4.6	1.1	20	4.5
1028 @	NGC 6475	C1750-348	355.86	-4.53	0.12	6.21	165	71	B5	b4	80	80	3.8	3.8	50	224
1030 @	NGC 6405	C1736-321	356.58	-0.70	0.44	8.22	360	71	B5	b3	20	15	2.1	1.6	50	51
1039 @	Cr 347	C1743-292	359.78	-0.32	3.48	13.63	1070	71	--	b0.5[a]	10	4.5	3.1	1.4	--	6.3

ASS#	OBJ.	IAU#	l	b	A	m-M	r	F	eSp	esp	d1	d2	D1	D2	γ1	γ2
25	I Lac	--	97.00	-17.15	0.29	8.70	480	80	O9	--	--	--	--	--	--	2.5°
30	III Cep	--	111.15	+3.75	2.40	11.40	630	86	O5	b1	--	--	--	--	--	1.6°
31	V Cas	--	112.05	+0.25	2.17	13.24	1640	82	O7*	b1	--	--	--	--	--	--
47	II Per	--	159.25	-17.25	0.30	8.08	360	89	O7	σ	--	--	--	--	--	1.3°
52	I Ori	--	202.30	-17.10	0.30	8.02	350	85	O	σ	--	--	--	--	--	4.5°
57	II Pup	--	244.00	+0.50	1.65	13.50	2350	82	O6*	--	--	--	--	--	--	4.0°
66	I Ara	--	338.00	+0.00	1.35	11.78	1220	87	O	σ	--	--	--	--	--	13°
68	II Sco	--	350.05	+17.80	0.36	5.93	130	82	B0	--	--	--	--	--	--	--

The spectral types are generally taken from |8| and |9|. There are a few exceptions:
* : |3|, |4|; + : |6|; - : |10|; □ : |11|, |12|.

REFERENCES

|1| Balázs, B.A.: 1978, Publ. Astron. Dept. Eötvös Univ. No. 5; 95.

|2| Balázs, B.A.: 1986, D. Sc. dissertation (in hungarian), 40.

|3| Alter, G., Ruprecht, J., Vanýsek, V.: 1970, CSCA, eds. Alter, Balázs, Ruprecht, Akadémiai Kiadó, Budapest.

|4| Ruprecht, J., Balázs, B.A., White, R.E.: 1981, CSCA Sup 1, ed. Balázs, " .

|5| Lyngå, G., Alcaino, G., Balázs, B.A., Moffat, A.F.J.: 1980, IAU Comm. 37 Circular, 1.

|6| Lyngå, G.: 1981, Catalogue of Open Cluster Data, CDS No. VII-30.

|7| Piskunov, A.: 1980, private communication.

|8| Becker, W., Fenkart, R.: 1971, Astron. Astrophys. Suppl. 4, 241.

|9| Fenkart, R.P., Bingelli, B.: 1979, Astron. Astrophys. Suppl. 35, 271.

|10| Janes, K., Adler, D.: 1982, Astrophys. J. Suppl. 49, 425.

|11| Vogt, N., Moffat, A.F.J.: 1975, Astron. Astrophys. 39, 477.

|12| Moffat, A.F.J., Vogt, N.: 1973, Astron. Astrophys. 23, 317.